



Esmail Najafi Saatlou

**Techno-Economic Environmental Assessment of Advanced
Intercooled Propulsion Systems**

SCHOOL OF ENGINEERING
DEPARTMENT OF POWER AND PROPULSION

PHD THESIS

Academic Year: 2009 - 2012

Supervisors: **Dr. Vishal Sethi**
Prof. Pericles Pilidis

September 2012

CRANFIELD UNIVERSITY
SCHOOL OF ENGINEERING
DEPARTMENT OF POWER AND PROPULSION

PHD THESIS

Academic Year 2009 - 2012

Esmail Najafi Saatlou

**Techno-Economic Environmental Assessment of Advanced
Intercooled Propulsion Systems**

Supervisors: **Dr. Vishal Sethi**
Prof. Pericles Pilidis

September 2012

This thesis is submitted in partial fulfilment of the requirements for
the degree of Doctor of Philosophy.

© Cranfield University 2012. All rights reserved. No part of this
publication may be reproduced without the written permission of the
copyright owner.

ABSTRACT

A tool based on a Techno-economic and Environmental Risk Assessment (TERA) framework is useful at the preliminary stage of an aero engine design process, to conceive and assess engines with minimum environmental impact and lowest cost of ownership, in a variety of emission legislation and taxation policy scenarios.

This research was performed as part of the EU FP6 New Aero engine Core concepts (NEWAC) programme which was established to assess the potential of innovative gas turbine core technologies to enhance thermal efficiency thereby reducing CO₂ emissions and fuel consumption. A representative prediction of engine life and mission fuel burn at the earliest possible design stage is a crucial task that can provide an indication of the approximate overall engine direct operating costs. Two aero engines, a conventional turbofan and a conceptual intercooled turbofan, were assessed and optimised using the TERA approach to identify the designs that provided the maximum time between overhaul (and therefore the minimum maintenance costs). In order to perform these assessments (which included sensitivity and parametric analyses, and optimisation studies) several models were developed and integrated in an optimisation framework. A substantial effort was devoted to the development of a detailed lifing model that calculates the engine life with a reasonable level of accuracy by integrating physics based oxidation, creep and fatigue models.

The results obtained from the study demonstrate that an engine optimised for maximum time between overhaul requires a lower overall pressure ratio and specific thrust but this comes at the cost of lower thermal efficiency and therefore higher mission fuel burn.

The main contribution to knowledge of this work is a multidisciplinary TERA assessment of a novel intercooled conceptual aero engine. Particular emphasis is placed on the design space exploration and optimisation studies to identify the designs that may offer the largest time between overhaul. The consequent implications therefore this may have on mission fuel burn and direct operating costs.

In addition to refining the various TERA models, one of the main recommendations for further work is to optimise the engines for minimum direct operating cost to identify the best economic compromise between engine life and mission fuel burn. This can be done by considering different fuel prices and under a variety of hypothetical emission taxation scenarios, to identify the circumstances in which intercooled engine technology may become economically viable.

ACKNOWLEDGEMENTS



In the name of God, the Most Gracious and the Most Merciful

I would like to extend my sincere gratitude to my supervisors, Dr. V. Sethi, and Professor P. Pilidis, for their encouragement, invaluable guidance and giving me the opportunity to commence this PhD research at Cranfield University. Also, I would like to express my thanks to all the staff in the Department of Power and Propulsion in providing guidance and support throughout the entire research project, especially the ever helpful Ms. G. Hargreaves and Ms. N. Datt.

Several individuals have provided invaluable assistance and guidance to me to complete this doctorate. Special thanks go to my brother Seyed Mohammed Mohseni for his encouragement, support and faith. I would also like to sincerely thank Dr. Konstantinos G. Kyprianidis for his valuable technical support, expertise and guidance throughout the project. I also wish to express my deepest thanks to Abu Abdullahi Obonyegba for his assistance and all the wonderful times we had while I have been at Cranfield University.

The present work was performed as part of the NEWAC research program (European Commission Contract No. AIP5-CT-2006-030876). The collaborative support of WP1.3 partners and the financial support from the EU are gratefully acknowledged. I would particularly like to thank Andrew M. Rolt (Rolls-Royce) and John Borradaile for their technical advice and suggestions.

I dedicate this work to my family: my father Mr. Jamshid Najafi Saatlou, my mother Mrs. Ghandab Safari, my dear sister Fariba Najafi Saatlou, my beloved wife Seyedeh Maryam Faghany; without her prayers, encouragement, understanding and patience, it would have been impossible for me to accomplish this work, and to my son Alisan for his lovely smiles.

TABLE OF CONTENTS

ABSTRACT.....	i
ACKNOWLEDGEMENTS.....	iii
TABLE OF CONTENTS.....	v
LIST OF FIGURES.....	vii
LIST OF TABLES.....	x
LIST OF EQUATIONS.....	xi
NOMENCLATURES.....	xii
CHAPTER 1 INTRODUCTION AND SCOPE.....	1
1.1 Environmental Impact of Civil Aviation.....	1
1.2 Objectives and Scopes.....	4
1.3 Contribution to Knowledge.....	5
1.4 Methodology.....	5
1.5 Thesis Outline.....	6
1.6 Publications.....	7
CHAPTER 2 BACKGROUND.....	9
2.1 Mitigation of Aviation Impact.....	9
2.2 Multidisciplinary Design Optimisation.....	12
2.3 Aero Engine Conceptual Design Frameworks.....	15
2.3.1 EDS.....	15
2.3.2 NPSS.....	16
2.3.3 PMDO.....	16
2.3.4 TERA.....	17
2.4 Commercial Optimisation Frameworks.....	26
2.5 Gas Turbine Lifting Concepts.....	26
2.5.1 Fatigue failure mechanism.....	28
2.5.2 Creep failure mechanism.....	33
2.5.3 Oxidation failure mechanism.....	35
2.6 NEW Aero Engine Core Concepts (NEWAC).....	37
2.6.1 Intercooled core (DDIC).....	39
2.6.2 Intercooled Recuperative Core (IR).....	40
2.6.3 Flow Controlled Core (FCC).....	42
2.6.4 Active Core.....	43
CHAPTER 3 TERA2020 FRAMEWORK.....	45
3.1 Introduction.....	45
3.2 TERA2020 Modules.....	46
3.2.1 Engine performance module.....	48
3.2.2 Weight and plant production cost module (WeiCo).....	50
3.2.3 Aircraft performance module (HERMES).....	51
3.2.4 Emission and environmental module (HEPHAESTUS).....	53
3.2.5 Noise module (SOPRANO).....	53
3.2.6 Economics module (HESTIA).....	54
3.3 TBC Oxidation Model.....	57
3.4 Integration and Optimisation Environment.....	63
CHAPTER 4 TERA 2020 ASSESSMENT PROCESS.....	67
4.1 Assumptions.....	67

4.2 Constraints	69
4.3 Sensitivity Analysis.....	70
4.4 Parametric Studies	72
4.5 Design Space Approximation and Optimisation.....	75
CHAPTER 5 AERO ENGINES LIFE ASSESSMENT	79
5.1 Introduction.....	79
5.2 BASELR Configuration.....	81
5.2.1 Sensitivity Analysis of BASELR Configuration	83
5.2.2 Parametric Study of BASELR Configuration	88
5.2.3 Optimisation of BASELR Configuration	100
5.2.4 BASELR Optimised Design	113
5.3 DDICLR Configuration.....	116
5.3.1 Sensitivity Analysis of DDICLR Configuration	118
5.3.2 Parametric study of DDICLR Configuration	123
5.3.3 Optimisation of DDICLR Configuration.....	135
5.3.4 DDICLR Optimised Design.....	152
5.4 Results Verification.....	155
CHAPTER 6 CONCLUSIONS AND FURTHER WORK.....	157
6.1 Conclusion.....	157
6.2 Recommendations for Further Work	161
REFERENCES	163
APPENDICES.....	173
Appendix A BASELR Design Parametric Study.....	173
Appendix B BASELR Design Space Exploration and Optimisation	182
Appendix C DDICLR Design Parametric Study	190
Appendix D DDICLR Design Space Exploration and Optimisation.....	203
Appendix E Publications.....	211

LIST OF FIGURES

Figure 1-1 Boeing's forecast of air traffic [3].....	2
Figure 1-2 Airbus's forecast of air traffic [4].....	2
Figure 1-3 Air traffic and CO ₂ emissions [7].....	3
Figure 2-1 Design space exploration [21].....	14
Figure 2-2 TERA Philosophy	19
Figure 2-3 TERA Structure for Aviation [36].....	20
Figure 2-4 TERA Structure for LNG Application [38].....	21
Figure 2-5 TERA Structure for Heavy Oil Recovery Applications [44].....	23
Figure 2-6 GT Power and Ship Speed Characteristic [36].....	24
Figure 2-7 GT Fuel Flow and TET Characteristic [36].....	24
Figure 2-8 The S-N curve [56]	29
Figure 2-9 Stress-strain behaviour after a reversal [57]	30
Figure 2-10 Typical cyclic Stress-Strain curve [57].....	31
Figure 2-11 Typical Strain-Life curve [57].....	31
Figure 2-12 The general creep curve [55]	33
Figure 2-13 TBC on a substrate material [62].....	37
Figure 2-14 NEWAC innovative core concepts [7]	39
Figure 2-15 Intercooled core architecture [69].....	40
Figure 2-16 Intercooled recuperated core architecture [66].....	41
Figure 2-17 Flow controlled core engine architecture [66].....	42
Figure 2-18 Active core engine architecture [66].....	43
Figure 3-1 TERA2020 algorithm [71].....	48
Figure 3-2 Engine design and manufacturing process [30].....	52
Figure 3-3 Blade thermal barrier coating schematic [63].....	59
Figure 3-4 A typical oxidation model output.....	62
Figure 3-5 TERA2020 architecture and data flow chart.....	65
Figure 5-1 BASELR configuration schematic [77]	82
Figure 5-2 BASELR Block fuel sensitivity analysis	85
Figure 5-3 BASELR SFC at top of climb sensitivity analysis.....	86
Figure 5-4 BASELR TBO sensitivity analysis around nominal point.....	87
Figure 5-5 BASELR Fan tip pressure ratio variation at top of climb	89
Figure 5-6 Example of LPT stage count change	90
Figure 5-7 BASELR Fan mass flow variation at top of climb.....	91
Figure 5-8 BASELR Core mass flow variation at top of climb	93
Figure 5-9 BASELR IPC pressure ratio variation at top of climb	95
Figure 5-10 BASELR HPC pressure ratio variation at top of climb.....	96
Figure 5-11 BASELR HPT Cooling mass flow variation at top of climb.....	97
Figure 5-12 BASELR Combustor outlet temperature variation at TOC.....	99
Figure 5-13 Variation of SFC with core mass flow and fan pressure ratio.....	102
Figure 5-14 Variation of time between overhaul with fan mass flow and fan pressure ratio.....	103
Figure 5-15 Variation of engine maintenance costs with fan mass flow and fan pressure ratio.....	104
Figure 5-16 Variation of block fuel burn with core mass flow and fan pressure ratio.....	105

Figure 5-17 Variation of engine time between overhaul with core mass flow and fan pressure ratio.....	106
Figure 5-18 Fan tip pressure ratio variation at top of climb	107
Figure 5-19 Variation of TBO with IPC and HPC pressure ratio.....	108
Figure 5-20 Variation of HPC delivery temperature and HPT metal temperature with IPC and HPC pressure ratio.....	109
Figure 5-21 Variation of take-off distance with IPC and HPC pressure ratio...	110
Figure 5-22 Variation of HPT metal temperature with combustor outlet temperature and HPT cooling mass flow.....	111
Figure 5-23 Variation of take-off distance with combustor outlet temperature and HPT cooling mass flow	111
Figure 5-24 Variation of block fuel with combustor outlet temperature and HPT cooling mass flow	112
Figure 5-25 Variation of direct operating cost with combustor outlet temperature and HPT cooling mass flow	113
Figure 5-26 DDICLR configuration schematic [77]	117
Figure 5-27 DDICLR TBO sensitivity analysis	119
Figure 5-28 DDICLR block fuel sensitivity analysis	121
Figure 5-29 DDICLR SFC sensitivity analysis	122
Figure 5-30 DDICLR Fan tip pressure ratio variation at top of climb	124
Figure 5-31 DDICLR Fan mass flow variation at top of climb.....	126
Figure 5-32 DDICLR Core mass flow variation at top of climb	128
Figure 5-33 IPC pressure ratio variation at top of climb	129
Figure 5-34 HPC pressure ratio variation at top of climb.....	130
Figure 5-35 Intercooler effectiveness variation at Take-off.....	132
Figure 5-36 HPT cooling mass flow variation at top of climb.....	133
Figure 5-37 Combustor outlet temperature variation at top of climb.....	135
Figure 5-38 Variation of block fuel burn with fan inlet mass flow and fan tip pressure ratio.....	138
Figure 5-39 Variation of maintenance costs with fan inlet mass flow and fan tip pressure ratio.....	139
Figure 5-40 Variation of direct operating costs with fan inlet mass flow and fan tip pressure ratio.....	140
Figure 5-41 Variation of block fuel burn with core mass flow and fan tip pressure ratio.....	141
Figure 5-42 Variation of time between overhaul with core mass flow and fan tip pressure ratio.....	142
Figure 5-43 Variation of engine maintenance costs with core mass flow and fan tip pressure ratio.....	143
Figure 5-44 Optimum fan tip pressure ratio for maximum TBO.....	144
Figure 5-45 Variation of HPT metal temperature with IPC and HPC pressure ratios.....	145
Figure 5-46 Variation of TBO with IPC and HPC pressure ratio.....	146
Figure 5-47 Variation of block fuel with Combustor Outlet Temperature and HPT cooling mass flow	147
Figure 5-48 Variation of TBO with combustor outlet temperature and HPT cooling mass flow	148

Figure 5-49 <i>Variation of engine weight with Intercooler effectiveness and Intercooler cold mass flow</i>	150
Figure 5-50 <i>Variation of block fuel with Intercooler effectiveness and Intercooler inlet mass flow</i>	150
Figure 5-51 <i>Variation of engine time between overhaul with Intercooler effectiveness and Intercooler inlet mass flow</i>	151
Figure 5-52 <i>Variation of engine maintenance costs with Intercooler effectiveness and Intercooler inlet mass flow</i>	152
Figure A-1 <i>BASELR Fan tip pressure ratio variation at top of climb</i>	173
Figure A-2 <i>BASELR Fan mass flow variation at top of climb</i>	174
Figure A-3 <i>BASELR Core mass flow variation at top of climb</i>	176
Figure A-4 <i>BASELR IPC Pressure ratio variation at top of climb</i>	177
Figure A-5 <i>BASELR HPC pressure ratio variation at top of climb</i>	178
Figure A-6 <i>BASELR HPT cooling mass flow variation at top of climb</i>	179
Figure A-7 <i>BASELR Combustor outlet temperature variation at top of climb</i> ..	181
Figure B-8 <i>BASELR Fan tip pressure ratio and fan mass flow variation</i>	183
Figure B-9 <i>BASELR Fan tip pressure ratio and core mass flow variation</i>	184
Figure B-10 <i>BASELR Fan tip pressure ratio variation</i>	186
Figure B-11 <i>BASECLR HPC and IPC pressure ratio variation</i>	188
Figure B-12 <i>BASECLR Fan tip pressure ratio and core mass flow variation</i> ..	189
Figure C-13 <i>DDICLR fan tip pressure ratio variation at top of climb</i>	191
Figure C-14 <i>Fan mass flow variation at top of climb</i>	193
Figure C-15 <i>Core mass flow variation at top of climb</i>	195
Figure C-16 <i>IPC pressure ratio variation at top of climb</i>	197
Figure C-17 <i>HPC pressure ratio variation at top of climb</i>	199
Figure C-18 <i>Intercooler effectiveness variation at take-off</i>	200
Figure C-19 <i>HPT cooling mass flow variation at top of climb</i>	201
Figure C-20 <i>Combustor outlet temperature variation at top of climb</i>	202
Figure D-21 <i>Variation of fan inlet mass flow and fan tip pressure ratio</i>	204
Figure D-22 <i>Variation of core mass flow and fan tip pressure ratio</i>	205
Figure D-23 <i>Optimum fan tip pressure ratio for maximum TBO</i>	206
Figure D-24 <i>Variation of IPC and HPC pressure ratio</i>	208
Figure D-25 <i>Variation of combustor outlet temperature and cooling mass flow</i>	209
Figure D-26 <i>Variation of intercooler effectiveness and intercooler inlet mass flow</i>	210

LIST OF TABLES

Table 2-1 <i>Fuel Consumed and Journey Times [36]</i>	25
Table 3-1 <i>Economic module output parameters</i>	55
Table 3-2 <i>Oxidation model input parameters</i>	61
Table 5-1 <i>BASELR engine performance specifications</i>	81
Table 5-2 <i>BASELR sensitivity parameters</i>	83
Table 5-3 <i>BASELR design space parameters and investigated range</i>	88
Table 5-4 <i>BASELR engine optimisation steps, variables and ranges</i>	101
Table 5-5 <i>BASELR engine design space constraints</i>	101
Table 5-6 <i>BASELR configuration design variables and optimum values</i>	114
Table 5-7 <i>Comparison of the TBO optimal design of BASELR engine with respect to the nominal design</i>	115
Table 5-8 <i>DDICLR engine performance specifications</i>	116
Table 5-9 <i>DDICLR sensitivity parameters</i>	118
Table 5-10 <i>DDICLR design space parameters</i>	123
Table 5-11 <i>DDICLR engine optimisation steps, variables and ranges</i>	136
Table 5-12 <i>DDICLR engine design space constraints</i>	137
Table 5-13 <i>DDICLR configuration design variables and optimum values</i>	153
Table 5-14 <i>Comparison of the TBO optimal design of DDICLR engine with respect to the nominal design</i>	154

LIST OF EQUATIONS

(2-1)	10
(2-2)	10
(2-3)	10
(2-4)	32
(2-5)	34
(2-6)	35
(2-7)	35
(3-1)	59
(3-2)	60
(3-3)	61

NOMENCLATURES

GENERAL ACRONYMS

Abbreviation ***Definition***

ACARE	Advisory Council for Aeronautical Research in Europe
AEO	All Engines Operative
ANTLE	Affordable Near-Term Low Emissions
APP	Approach
ARTNE	Air Transportation Noise and Emissions
ASA	Adaptive Simulated Annealing
BPR	Bypass Ratio
CAEP	Committee on Aviation Environmental Protection
CAPEX	Capital Expenditure
CLEAN	Component Validator for Environmentally-friendly Aero-Engine
CR	Cruise
CRFC	Counter Rotating Flow controlled Core
CRTF	Counter Rotating Turbo Fan
CU	Cranfield University
DDICLR	Direct Drive fan Intercooled Core turbofan for Long Range
DDICSR	Direct Drive Intercooled Core turbofan for Short Range
DDTF	Direct Drive Turbo Fan
DLL	Dynamic Link Library
DOC	Direct Operating Costs
DREAM	Validation of Radical Engine Architecture Systems
DTAMB	Ambient temperature relative to ISA
EEFAE	Efficient and Environmentally Friendly Aircraft Engine
EC	European Commission

EI CO ₂	Emission Index for Carbon Dioxide
EI NO _x	Emission Index for Nitrogen Oxides
EIS	Entry Into Service
EOR	Enhanced Oil Recovery
EPNL dB	Effective Perceived Noise Level in decibels
ETA	Efficiency
EVA	EnVironmental Assessment
EU	European Union
FAR	Federal Aviation Regulations
FCC	Flow Controlled Core
FP	Framework Package
FPR	Fan Pressure Ratio
GDP	Gross Domestic Product
GTIRLR	Geared Turbofan Intercooled Recuperative for Long Range
GWP	Global Warming Potential
HPC	High Pressure Compressor
HPT	High Pressure Turbine
IATA	International Air Transport Association
IC	Intercooler
ICAO	International Civil Aviation Organisation
IPCC	Intergovernmental Panel on Climate Change
IPC	Intermediate Pressure Compressor
IPT	Intermediate Pressure Turbine
JTI	Joint Technology Initiative
LDI	Lean Direct Injection
LLP	Life Limited Parts
LNG	Liquefaction of Natural Gas
LPC	Low Pressure Compressor (booster)
LPP	Lean Premixed Pre-vaporised

LPT	Low Pressure Turbine
LTO NO _x	Landing Take-Off Nitrogen Oxides
MDO	Multidisciplinary Design Optimization
MTBF	Mean Time Between Failure
MTOW	Maximum Take-Off Weight
MTTR	Mean Time To Repair
NPC	Net Present Cost
NPV	Net Present Value
NEWAC	New Aero engine Core concepts
NTUA	National Technical University of Athens
OEI	One Engine Inoperative
OEM	Original Engine Manufacturer
OEW	Operating Empty Weight
OPR	Overall Pressure Ratio
PARTNER	Partnership for Air Transportation Noise and Emissions
PERM	Partially Evaporating Rapid Mixing Combustor
RPK	Revenue Passenger Kilometres
PROOSIS	Propulsion Object-Oriented Simulation Software
RTDF	radial temperature distortion factor
SP	Sub Programme
SRA	Strategic Research Agenda
TBC	Thermal Barrier Coating
TBF	Time Between Failure
TERA2020	Techno-economic Environmental and Risk Assessment for 2020
TET	Turbine Entry Temperature
TEOR	Thermal Enhanced Oil Recovery
TMF	Thermo mechanical fatigue
TOC	Top Of Climb
TO	Take-Off

TRL	Technology Readiness Level
TTR	Time To Repair
USTUTT	University of Stuttgart
VITAL	Environmentally Friendly Aero Engines
VIVACE	Value Improvement through a Virtual Aeronautical Collaborative
VGW	Variable Guide Vanes
WP	Work Packages

TERA ACRONYMS

In the list below the TERA abbreviations are included for the benefit of the future users. Note that “d” in the abbreviations stands for the fractional percentage variation of the parameters value from the nominal value. Few other abbreviations are defined in the local text.

<i>Abbreviation</i>	<i>Definition</i>	<i>Unit</i>
AcClimbDes	Climb time to 35000 [ft]	min
AcTODDes	FAR take-off distance	km
ddP4Q31	Combustor pressure loss	-
dFanBPPR	Fan tip pressure ratio	-
dFanBPeff	Fan tip polytropic efficiency	-
dFanBPETApol	Fan tip polytropic efficiency	-
dHPCETApol	HPC Polytropic efficiency	-
dHPCPR	HPC Pressure ratio	-
dHPTETApol	HPT Polytropic efficiency	-
dIDPC	Intercooler cold stream pressure loss	-
dIDPH	Intercooler hot stream pressure loss	-
dIEFFCR	Intercooler effectiveness at cruise	-
dIEFFTO	Intercooler effectiveness at take-off	-
dIEFFTOC	Intercooler effectiveness at top of climb	-
dIPCETApol	IPC Polytropic efficiency	-
dIPCPR	IPC Pressure ratio	-
dIPTETApol	IPT Polytropic efficiency	-
dLPTETApol	LPT Polytropic efficiency	-
dT4APP	TET for descent rating	-
dT4CR	TET for cruise rating	-
dT4TO	TET for take-off rating	-

dT4TOC	TET for climb rating	-
dW1	Fan inlet mass flow	-
dW132	Intercooler cold inlet mass flow	-
dW23	Core mass flow	-
dW41CQW26	HPT cooling mass flow	-
dW44CQW26	IPT cooling mass flow	-
TBO	Time Between Overhaul	hr
T30TOC	HPC delivery temperature at top of climb	K
T40TOC	Combustor outlet temperature at top of	K
T41mTOC	HPT blade metal temperature at top of climb	K
P25Q24TOC	IPC design pressure ratio at top of climb	-
P3Q26TOC	HPC design pressure ratio at top of climb	-

SYMBOLS

<i>Symbol</i>	<i>Definition</i>	<i>Unit</i>
Alt	Altitude	m
amb	Ambient	-
C	Fatigue ductility coefficient	-
CO ₂	Carbon Dioxide	-
E	Elastic module of the material	-
kE	Thousand Euros	€
N _f	Number of cycles to failure	-
NO _x	Nitrogen Oxides	-
pax	Number of passengers	pax
Rel.	Relative to the design point	-
W ₂	Fan mass flow	Kg/s

GREEK SYMBOLS

<i>Symbol</i>	<i>Definition</i>	<i>Unit</i>
η	Efficiency	-
σ	Stress	MPa
σ_f	Fatigue strength coefficient	-
ε	Strain	MPa
ε_t	Total strain	MPa
ε_f	Fatigue ductility coefficient	-
Δ	Difference	-

CHAPTER 1 INTRODUCTION AND SCOPE

This chapter provides a general introduction to the context of the present research project and defines the scope and specific objectives addressed in the research. The main contribution of the research is introduced along with the methodology to accomplish the objectives. Lastly, the outline of the thesis structure is highlighted.

1.1 Environmental Impact of Civil Aviation

The environmental impact of commercial aviation has been of concern since its foundation and is becoming more pressing as the demand for air transport grows. After the Second World War, the commercial aviation industry has experienced a very fast expansion due to the improvement in the global economy and advancement in air transport technology. This economic sector is also growing faster than the world Gross Domestic Product (GDP) and has consequently become a means of mass transportation [1].

Historically, air travel outpaced economic growth, represented by GDP. This is reflected by the increase of the air traffic which rose at an average annual rate of about 10% from 1945 to 1999 where the GDP increased 3.8% during the same period. Therefore, one can state that the worldwide economic growth is the main driver for increasing demand of commercial air transport [1].

The future forecasts of civil aviation growth by ICAO and industry estimates the global average annual rate of the passenger traffic demand growth of around 5% with passenger traffic projected to double over the next 15 years [2]. However, environmental problems associated with aviation will increasingly limit the expansion of air travel and the social benefit that it brings. Boeing's and Airbus' outlook for the future forecast of air traffic growth are depicted in Figure 1-1 and Figure 1-2 respectively.

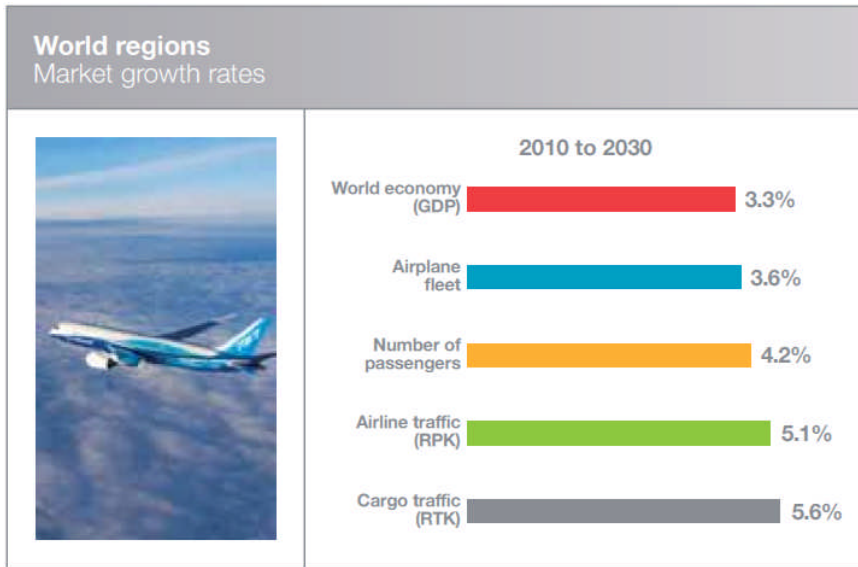


Figure 1-1 Boeing's forecast of air traffic [3]

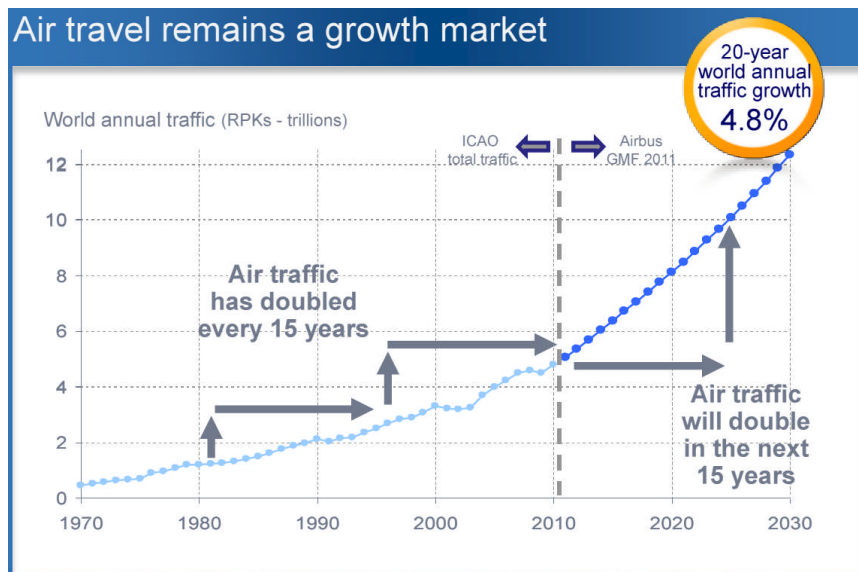


Figure 1-2 Airbus's forecast of air traffic [4]

Although the effect of aircraft emissions on air quality became a matter of public concern rather later than noise, work to develop more efficient combustion chambers had been in progress from the beginning of the jet engine age. The International Civil Aviation Organisation (ICAO) and its Committee on Aviation Environmental Protection (CAEP) introduced its first aircraft emissions

certification regulation in 1983. Since then, ICAO adopted more demanding standards in order to mitigate the negative environmental impact of aviation. [5]

As civil aviation continues to grow, main contributors to the climate change such as CO₂ and NO_x emissions increase and the emissions legislation is becoming ever more stringent. Both Europe and United States have set ambitious environmental targets for vision 2020 through numerous research and technology development programmes and collaborations to sustainable reduction in aircraft pollutants. According to Advisory Council for Aeronautic Research in Europe (ACARE) the environmental goals of vision 2020 and vision 2050 are set to reduce noise and emission produced by the ever increasing global air traffic. The solution for targeted improvements can be divided into significant changes to the aircraft, aircraft engine, and air traffic management systems.[6]

Also, the International Air Transport Association (IATA) has set ambitious targets to reduce CO₂ emissions produced by 50% by the ever increasing global air traffic (Figure 1-3). However, with the current technology level it is too optimistic to achieve this goal. Therefore, technology research and development is essential in order to create the potential for future aircraft/ engine systems.

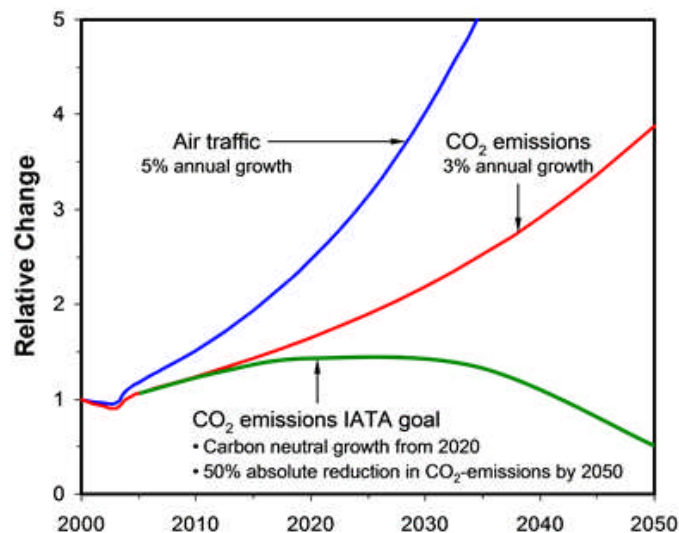


Figure 1-3 Air traffic and CO₂ emissions [7]

1.2 Objectives and Scopes

The current research contributes to knowledge by using a structured conceptual design tool to generate optimised preliminary conceptual engine designs based on specified design parameters, objective functions (defined target functions) and constraints. Thus, the overall objective of this work is to evaluate and optimise conceptual and novel aero- engine cycles, taking into account the multidisciplinary aspects such as engine/ aircraft performance, fuel burn, weight, and economics. Hence, the main objectives comprise the following:

- Contribution to the development and integration of a multi-disciplinary framework (i.e. TERA) which consists of integrated models such as aircraft/engine performance, power plant weight and cost, emissions, environmental impact, noise and economics in order to optimise conventional and conceptual aero engines.
- Development of a physics based oxidation model for HPT blades life prediction to make possible the assessment of potential performance and running cost benefits resulting from the adoption of new engine technologies and concepts.
- Assessment and optimisation of the conventional and conceptual aero engines with respect to the engine time between overhaul (TBO), taking into account the multidisciplinary aspects such as performance, block fuel burn, engine weight, production cost, maintenance and direct operating costs (DOC).

1.3 Contribution to Knowledge

There is limited information in the public domain with respect to MDO of aero engine cycles trade-offs between overall mission fuel burn and engine life. Therefore, investigating the engine design at the conceptual design stages in order to optimise engine life (thus reducing operating costs) and assess the consequent trade-off in fuel consumption provide a contribution to knowledge. Consequently, the main contributions of this work to knowledge involve the following:

- Multidisciplinary TERA assessment of a novel intercooled conceptual engine with a particular emphasis on design space exploration and optimisation studies to identify the designs that may offer the largest time between overhaul and the consequent implications this may have on mission fuel burn and direct operating costs (DOC).
- Development of a more comprehensive lifing model that calculates the engine life with reasonable level of accuracy by integrating physics based oxidation, creep and fatigue models.

1.4 Methodology

In order to successfully accomplish the objectives initially proposed in this research project, a set of computational tools currently available at Cranfield University has been used. However, new computational tools or modifications to the existing ones are implemented in order to perform the tasks proposed. One particular contribution is the high pressure turbine blade oxidation life prediction model, which estimates more accurately the used life from current and potential future aircraft gas turbine engines. This is a physics based oxidation model developed to estimate the TBC life of the high pressure turbine blades of the first stage and represents the oxidation effect on turbine blade failure. The first stage of the high pressure turbine is the part of the aero engine that bears the

highest stresses due to pressure, temperature and rotational speeds. Hence in this model the focus is on high pressure turbine blade, being the component that usually limits gas turbine life. This model, along with creep and fatigue models is used by the lifing module to better predict time between overhaul (TBO) of the aero engines. Then the value of TBO is taken as the baseline distribution to calculate the life of other important modules of the engine and used in the economic module calculations. Finally, engine/aircraft performance, plant weight and cost, emissions, environment and economic models are integrated into the TERA framework with a commercially available optimiser (iSIGHT) to perform optimisation, sensitivity analysis, trade off and parametric studies of two aero engine cycles, a conventional turbofan and a conceptual intercooled turbofan, for a range of mission profiles.

1.5 Thesis Outline

The content of the present research project is organised in six chapters. Chapter 1 provides an overview to the current research project and summarises the general context of the work; objectives and scopes, contribution to the knowledge, methodology, thesis outline and publications.

The literature survey and background, including; mitigation of aviation impact, multidisciplinary design optimisation, aero engine conceptual design frameworks, commercially available integration and optimisation tools, gas turbine failure mechanisms, European sixth frame work programme and new aero engine core concepts for year 2020 entry into service are presented in Chapter 2.

Chapter 3 describes the TERA2020 methodology and architecture in particular, the incorporated modules for modelling different aspect of aero engines. The underlying assumption and simplification of the TERA2020 is explained. The commercially available optimiser for integration, automation, and optimisation purpose is briefly discussed. Additionally, development to the lifing module (in

particular the development of an TBC oxidation model) of the HESTIA code is presented. The integration and automation aspect of TERA2020 is explained.

Chapter 4 describes the approaches adopted for life assessment and optimisation of conventional turbofan and conceptual intercooled turbofan aero engines using TERA2020 tool. For a better understanding and interpretation of the presented results, the TERA assumptions and simplification are presented. The sensitivity analysis and its application are explained. The parametric study and the applied techniques for identifying an appropriate design space are described. Exploring the design space and optimisation process is presented.

The discussion of results generated by the multi-disciplinary design tool for sensitivity analysis and optimisation of novel engines for maximum time between overhaul and possibly minimum fuel consumption and low direct operating cost is the focus of Chapter 5.

Finally, in Chapter 6 the research conclusions are discussed and possible topics for the future work included.

1.6 Publications

The outcomes of this research work are highlighted in the publications which are included in Appendix E.

CHAPTER 2 BACKGROUND

This chapter summarises the initial literature review performed at the early stage of the current research project. It presents an overview of the new technologies and procedures applied within the aviation industry to reduce the negative environmental impacts. However, at this point it should be clarified that the literature background requirements for each task is also included within the chapters of this thesis.

2.1 Mitigation of Aviation Impact

In the past 30 years, society awareness over the environmental impact associated with the aviation industry has increased and made the environmental consideration of the commercial aviation most challenging. Currently, the emphasis has shifted towards increasing safety and security, while reducing the environmental impact arising from the ever increasing demand for air travel.[8]

In Europe, the aeronautical research community has established the Advisory Council for Aeronautical Research in Europe (ACARE) and has set out a Strategic Research Agenda which gives high priority to, and sets ambitious goals for, reducing environmental impact. [2] According to ACARE there are multiple mitigation options in the transport sector, but their effect may be offset by growth in the sector. The following objectives are fixed by ACARE with respect to environmental concerns, as described in the Strategic Research Agenda (SRA) for target year 2020:

- A 50% reduction in CO₂ emissions per passenger-kilometre with the engine contribution corresponding to a reduction of 15 to 20 % in specific fuel consumption.
- A reduction in perceived noise (EPNdB) to one half of the current average level, considered as equivalent to a 10 dB reduction per aircraft

operation, taking into account that the engine is the major contributor to noise.

- An 80% reduction in NOx emissions, where the engine combustion is the only contributor.

Reduction of CO₂ emissions is strongly linked with the improvement of engine specific fuel consumption (SFC). Reducing specific fuel consumption can be broken down into improving propulsive efficiency and thermal efficiency. Thermal efficiency (η_{th}) is defined as the ratio of the output power given by the engine to the airflow, to the input energy amount given by the fuel combustion.

$$\eta_{th} = \frac{\text{Jet Kinetic Power}}{\text{Fuel Power}} = \frac{PW_{airflow}}{PW_{fuel}} \quad (2-1)$$

Propulsive efficiency (η_{pro}) in aero engines is a measure of the low pressure system effectiveness and defined as the ratio of the power given to the aircraft (thrust work) to the power given by the engine to the airflow [9], [10].

$$\eta_{pro} = \frac{\text{Thrust Power}}{\text{Jet Kinetic Power}} = \frac{PW_{aircraft}}{PW_{airflow}} \quad (2-2)$$

$$\eta_{overall} = \eta_{th} \times \eta_{prop} \quad (2-3)$$

European Union (EU) Projects VITAL and DREAM are focused on propulsive efficiency improvement of the aero engines, while the EU project NEWAC, focused on thermal efficiency core concepts.

Since currently available mitigation options will probably not be enough to prevent growth in air transport emissions, technology research and development is essential in order to create sustainable development for the future. Medium term mitigation potential for CO₂ emissions from the aviation sector can come from improved fuel efficiency, which can be achieved through a variety of means, including technology, operations, air traffic management and product life cycle [11]. Particular examples of these projects include the PARTNER (Partnership for AiR Transportation Noise and Emissions Reduction) project [12] , and the European Clean Sky JTI (Joint Technology Initiative) project [13].

The design of aircraft/engine to reduce fuel burn and hence CO₂ emission remains a key long-term objective. A large variety of promising concepts are being proposed to reduce CO₂ and other emissions, although the best option to pursue for investment is difficult to select.

On the other hand, airline companies need to continuously reduce their operating costs in order to increase, or at least maintain, their profitability. Therefore the main focus of commercial aircraft design has been on producing airplanes that meet performance goals at minimum operating costs and this introduces an additional design challenge as new aero-engine designs need to be conceived for reduced environmental impact as well as direct operating costs. Due to the gradual tightening of environmental requirements, the cost and complexity of meeting this environmental performance in the post design phase has increased significantly. It has been concluded that there is a need for integrating environmental considerations at an early stage of the aircraft/engine design process [14].

Clearly, decision making on optimal engine cycle selection needs to consider mission (pay load and range) fuel burn, direct operating costs, engine and airframe noise, and emissions and global warming impact (radiative forces) for investigations and quantifications of the trade-offs involved in meeting the associated specific environmental effects of aviation constraints. It implies the use of multidisciplinary design optimisation (MDO) processes in order to

evaluate and quantify aircraft/engines design trade-offs originated as a consequence of addressing conflicting objectives such as low environmental impact and low operating costs.

To conceive and assess gas turbine engines with minimum global warming impact and lowest cost of ownership in a variety of emission legislation scenarios and emissions taxation policies a tool based on a Techno-economic and Environmental Risk Assessment philosophy is required. Such a tool was conceived and is currently being developed by Cranfield University and its capabilities are explored in detail in CHAPTER 3.

2.2 Multidisciplinary Design Optimisation

A preliminary aero engine design and development cycle is a complex, multidisciplinary, sequential and iterative process. Designing of this highly integrated mechanical system puts many engineering disciplines into conflict such as thermodynamics, aerodynamics, rotor dynamics, mechanical integrity, structures, manufacturability, pollutants, mechanical stress, material properties, as well as life cycle disciplines of direct operating costs, reliability, maintainability and more [15]. At the same time, short design cycle, long life, reduction of the risk involved with the project, low production and maintenance costs are demanded by the highly competitive aircraft engine market.

The current tightening legislation as a result of the environmental impacts of aviation industry adds more complexity to the engine design options. This increasing complexity of aero engine design has encouraged the gas turbine engine designers and manufacturers towards developing and implementing multidisciplinary design optimisation approach from the earliest design stages, where the great influence on the final product is recognised thereby preventing the need for expensive changes during full-scale development.

The success or failure of an aero engine business depends on a careful selection of a conceptual engine. In other words identification of an appropriate

concept in the early design phases is a crucial exercise. “*The best engineering effort cannot totally right a poor concept selection*”. [16] Although, during the preliminary design phase there is little product knowledge, there is a powerful impact on the final design. Therefore, any decisions made at the preliminary stages are crucial, as they freeze the overall configuration of the alternative product and stimulate huge efforts and investment towards developing that novel concept.

Sobieszczanski-Sobieski and Haftka define Multidisciplinary optimisation (MDO) as methodology for the design of systems in which strong interaction between disciplines motivates designers to simultaneously manipulate variables in several disciplines.[17]

The initial developments of MDO methodology occurred in 1970s and still have been continuing. It has found extensive application in the industry, particularly in aerospace. The potential advantages of using such an automated design methodology over the traditional, human-based, approach are as follows:

- Easy access to all the in-house knowledge
- Fast investigation of the design space
- Reduced human errors

The aim therefore of any preliminary design tool set or process is to eliminate as much uncertainty as possible, to increase product knowledge and enable design trades and options to be understood. In order to reliably understand the effects of design decisions at conceptual stage, it is necessary to have a reliable design tool, one that is also able to produce solutions quickly and enable the whole of the design space to be explored. [18]

Mathematical Modelling, Design-Oriented Analysis, Approximation Concepts, Optimization Procedures, System Sensitivity, and Human Interface are the main components for the MDO tools as stated by Sobieszczanski-Sobieski. [19] Although the current computer technologies have increased the design capabilities, gas turbine engineers remain the key component of the system.

They will always be needed to monitor the design process and verify the solutions manifested by the computer codes.

Whellens [20] indicates that the MDO can be classified based on the following criterion: the number of disciplines considered, the fidelity of the models of the various disciplines, the number of available optimisation strategies and to the level of generalisation of the tool. Computational costs and organisational difficulties are the main challenges involved with the development of MDO systems along with the advantages such as reducing product development time and ownership cost. Figure 2-1 shows the entire design space exploration of conceptual aircraft by utilising MDO technique.

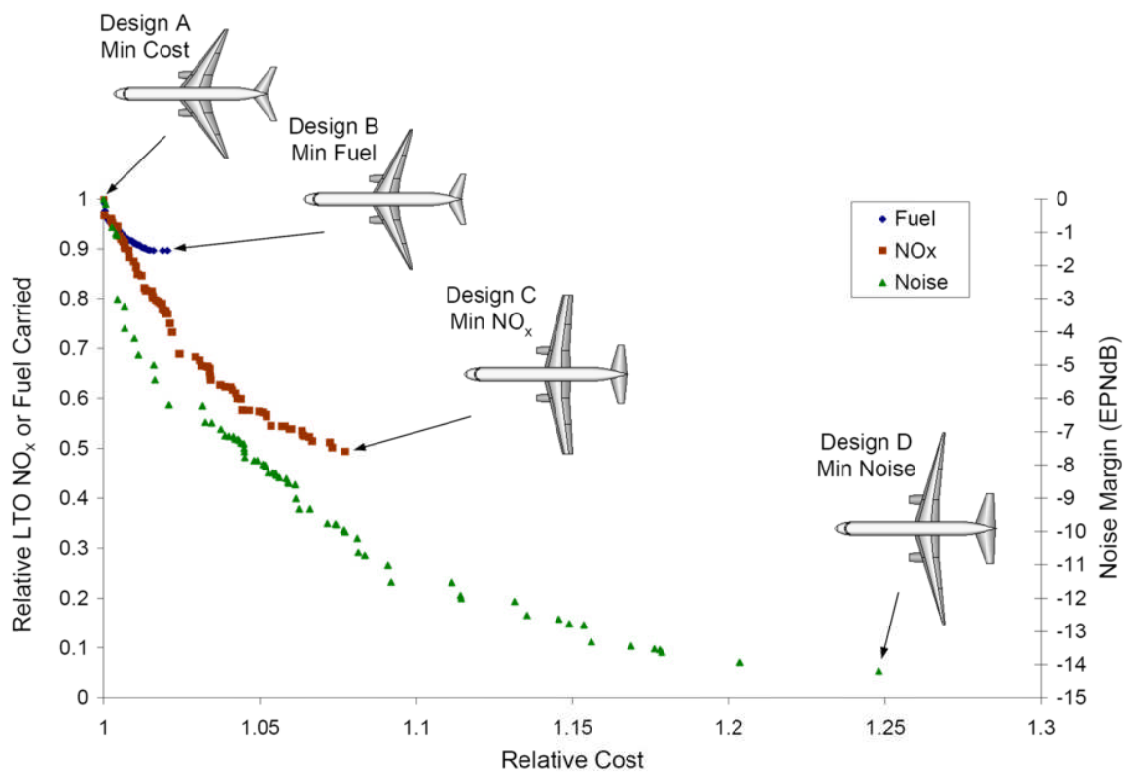


Figure 2-1 Design space exploration [21]

2.3 Aero Engine Conceptual Design Frameworks

Since the gas turbine engine evolved so rapidly, automated design process finds numerous applications particularly in the aviation industry. Different organisations based on their own requirements are developing comprehensive preliminary design tools that allow for constant assessment of the environmental effects of aviation system. The fast moving and competitive nature of the gas turbine industry means that design and development, equipment selection, as well as operation and maintenance need careful consideration. Within the increasingly strict demands of the industry the main concern, for plant operators and engine manufacturers alike, is to find a viable solution for a given application with minimum expenditure. At the same time stringent legislation on carbon emissions, noise pollution and industry specific regulations means the analysis for new technologies needs to be broad in its outlook. Vivaly, one must consider not only the performance assessment but also the emissions and environmental impact, concerns of noise regulations, technology failure and risk, maintenance scheduling and of course total plant life costs. The problem is multidisciplinary and has led many within the industry to adopt techno-economic tools. In this section a review of the most common frameworks is given.

2.3.1 EDS

EDS (Environmental Design Space) is being developed collaboratively by The Georgia Institute of Technology and the Massachusetts Institute of Technology as part the PARTNER Centre of Excellence. PARTNER — the Partnership for AiR Transportation Noise and Emissions Reduction — is a leading aviation cooperative research organisation, and an FAA/NASA/Transport Canada-sponsored Centre of Excellence. The main goals of this large activity are to better understand the relationship between noise and different types of emissions, and to provide the cost benefit analysis capability necessary for data-driven decision making. [22][23] The main elements of this framework

comprise: Environmental Design Space (EDS) to estimate source noise, exhaust emissions, performance and economic parameters for existing and future aircraft designs under different technological, operational, policy, and market scenarios, Aviation Environmental Design Tool (AEDT) to provide an integrated capability of assessing interrelationships between noise and emissions and amongst emissions at both local and global levels, and Aviation Environment Portfolio Management Tool (APMT) to provide the common, transparent benefit-cost methodology needed to optimize aviation policy in harmony with environmental policy. [24][25][26]

2.3.2 NPSS

NPSS (Numerical Propulsion System Simulation) is an advanced engineering environment developed by NASA Glenn Research Centre, the aerospace industry, government agencies and academia for the analysis and design of advanced aerospace propulsion systems. This multidisciplinary simulation system known as “Virtual wind tunnel” raise the design confidence and provides crucial information about propulsion system that should be determined in the early stage of the design project. The key elements of NPSS are: the engineering models, simulation environment and high performance computing environment. Using a modular and object-oriented approach for the structural development of NPSS provides a common interface which allows the simulation framework accessible for a variety of users. It is expected that this simulation environment could reduce the time and cost of the design and development about 30 to 40 percent.[28] [29]

2.3.3 PMDO

PMDO (Preliminary Multi-Disciplinary Design Optimisation) is an automated integration and optimization system tool developed at Pratt & Whitney Canada for use in the Advance Engineering team for concept design studies. The

engineering disciplines considered in this tool include aerodynamic flow path, air-system, dynamics, weight, cost, noise, emissions. The commercial software package, Isight, has been applied for the integration of disciplines, modelling code and optimisation tasks. The expected gains of using PMDO consists of automated data transfer between analytical tools, improved turnaround time, reduced design costs, and improved designs. [30]

2.3.4 TERA

TERA (Techno-economic Environmental and Risk Assessment) is an approach pioneered at Cranfield University, UK. It can be used to evaluate the power systems for use on land, at sea and in the air. For different applications its architecture and encompassed disciplines vary. It is a tool which can analyse various disciplines within a given framework. It is also a tool for complete engine management and strategic decision making system [31]. Therefore, the concept of TERA can be interpreted as a formal methodology that facilitates exploration and exploitation of interdisciplinary interactions to achieve a better overall system. TERA is a comprehensive suite of software tools which are applicable for academia, industry, government agencies, and regulatory bodies for setting technology assumptions and forecasting scenarios.

It is a quick and reliable assessment approach with the capability of adaptation to a variety of mechanical systems and evaluating their environmental and economic characteristics at an early stage of the design process. The essential function of TERA is to rapidly explore the design space and identify solutions and minimising computational time and costs. Furthermore, it can be used as an optimisation tool, given an objective function, such as noise minimisation, better fuel consumption or reducing total plant life cost. The TERA framework can be described as: "*An adaptable decision making support system for preliminary analysis of complex mechanical systems*".

The earliest developments of this tool occurred in the 1990s and have been progressing ever since revealing great potential to improve product quality and significantly reduce development time, thus, helping the product to remain competitive in a global market.

Techno-economic assessments of industrial gas turbines were carried out by Gayraud [32] at Cranfield University, focusing on gas turbine selection decision support systems for combined cycles. Whellens and Singh [33] exemplify simplification of the design procedure by implementing TERA, thereby making the decision making process faster, easier and cheaper. TERA has been successfully applied in the aviation and power generation fields [34][35] and has also been extended to marine applications [36][37]. Some of the latest projects focus on the Oil and Gas industry, especially in Enhanced Oil Recovery (EOR) and Liquefaction of Natural Gas (LNG) [38].

Work on complex energy and power systems were carried out within a variety of contexts and for different customers. This included work on aero-derivative power generation plant [39], use of coal synthetic gas [40][41], work on degradation and diagnostics [42], nuclear gas turbines [43] and other topics. Much work carried out for industrial customers has not been published. This list includes research on novel bottoming cycles, advanced hydrogen fuel cycles for power generation, further nuclear gas turbine work, fog injection, turbomachinery for renewable energy sources, a novel piston engine system and others.

This interest is coupled with work and experience on environmental issues and economic performance, given that these are key selection criteria. It was then natural, over the years, to develop modelling techniques that encompassed combined thermodynamic, economic and environmental algorithms. These gave rise to a very interesting method, the TERA. A schematic of the TERA philosophy is shown in Figure 2-2.

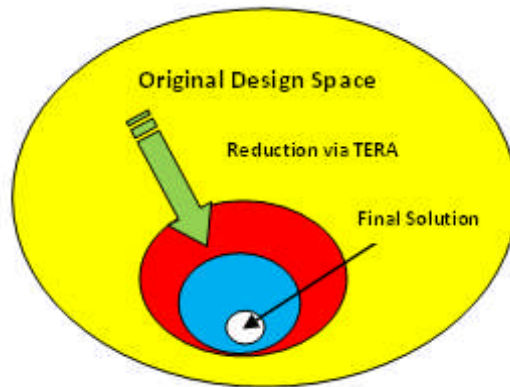


Figure 2-2 *TERA Philosophy*

2.3.4.1 TERA for Aviation

The TERA approach was originally conceived in order to assess engines with minimum global warming impact and lowest cost of ownership in a variety of emission legislation scenarios, emission taxation policies, fiscal and air traffic management environments [31]. This method evaluates the engine at an early stage of the aircraft design process due to the cost and complexity of meeting environmental performance in the aircraft post design process.

TERA-oriented developments on aircraft and weight models were initiated in an attempt to study the effect of bypass ratio on commercial aero engines designed for long-range subsonic aircraft. The general objectives of TERA approach for aviation application are as a quick assessment tool to rapidly explore the design space for more economical and greener engine concepts and to provide a starting point for in depth studies using OEM proprietary detailed design software suites. Also, assessments of the benefits of different technologies for different economic and environmental conditions are considered. Optimisation of a group of engine technologies by relatively simple algorithms for different economic and environmental scenarios can be conducted. Finally, TERA aims to progressively incorporate novel technologies.

The core of this tool is a detailed thermodynamic model of the power plant which provides data required by other modules. This core module is integrated

with some additional modules to represent a multidisciplinary tool. These preliminary design modules are integrated with a commercial optimiser and provide a means for cycle studies. It is expected that new legislative and fiscal constraints on air travel will demand an extension to the customary range of asset management parameters. In such a business environment there is potential for TERA to develop into a useful tool for aircraft and engine asset management. This tool can then be applied to the optimisation of one or more objective functions, such as mission fuel burn, engine noise, engine gaseous emission i.e. NO_x, global warming potential (GWP) and engine direct operating cost (DOC). The present modular structure of the aviation TERA based tool consists of the disciplines as shown in Figure 2-3, along with a commercial optimiser.

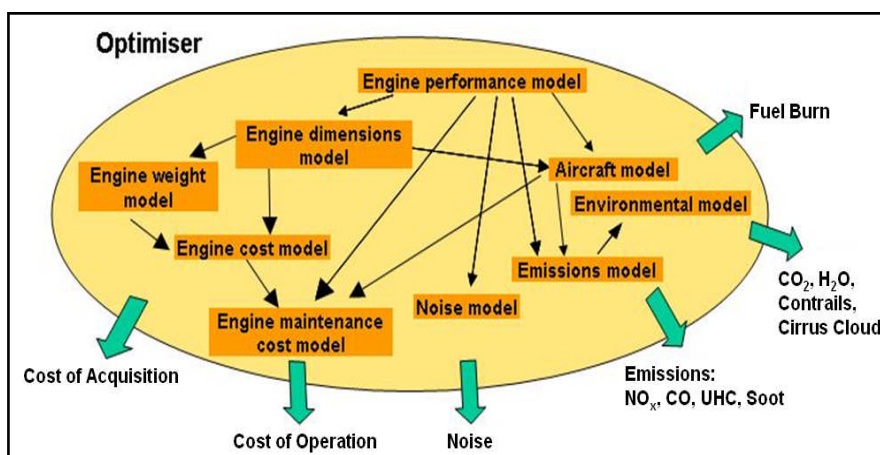


Figure 2-3 TERA Structure for Aviation [36]

All these modules are individual and can be utilised as standalone executable. The multi-modular platform was chosen for extra flexibility and exchangeability of the modules. However, the multi-modular structure of this tool leads to more integration challenges. By using the civil framework and developing the necessary components, future applications that TERA could support include chemical processing, and submarine propulsion.

2.3.4.2 TERA for Oil and Gas

TERA has been successfully used for land based applications. Whilst projects were previously conducted in electrical power generation for major companies in the UK, this has now been extended to the Oil and Gas field where new modules have been created to capture the diverse nature of the field. The following section highlights some of these.

TERA for the production of liquefied natural gas (LNG) is sponsored by a major oil and gas company [38]. Gas turbines are being used as mechanical drivers for the liquefaction process to liquefy natural gas to -160°C for more economical transfer by shipment over longer distances compared to traditional pipeline transfer that requires many expensive pumping stations. As well as performance modelling, emissions predictions and economics, the LNG TERA has some unique additional features. It looks at technical risk and failure of turbomachinery in a quantitative way. The system architecture is depicted in Figure 2-4.

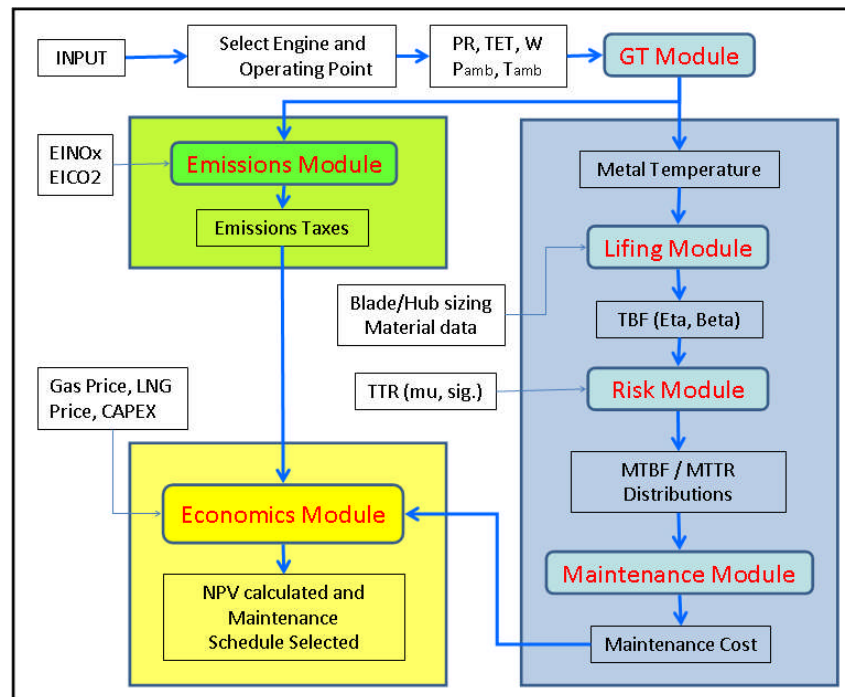


Figure 2-4 TERA Structure for LNG Application [38]

As can be seen, the GT Module is core to the emissions, risk and economics modules. The risk is depicted in the left hand shaded box and incorporates sub-modules of lifing, central risk, and maintenance. The aim is to life the major components in the hot gas path and creates failure distributions using the central risk module. This involves Monte Carlo simulations and also uses statistical techniques such as the Weibull distribution to model failure. The risk then feeds the maintenance module which better informs the operator how engine performance and operation is affecting the economics of maintenance and total plant life cycle costs.

A TERA for Thermal Enhanced Oil Recovery (TEOR) project is being developed [44]. Thermal recovery is one of the most effective and widely used heavy oil production techniques. It involves the injection of large quantity of steam into the oilfield in order to reduce oil's viscosity and improve its permeability. A significant quantity of energy is required to produce steam and therefore project's profitability is very sensitive to steam production costs. Furthermore, steam generation activities have severe environmental problems associated with the production of Greenhouse Gases, GHG. With stricter environmental regulations and possible future emission tax, heavy oil producers have found themselves in mounting economic and environmental pressures.

Gas turbine based cogeneration system is seen as one of the solutions to reduce both steam generation costs and GHG emission from such oil recovery processes. The use of cogeneration, although not new, has not been studied and reported in details in the past. Especially, there is the lack of appreciation of the interaction between cogeneration system selection and operation and oil field steam requirements. The problem is multi-dimensional in nature, where both surface and subsurface operation are assessed simultaneously, and hence multi-disciplinary assessment framework and tool is required.

The TERA concept is being utilised to fill in the gap between surface and subsurface design and operation. The proposed architecture is illustrated in Figure 2-5. Initially, the required quantity of steam required for field injection is determined using the Oil Recovery Model. Then the quantity, quality and

pressure of steam are fed into the cogeneration performance model. Output from the cogeneration model such fuel consumption and parameters required to emission calculation are fed into the emission and economic models accordingly.

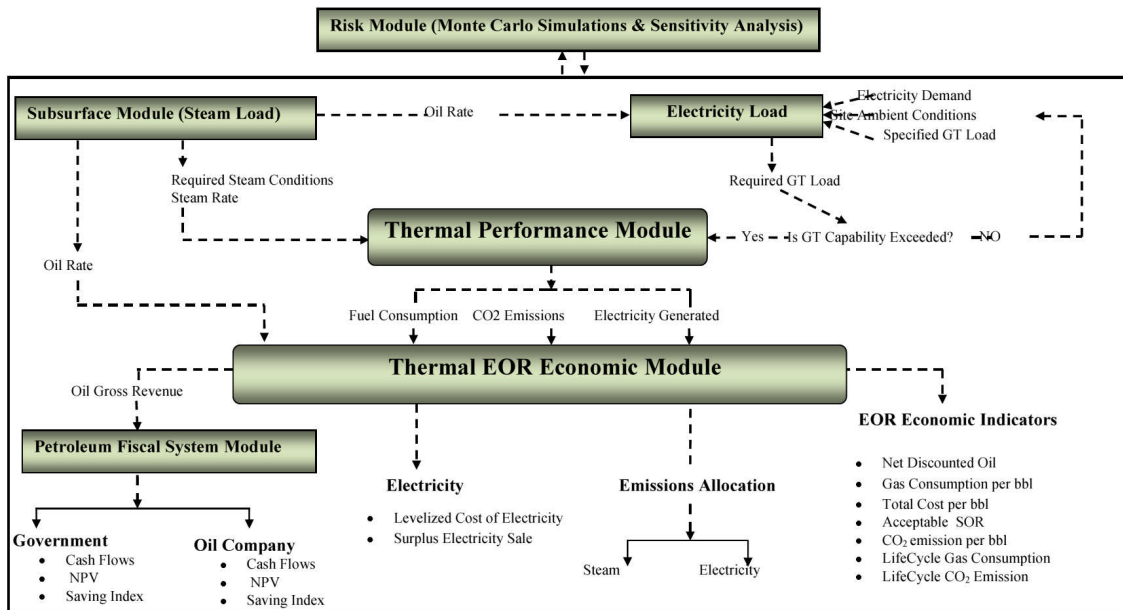


Figure 2-5 TERA Structure for Heavy Oil Recovery Applications [44]

2.3.4.3 TERA for Marine Application

The case study described below is related to a Marine TERA Framework application and is based on the ship analysis described in [36] [37]. An input of the time domain of the mission is required. This can be a description of the flight details (mission profile) of an aircraft, the journey of a ship, the daily duty of a power station and others. In the case of the marine application, a comparison of a journey in three different scenarios was examined; S1, Calm sea and “clean” ship, S2, Stormy sea and “clean” ship and finally S3, Stormy sea and fouled hull. The engine rating was based on the hot section temperature. The outcomes of the three scenarios are illustrated in Figure 2-6 and Figure 2-7.

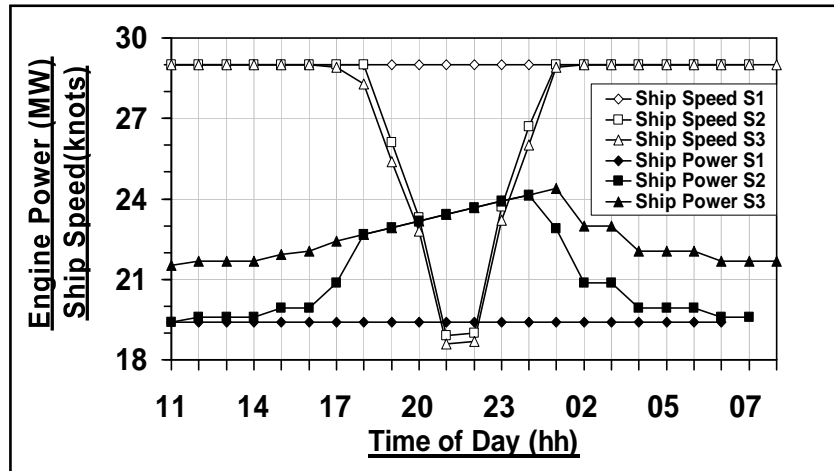


Figure 2-6 GT Power and Ship Speed Characteristic [36]

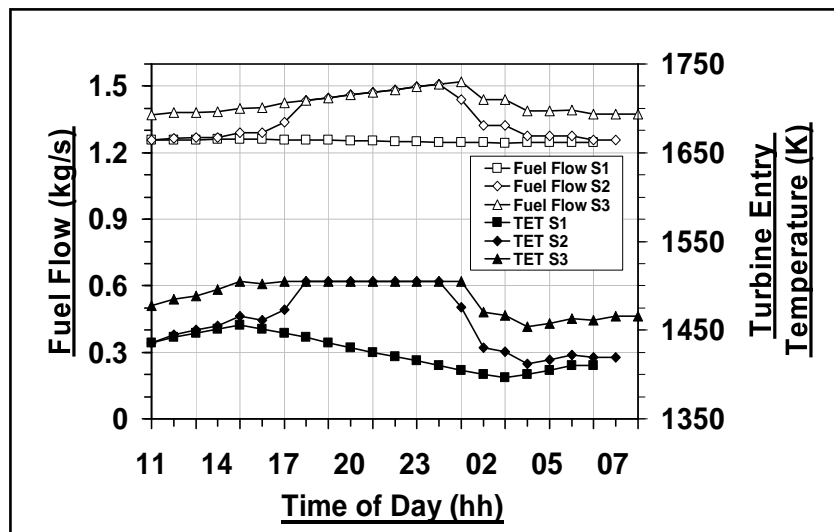


Figure 2-7 GT Fuel Flow and TET Characteristic [36]

Figure 5 shows, for S1 (the calm sea with “clean” hull scenario) a departure in the middle of the morning and a journey, where the ship travels at a constant speed and the power required from the power plant is always the same. For this scenario, Figure 6 shows the change of turbine entry temperature needed to offset the effect of changing ambient temperature during the journey. The fuel flow is also shown. There are some small variations in fuel flow, not

discernible in the graph, due to the small changes in thermal efficiency arising from the change of power setting of the engine.

Scenario S2 shows the effect of a storm that takes place during the journey. The ship leaves harbour and nearly immediately a storm starts. This hampers the progress of the ship. To keep the service speed, the engine needs to deliver increasingly higher levels of power. At 1800 hours, the maximum power of the engines is needed. From 1800 to 2400 hours the engine is run at maximum power. This maximum power increases because as ambient temperature falls, an engine rated on temperature delivers higher power. However this maximum power is not enough to allow a constant ship speed to be maintained. The ship speed thus falls to slightly below 19 knots. As the storm abates, the ship speed starts to rise gradually to the service speed of 29 knots. When this is reached, the engine power is gradually reduced given the lessening resistance from the rough sea. When the ship arrives in port after a slightly longer journey, the sea is calm again. In scenario S3, the hull of the ship is fouled, therefore at any speed it presents a higher resistance to the motion of the ship. The ship makes the journey through the same storm of scenario S2. It can be seen that at any point, higher engine power is needed to propel the ship through at sea. When the maximum engine power is reached, the effect of hull fouling manifests itself as a lower speed than that of S2. For each of the three scenarios, the fuel consumed and the journey time is summarised in Table 2-1.

Table 2-1 *Fuel Consumed and Journey Times [36]*

Scenario	Fuel	Journey
S1	93.3 tonnes	20h 41min
S2	106.7 tonnes	21h 56min
S3	113.3 tonnes	22h 04min

2.4 Commercial Optimisation Frameworks

With the increasing interest and application of MDO methodology, a verity of integration and optimisation frameworks have been developed for design space exploration. The detailed description of these frameworks is well beyond the scope of this research work and only a few are frequently used frameworks are listed as follows:

- Isight by Engineous software Inc. [45]
- Boss Quattro by Samtech s.a. [46]
- Model Center by Phoenix Integration Inc. [47]
- modeFRONTIER by Engine Soft [48]
- DAKOTA by Sandia National Laboratories [49]
- MDICE by CFD Research Corporation [50]

2.5 Gas Turbine Lifting Concepts

Aero engines hot section components, namely first stage HPT disk and blades, are subject to difficult operating conditions; elevated and varying temperature transients, hostile gas pressure coming from the combustion chamber and severe centrifugal forces. These critical components can significantly influence the overall engine life cycle costs. A reliable prediction of the turbine disk and blades life at the preliminary design stage is therefore necessary to ensure both the safety and economics of gas turbine operation.

The blade life is of course affected by many matters. Creep, fatigue, corrosion and oxidation are the prime modes of failure for the high pressure turbine blades and disc. Creep and fatigue life are highly dependent on the stresses and working temperatures of the material which the component is made from. These temperatures and stresses can be calculated during the preliminary design process as well as the geometry, material properties and operating conditions through the performance analysis and turbine aerodynamic &

mechanical design. The results may be imprecise for practical use, but will be helpful to identify potential design problem. So the life prediction can be made and the system designer can investigate the design more thoroughly and accurately at an earlier stage of the design [51].

The life methodologies may be classed into two distinct approaches to determine turbine hot section component service life for a specific plant. These approaches are probabilistic (un-deterministic) methods and physics based methods. Probabilistic methods are based on mathematical models to describe the physical processes of the phenomenon. Their mathematical models are either stochastic themselves or take in stochastic inputs. This allows proper accounting for possible material, manufacturing induced defects, uncertainties associated with the collected data either from test results or in-service monitoring, variations in operating conditions due to changing mission profile or any other type of data variations that could affect the life of a component of interest. The key is to get the required probability distributions for each applicable variable right. Hence, these methods normally require a large amount of basic data on each variable to be modelled probabilistically, or proper expert opinion on the distribution of these variables [52].

Conventional approach implies the use of non-stochastic mathematical models with known or assumed inputs to estimate the useful life of a given part for a given application. The known or assumed inputs are normally based on maximum requirements, experience or laboratory testing. This approach combines engine operating history with the mechanical and metallurgical aspects of individual turbine components for remaining serviceable life assessment. By identifying life limiting factors and predicting the rate at which damage occurs, optimum repair, replacement and overhaul intervals can be established. To validate the computer model, periodic metallurgical analysis of components from certain key engines needs to be performed to monitor deterioration rates and identify any unforeseen failure mechanisms [53].

In the current research work, a physics based life model is used. The focus is on the high pressure turbine, and the analyses are based on creep, low cycle

fatigue and oxidation failure mechanisms. The result in term of hours between engine overhaul allow the user to predict with a certain accuracy the influence of the maintenance cost on the total cost of an airplane in service, over a certain amount of time with the aim prolonging asset life and optimizing long term operational costs.

2.5.1 Fatigue failure mechanism

A survey of 3824 aircraft incidents during the period from 1963 to 1978 conducted by the USAFML showed that 1664 incidents (43% of all incidents) were due to engine structural failure. Almost 28% of the engine structural failures were caused by Low Cycle Fatigue and about 8% were due to High Cycle Fatigue. [54]

Fatigue loading of turbine components associated with continuous aircraft take-off, cruise and landing cycles is a principal source of degradation in turbo machines. These machines are subject to non-steady loads, which produce fluctuations in the stresses and strains in their components. If the fluctuating stress is large enough, failure may occur after several applications of the load, even though the maximum stress applied is lower than the static strength of the material. If the nature of a stress is thermal, then the process of failure due to fatigue is known as Thermal fatigue (TMF). Thermal fatigue is usually characterized by a LCF failure because of the high peaks of temperature the component (i.e. the turbine) is usually subjected to. Obviously, the components most susceptible to thermal fatigue are the one into direct contact with the high temperatures gases, namely turbine blades, nozzle guide vanes and the turbine discs.[55]

The process of fatigue is usually divided into the following three phases:

- Primary stage: crack initiation. It usually takes place at the surface of a component, where the stress is more concentrated.

- Secondary stage: crack propagation. This phase is very important, since most of the components start working with micro-cracks already existing in them. There are two different stages of propagation: during the first, the crack continues propagating along a plane of high shear stress, whereas during the second stage growth occurs along a plane normal to the maximum stress.
- Final or tertiary stage: failure by fracture. Usually a fast running brittle fracture causes a sudden failure of the component.

Low cycle fatigue is a fatigue failure of components at relatively low number of cycles (normally 10^3 - 10^5 Cycles) of load applications at very high stress levels. If a material is subjected to very high cyclic stresses or strains, there will be significantly greater accumulation of energy in the form of plastic deformation per cycle. When sufficient plastic energy accumulates, a crack will form. The basic method of presenting fatigue data is by means of the S-N curve which is shown in Figure 2-8. [55]

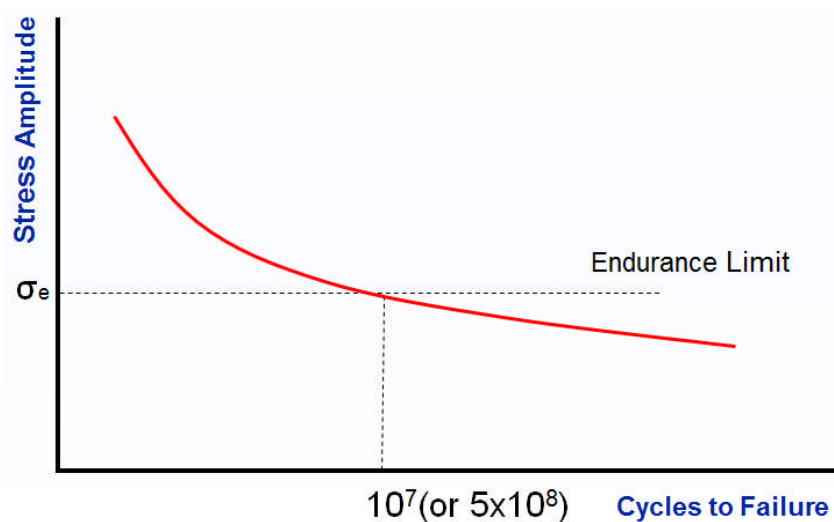


Figure 2-8 The S-N curve [56]

As damage is usually associated with plastic deformation, LCF is often known as 'high-strain fatigue'. At high stresses, low cycles, the materials deform

plastically in a highly localized way, the fatigue life is reduced, but the gross plastic deformation makes it difficult to interpret in terms of stress. Therefore, at the 'Low-cycle fatigue' region, it is more reasonable to study cyclic strain response of materials instead of cyclic stress.

When components are subjected to large loads, plastic deformation may take place and the load will be redistributed. If no plastic deformation occurs in the material, the load will simply produce elastic deformation up and down along the elastic line. If the plastic strain is large enough, some plastic deformation will be evident (Figure 2-9). On the other hand, if the plastic strain (ϵ_p) is large enough, some plastic deformation in the second part of the cycle will take place. The subsequent cycles, and the effects they will have on the component, will depend on the material and the load condition.

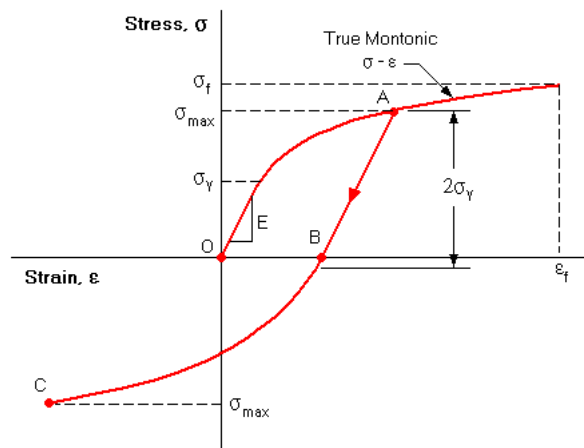


Figure 2-9 Stress-strain behaviour after a reversal [57]

When the loading process is reversed and the specimen is unloaded after yielding, the stress-strain relationship will follow line A-B with a slope equivalent to the elastic modulus E. When the specimen is subjected to a compressive load ($-\sigma_{max}$) the material will yield at a stress level that is less than the initial yield stress (σ_Y) this phenomenon is called the Bauschinger effect.[55] [57]

If reloading in tension then a hysteresis loop will develop as shown in Figure 2-10. This hysteresis loop defines a single fatigue cycle in the strain-life method. The dimensions of the loop are described by the total strain range $\Delta\varepsilon$ as the width, and the stress range $\Delta\sigma$ as its height. The total strain range $\Delta\varepsilon$ equals to the summation of an elastic strain component $\Delta\varepsilon_e = \Delta\sigma/E$ and the plastic strain component $\Delta\varepsilon_p$.

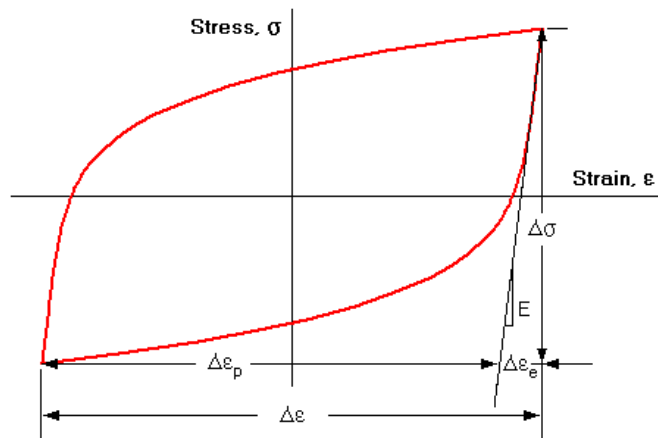


Figure 2-10 Typical cyclic Stress-Strain curve [57]

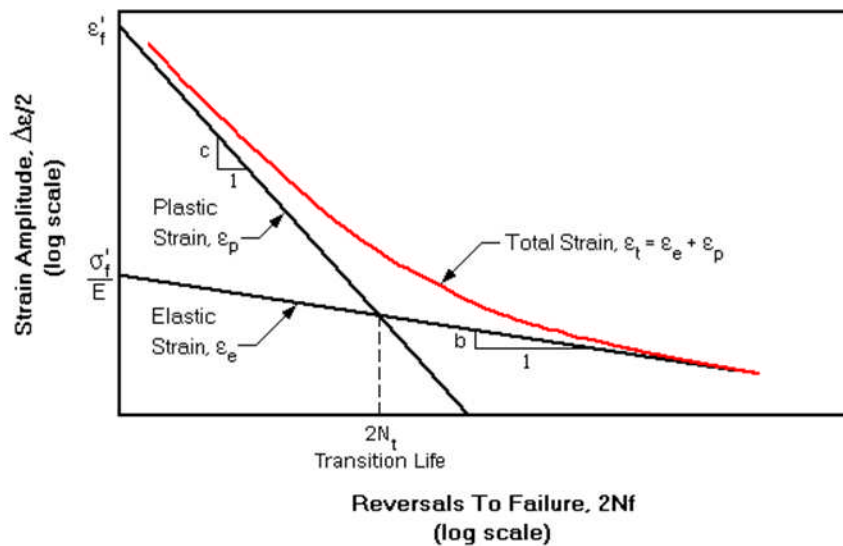


Figure 2-11 Typical Strain-Life curve [57]

The stress-strain response of a material can change as plastic deformation is not completely reversible which lead to modifications to the material structure. The material may undergo cyclic hardening if the maximum stress increases with each successive cycle, or softening if the maximum stress decreases, otherwise remain cyclically stable if the maximum stress level does not change. Generally this change in stress-strain response of a material behaviour tends to stabilize after a relatively small number of cycles - typically about 100 cycles. The influence of the elastic and plastic components on the strain-life curve is shown in Figure 2-11.

Usually, LCF test results are plotted as cycles to failure N_f against the total strain range ($\Delta\varepsilon_T$) sum of the plastic and the elastic component, as mentioned before. Manson suggested that both the strain components (plastic and elastic) produce straight lines when plotted logarithmically against N_f (number of cycles to failure). From this he evolved his so-called the 'universal slope method', based upon the Manson–Coffin relationship that Manson himself found to be sufficiently accurate for initial design. The Strain-Life curve can be written by summing the elastic and plastic components as follows:

$$\varepsilon_t = \frac{\Delta\varepsilon}{2} = \frac{\sigma_f}{E} (2N_f)^b + \varepsilon_f (2N_f)^c \quad (2-4)$$

Where:

ε_t = total strain

E = elastic module of the material

σ_f = fatigue strength coefficient

ε_f = fatigue ductility coefficient

N_f = number of cycles to failure

C = fatigue ductility exponent

2.5.2 Creep failure mechanism

Creep can be defined as a time dependent progressive deformation of a material caused by the operating stresses and temperatures. Being a function of stress, temperature, time and strain, creep is a complex quantity to define. Usually, if the metal temperature is above 0.3 to 0.4 melting temperature of the metal then the creep will occur. The higher the temperature is, the shorter the creep life will be. It is based on the mobility of dislocations and discontinuities in the material, caused by the operating stresses and temperatures.[58] This phenomenon is generally accepted to be a four-stage process:

- Instant elastic stage: namely a pure elastic deformation
- Primary creep: predominant stage at low stress levels and low temperature
- Secondary creep: the creep rate is constant, therefore the curve is linear and the creep rate is minimum
- Tertiary creep: strain-rate increases rapidly until fracture (rupture) occurs

The general creep process is shown in Figure 2-12.

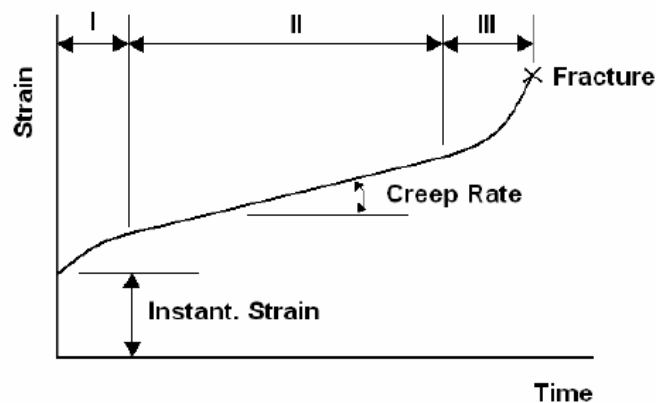


Figure 2-12 *The general creep curve [55]*

The creep rate is dependent on the material properties, working time, working temperature and the applied structural load. The process of creep is so complex that up to now predicting creep strain or rupture from a theoretical model is not possible. In preliminary designs the common method is to compare the calculated maximum stress with a creep value from experience. This creep value is the stress (at the maximum temperature) to produce 0.1% strain in 100 hours for aero gas turbines and the stress to produce 0.1% strain in 10,000 hours for industrial gas turbines.[55]

Creep testing is a time consuming task. It will take a long time to generate the design data thus making the creep test expensive. Therefore the normal way to deal with this problem is to extrapolate the short term creep tests to longer times than have been tested. When doing this, an assumption is made that the same rate will apply throughout the components' life and no structural changes occur in the region of extrapolation.

Relationships known as time-temperature parameters have been used to extrapolate from short to longer times. This is based on the assumption that an increase in operating temperature will reduce the time to reach a particular creep state so that we can 'buy' time with temperature and vice versa('trade off' between time and temperature). This assumption can only be true if the same reaction controls the process over the whole temperature range investigated.

The most popular of the time-temperature parameters is the Larson-Miller parameter.

$$P = \frac{T}{1000} (\log t_r + C) \quad (2-5)$$

Where:

T = Absolute operating temperature [K]

t_r = time to rupture in hours

C = constant, between 15 and 30

Note: for most of the industrial applications it is assumed that C equal to 20.

Considering a simple flight envelope, it could be possible to divide it up into several sections (i.e. take-off, climb, cruise, descent, and landing); obviously each flight segment will be characterized by different operating conditions, which are different stresses and temperatures. The difficulty lies in adding together the effects of each segment. One way of solving this problem, is to adopt the so-called Miner's Law, an inverse sum law which states that the sum of life fractions should be unity:

$$\sum_i (\text{Life fraction}) = 1 \quad (2-6)$$

Through the use of the Larson-Miller parameter, it is possible to determine the life to failure for each operating condition; hence, by dividing the real time spent at these conditions by the total life to failure, the life fraction is determined. Logically, the sum of these life fractions should be unity.

2.5.3 Oxidation failure mechanism

Oxidation is a chemical reaction resulting in the formation of an oxide due to the reaction of a metal and oxygen. The oxidation of metals consists of two main factors: thermodynamics and kinetics. Metallic elements absorb oxygen and react with oxygen to form oxides if it is energetically feasible. Thermodynamics show whether or not a reaction can take place. When the oxidation reaction is possible, kinetics tell how fast the reaction happens to form an oxide scale on the metal surface. The oxidation rate is defined by the change in the oxide thickness or weight. [59] The formation of an oxide can be described by the following reaction:



Oxidation is often the most important high temperature corrosion reaction and is described via different oxide growth laws where the parabolic growth law is the commonly used approach. [60] As the resulting oxide is solid it can grow to form a scale on the metal surface. This scale also may protect the underlying metal.

As a consequence of increasing operating temperature in gas turbine engines, oxidation has become a critical life limiting phenomenon. Therefore, thermal barrier coatings (TBC) were introduced for thermal protection of high temperature components such as combustor, turbine vanes and HPT blades. TBC reduce substrate metal temperatures by being an isolating layer between the hot gas on the outside of a component and the base metal.

The thermal barrier maintains the metal temperature of a coated component at moderate temperature levels during turbine operation. If the coating spalls off, the underlying metal will suffer from creep damage and oxidation with risk of severe machine damage. Therefore coating integrity must be maintained, putting forward demands on a reliable assessment of coating life. This is especially crucial if a design with long inspection intervals is required. A typical TBC structure is shown in Figure 2-13.

Basically, the TBC failure is due to a combination of oxidation damage and crack damage from thermal cycling. The oxidation failure process involves both the formation and spallation of oxides. [61] A thermally grown oxide layer (TGO) forms at the interface between the bond coat and the ceramic coating. Spallation of the ceramic coating occurs when the TGO reaches a critical thickness where the internal stresses exceed the TGO properties and delamination of the ceramic occurs. Cracks propagate through the ceramic and TGO layers, driven by thermally induced cyclic stresses until the cracks link together and the coating spalls.

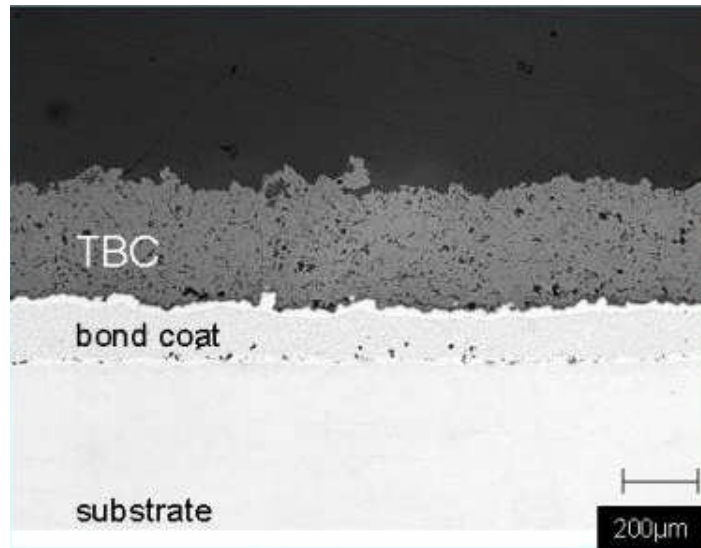


Figure 2-13 *TBC on a substrate material [62]*

2.6 NEW Aero Engine Core Concepts (NEWAC)

In order to address the environmental effects of aviation industry and find a promising solution, large collaborative projects are running worldwide. Both Europe and United states have conducted extreme programmes to meet the targets set by the ACARE in 2020. In this section the European Union collaborative project, NEWAC, is explained in more detail. Parts of the contexts are quoted directly from the official website of the NEWAC project.

NEWAC stands for 'NEW Aero engine Core concepts' which is addressed to improve environmental impact of civil aviation subject to the future low-emission aero engines. This is an integrated programme, co-funded by the European Union (EU) within the Sixth Framework Package (FP6) under Thematic Priority 4 Aeronautics and Space under the leadership of MTU Aero Engines. NEWAC researches four new engine core concepts and lean-burn combustion.

The research is conducted by these major European engine manufacturers assisted by universities, research institutes and enterprises to investigate on new core engine concepts. The project commenced in May 2006 and concluded in April 2011. It aims to reduce fuel burn and hence emissions by improving

thermal efficiency and lean combustion technology, contributing to the attainment of the Advisory Council for Aeronautics Research in Europe (ACARE) targets. NEWAC builds on some past and existing EU Framework programmes in the field, such as EEFAE (CLEAN and ANTLE) developed in FP5 EU project and VITAL in FP6. [65]

NEWAC is looking for enabling technologies for environmentally friendly and economic propulsion solutions to be able to close the gap between the current emissions and the ACARE ambitious targets. It is a complementary to VITAL integrated programme in terms of engine component modelling. VITAL is focusing on noise and propulsive efficiency by addressing low pressure (LP) component design. The main focus of NEWAC project was on thermal efficiency and fuel consumption by introducing novel innovative core configurations to reduce CO₂ and NO_x emissions.

This project will deliver a major contribution to the global environment. Its main objectives were to achieve a 6% reduction in CO₂ emissions and a further 16% reduction in NO_x relative to ICAO-LTO cycle thereby making major steps towards achieving the environmental targets set by ACARE. These goals, which are to be realised in 2020, include, reductions in CO₂ and NO_x emissions of 50% and 80%, respectively.[66]

The NEWAC enabling technologies for low emission engines consists of four innovative core configurations, namely, Intercooled core operating at high OPR, Intercooled Recuperated Core operating at low OPR, Flow Controlled Core and Active Core operating at medium OPR, improved combustion, active systems and improved core components. NEWAC engine configurations are illustrated in Figure 2-14. In the following sections these configurations are briefly discussed.[67]

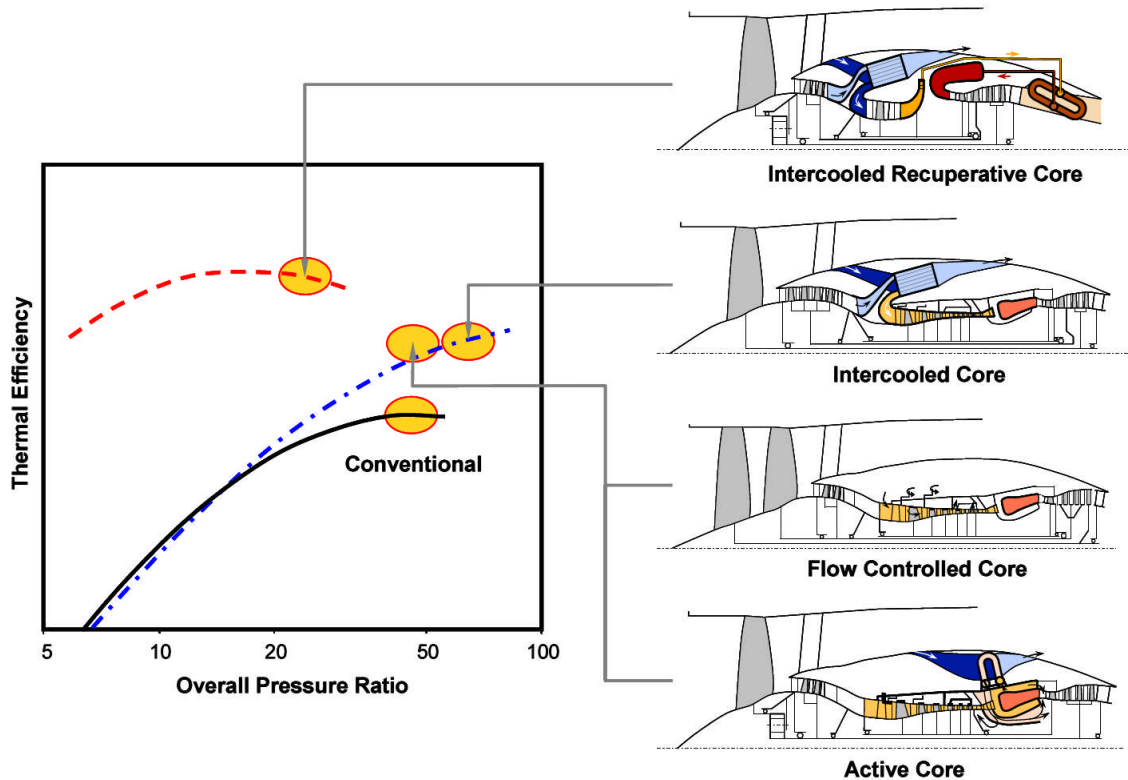


Figure 2-14 *NEWAC innovative core concepts [7]*

2.6.1 Intercooled core (DDIC)

The intercooled core concept is a high OPR ratio configuration based on three-shaft direct drive turbo fan (DDTF) architecture with separate hot and cold jet nozzles. This configuration is equipped with staged Lean Direct Injection (LDI) combustion technology. The original concept of direct drives turbofan engine was developed by Rolls-Royce under the sixth framework program.

This configuration features an intercooler which is placed between the intermediate and high pressure compressor. Introduction of an intercooler allows increasing overall pressure ratio while keeping combustor entry temperature relatively low. Hence leads to improved specific fuel consumption by reducing the compression work combined with lower NOx emissions. Consequently it gives an improvement of the core specific output and the bypass pressure ratio [68]. In comparison with conventional core turbofan

engines, the intercooled core can be designed for significantly higher OPR, reduced cooling air requirements and higher thermal efficiency.

Intercooled core concept is expected to enter into service around 2025 for intercooled aero engines. It contributes to reducing CO₂ by 4% and NO_x emission by 16% [67] compared to the reference technology, established in EEFAE ANTLE. The intercooled engine architecture for long range application is given in Figure 2-15.

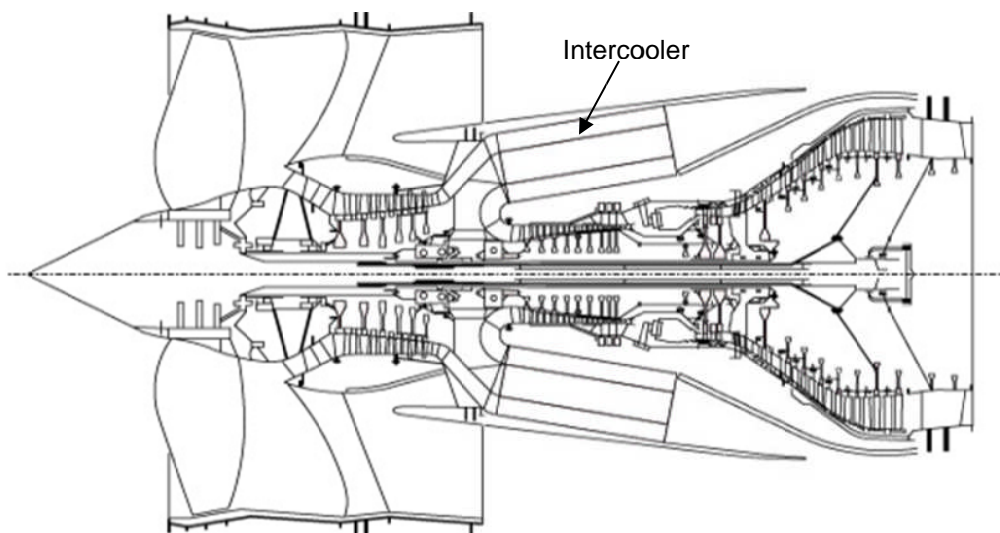


Figure 2-15 *Intercooled core architecture [69]*

2.6.2 Intercooled Recuperative Core (IR)

The intercooled recuperated core concept is a low overall pressure ratio (OPR) with geared fan architecture and making use of Lean Premixed Pre-vaporised (LPP) combustion system. The original concept of intercooled recuperated core engine is developed by MTU Aero Engines. This concept results from the integration of intercooler, placed between the intermediate and high pressure compressor, and heat exchanger, installed in the hot gas exhaust nozzle, into an aero engine.

The intercooler component reduces the air temperature at the inlet of HPC in order to decrease the amount of work needed in compression section and also keeping compressor outlet temperature level low. On the other hand the recuperator component exploits the remaining heat of the engine exhaust gas and transfers it to the high pressure discharge air at the combustor inlet. Thus substantial benefits of thermal efficiency with a potential of up to 20% fuel consumption reduction. Due to more complexity and weight problems, this configuration is considered for long range flight mission. [70]

Intercooled recuperative core concept contributes to reducing CO₂ by 2% and NO_x emission by 10% [67] compared to the reference technology, established in EEFAE CLEAN. The intercooled recuperated engine architecture for long range application is shown in Figure 2-16.

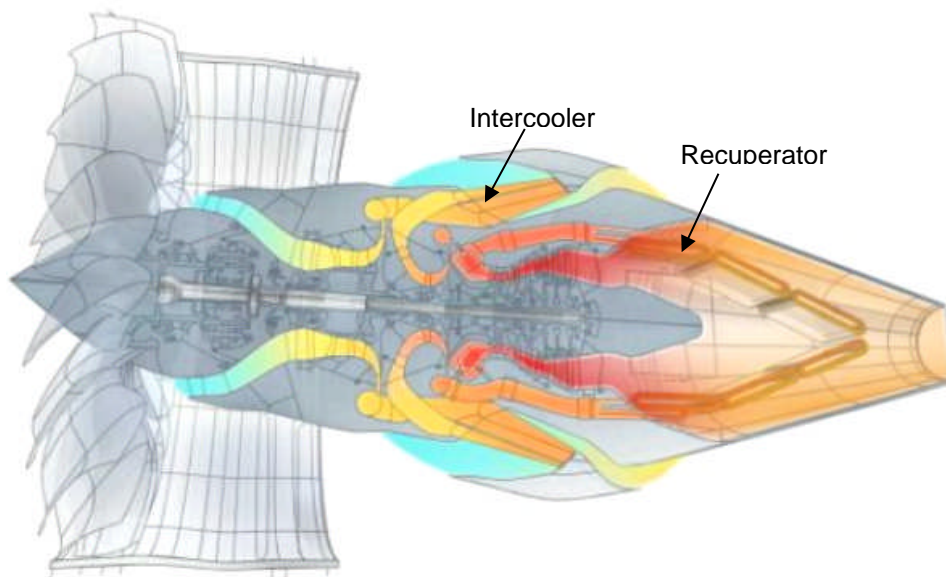


Figure 2-16 *Intercooled recuperated core architecture [66]*

2.6.3 Flow Controlled Core (FCC)

The flow controlled core concept is a high by pass ratio engine based on three-shaft counter rotating turbo fan configuration where two independent shafts are rotating in opposite direction. The LP spool of the FCC has been designed with counter rotating fan which is joined to a low pressure turbine with several stages of counter-rotating blades. The main point in this fan design is the low fan tip speed and the ratio between the speed of the front fan and the speed of the second fan. For this configuration a LDI or a PERM combustion system can be used.

Number of flow control technologies is applied in flow controlled core concept such as stall active control, blade/casing rub management for tight tip clearance and air aspiration. The main focus in the flow controlled configuration is on the engine component efficiencies mainly HP compressor module. Increased stall margin and efficiency is resulted by high aerodynamic load of high pressure compressor (HPC) in order to reduce consumption and emissions. Flow controlled core is expected to contribute to reducing CO₂ by 3% and NO_x emission by 12% [67] compared to reference technology, established in EEFAE CLEAN and ANTLE.

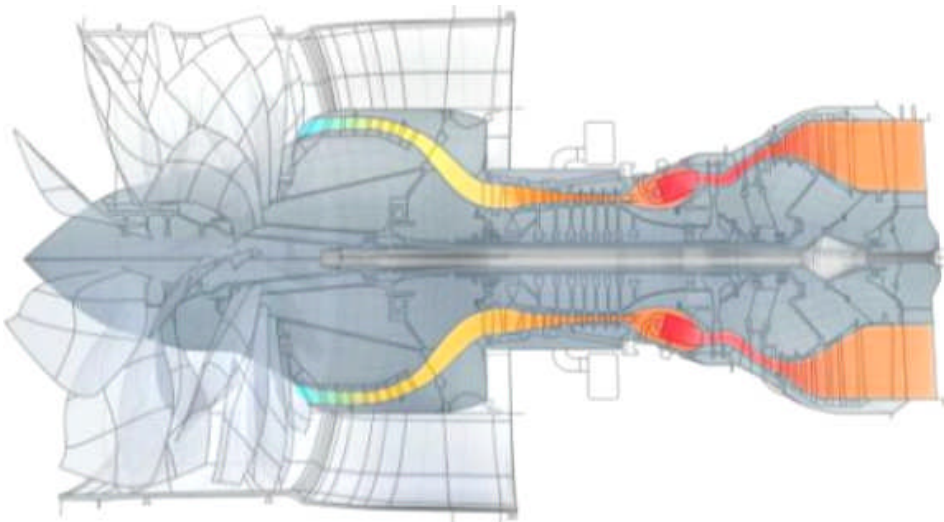


Figure 2-17 Flow controlled core engine architecture [66]

2.6.4 Active Core

The active core concept is a high pressure ratio core with geared fan architecture and making use of Partially Evaporation and Rapid Mixing (PERM) combustion system. With this concept the core engine can be adapted to each operating condition (Climb, Cruise, decent, etc.). The main objective of this configuration is to improve efficiency, operability and weight of a high pressure ratio core by using active technologies such as active cooling air cooling system, casing active tip clearance control for compressor rear stages and active surge control for compressor front stages. These systems offer significant improvement of HPC efficiency and size through increased surge margin and clearance control. In general these active technologies can help to increase the average thermal efficiency significantly.

Active core concept is expected to contribute to reducing CO₂ by 4% and NO_x emission by 12% [67] compared to reference technology, established in EEFAE CLEAN and ANTLE.

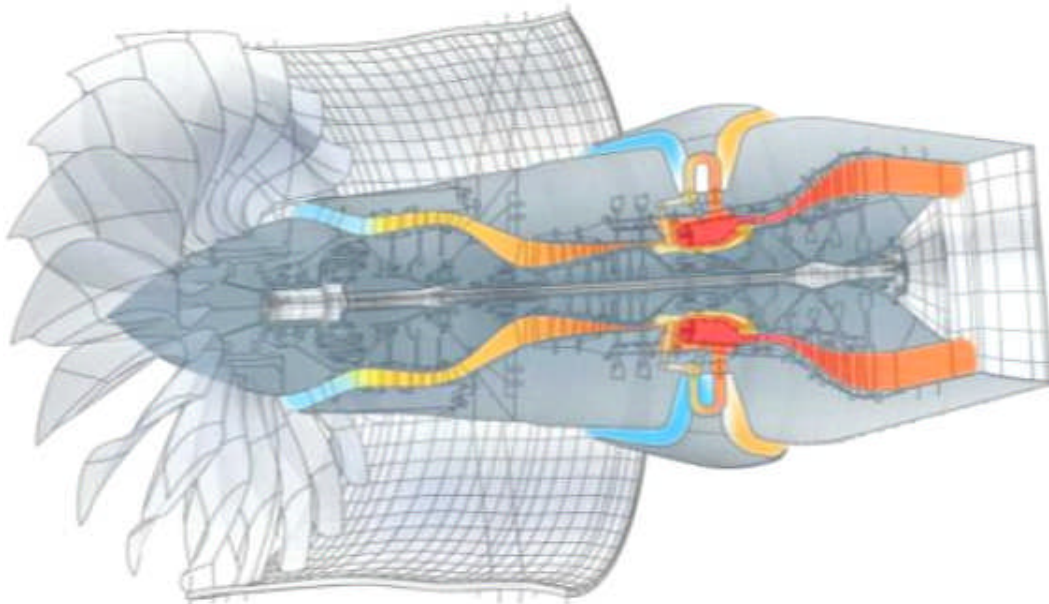


Figure 2-18 Active core engine architecture [66]

CHAPTER 3 TERA2020 FRAMEWORK

In this chapter the TERA2020 methodology and architecture, in particular, the incorporated modules for modelling different aspect of aero engines is described. The underlying assumption and simplification of the TERA2020 is explained. The commercially available optimiser for integration, automation, and optimisation purpose is briefly discussed. Additionally, development to the lifing module (in particular the development of an oxidation model) of the HESTIA code is presented.

3.1 Introduction

The environmental impact of civil aviation is currently one of the most serious public concerns due to increasing demand of air travel and the subsequent contribution it has towards global warming. As a consequence, the aviation industry is constantly changing to satisfy restrictive legislations worldwide. A large variety of power plant technologies are being proposed to reduce aviation pollutants, however selection of the best candidate is difficult due to the number of variables and criteria that need to be met. Therefore, a multi-disciplinary methodology and tool for assessing aero engines at the conceptual and preliminary design stages to address conflicting objectives is highly justified and valuable.

TERA2020 is a modular multidisciplinary aero engine conceptual and preliminary design software tool. This tool is made up of six simulation modules to calculate many aspects of engine design. It provides a virtual platform for assessments (design space exploration, sensitivity analyses, and multi-disciplinary optimisation and trade-off studies) of various power plant concepts at system level. The incorporated disciplines provide sufficient accuracy for the purpose of a conceptual study. This preliminary design tool enables the designer and interested bodies (government, airlines) to assess the affordability of the alternative engine architecture at the concept stage of an engine design.

This approach was originally conceived in order to assess engines with minimum global warming impact and lowest cost of ownership in a variety of emission legislation scenarios, emission taxation policies, fiscal and air traffic management environments. This method evaluates the engine at an early stage of the engine design process due to the cost and complexity of meeting environmental performance in the engine post design process. To fully understand the challenges associated with the innovative aero engine configuration, a conceptual multidisciplinary analysis tool is required to address the request of different interested parties. Choosing the right configuration of the power plant will need to take all the contradictory parameters into consideration such as fuel efficiency, prolonged engine life, reduced ownership cost amongst others.

The core of this tool is a detailed thermodynamic model of the power plant which provides data required by other modules. This core module is integrated with some additional modules to represent a multidisciplinary tool. These preliminary design modules are integrated with a commercial optimiser and provide a means for cycle studies. It is expected that new legislative and fiscal constraints on air travel will demand an extension to the customary range of asset management parameters. In such a business environment there is potential for TERA to develop into a useful tool for aircraft and engine asset management. This tool can then be applied to the optimisation of one or more objective functions, possibly including but not limited to mission fuel burn; engine noise, engine gaseous emission i.e. NO_x, global warming potential (GWP) and engine direct operating cost (DOC).

3.2 TERA2020 Modules

Cranfield University has developed several design tools to enable the design space exploration be carried out in the preliminary design stage of a new or derivative gas turbine engine. The current developed framework, TERA2020, is a collaborative effort of European academia within the VITAL and NEWAC

projects. The modular structure of the aviation TERA based tool consists of 7-modules, which are designed to function with the thermodynamic cycle model within the TERA2020 framework. The codes other disciplines have been successfully integrated into the framework. All these modules are individual and can be utilised as standalone executable and the multi-modular platform was chosen for extra flexibility and also to allow for maximum of future exchangeability of the modules. This physics based modelling environment extends the simulation capability from components to the full system level. However, the multi modular structure of this tool leads to more integration challenges. The following are the considered disciplines and are explained in more detail:

- Engine performance module
- Engine dimensions and weight module
- Engine production cost module
- Aircraft performance and dimension module
- Emissions module
- Noise module
- Economic module

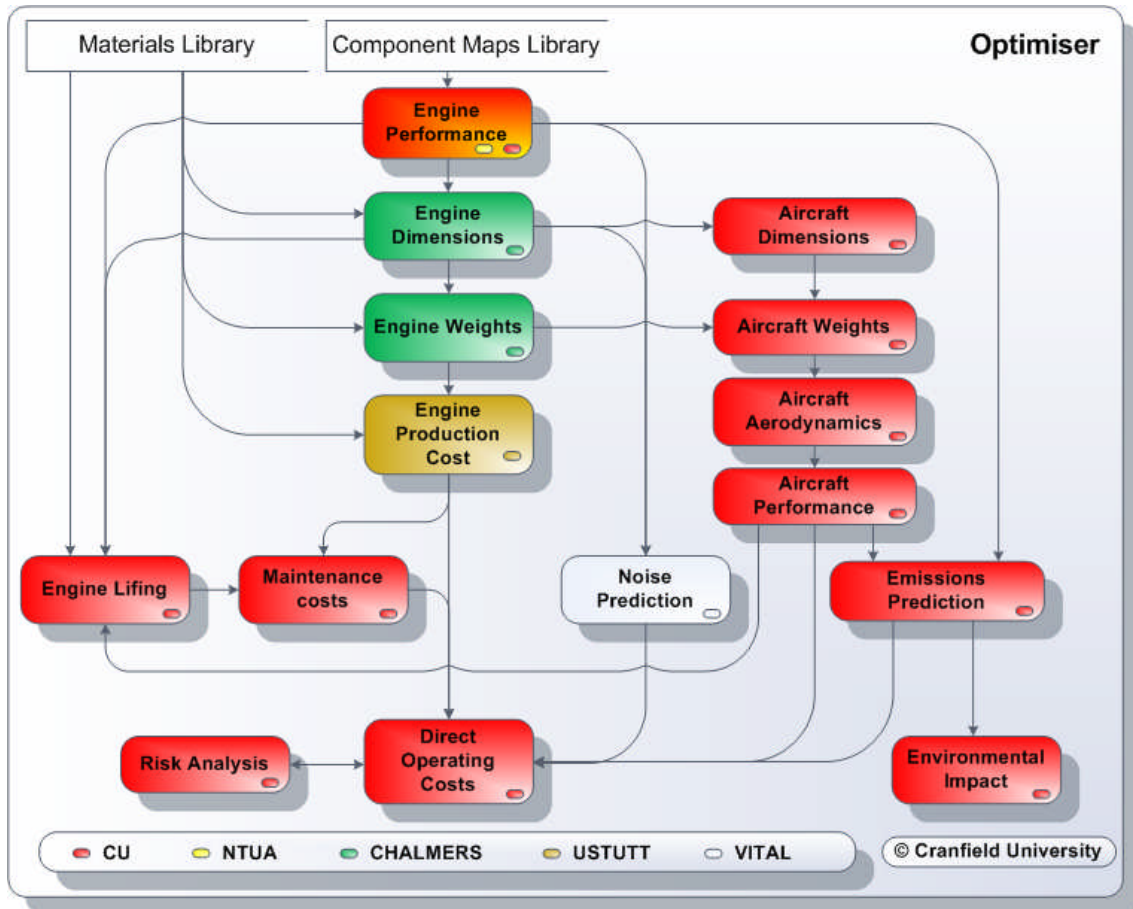


Figure 3-1 TERA2020 algorithm [71]

3.2.1 Engine performance module

As the engine performance model in the core of all information exchange in the TERA method, the need for a fast and robust engine thermodynamic simulation code is necessary. In the VITAL and NEWAC engine performance models are developed by CU and NTUA using TURBOMATCH [72] [73], EVA [75] [76] and PROOSIS [78] [79] codes. The engine performance module is the starting point in the TERA2020 calculation procedures.

TURBOMATCH is the gas turbine performance simulation and diagnostic code which has been developed by Cranfield University for more than a decade. This computational tool was developed to facilitate design point, off-design (steady state) and complex transient performance calculations for gas turbines engines.

It can be used to simulate the performance of an extensive range of both Aero and Industrial engines cycles ranging from a simple single shaft turbojet to complex multi-spool turbofans with mixed exhausts and complex secondary air systems. It can also be used to simulate the performance of novel and conceptual cycles including wave rotors and intercooled / recuperated cycles among others. This simulation tool uses the component matching approach and comprises several pre-programmed modules (using FORTRAN 90), known as Bricks and connected to each other to create an engine cycle. Most Bricks correspond to models of individual gas turbine components e.g. Compressors, Burners, Turbines, Mixers, Nozzles, Heat Exchangers, Afterburners, and Power Turbines, among others [74].

EVA has been developed by Cranfield University using the TERA methodology for environmental assessment of novel propulsion systems. This tool is capable of modelling engine performance to explore the design space for the preliminary design analysis. The engine components such as intake, duct, fan, bleed, compressor, combustor, etc. are connected together to produce the engine thermodynamic model. This tool is adopted in NEWAC project for developing performance models of the intercooled and intercooled recuperated engines [75].

PROOSIS is a cost effective gas turbine simulation environment developed by the European Framework 6 collaborative project VIVACE. This tool is capable of modelling any kind of dynamic system implementing object-oriented approach, visual environments, and shared standards for the European Union gas turbine community. PROOSIS is used successfully by leading companies in the aerospace and energy sectors [79].

In TERA2020 algorithm the calculation procedure initiates from the engine performance module. The executable decks (Performance.exe) of the aforementioned codes are used to simulate the performance of the proposed engine configuration at cycle design and off-design operating conditions. The engine design point is set at top of climb (TOC) with altitude of 10668 [m] at hot

day condition (ISA+10) to determine the map scaling factors of the components and the area of the nozzle.

Then the numerous off-design points are performed using the engine off-design operating point input data file and producing all the necessary engine performance information required by other TERA modules. In fact the TERA2020 algorithm first defines an engine cycle and then the engine performance module provides the engine performance information as an input for weight, aircraft, noise, emissions, and the economic modules.

3.2.2 Weight and plant production cost module (WeiCo)

WeiCo is an acronym for the engine weight and plant cost model. In TERA2020 these two are refined and merged as a single framework. The weight model was originally developed by Chalmers University while the plant production cost model was developed by University of Stuttgart. WeiCo is the second module in the TERA2020 calculation procedures.

The weight model is written in FORTRAN 90 and developed based on the established methodology of Onat and Kless [80] [81]. This semi-generic model uses two types of data to estimate the engine weight; the mandatory data provided by engine performance model and the default values stored in an input text file. The code converting thermodynamic cycle data such as airflows, temperatures, and pressures, etc. into an outline of the engine cross section that is required for sizing the components and weight calculations. It calculates the weight and dimension of major engine components, such as fan, compressor, burner, turbines and frames. Aerodynamic and mechanical design for most components is carried out at top of climb; some components such as the intercooler, combustor and recuperator components are designed at take-off conditions. Substantial efforts have been made to harmonize the code with the plant cost model and other TERA2020 modules.

The plant cost model is also written in FORTRAN 90. This tool is developed to calculate the production cost of the various engine configurations within the VITAL and NEWAC projects. Estimating the plant costs is a complex problem due to the numerous factors involved such as material prices, wage rate, production number and technology level. The current model calculates the direct production costs while assuming equal manufacturing conditions for the entire selected concepts. Therefore, the production cost model use the calculated dimensions by the weight model via a component by component approach. Where the final value added by the factory are considered. This model is linked to the weight model using a Dynamic Link Library (DLL) communicate technique.

3.2.3 Aircraft performance module (HERMES)

In the aviation industry the aero engine design process starts at the overall aircraft system level and gradually moves down to the component level where the aircraft is optimised first. Then the optimum engine is chosen taking into account the engine characteristics for the aircraft design. However, the design algorithm adapted in TERA system works in different manner implementing a different approach that offers clear advantages in system design. A rubberised wing aircraft model is implemented in TERA2020 to cover the main aircraft/engine design interactions. In this method an aircraft geometry and weight is optimised to meet the performance specification of the integrated engine. It allows engine sizing and investigation of certain engine parameters. This model also allows for the modelling of different aircraft and engines. A typical engine design and manufacturing process in industry is illustrated in Figure 3-2.

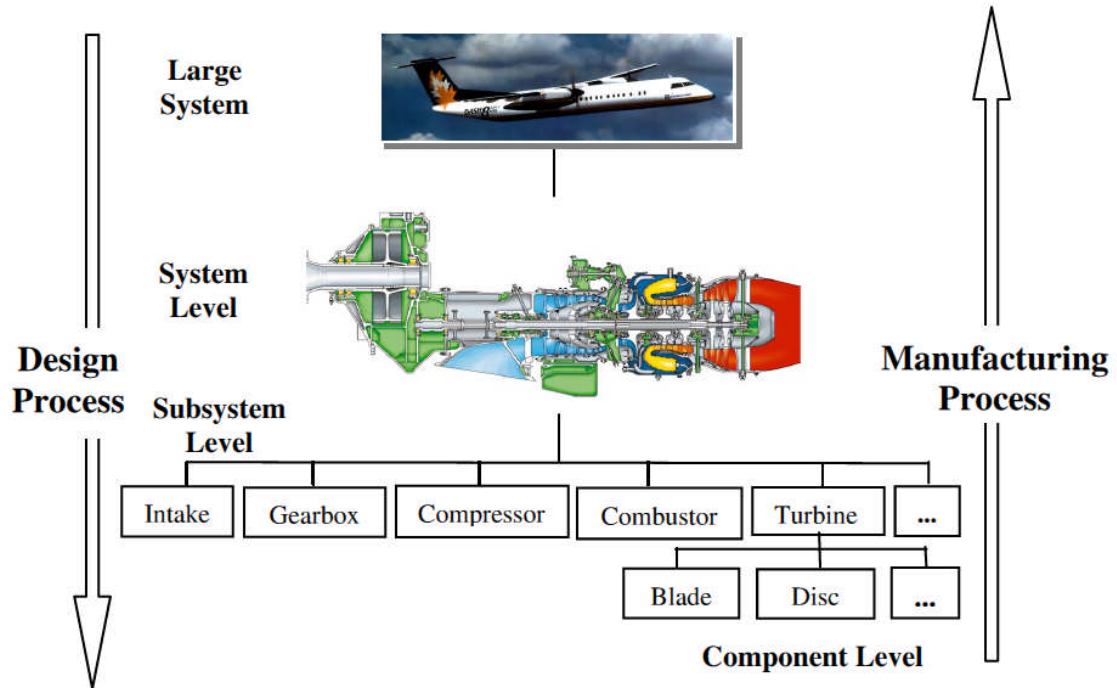


Figure 3-2 Engine design and manufacturing process [30]

The aircraft module (HERMES) is the third module in the TERA2020 calculation sequence. This code was originally developed by Cranfield University [82] [83] and is further developed for use in NEWAC project. It can predict aircraft dimensions, weights, aerodynamics and performance. The programming language for the aircraft performance model is FORTRAN 90.

When the engine cycle is defined from a set of performance parameters, it provides the engine performance data (engine rating) at different operating conditions (take-off, climb, cruise, etc.) for use in aircraft model along with the engine weight and dimensions data provided by WeiCo module. Then the given aircraft configuration is adapted, on a constant wing loading and aspect ratio criterion, in order to suit to this new engine design as well as satisfy the defined payload-range requirements.

Whole flight mission profile including diversion is considered for fuel burn calculation which allow for adequate fuel planning. At cruise condition as the aircraft gets lighter, a step-up cruise procedure is applied. Lighter aircraft

requires less thrust where the engine operates at a lower combustor outlet temperature. On the other hand a lighter and more efficient engine means the aircraft will be lighter, thus lower aircraft maximum take-off weight (MTOW) is needed. Therefore, the block fuel burn is affected by both engine and aircraft.

3.2.4 Emission and environmental module (HEPHAESTUS)

The emission and environmental impact module is developed by Cranfield University to evaluate the environmental impact of the NEWAC innovative combustor technologies and provides the required information for direct operating cost calculations in economic module. In NEWAC TERA2020 two individual modules, Emission prediction model and Environmental impact model were merged into a single software unit to speed up the code and reduce the integration challenges involved.

This module utilises the thermodynamic cycle parameters provided by aircraft module, public domain methods and correlations (i.e. P3T3 and Boeing method) to predicts the LTO NO_x emissions as well the NO_x, CO₂, and H₂O emissions (and GWP) for the entire flight mission profile. This code was developed on the basis of open literature correlation for a conventional combustor for year 2020 entry into service technology level.

3.2.5 Noise module (SOPRANO)

SOPRANO is the noise module developed in SilenceR research program by ISAE (SUPAERO) [84] and integrated in TERA2020 to assess the noise levels of the VITAL and some of the NEWAC engine configurations. The noise module utilises engine performance data and dimensions from WeiCo to calculate the noise produced by each engine component for the main noise operating points: side line, flyover and cutback. These are the key certification points that need to be addressed with respect to ICAO certification policy.

3.2.6 Economics module (HESTIA)

With the increased importance of economics in the aero engine design process, the development of computational models for simulating the engine components life, maintenance and direct operating cost is necessary.

The last module in TERA2020 calculation sequence is called HESTIA which has been developed by Cranfield University and written in FORTRAN 90 language. This module evaluates the potential performance and running cost benefits resulting from the implementation of new engine technologies and concepts. Economic module applies engine performance data, dimensions and production cost, LTO NO_x and CO₂ data from the emissions module and of course EPNL information from the noise module which are the upper stream of the TERA2020 algorithm. It calculates the cost of maintenance and direct operating costs for the proposed engine design and estimates the net present costs over a period of 30 years.

The existing economic module is composed of three main sub models: a lifing model, an economic model and a risk model. The lifing model measures preliminary serviceable life of the engine, namely high pressure turbine blade, through the analysis of creep, fatigue and oxidation over a full working cycle of the engine.[85] The economic model utilises the calculated time between overhaul from the lifing model to estimate the direct operating costs (DOC) and net present cost (NPC) of engine and aircraft. The risk model uses the Monte Carlo method with a Gaussian distribution to study the impact of the variations in some parameters such as fuel price, interest percentage on total investment, inflation, downtime, maintenance labour cost, emission and noise taxes on the NPC. [86] The output parameters of the economic module are listed in Table 3-1.

Table 3-1 *Economic module output parameters*

Parameter	Description	Unit
BladeCreepLife	HPT blade creep life	hr
BladeFatigueLife	HPT blade fatigue life	hr
BladeOxidationLife	HPT blade oxidation life	hr
DiscCreepLife	HPT disc creep life	hr
LifingTBO	HPT time between overhaul	hr
WeibullTBO	Probabilistic time between overhaul	hr
TBO	Engine time between overhaul	hr
NPCTotal	Total net present cost of the engine and aircraft over 30 years	kE
NPCTotalYr	Average annual net present cost of the engine and aircraft	kE/yr
AirportTax	Total airport charges per year	kE/yr
CarbonTax	Airport CO ₂ emission charges per year	kE/yr
NoxTax	Airport No _x emission charges per year	kE/yr
NoiseTax	Airport Noise emission charges per year	kE/yr
DOCTotalYr	Total engine and aircraft direct operating cost per year	kE/yr
DOCTotalFlight	Total engine and aircraft direct operating cost per flight	kE/flight
DOCTotalHr	Total engine and aircraft direct operating cost per hour	kE/hr
DOCMtceTotalHr	Total engine and aircraft maintenance direct operating cost per hour	kE/hr
DOCMtceEngHr	Single engine maintenance direct operating cost per hour	kE/hr
AcFuelEff	Transport fuel efficiency parameter	lt/(100km*pax)
AcCostEff	Transport cost efficiency parameter	E/(100km*pax)
CFUELYr	Cost of fuel per year	kE/yr
MtrlsEngBlockHr	Single engine materials cost per hour	kE/hr

Aero engines hot section components, namely first stage HPT disk and blades, are subject to arduous operating conditions; elevated and varying temperature transients, hostile gas pressure coming from the combustion chamber and severe centrifugal forces. These critical components can significantly influence the overall engine life cycle costs. The accurate prediction of turbine disk and blades life at the preliminary design stage is therefore necessary to ensure both the safety and economics of gas turbine operation.

The blade life is of course affected by different phenomenon. Creep, fatigue, corrosion and oxidation are the prime modes of failure for the high pressure turbine blades and disc. Creep and fatigue life are highly dependent on the stresses and working temperatures of the material which the component is made from. These temperatures and stresses can be calculated during the preliminary design process as well as the geometry, material properties and operating conditions through the performance analysis and turbine aerodynamic & mechanical design. The result may be inaccurate for practical use but will be helpful to identify potential design problem. So the life prediction can be made and the system designer can investigate the design more thoroughly and accurately at an earlier stage of the design [87].

The life methodologies may be classed into two distinct approaches to determine turbine hot section component service life for a specific plant; probabilistic (un-deterministic) methods and physics based methods. Probabilistic methods are based on mathematical models to describe the physical processes of the phenomenon. Their mathematical models are either stochastic themselves or take in stochastic inputs. This allows to properly accounting for possible material, manufacturing induced defects, uncertainties associated with collected data either from test results or in-service monitoring, variations in operating conditions due to changing mission profile, or any other type of data variations that could affect the life of a component of interest. The key is to get the required probability distributions for each applicable variable right. Hence, these methods normally require a large amount of basic data on each variable to be modelled probabilistically, or proper expert opinion on the distribution of these variables [88].

Conventional approach implies the use of non-stochastic mathematical models with known or assumed inputs to estimate the useful life of a given part for a given application. The known or assumed inputs are normally based on maximum requirements, experience or laboratory testing. This approach combines engine operating history with the mechanical and metallurgical aspects of individual turbine components for remaining serviceable life

assessment. By identifying life limiting factors and predicting the rate at which damage occurs, optimum repair, replacement and overhaul intervals can be established. To validate the computer model, periodic metallurgical analysis of components from certain key engines needs to be performed to monitor deterioration rates and identify any unforeseen failure mechanisms [89] .

In the current research work, using physics based life model, the attention has been focused on the high pressure turbine, and the analyses based on creep, low cycle fatigue and oxidation life approaches. The result in term of hours between engine overhaul allow the user to predict with a certain accuracy the influence of the maintenance cost on the total cost of an airplane in service, over a certain amount of time with the aim prolonging asset life and optimizing long term operational costs.

3.3 TBC Oxidation Model

In aero gas turbine engines, creep, fatigue, oxidation and corrosion are the most important failure mechanisms of high pressure and high temperature components. As a consequence of increasing turbine entry temperature, oxidation has become a critical life limiting phenomenon. Although there are other factors that affect the oxidation life of the engine components, exposure time and temperature are identified as the dominant factors.

The current oxidation model is a physics based model developed to estimate the TBC life of the high pressure turbine blades of the first stage. This model represents the oxidation effect on turbine blade failure and enables the calculation of failure due to oxidation. The first stage of the high pressure turbine is the part of the aero engine that bears the highest stresses due to pressure, temperature and rotational speeds. Hence in this model the focus is on high pressure turbine blade, being the component that usually limits gas turbine life. This model, along with creep and fatigue models is used by the lifing module to better predict time between overhaul (TBO) of the aero engines for

both short and long range missions. Then the value of TBO is taken as the baseline distribution to calculate the life of other important modules of the engine and used in the economic module calculations.

The oxidation algorithm calculates oxidation life using engine performance data and material property of the engine component. The oxidation model as part of the Economic module is called by the main program, which provides some input data and displays the final outputs. Basically, the flight envelope has to be split into several segments. Each segment characterised by a time length and a well-defined operating condition, that is operating temperature, cooling effectiveness and cooling flow temperature. This oxidation model offers the user the option of including a blade cooling flow system, in to the lifing calculation. The calculations used in the model are based on a simple one dimensional model of convection cooling. It is assumed that equilibrium exists between the heat flux entering the blade and that leaving it (heat absorbed by the coolant). The process is based on a certain amount of air bled from the last stages of the HP compressor, just before entering the combustor, and transferred to the HP turbine, where it will cool the blades.

Thermal barrier coating is further used to make cooling easier, causing a drop in temperature inside the blade. Because of their low thermal conductivity, thermal barrier coatings are able to provide a temperature drop of roughly 150°C [63] across a 200µm thickness. This means that the metal surface will experience 150°C drop compared to the situation before being coated. Therefore, the oxidation model is able to estimate blade interface temperature and the blade metal temperature, applying a cooling mechanism and thermal barrier coating temperature reduction. In spite of the presence of the ceramic layer (TBC), the bond coat usually operates at relatively high temperatures and its oxidation is impossible to avoid. The oxide layer produced as a consequence of this reaction is the Thermally Grown Oxide (TGO). The schematic of a thermal barrier coating on a blade is shown in Figure 3-3.

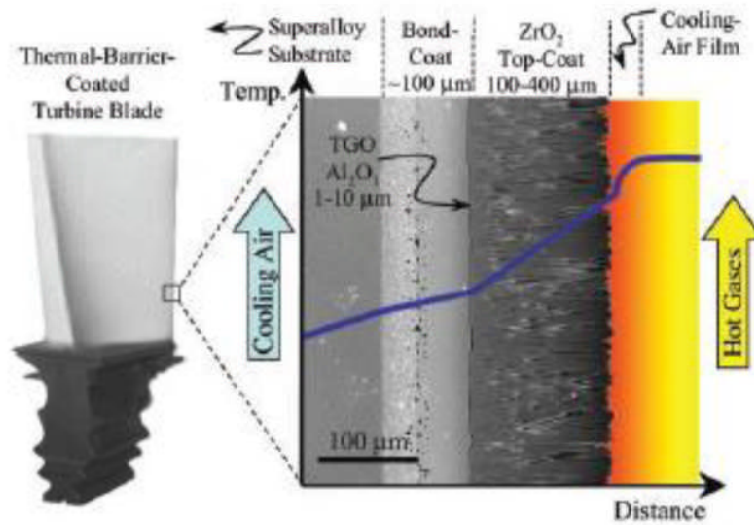


Figure 3-3 Blade thermal barrier coating schematic [63]

The substrate is the material that needs to be protected, usually a nickel base super-alloy. The bond coat is either a metal with high contents of chromium and aluminium or it is made of diffusion aluminides of nickel or platinum. The TBC usually consists of a thin layer of yttria-stabilized zirconia which provides thermal isolation and is a highly compliant and strain tolerant material, with a low thermal conductivity and high thermal-expansion coefficient [63].

At high temperatures the oxidation of many metals is found to follow parabolic time dependence and this behaviour is described by Wagner's Theory, whose detailed description can be found in literature. By applying parabolic growth law, the model is able to calculate oxide thickness at different flight segments. As temperature varies along time the component will oxidize. The TGO growth presents Arrhenius behaviour. [64]. The following oxide thickness model was applied to quantify the oxide layer thickness growth per flight cycle:

$$\delta = \left\{ \exp \left[Q \left(\frac{1}{T_0} - \frac{1}{T} \right) \right] t \right\}^n \quad (3-1)$$

Where:

δ = oxide thickness (μm)

$Q = \Delta H/R$ = the ratio between the apparent activation energy and universal gas constant

T_0 = temperature constant (K)

T = blade metal temperature (K)

t = operating time

$n = 0.332$

Thermal stresses arise when the oxidized sample is heated or cooled. At higher temperature the stresses will be higher and this phenomenon is more noticeable. As the thermal expansion coefficients of substrate and oxide differs, one will tend to expand (or contract) more than the other. The coefficient of thermal expansion for TGO was assumed to be linearly dependent on temperature, which is obtained for aluminium oxide from literature. Then the code is able to calculate the free elongation of the TGO and accordingly it's mechanical strain:

$$\epsilon(T) = \epsilon_{ss}(T) - \delta L/L \quad (3-2)$$

Where:

ϵ = mechanical strain in the TGO

ϵ_{ss} = substrate total strain

$\delta L/L$ = free elongation of TGO

Failure as a result of thermally induced stresses arising from the large thermal expansion mismatch between substrate and scale spallation manifests as the detachment of either the oxide layer or TBC subsequent to their cracking. Once the free elongation, mechanical strain and oxide thickness of the TGO are

calculated, the oxidation model estimates the spallation of the TBC during each segment of flight for one cycle. Hence, the cyclic life of thermal barrier coating at each flight segment is given as:

$$N = \left[\left(\frac{\epsilon_{ff}}{\epsilon} \right) \left(1 - \frac{\delta}{\delta_c} \right)^c + \left(\frac{\delta}{\delta_c} \right)^c \right]^b \quad (3-3)$$

Where:

N= cyclic life

ϵ_{ff} = mechanical strain range constant

ϵ = mechanical strain in the TGO

δ = oxide thickness (μm)

δ_c = critical oxide thickness (mm)

$c = 1.0$

$b = 7.64$

The last step is the calculation of TBC life fraction consumed at each flight segment and total oxidation life (either in hour of flight or in cycles) through the use of Miner's cumulative law. Some key parameters required by the oxidation model and their sources are shown in Table 3-2.

Table 3-2 Oxidation model input parameters

Parameter	Data Flow Source
Operating temperature during each segment of flight	Performance module
Time spent during each segment of flight	Performance module
Cooling effectiveness during each segment of flight	Performance module
Cooling flow temperature during each segment of flight	Performance module
Linear coefficient of thermal expansion	Material database
Elastic modulus of the material	Material database

The oxidation model gives the following outputs:

- Oxidation layer thickness at each flight segment
- Segment thermal barrier coating life
- Blade TBC life fraction consumed
- Total blade oxidation life

The blade cooling selector and number of flight segments would be defined by the user. A typical output from of the oxidation model for short range application is shown in Figure 3-4.

T U R B I N E B L A D E O X I D A T I O N A N A L Y S I S

Number of flight segments:	5
Blade cooling selector:	Cooled Turbine Blade
Segment oxide layer thickness growth:	1 0.43E-01 [micro m] 2 0.16E-01 [micro m] 3 0.12E-01 [micro m] 4 0.28E-03 [micro m] 5 0.27E-01 [micro m]
Segment thermal barrier coating life:	1 0.11E-10 [cycle] 2 0.45E+00 [cycle] 3 0.27E+01 [cycle] 4 0.23E+04 [cycle] 5 0.12E-01 [cycle]
Blade TBC life fraction consumed:	1 0.12E+14 [-] 2 0.45E+00 [-] 3 0.27E+01 [-] 4 0.23E+04 [-] 5 0.12E-01 [-]
Cycle duration:	6.5 [hr]
Total number of cycles:	32000 [-]
Total blade oxidation life:	15000 [hr]

Figure 3-4 A typical oxidation model output

3.4 Integration and Optimisation Environment

For the modular structure of the TERA2020 framework (Figure 3-5) where the parameters and results from one module code are required as inputs to another module code; an integration, automation, and optimisation of design processes simulation is therefore necessary.

Commercially available simulation process automation and design optimisation solution, Isight, was applied to implement the multidisciplinary structure of the TERA2020. It significantly reduces the preliminary design time and improves the product quality and reliability as the manual simulation process of entering the required data can reduce efficiency, slow product development, and introduce errors in modelling and simulation assumptions. [45]

Using Isight drag-and-drop capability one can create automated simulation process flows. It provides an extensive library of parallel process components, such as Design of Experiments and Optimisation as well as Approximation methods that enable engineers to thoroughly and quickly explore the design space. This integration tool allows for multi-objective optimisation, design studies, parametric studies, and sensitivity analysis. The mathematical modelling for disciplines interacts by exchanging data using its data exchanger capability. This tool has been employed by different industries over a decade to improve and enhanced their products.

The following are the powerful design drivers available in Isight software:

- Multi-disciplinary optimisation
- Design of experiments
- Approximation methods
- Monte Carlo analysis
- Stochastic design improvement

- Taguchi robust design
- Design for six sigma

In Isight there are four main categories of Optimisation Techniques, as follows:

- Numerical Optimisation Techniques: They assume the parameter space is unimodal, convex and continuous.
- Exploratory Techniques: Exploratory techniques avoid focusing only on a local region. They generally evaluate designs throughout the parameter space in search of the global optimum.
- Expert System Techniques: Expert system techniques follow user defined directions on what to change, how to change it, and when to change it. The technique included in iSIGHT is Directed Heuristic Search
- Optimisation Strategies: Optimisation strategies are one level above other optimization techniques, because they incorporate another optimization technique into their execution. The technique included in iSIGHT is Satisficing Trade-off Analysis. This technique is considered an optimization strategy because it internally executes Sequential Quadratic Programming - NLPQL multiple times.

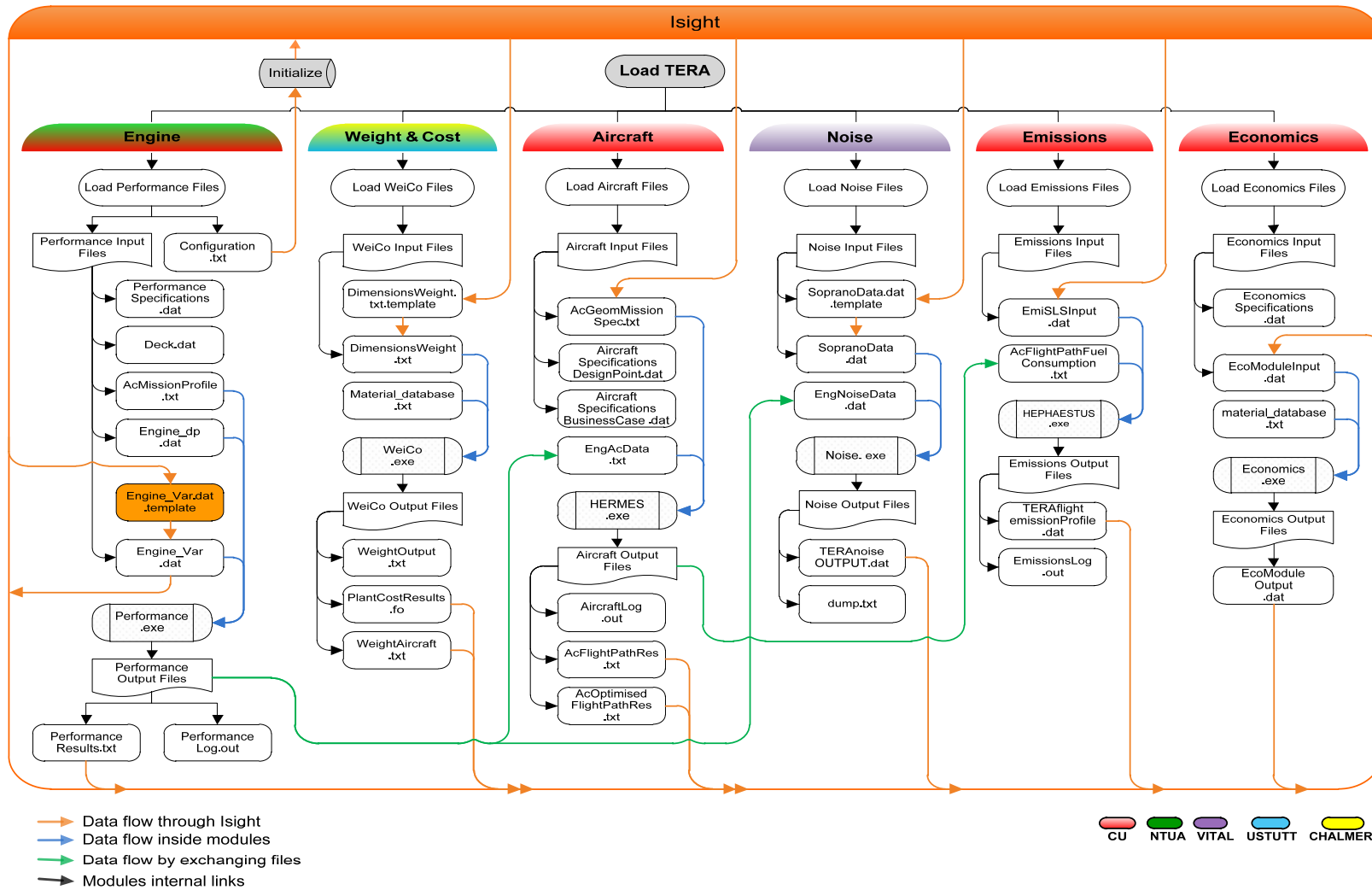


Figure 3-5 TERA2020 architecture and data flow chart

CHAPTER 4 TERA 2020 ASSESSMENT PROCESS

This chapter describes the approaches adopted for life assessment and optimisation of conventional turbofan and conceptual intercooled turbofan aero engines using TERA2020 tool. For a better understanding and interpretation of the presented results, the TERA assumptions and simplifications are presented. The sensitivity analyses and their applications are explained. The parametric study and the applied techniques for identifying an appropriate design space are described. Exploring the design space available and optimisation process is presented.

4.1 Assumptions

This section describes the primary assumptions and simplification of the TERA2020 system for a better understanding and interpretation of the performed studies presented in the result section. These assumptions are mainly related to the engine and aircraft interactions. Parts of this section are quoted directly from the internal documents of the NEWAC project.

The engine design point (match point) with respect to the performance was set at top of climb (TOC) with an altitude of 10668 [m] and 0.82 Mach number at hot day condition (ISA+10[K]) to determine the map scaling factors of the turbo machinery components and the areas of the core and by pass nozzle.

The following design parameters are fixed at top of climb point:

- Combustor output temperature
- Fan mass flow
- Core mass flow
- Compressor pressure ratio

- Cooling mass flow
- Cooling temperature
- Intercooler effectiveness
- Intercooler pressure loss

Consequently, the following engine output parameters are allowed to vary:

- Engine thrust
- Engine specific thrust
- Bypass ratio (if fan mass flow or core mass flow allowed to vary)
- Velocity ratio
- Overall pressure ratio

The following parameters are allowed to vary at off-design operating conditions:

- Combustor output temperature for climb rating
- Engine thrust
- Engine specific thrust
- By pass ratio
- Velocity ratio
- Overall pressure ratio
- Cooling temperature

The aerodynamic and mechanical design for most components was performed at top of climb operating condition. However, some components such as the

intercooler and combustor components are designed at take-off conditions due to the highest heat transfer.

A step-up cruise approach is used for cruise condition, where the cruise Mach number (0.82) is fixed by the engine performance model. The mid-cruise point was selected to be the middle point in the distance covered during cruise. During the flight mission as the aircraft gets lighter, less thrust is required for cruise which means that the engine operates at lower combustor output temperature, thus lighter and efficient engine. This results in a lighter aircraft and lower maximum take-off weight (MTOW). Therefore, the aircraft wing length is varied on the basis of constant wing loading and aspect ratio criterion. It is noteworthy that the thrust and combustor output temperature variation at cruise not only vary due to the aircraft getting lighter, but also vary because the engine design changes.

4.2 Constraints

In the TERA2020 environment there are three main alternatives that the designer can apply in order to constrain the design space:

- Applying a 'hard-coded' limits the module codes, with respect to underlying physics limitations of the model.
- Setting a specific range for each design variable to constrain the optimiser algorithm on the basis of engineering experience
- Using practical constraints set at the end of the calculation procedure with respect to components aerodynamic design, material properties and customer requirements.

In the current study the feasibility of the final engine design was realised at the end of the calculation sequence, after the economics module execution, using the constraint sets in the optimiser environment. Subsequently during the

calculation procedures, unrealistic designs that affect the stability and underlying assumptions in TERA2020 modules were automatically excluded by interruptions of the single modules code. Therefore, the complicated internal iteration sequence between the performance module, the WeiCo module and the aircraft module was unnecessary and kept to minimum. For example, there is no iterative loop for the take-off rating and the calculated FAR take-off field length is an output.

All design parameters was chosen for optimisation studies have a certain limitation. The HPC last stage blade height is restricted due to manufacturability and the effect of the losses from tip clearance on compressor efficiency. Also the HPC delivery temperature is controlled because of the HPC disc and HPT blades material properties. Similarly, the combustor output temperature is limited by HPT blade material consideration. The IPC pressure ratio is constraint with respect to icing. A very low IPC PR coupled with high intercooler effectiveness. This results in very low temperatures inside the intercooler. The intercooler is particularly susceptible to that as ice can form more easily within the small diameter tubes. The HPT blade metal temperature is limited by the available cooling system technology and the failure mechanism such as creep and fatigue. Auxiliary nozzle area cannot go beyond certain limit due to installation and aerodynamics considerations. It is expected that the aircraft to be able to take-off from majority of the airports. The climb time is constrained by the air traffic control requirements. Finally, for the propose of this study the block fuel burned was constraint to nominal design point as the main objective of conceptual aero engine design was to reduce fuel consumption, hence emission reduction.

4.3 Sensitivity Analysis

Prior to the optimisation studies of each engine configuration a sensitivity analysis was performed to decide the influence of small deviations of the major performance parameters. Consequently, the exchange rates are used.

Exchange rate is the term associated with the effects of slightly changing a particular parameter on all other engine parameters for a specified engine. For instance, the effect of 1% increase in HP compressor efficiency may result in increase or decrease of the specific fuel consumption of the engine. This process is also referred to as sensitivity analysis which indicates the extent to which the viability of an engine design is influenced by the variation of a particular design parameter.

The performed sensitivity analyses, using TERA2020 tool, are essential for successful design of experiments and optimisation studies. These results are helpful for a better understanding of the design domain for each engine configuration. In particular, the compiled sensitivity parameters allow to assess the impact of changes in a certain design variable and determine which design parameter is the key driver to concentrate more efforts on. These factors also allow assessing the importance of progress in specific component technologies for each engine configuration. Furthermore, these exchange factors help to quantify the impact of technology shortcomings and assess the impact of missing some technology targets. In general the sensitivity studies are conducted for the following purposes:

- Assessing the impact of input parameters on output parameters
- Identifying significant parameter interaction
- Quantify the impact of technology weaknesses

From the available algorithms provided by the integration environment, Isight, “Parameter Study” technique was chosen to study the sensitivity of the design to each factor independent of all other factors by executing $\pm 2\%$ single parameter variations from the nominal design points. The weak point of using “Parameter Study” is that one cannot look at the interaction among different factors.

Each variable allowed varying up to 19 levels in a specified bound. Whilst a single design parameter was varied each time, the rest of the design

parameters were kept frozen. In other words, each factor is studied at all of its specified levels (values) while all other factors are held fixed at their baseline. The specified ranges for the sensitivity analysis presented in CHAPTER 5 should be perceived as fractional percentage variations from the technology target value that was assumed. The study aims to investigate the effect of technology parameter deviations on engine time between overhaul, block fuel and specific fuel consumption.

It should be noted that the listed sensitivity parameters are the main engine design parameters for a certain configuration. Some of these parameters were used for the design space exploration and optimisation process and the rest were kept frozen. For the engine performance the main technology level indicators would be component polytropic efficiencies, duct pressure losses and allowable metal temperature. The metal temperature is chosen to assess the engine life in the Economics module and in this study it is not considered as technology parameter.

4.4 Parametric Studies

Before starting the design space exploration and optimisation, assessing the effect of major design parameters on the final engine design with respect to the time between overhaul, direct operating costs, block fuel burn, specific fuel consumption and engine weight is desirable. These assessments provide a rough estimate of optimal designs which can then be used as a starting point for the design space approximations and numerical optimisations.

Multidisciplinary framework of the TERA2020 tool was developed by the contribution of different organisations and teams. The modules of each discipline was delivered as standalone executable file (black box) and then integrated with the surrounding modules within an optimiser environment. Therefore, it was not possible to track the codes failure and modify the underlying assumptions when the models were not converging. Therefore,

using the Design of Experiment (DOE) techniques was an effective practice to identify the upper and lower bounds of the design parameters. Several iterations were performed to establish an appropriate range for each design variable. Finding a suitable range is therefore realised by subsequently reducing variable limits and employing the 2-D, 3-D and scatter graphs.

In general Design of Experiment (DOE) is a collection of statistical techniques providing a systematic way to sample the design space and then graphically illustrate the available design space in order to improve the original design. It is an essential technique for doing systematic statistical experiments to study the effects of multiple input variables on one or more output parameters. DOE is useful when tackling a new problem for which you know very little about the design space. Through the design of experiment critical factors can be highlighted and initial design point identified. Also these techniques allow the designers to determine the individual and interactive effects of design parameters that could affect the output results and identify those factors which have a relevant impact on the system's response.

Design of Experiment is often used before setting up a formal optimisation problem in order to identify key drivers among potential design variables, appropriate design variable ranges and achievable objective function values. Furthermore, the created data set by DOE can be used to generate approximation models of the design space. These surrogate models are intended to reduce the computational effort and allow the visualisation of the results.

In the current study in order to create the design space, "Full Factorial" and "Latin Hypercube" techniques among the others were applied during which a number of engine design parameters can be specified to vary as a percentage from their nominal value at top of climb (design parameters at TOC are varied around their nominal point). For Latin Hypercube technique the number of levels for each factor is equal to the number of points with random combinations. This technique allows many more points and more combinations can be studied for each factor. The engineer has total freedom in selecting the number of designs

to run as long as it is greater than the number of factors. However, they are not reproducible unless the same random seed is used consecutively. As the number of points decreases, the chance of missing some regions of the design space increases.

In Full Factorial technique the number of levels for each factor is specified and all combinations of all factors at all levels are studied. For p levels, all $p-1$ order effects can and all possible factor interactions can be evaluated. However, this technique can be very expensive for multiple factors at multiple levels. For example, 5 factors studied at 5 levels require 3125 design points.

The available techniques of the DOE is summarised as follow:

- Parameter Study:
 - ✓ Specify levels for each factor (design variable)
 - ✓ Change one factor at a time, all others at base level
 - ✓ Consider each factor at every level
- Full-Factorial Design:
 - ✓ Specify levels for each factor
 - ✓ Evaluate outputs at every combination of values
- Orthogonal Arrays:
 - ✓ Specify levels for each factor
 - ✓ Use arrays to choose a subset of the full-factorial experiment
 - ✓ Subset selected to maintain orthogonality between factors
 - ✓ Does not capture all interactions, but is efficient
 - ✓ Experiment is balanced

- Latin Hypercubes:
 - ✓ Divide design space uniformly into I divisions for each factor
 - ✓ Combine levels randomly: specify I points and use each level of a factor only once
- Optimal Latin Hypercube:
 - ✓ A modified Latin Hypercube, in which the combination of factor levels for each factor is optimised, rather than randomly combined
 - ✓ Gives the best opportunity to model the true function or true behavior of the response across the range of the factors.
- Central Composite Design:
 - ✓ A statistically based technique in which a 2-level full-factorial experiment is augmented with a center point and two additional points for each factor (called “star points”)
 - ✓ A popular technique for compiling data for Response Surface.
- Data File:
 - ✓ Provide a convenient way to define a set of trials outside of Isight, and still make use of Isight’s integration and automation capabilities
 - ✓ Any file(s) used must simply contain a row of tab or space separated values for each data point and a column for each parameter to be used as a factor from that file.

4.5 Design Space Approximation and Optimisation

Different optimisation procedures can be applied for optimising the proposed engine configurations. For the purpose of this study a semi-manual (step-wise)

optimisation procedure was applied. This procedure is capable of taking into consideration the discontinuity involved with the engine design as a result of component aerodynamic loads variation such as HPT stage count change. Using this procedure both the core and the low pressure system were optimised effectively.

As a first stage, the engine design variables that have a key influence in the optimisation process were organised in different groups. During the step study, a number of DOE studies were carried out for each step to provide an appropriate design space. The design parameters were varied around their nominal point without constraining the involved design variables or objective functions. These procedures allow the designer to illustrate the trend or influence of the involved parameters.

After a large number of TERA2020 simulations were carried out using DOE studies, approximation techniques were applied to generate a mathematical model of the design space data, which can then be used for quick and efficient design studies or optimisation. The following two approximation techniques are available in the approximation component:

- RBF Model - a neural network-based approximation technique
- Response Surface Model - a polynomial-based approximation technique

Based on the multiple data points generated previously, response surface model (RSM), a polynomial based approximation technique, was used to create and initialise the mathematical model. The available Error Analysis tool in the approximation environment indicates the degree of fit of approximation model to the exact model. For the approximation errors more than 1% the mathematical model is discarded and the new design space is created where more points in DOE are defined to make the design space smooth. As already mentioned, the step changes in the design space were experienced mainly due to turbomachinery stage number variation. However, the turbomachinery stage count change is unavoidable which may cause design space discontinuities.

As a final step an optimisation was conducted using design search option to maximise engine time between overhaul. During the optimisation with TERA2020, different engine designs are continuously evaluated by the optimiser as it searches for the optimal solution. It is noted here already that the engine design space is non-linear and sometimes discontinuous. Therefore, selecting a suitable optimisation algorithm for the problem was very important.

Two techniques have been used in the optimisation; the adaptive simulated annealing algorithm (ASA) and Sequential Quadratic Programming (NLPQL). The ASA algorithm can handle discontinuities, it implies randomness to find a global optimum, and it does not need gradient information. The NLPQL algorithm was used to exploit local area around initial design point: this enabled the rapid achievement of the local optimum design and handling of the inequality constraints used. It is gradient-based and therefore converges quickly and precisely to a local optimum. It cannot go around discontinuities, though. A combination of both algorithms was applied which can lead to very precise and global optima even in discontinuous nonlinear design spaces. [90]

The design space explored using the approximate models where the selected optimisation algorithms employed to find the maximum time between overhaul that obeys a given set of design constraints. As the NEWAC engines originally were designed to reduce fuel burn, during the optimisations for maximum TBO the block fuel burn was constrained to nominal design point block fuel burn values. Designs that fail to meet the constraints set by the user are discarded as infeasible. There are two ways to rule out infeasible combinations during optimisation; applying constraint set or limiting the variables range. Finally the results are presented in the form of contour plots and tables.

CHAPTER 5 AERO ENGINES LIFE ASSESSMENT

This chapter presents the results achieved from the course of evaluation and optimisation of a conventional turbofan engine and an intercooled turbofan aero engine. Both the core and the low pressure system were assessed and optimised with respect to maximum time between overhaul.

5.1 Introduction

The competitive civil aviation market addresses a need for fuel efficient, environmental friendly propulsion systems with prolonged service life for the future. Every innovative technological solution is in fact associated with acquisition, maintenance, and operative cost of the power plant. The optimum engine cycle for performance and engine life are different. Consideration of these challenging aspects of gas turbine development programs are significant and need to be addressed at the earliest possible stage of the design procedure where the fundamental decisions are taken which will be influential in the overall cost of the project.

Therefore, the objective of this section is to assess the effects of engine design parameters on time between overhaul and maintenance cost of the engine, for a typical long range mission. Particular attention is paid to explore the design space and matching the engine key design parameters in order to extend the gas turbine service life (time between overhaul). This should allow an optimum thermodynamic cycle design to be chosen for best economy.

The reduced direct operating costs are attributed to the significantly reduced engine production and maintenance costs of the fuel optimal design; the reduction in the cost of fuel also benefits direct operating costs. The direct operating cost of the engine is derived as a function of maintenance cost with the cost of taxes on emissions and noise, the cost of fuel, the cost of insurance and the cost of interest paid on the total investment. Thus great attention is paid

to improve the engine time between overhaul which means lower maintenance cost and direct operating cost accordingly. The life estimation methods are discussed in CHAPTER 2.

The simulation results obtained from the process of evaluation and optimisation of aircraft propulsion systems using TERA2020, a multidisciplinary assessment environment, are described. Different engine configurations will be optimised for minimum direct operating cost (DOC) and maximum time between overhaul (TBO) for their respective business case. These simulations focused around the nominal design and intended to analyse the engine life extension criterion both at design point and off-design conditions. The main economic drivers of the civil aero engines are the fuel consumption and the time between overhauls. In the previous studies of the NEWAC project, new core engine concepts are investigated and optimised for minimum fuel consumption. In the current study the NEWAC engines optimised for maximum time between overhaul. However, these contradicting objectives should be considered simultaneously to find an optimal economical solution.

The design space of each configuration is then explored to illustrate the trend or influence of the involved parameters and visualise the design space. From the available design of experiments (DOE) algorithms the most suitable one is chosen since, during the search for optimal points, discontinuities could be encountered. Finally two different approaches, manual and automatic, have been utilised to optimise the engine/aircraft combination for minimum direct operating costs (DOC) and maximum time between overhaul (TBO). The life of the conceptual engines is studied at the different operating conditions.

Both the core and the low pressure system of the conventional baseline engines and innovative conceptual engines have been assessed from economics point of view. It should be noted that the sensitivity analysis, approximation and optimisation results presented in this chapter are only reasonable within the validity of the underlying assumptions. Therefore, to realise the results presented in this chapter, the underlying assumptions and simplification of the TERA system need to be understood first. Hence, the reader is referred to

TERA assessments process in CHAPTER 4. In the current study noise criterion was not considered since the noise model is unable to calculate the noise of 3-nozzle engines and heat-exchanger noise effects. To have a complete overview of the NEWAC technology development, two different aircraft are taken into account. These are the A320 aircraft type for short range application and A330 type for long range application

5.2 BASELR Configuration

The basis of the work reported herein is the Rolls-Royce Trent 772B-60 engine. The EVA code [76] has been introduced in NEWAC by Cranfield University for developing the performance model of the Baseline for long range application. This is a 3-shaft configuration turbofan with the separate exhausts for the bypass and core flow. It has a single stage fan, eighth stages IP compressor, six stages HP compressor, single stage HP turbine, single stage IP turbine and four stages LP turbine. The design point is set at Top of climb (TOC) with altitude of 10668 [m] at hot day condition (ISA+10). A summary of the engine specification and power setting is given in Table 5-1.

Table 5-1 *BASELR engine performance specifications*

Parameter	Unit	Rating		
		<i>Take-off</i>	<i>Top of Climb</i>	<i>Cruise</i>
Altitude	[m]	0	10668	10668
Mach number	[-]	0.25	0.82	0.82
DTAMB	[K]	15	10	0
Inlet mass flow	[kg/s]	924	360	341
Core mass flow	[kg/s]	154	62	55
Bypass ratio	[-]	5	4.9	5.3
Fan pressure ratio	[-]	1.77	1.8	1.66
Overall pressure ratio	[-]	37	38	31
Combustor outlet temperature	[K]	1794	1620	1381
SFC	[g/(kN*s)]	13	17.89	16.49
Thrust	[kN]	268	68	51

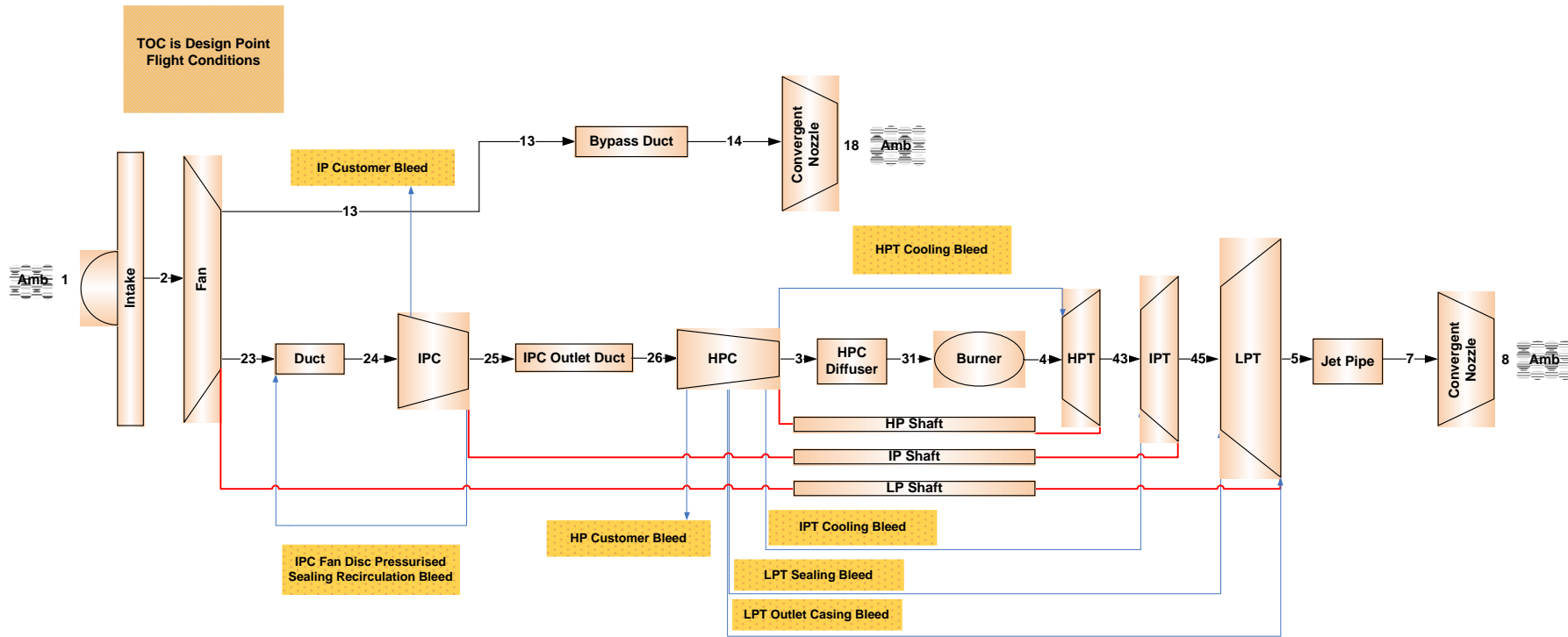


Figure 5-1 BASELR configuration schematic [77]

5.2.1 Sensitivity Analysis of BASELR Configuration

Initially, a sensitivity analysis is performed to distinguish the influence of small deviations of the main performance parameters from the engine nominal design point. The outcomes of these studies provides crucial basis for successful optimisation study. They provide the starting points for the optimisations through the identifying design variables and their reasonable range for the final optimisation. This procedure is carried out again when the engine configurations are optimised to assess the stability of the optimal engine design. More details about the sensitivity analysis are given in CHAPTER 4.

Both performance and engine service life are affected by many design features. It would consume many times the effort that all were considered. For the purpose of this study 18 parameters considered as listed in Table 5-2.

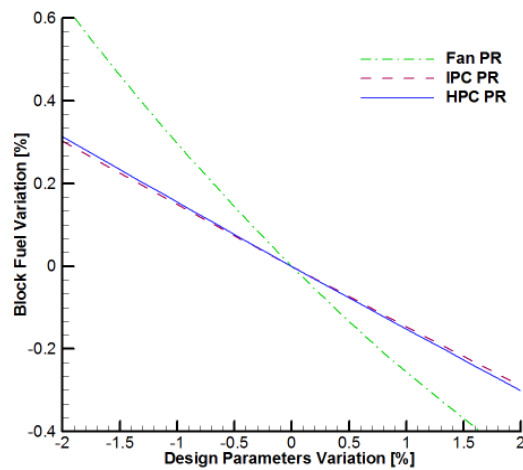
Table 5-2 BASELR sensitivity parameters

Parameter	Range	Unit
Fan tip pressure ratio	-2%... +2%	%
Fan tip polytropic efficiency	-2%... +2%	%
IPC pressure ratio	-2%... +2%	%
IPC polytropic efficiency	-2%... +2%	%
HPC pressure ratio	-2%... +2%	%
HPC polytropic efficiency	-2%... +2%	%
HPT polytropic efficiency	-2%... +2%	%
IPT polytropic efficiency	-2%... +2%	%
LPT polytropic efficiency	-2%... +2%	%
Fan inlet mass flow	-2%... +2%	%
Core mass flow	-2%... +2%	%
TET for climb rating	-2%... +2%	%
HPT cooling mass flow	-2%... +2%	%

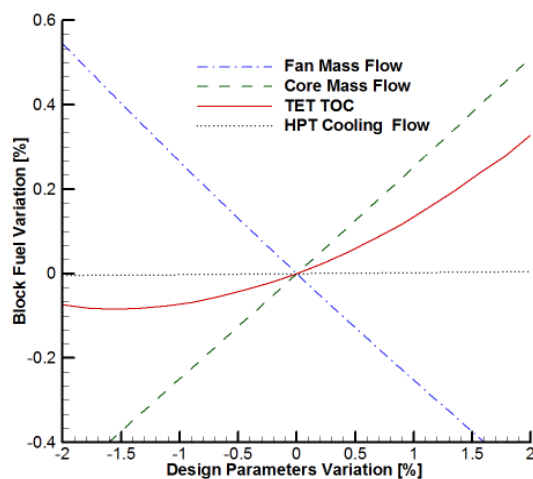
The sensitivity analysis shows that perturbation of design features has a sophisticated influence on engine service life rather than block fuel. These effects are presented in Figure 5-2 and Figure 5-4. The general trends of the

fan, IPC and HPC pressure on block fuel are similar, although it is noted that the influence of fan pressure ratio variation is more prominent.

As core mass flow increases, the block fuel tends to increase. Inversely, increasing fan mass flow improves the block fuel. It is well known that improving components efficiency gives plenty of block fuel benefits. Increasing the low pressure system component efficiency, namely fan and LPT, has a higher impact on the block fuel.



(a)



(b)

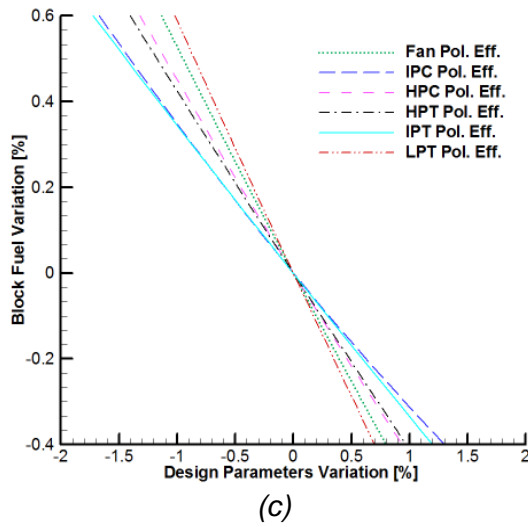
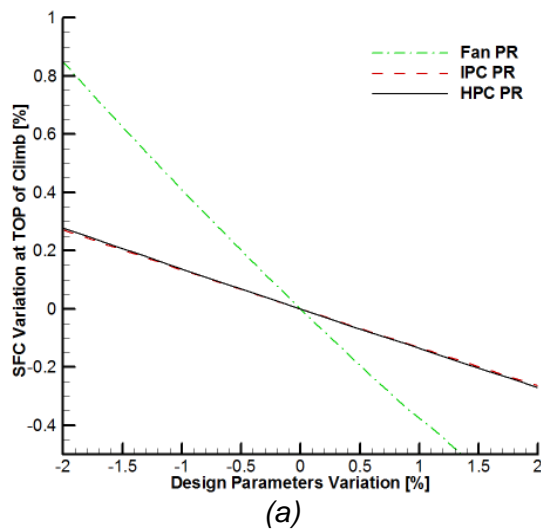


Figure 5-2 BASELR Block fuel sensitivity analysis

It should be noted that the variation of HPT cooling mass flow, definitely, effect the engine fuel consumption. As mentioned previously, the sensitivity studies are considered for small changes and for that reason the effect of HPT cooling mass flow on objective functions such as Block Fuel Burn are not pronounced. However, this variation is noticeable for the engine SFC as shown in Figure 5-3.



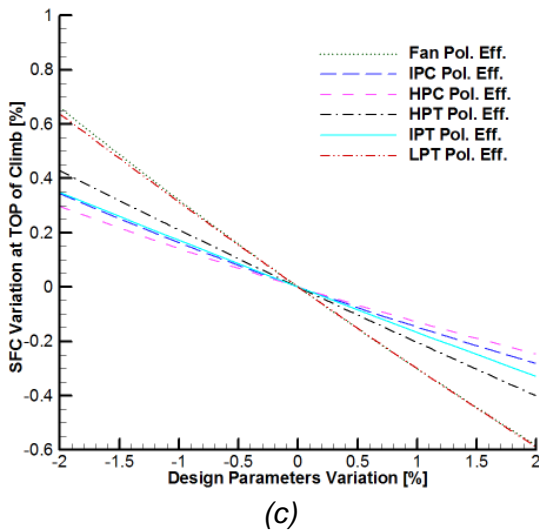
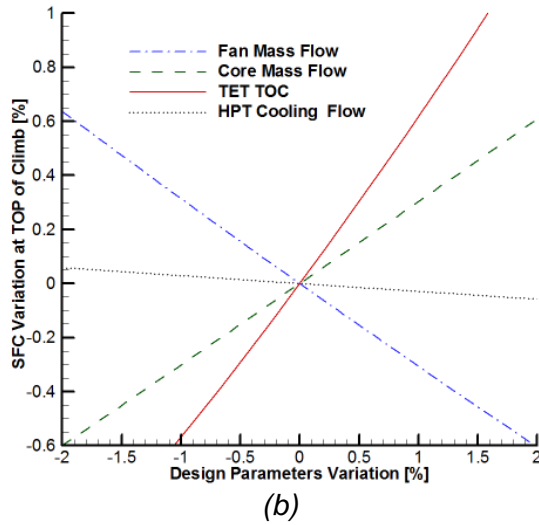
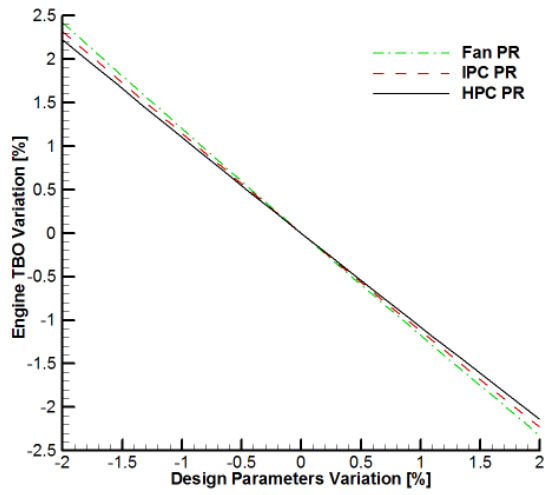


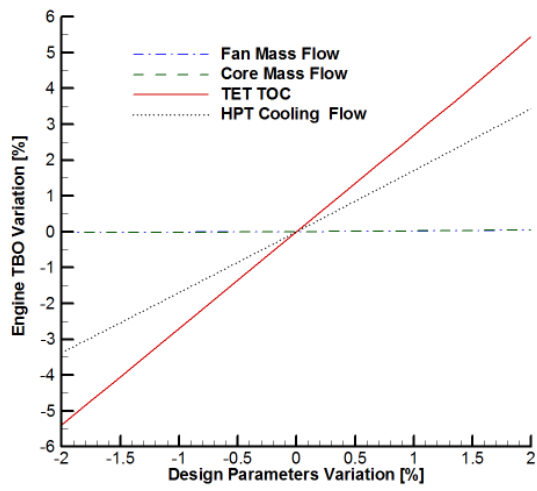
Figure 5-3 BASELR SFC at top of climb sensitivity analysis

The trend of the fan, IPC and HPC pressure ratio on the engine life is quite similar. It is shown, not surprisingly, that increasing both the combustor outlet temperature and HPT cooling mass flow improves the engine life. Increasing the former results in higher engine thrust and consequently reduces the time to climb. Hence the effect low cycle fatigue, as a time/temperature dependent mechanism, at top of climb is reduced.

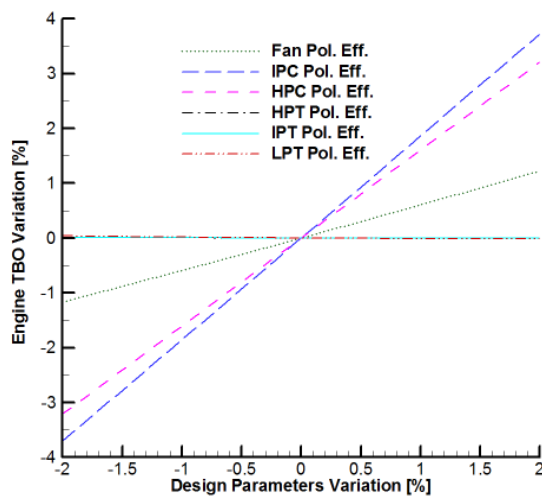
The effect of IPC and HPC component efficiency on engine life is more pronounced amongst the other component efficiencies (Figure 5-4).



(a)



(b)



(c)

Figure 5-4 BASELR TBO sensitivity analysis around nominal point

5.2.2 Parametric Study of BASELR Configuration

An attempt has been made here to investigate the effect that the main engine design parameters have on time between overhaul, DOC, specific fuel consumption, fuel burn and weight of the BASELR configuration. Both performance and engine life are affected by many engine design features, and if all were considered, it would consume many times the effort that could be put into a document such as this. The work presented herein is therefore restricted to matters associated with the effects of fan and core sizing, IPC/HPC pressure ratio and engine rating. This study is carried out at hot day top of climb conditions (TOC) and at variable thrust levels. Design parameters are allowed to vary in a reasonable range. Nevertheless, for some parameters wide ranges are considered to demonstrate the changes on objective functions. In the results presented in this section, the pink dot indicates the nominal design point. From the design parameters listed in Table 5-3 only one parameter at a time is being varied around the nominal point, while the rest are kept constant. It should be kept in mind that all parameters have certain bounds due to variety of reasons. These are explained in constraint section of CHAPTER 4.

Table 5-3 *BASELR design space parameters and investigated range*

Parameter	Range		Unit
	<i>Lower</i>	<i>Upper</i>	
Fan tip pressure ratio	-2.48	+1	%
IPC Pressure ratio	-30	+25	%
HPC Pressure ratio	-26	+22	%
Fan inlet mass flow	-4.25	+16	%
Core mass flow	-13	+4.32	%
TET for climb rating	-4.5	+1.5	%
HPT cooling mass flow	-23	+50	%

5.2.2.1 Fan tip pressure ratio

The engine fan tip pressure ratio at top of climb is varied (and hence the overall pressure ratio). As the fan tip pressure ratio is increased, the engine propulsive efficiency will improve leading to better SFC and engine weight. Inversely, the engine time between overhaul will drop leading to higher maintenance cost. This is attributed to the negative effect of increased overall pressure ration on the cooling flow temperature of the HPT component. On the other hand, the HPT metal temperature will increase which decreases the components life. These results are depicted in Figure 5-5. (Ref. Appendix A.)

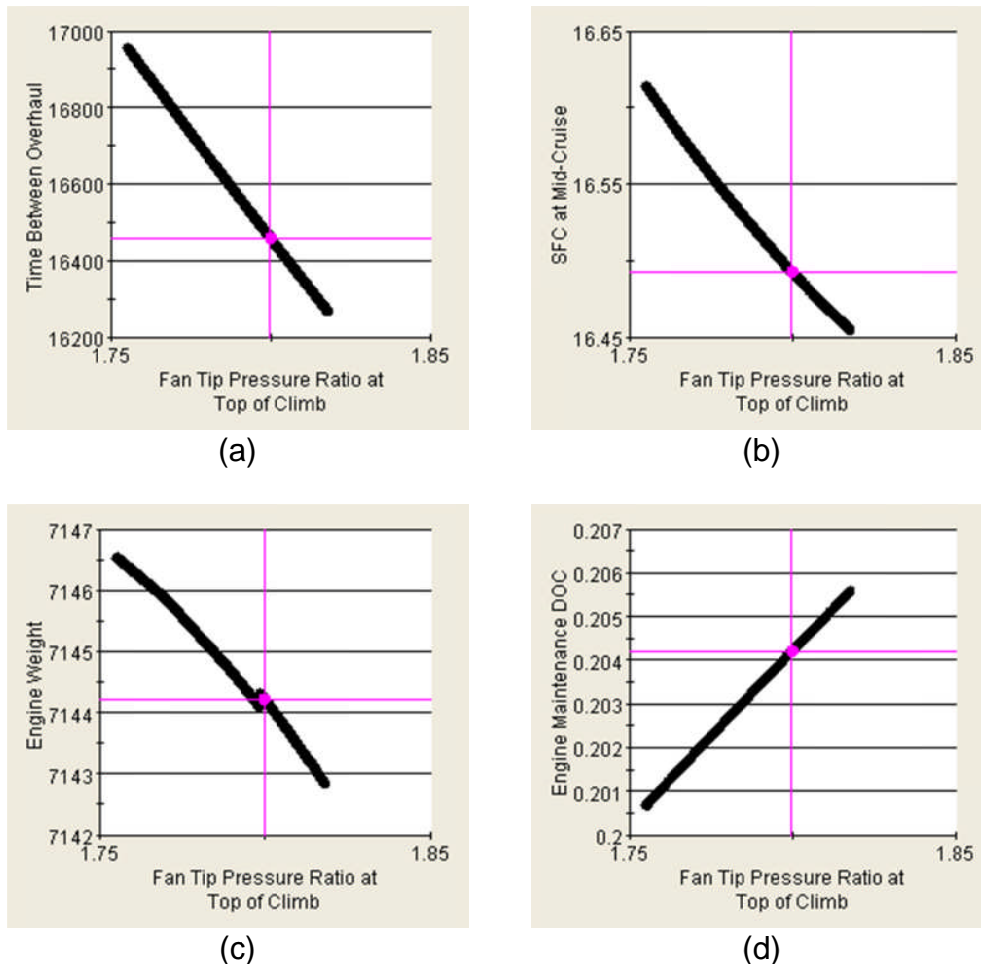


Figure 5-5 BASELR Fan tip pressure ratio variation at top of climb

The design space discontinuity observed in Figure 5-5 (c) as a result of the aerodynamic loads variation. At a fixed core size, increasing the fan tip pressure ratio requires more power supplied by the LPT unit. This leads to a change in the length or the stage count of the LPT. The magnified picture is shown in Figure 5-6.

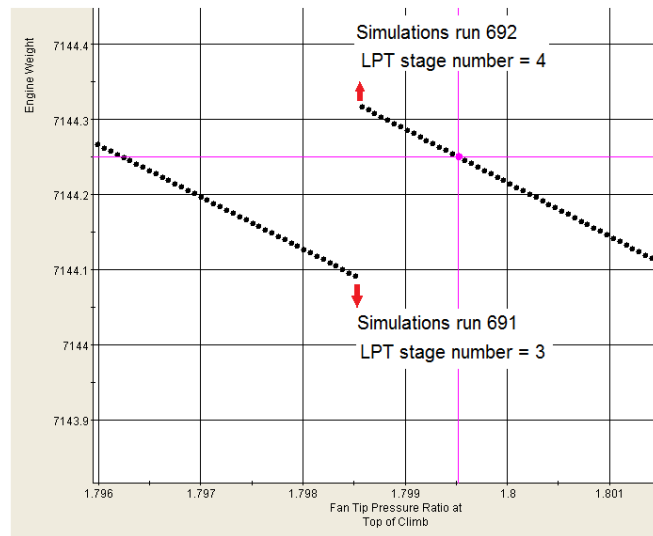


Figure 5-6 Example of LPT stage count change

5.2.2.2 Fan mass flow

The engine fan mass flow at top of climb is varied (and hence the bypass ratio). With a fixed core mass flow, increasing the engine fan mass flow will increase the bypass ratio and reduce the specific thrust. This will result with an increased propulsive efficiency which improves the engine fuel burn. Similarly, the engine time between overhaul will benefit from this. Mainly the increased thrust levels improve the climb time and hence the HPT blade materials are less exposed to severe thermal condition. Consequently, better fatigue, creep and oxidation life of the components are expected. On the other hand reduced specific thrust are directly linked with substantial increase in nacelle diameter and therefore engine weight. However, the rates of thrust level increase faster than engine weight. These are shown in Figure 5-7.

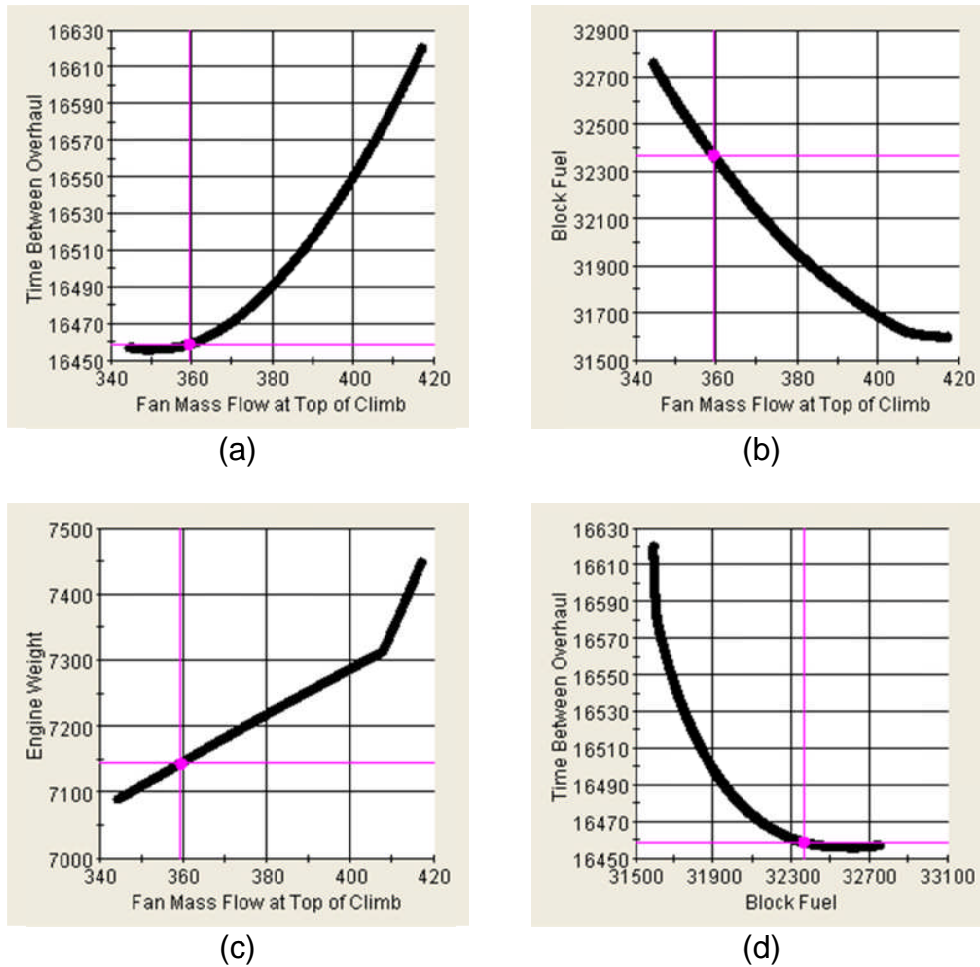


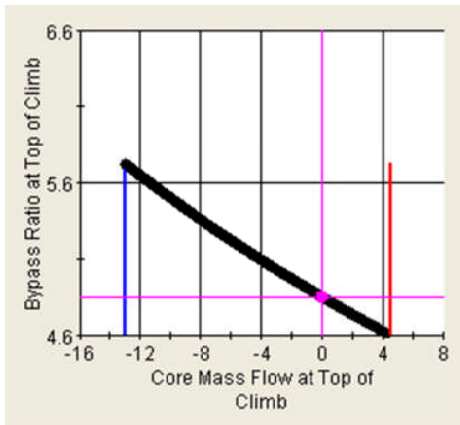
Figure 5-7 BASELR Fan mass flow variation at top of climb

5.2.2.3 Core mass flow

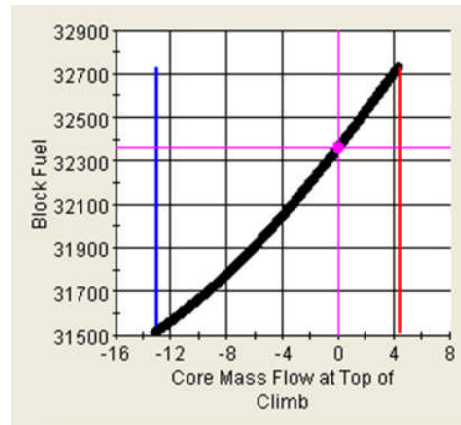
Core inlet mass flow at top of climb is varied (and hence the bypass ratio) where the engine fan mass flow is frozen. Increasing the core inlet mass flow at a fixed engine inlet mass flow essentially reduces the engine bypass ratio. Furthermore, increasing the core mass flow will result in an increase in engine SFC and block fuel burn. The reason for this is the increased amount of fuel flow for a given combustor outlet temperature.

In this investigation, no stage change is observed on the turbomachinery components. Thus, the increased density of the core air decreases engine weight as well as production cost. The production cost follows the trend of the

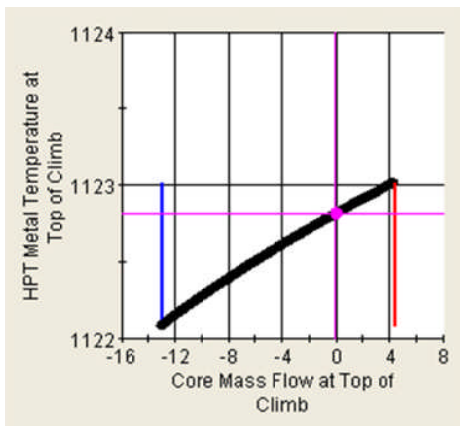
weight change. With the increased air density and fuel flow the HPT metal temperature increase and the blade life deteriorate. As a result, the engine maintenance cost goes up, even though the engine weight decreases due to increased air density. The effect of core inlet mass flow variation is illustrated in Figure 5-8.



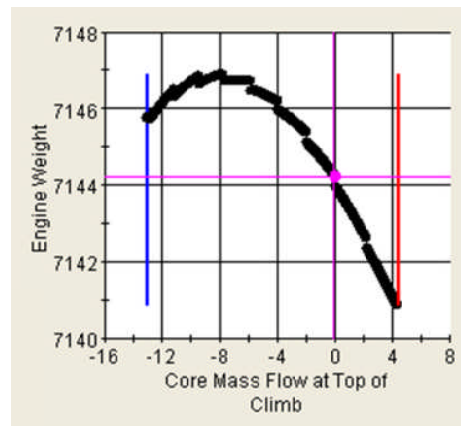
(a)



(b)



(c)



(d)

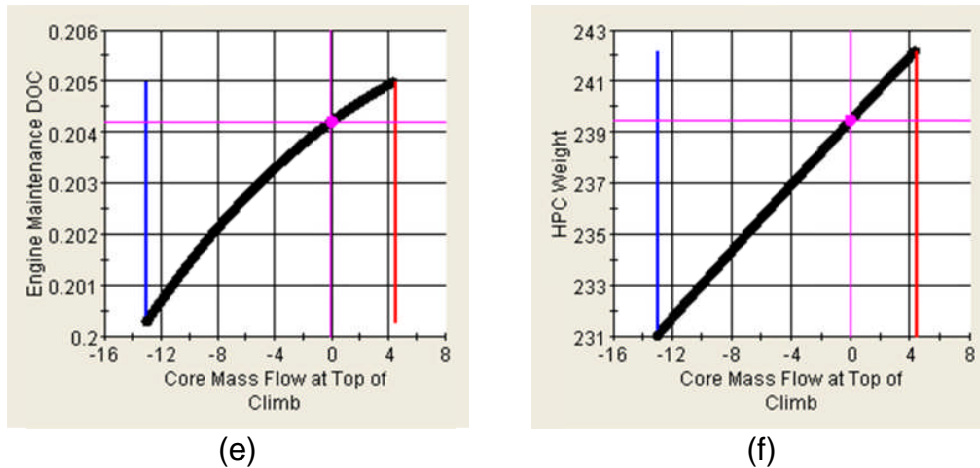
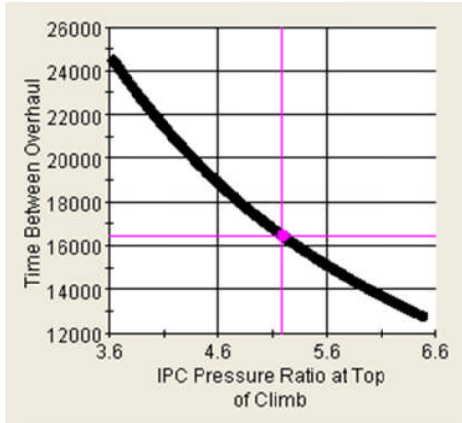


Figure 5-8 BASELR Core mass flow variation at top of climb

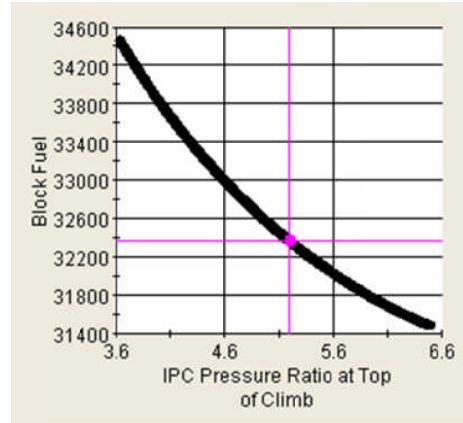
5.2.2.4 Intermediate pressure compressor pressure ratio (IPC PR)

Within this investigation the IPC pressure ratio at top of climb is varied and hence the overall pressure ratio (at fixed BPR). It can be seen in Figure 5-9 that increasing IPC pressure ratio has a negative effect on engine life and at the same time beneficial for fuel burn. This is effectively attributes to the OPR changes. As the engine overall pressure ratio moves towards the IPC pressure ratio, propulsive and overall efficiency of the engine improves due to increased jet velocity ratio. Therefore the SFC reduces. Nevertheless, there is an optimum value of the IPC pressure ratio for maximum thermal efficiency because of the reduced engine hot thrust.

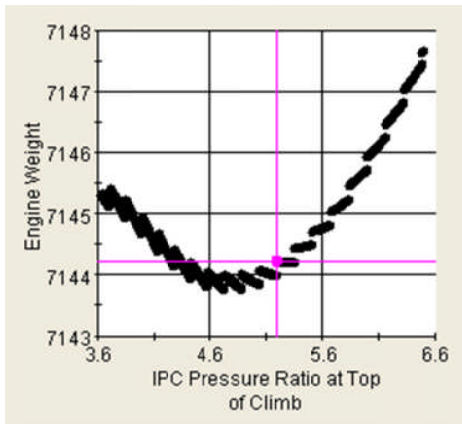
The negative impact of increasing IPC pressure ratio on engine life attributes to the increased cooling flow temperature and climb time as shown in Figure 5-9.



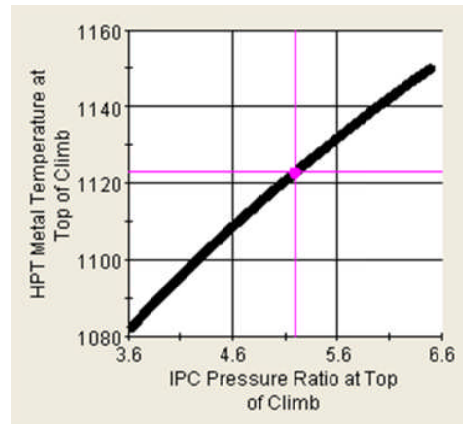
(a)



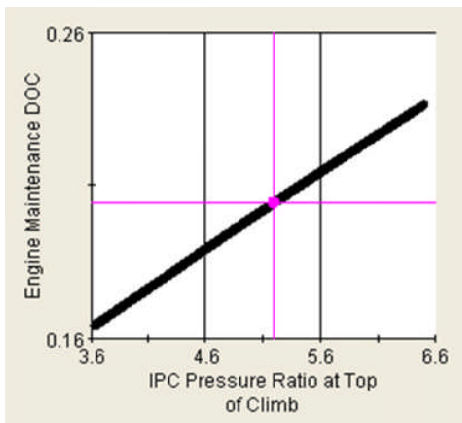
(b)



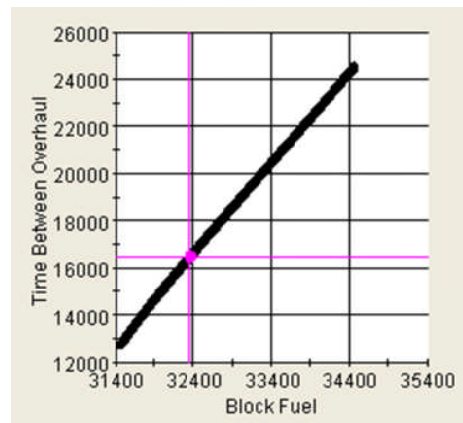
(c)



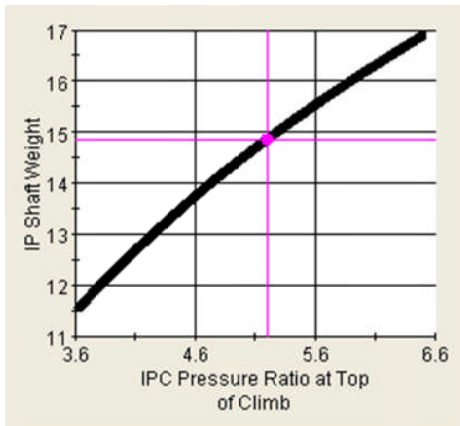
(d)



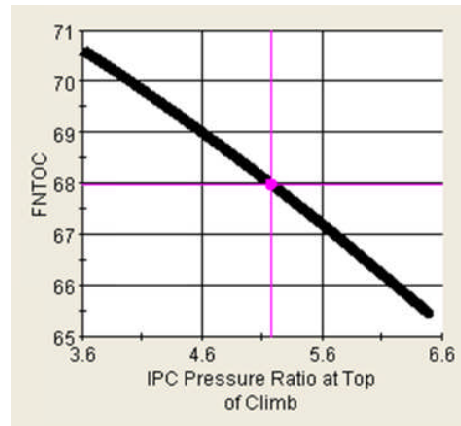
(e)



(f)



(g)

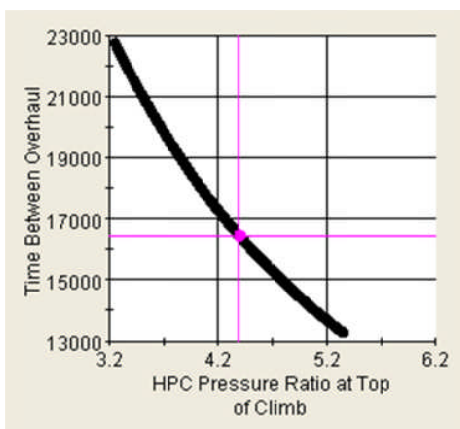


(h)

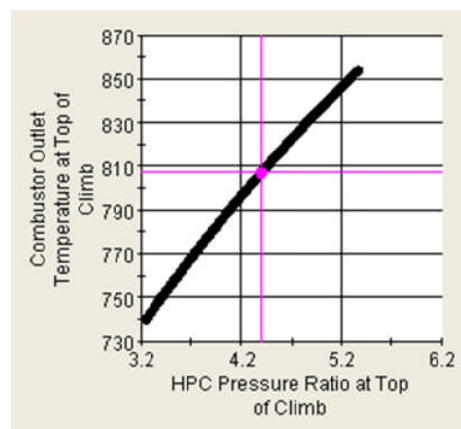
Figure 5-9 BASELR IPC pressure ratio variation at top of climb

5.2.2.5 High pressure compressor pressure ratio (HPC PR)

The HPC pressure ratio at top of climb is varied (and hence the overall pressure ratio). Similar effects of HPC pressure ratio on engine time between overhaul and block fuel burn is observed, compared to the IPC for the same reasons as illustrated in Figure 5-10. It is noted that there is a great potential of engine weight reduction through increasing HPC pressure ratio. Although, due to the increase in OPR, the optimum HPC pressure ratio is restricted by the maximum allowable HPC delivery temperature.



(a)



(b)

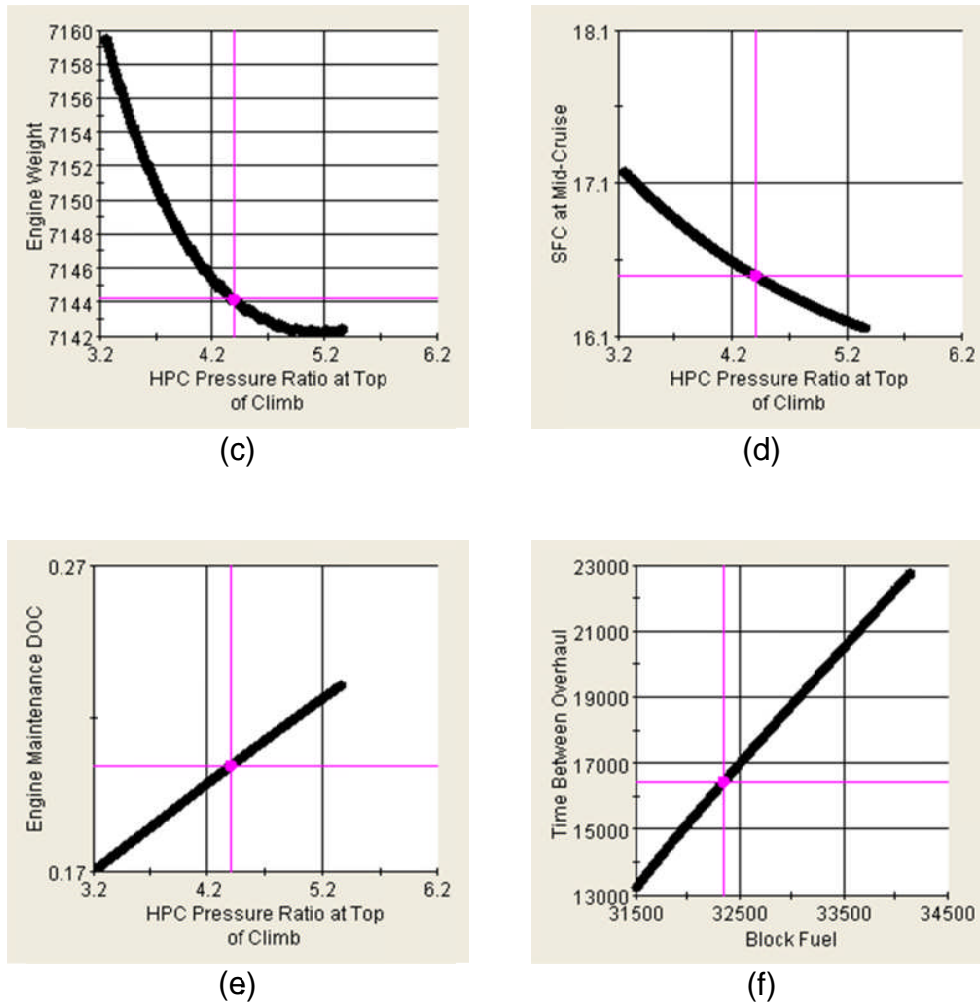
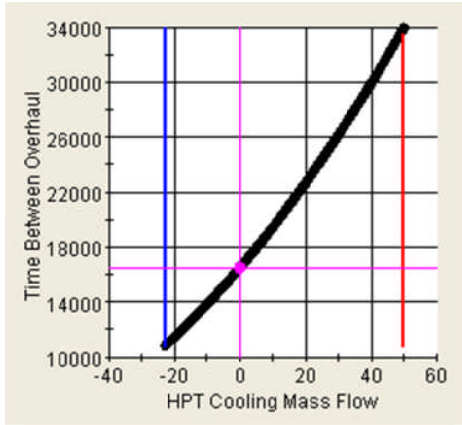


Figure 5-10 BASELR HPC pressure ratio variation at top of climb

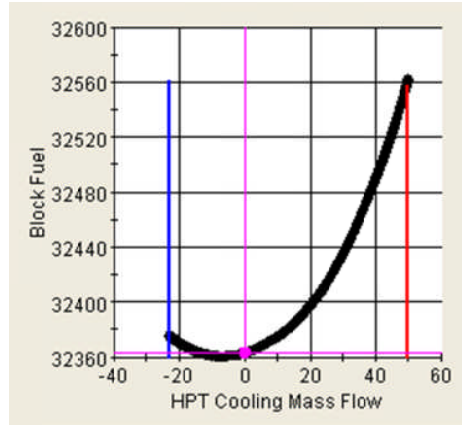
5.2.2.6 HPT Cooling mass flow

Herein the HPT cooling flow at top of climb is varied at a fixed Turbine entry temperature (TET), fan mass flow, bypass ratio (BPR), and compressor pressure ratio. Time between overhaul improvements was expected and can be observed in Figure 5-11.

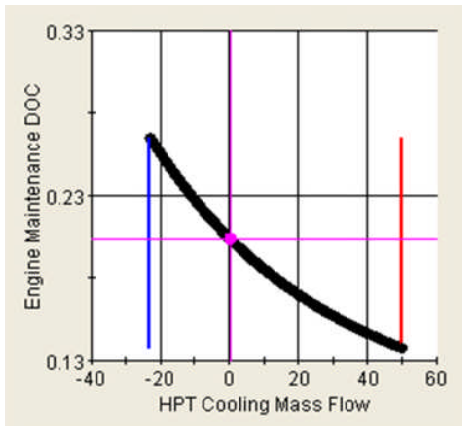
It can be seen that the amount of HPT cooling flow amplifies the engine life improvement. Thermal efficiency of the engine is strongly influenced by turbine cooling flow since the increasing the cooling flow increases HPC required power (and hence HPC, HP Shaft weight).



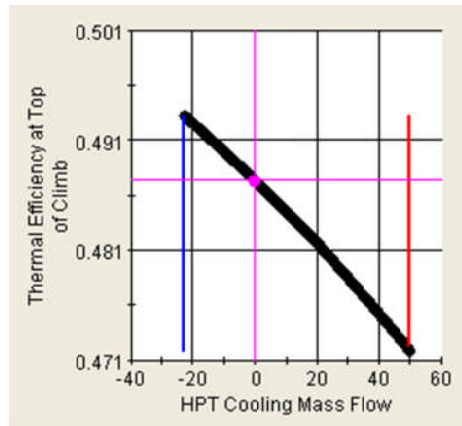
(a)



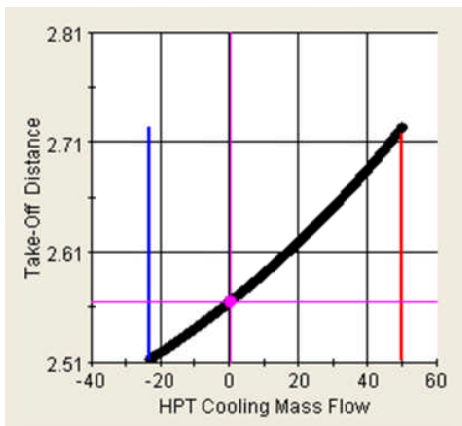
(b)



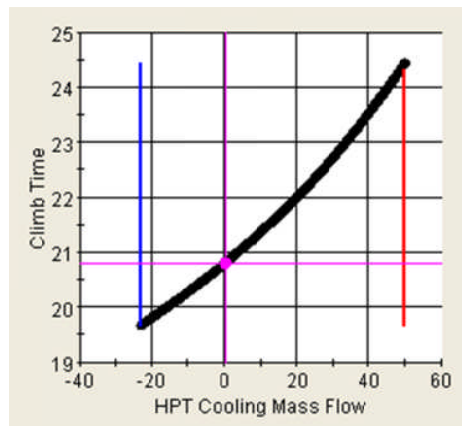
(c)



(d)



(e)



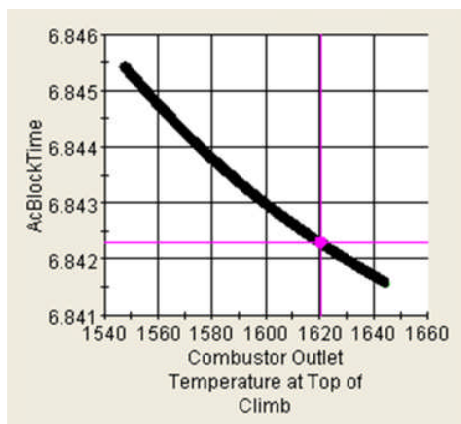
(f)

Figure 5-11 *BASELR HPT Cooling mass flow variation at top of climb*

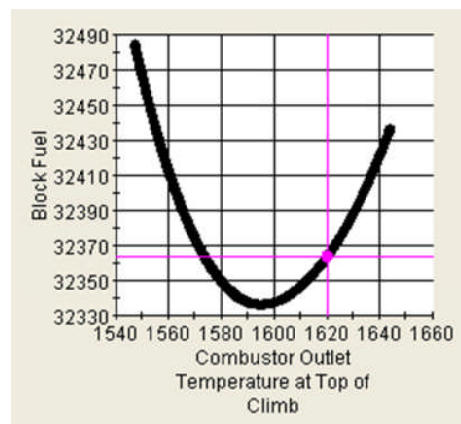
5.2.2.7 Combustor outlet temperature

Combustor outlet temperature at top of climb is varied and the corresponding engine thrust level (at constant combustor pressure loss and HPT cooling mass flow) to investigate the effects on the engine life and performance. Setting combustor outlet temperature is a complex process where the aircraft performance requirements, engine performance criterion, and engine service life should be considered. Higher combustor outlet temperature is limited with allowable HPT blade material, while the lower combustor outlet temperature restricted due to lower engine cycle efficiencies. Also, the engine with lower combustor outlet temperature cannot meet the customer requirements such as take-off length.

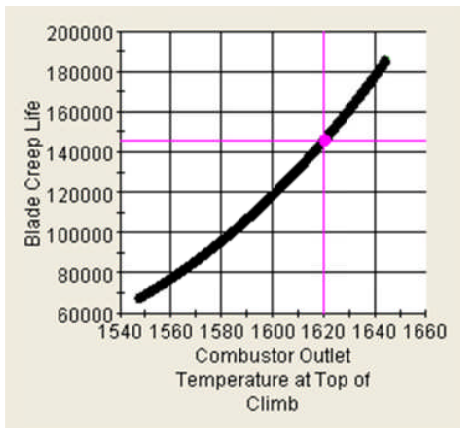
In Figure 5-12 it can be seen that at top of climb condition increased combustor outlet temperature interestingly improves time between overhaul. This is perceived to be related to a faster climb to height due to higher specific thrust of the engine. As the engine inlet mass flow is fixed at top of climb condition, increased combustor outlet temperature results in higher engine thrust with lower engine weight. A 6% increase in combustor outlet temperature (~100K) can reduce the flight mission time by 0.5% (at a fixed range). Therefore, one would say that at top of climb condition the time parameter dominates the temperature parameter in the engine life calculation algorithms, namely blade creep, fatigue and oxidation routines.



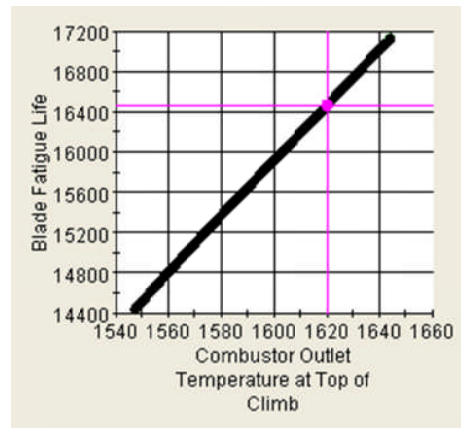
(a)



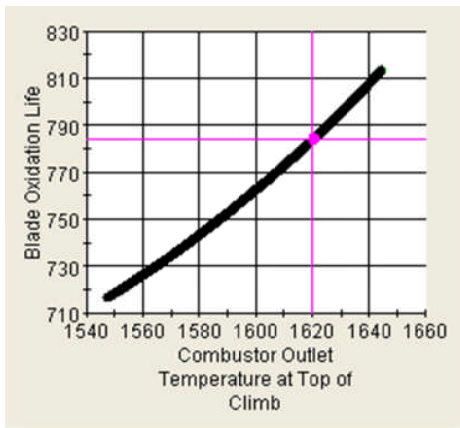
(b)



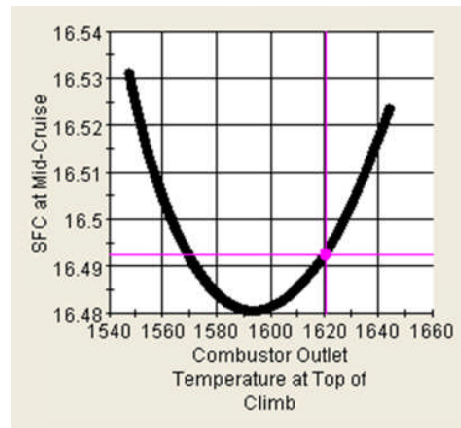
(c)



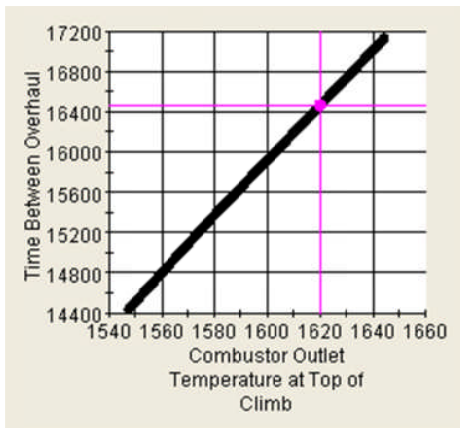
(d)



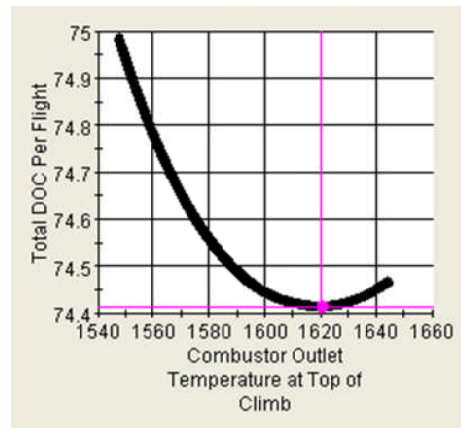
(e)



(f)



(g)



(h)

Figure 5-12 BASELR Combustor outlet temperature variation at TOC

5.2.3 Optimisation of BASELR Configuration

The thermodynamic cycle optimisation of the BASELR configuration with respect to the maximum time between overhaul is presented in this section. Based on the lessons learned from the sensitivity analysis and the parametric design space exploration, design variables were allowed to deviate from their nominal value. The range investigated is wide enough to create a design space without affecting the stability in TERA2020 modules. For instance, at a fixed core size, fan pressure ratio (FPR) and bypass ratio (BPR) cannot go beyond a certain limit where the fan eventually will require more power than that what can be delivered by the LPT. Due to the broad range of constraints, the number of infeasible designs is large at the beginning of the optimisation. Therefore, careful monitoring of the variable configurations is necessary. Thus non-feasible combinations can be discarded manually, limiting the boundary conditions to a reasonable design space.

Finding an optimum design is realised by subsequently reducing variable limits. The non-feasible designs cause interruptions in single modules of the code. The Performance and the WeiCo module are the two most likely to fail. Non-feasible designs are ruled out by either interruptions of the module codes (e.g. when maps cannot be extrapolated) or by constraints. It should be kept in mind that all parameters have certain bounds due to variety of reasons. These are explained in the “constraints” section of CHAPTER 4.

For a better understanding of the design space, the optimisation was performed in three steps. As a first step, the fan pressure ratio, fan mass flow and the core mass flow were optimised to achieve the best engine design in terms of time between overhaul. With these 3 design variables fixed at the optimal design values identified in step 1, the IPC pressure ratio and HPC pressure ratio were optimized next. After this, all the optimisation variables in step 1 and 2 were frozen to the optimal values and step 3 was carried out. The final optimum was the output of all three optimum steps. The following engine design variables that

have a major influence on engine and aircraft system were chosen for optimisation, as listed in Table 5-4.

Table 5-4 BASELR engine optimisation steps, variables and ranges

Step	Parameter	Range [%]
1	Fan inlet mass flow	-4.25...+16
	Core mass flow	-10...+2
	Fan tip pressure ratio	-6... +1
2	IPC Pressure ratio	-30... +15
	HPC Pressure ratio	-20... +15
3	Combustor outlet temperature	-6... +1
	HPT cooling mass flow	-25... +50

During the optimisation procedures using TERA tool, different engine design was evaluated to find the optimum design. The feasibility of the optimum design was judged using the constraints. The constraints set for the current optimisation problem are given in Table 5-5.

Table 5-5 BASELR engine design space constraints

Constraint	Bound		Unit
	Lower	Upper	
FAR take-off distance	-	2.5	km
Climb time to 35000 [ft]	-	22.5	min
IPC design pressure ratio	2.7	-	-
HPC design pressure ratio	-	5.5	-
HPC delivery temperature	-	800	K
Combustor outlet temperature	-	1700	K
HPT blade metal temperature	-	1150	K
Block fuel burn	-	32400	Kg

In the counter plots presented in this section, the Pink point indicates the engine design point and the Black ones represent the optimal design with respect to the time between overhaul.

5.2.3.1 Fan and core sizing

Fan pressure ratio, fan inlet mass flow and core mass flow are the main parameters of concern when sizing the engine. As a first step, these parameters were examined at top of climb to achieve an optimal engine design in terms of time between overhaul (TBO) using TERA2020 software. Increasing fan mass flow (and hence a bigger fan diameter) at a fixed core size would be beneficial for the engine SFC due to propulsive efficiency improvement as it can be seen from Figure 5-13. There is a limit on how far fan mass flow can be increased. The engine weight gets excessive in the upper left corner of the contour which violates the block fuel burn limit and further reduction of fan tip pressure ratio violates the take-off field length constraint. These limits are highlighted in the contour plot. With all the other parameters in Table 5-4 fixed at nominal design, the projected benefit from increasing fan mass flow of 3.8% at fan pressure ratio of -2% was about 0.3% reduction in specific fuel consumption.

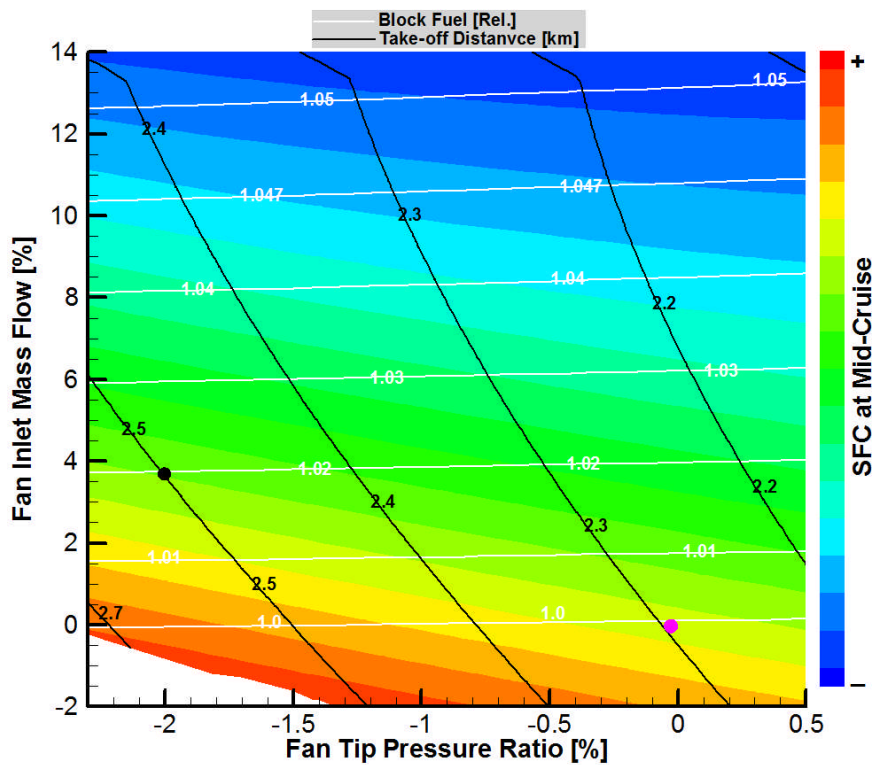


Figure 5-13 Variation of SFC with core mass flow and fan pressure ratio

On the other hand, increasing the fan diameter at a fixed tip speed reduces the fan rotational speed which can very well moderates the centrifugal loads of the HPT disc and blades. Also, the reduced fan tip pressure ratio improves the HPT cooling temperatures due to reduced overall pressure ratio. Thus, together with the block fuel, the time between overhaul was improved with about 2.4%, as illustrated in Figure 5-14.

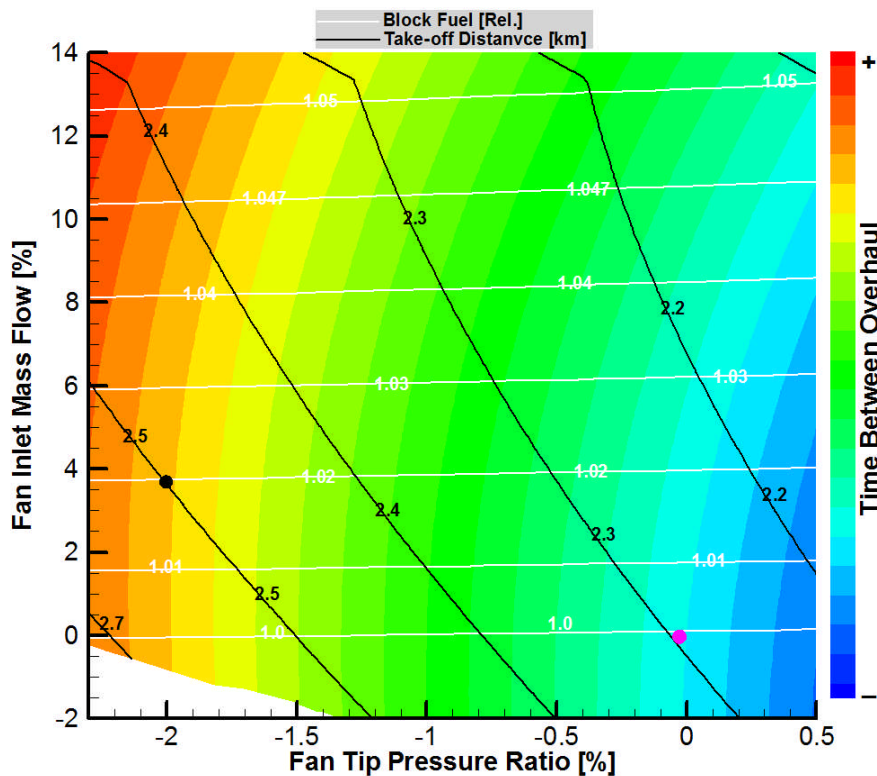


Figure 5-14 Variation of time between overhaul with fan mass flow and fan pressure ratio

The maintenance cost is proportional to the engine weight, production cost and time between overhaul. It was observed that some of the block fuel benefits were negated by the bigger fan diameter which results in a heavier engine with about 0.7% more than nominal design. Production cost follows the weight trend, which also increased by 0.1% and has had a negative influence on the maintenance costs. Nevertheless, the maintenance cost of the engine was

improved by 4.8% compared to the nominal engine. One would argue that the TBO is the main driver for the engine maintenance costs. As one moves towards the lower left corner of Figure 5-15 the maintenance cost reduces. Further reduction of fan tip pressure ratio violates the take-off field length and time to climb constraints.

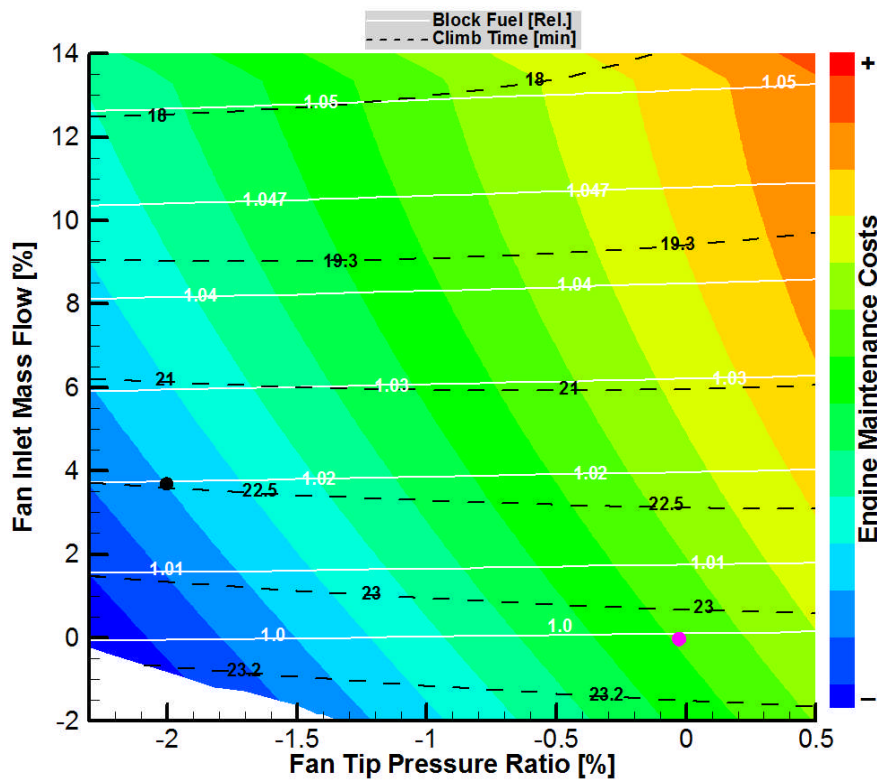


Figure 5-15 Variation of engine maintenance costs with fan mass flow and fan pressure ratio

Principally, decreasing the core mass flow (and hence core size) results in a reduced engine weight and contributes to the block fuel burn reduction. However, there is a lower bound on the core size which is imposed by the runway length and also the climb time to altitude. By reducing the core mass flow about 3.2% and fan pressure ratio about 2.7% from nominal design point a further fuel saving was achieved. A 0.8% reduction in SFC due to thermal efficiency improvements was achieved. On the other hand the engine take-off

and top of climb thrust drops with about 1.5% which extends the runway length and the climb time. Variation of block fuel burn with core mass flow and fan tip pressure ratio with a fixed fan size is illustrated in Figure 5-16.

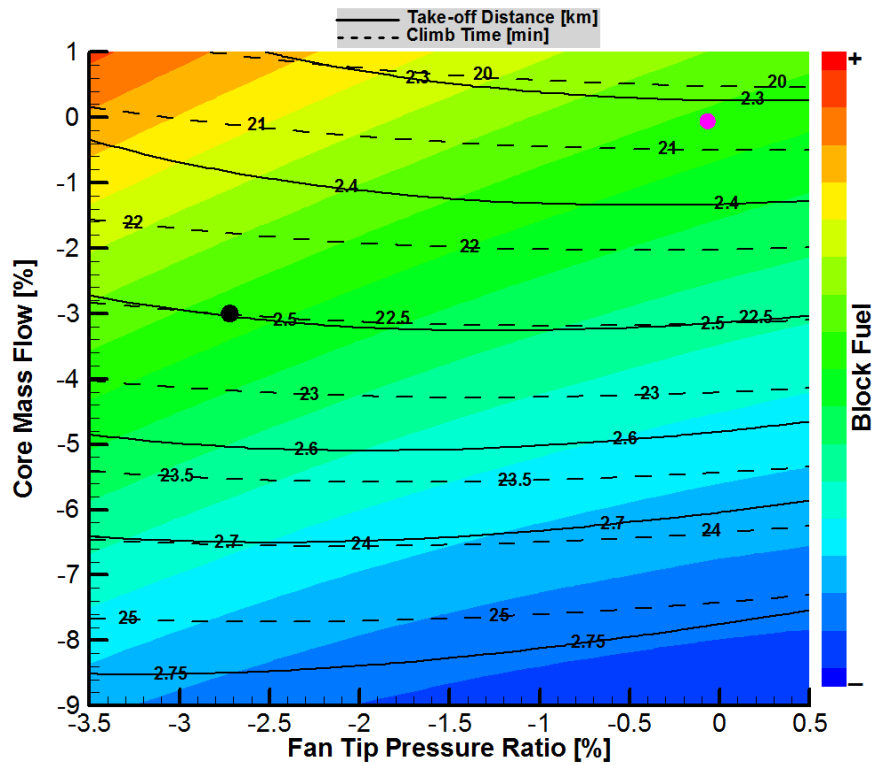


Figure 5-16 Variation of block fuel burn with core mass flow and fan pressure ratio

Nearly 3% improvement in the engine time between overhaul was realized. This is due to cooling treatment as a result of 1% reduction in HPC outlet temperature. Therefore, the engine maintenance cost reduces by 4.5% as a result of both decreasing engine production cost and increasing TBO. The time between overhaul counter with respect to fan tip pressure ratio and core mass flow is illustrated in Figure 5-17. Similar to the previous plot the highlighted area in Figure 5-17 represents the imposed constraint by the runway length and the climb time to altitude. Also, moving towards the upper left corner was constraint by the upper bound of the block fuel burn.

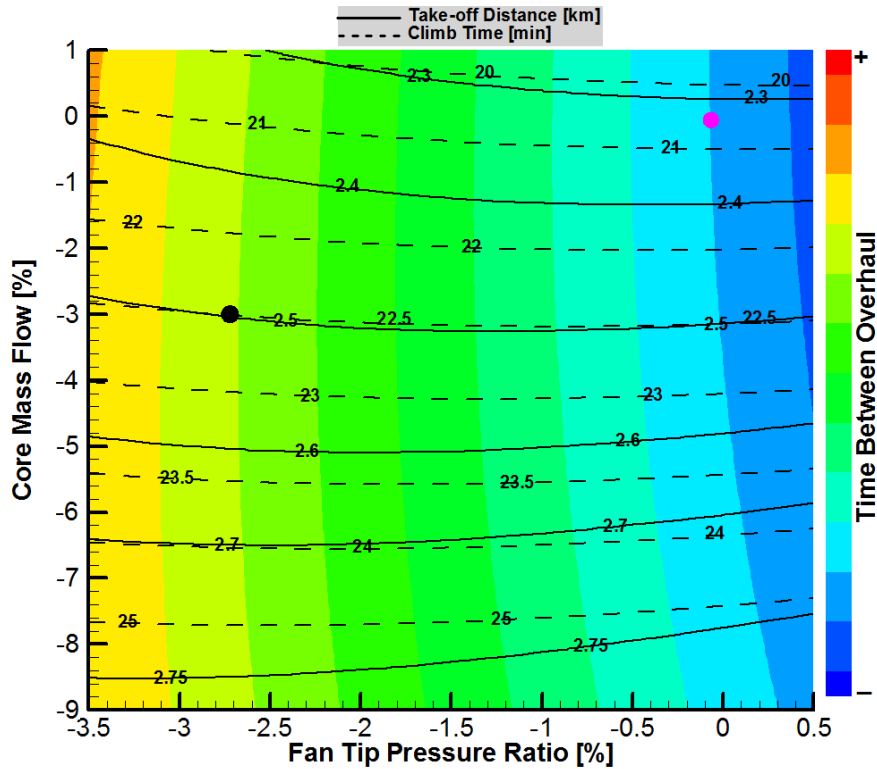


Figure 5-17 Variation of engine time between overhaul with core mass flow and fan pressure ratio

When the engine fan and core were both optimised for maximum time between overhaul with the lower possible block fuel burn, it was straightforward to find out the optimal fan pressure ratio with respect to the optimum engine life. At a fixed bypass ratio at top of climb, reducing the fan tip pressure ratio about 4% can improve the engine time between overhaul about 4.7% in comparison with the engine nominal design. Inversely the engine fuel burn was suffered with the reduced fan tip pressure ratio. Therefore, the optimum fan pressure ratio level is a trade-off between a better engine time between overhaul and block fuel burn as illustrated in the plot (a) of Figure 5-18.

With the fan tip pressure ratio of -1.1% from the engine nominal design the minimum take-off distance and climb time can be achieved as illustrated in the plots (e) and (f) of Figure 5-18. The reduced fan tip pressure ratio deteriorates propulsive efficacy where the increased fan tip pressure ratio value increase the LPT weight and hence the total engine weight. Please note that in the scatter

plots, the pink point indicates the engine design point and the green ones represent the optimal design.

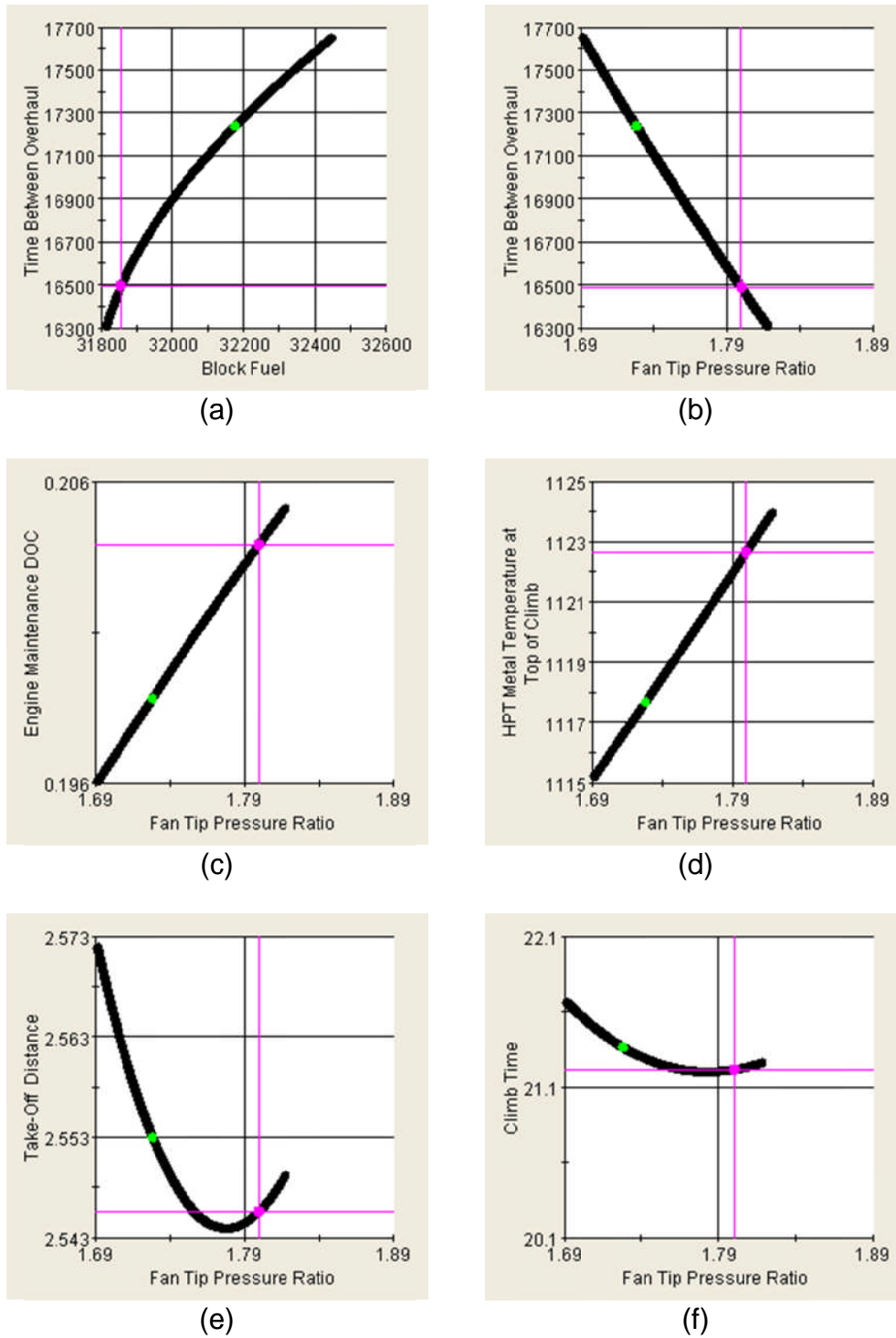


Figure 5-18 Fan tip pressure ratio variation at top of climb

5.2.3.2 IPC/HPC pressure ratio

With the value of the fan pressure ratio, fan mass flow and core mass flow fixed at the optimum point, the IPC and HPC pressure ratios were varied (and hence the overall pressure ratio) at top of climb in order to improve the engine life. The time between overhaul counter with respect to these variables is shown in Figure 5-19.

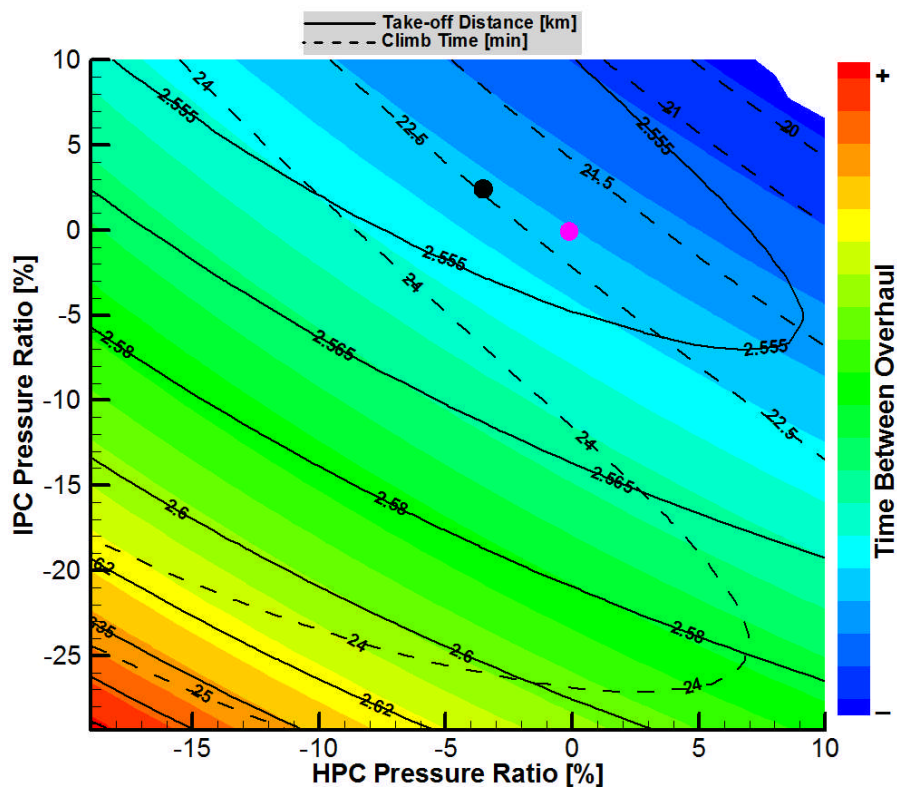


Figure 5-19 Variation of TBO with IPC and HPC pressure ratio

Increasing engine OPR has contradictory effects on the engine time between overhaul and block fuel burn. Thus the trade-off is between these two objective functions. Thermal efficiency of the engine improves as a result of increased IPC and HPC pressure ratios. Inversely, the time between overhaul strongly influenced as a result of increased HPC delivery temperature which provides

the required cooling flow of the HPT cooling system as depicted in Figure 5-20. The HPT metal temperature follows the same trend.

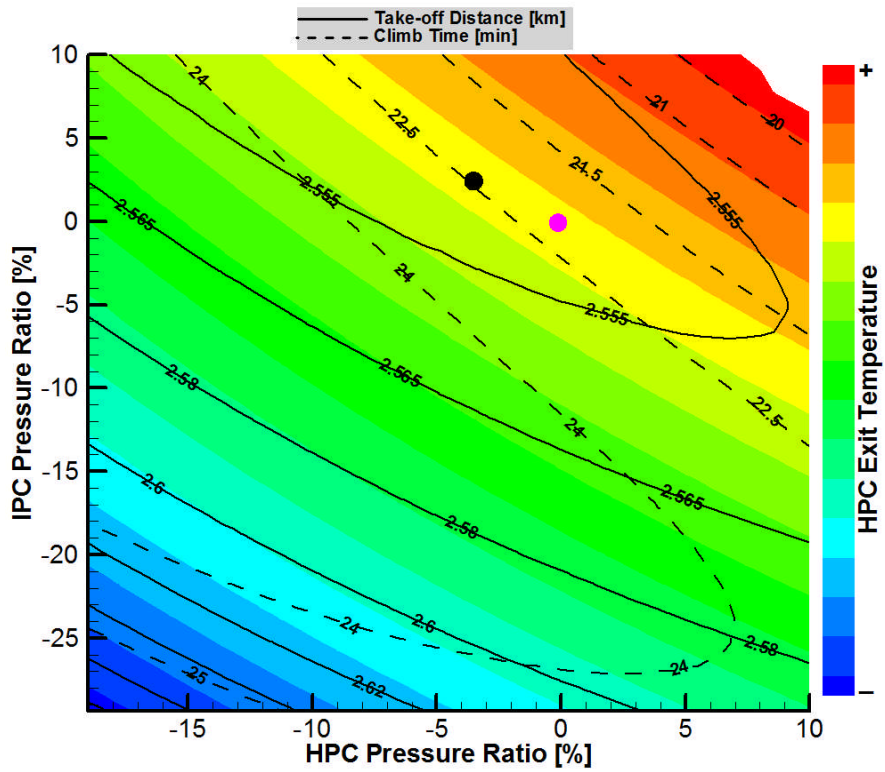


Figure 5-20 Variation of HPC delivery temperature and HPT metal temperature with IPC and HPC pressure ratio

The simulation results show that to achieve a better engine life, the IPC should have higher pressure ratio while the HPC pressure ratio should decrease. However, as one moves towards the lower left corner of Figure 5-20 the engine take-off and top of climb thrust reduces.

With 2.7% increase in IPC and 3.5% decrease in HPC pressure ratios, the engine TBO can increase 5.6% in comparison with the nominal design. At this optimal point, all the constraint sets are satisfied. Variation of take-off distance with IPC and HPC pressure ratio is shown in Figure 5-21.

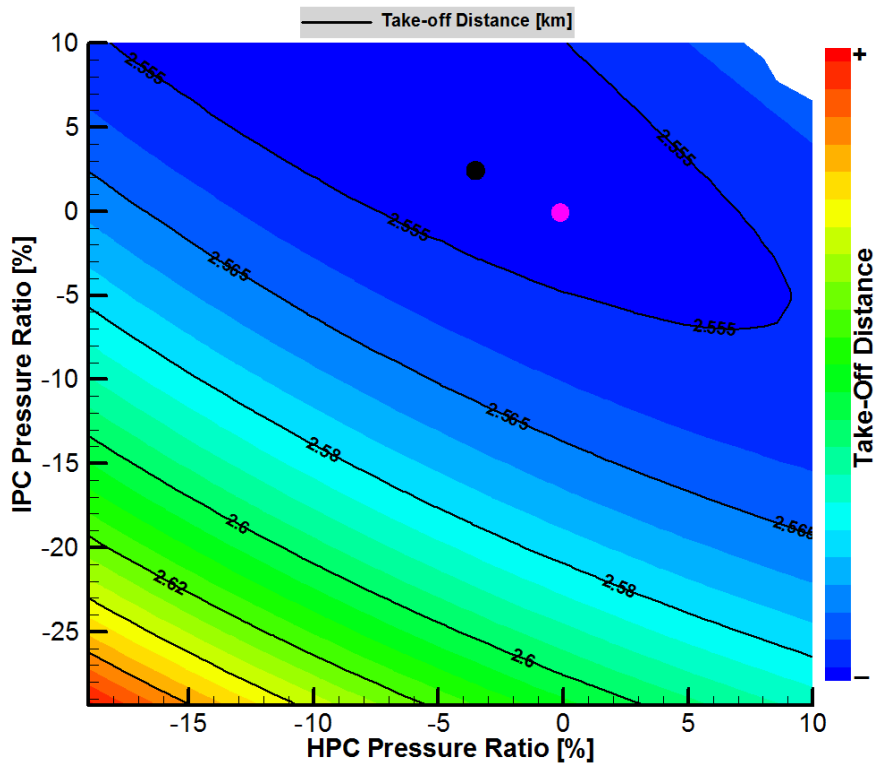


Figure 5-21 Variation of take-off distance with IPC and HPC pressure ratio

5.2.3.3 Combustor outlet temperature and HPT cooling flow

With the values from previous steps fixed at optimum point, fraction percentage variation of combustor outlet temperature and HPT cooling mass flow (at top of climb) from the nominal engine design was performed.

Combustor outlet temperature is an important parameter for engine optimisation. Both engine life and the amount of fuel consumption need to be considered. Values of combustor outlet temperature -0.6% and cooling mass flow +7% display reasonable improvement in engine life where upper limit was set for the block fuel burn. Introducing higher HPT cooling mass flow deteriorates engine performance. However, due to increasing cooling mass flow and slightly reducing combustor outlet temperature, HPT metal temperature drops, as illustrated in Figure 5-22.

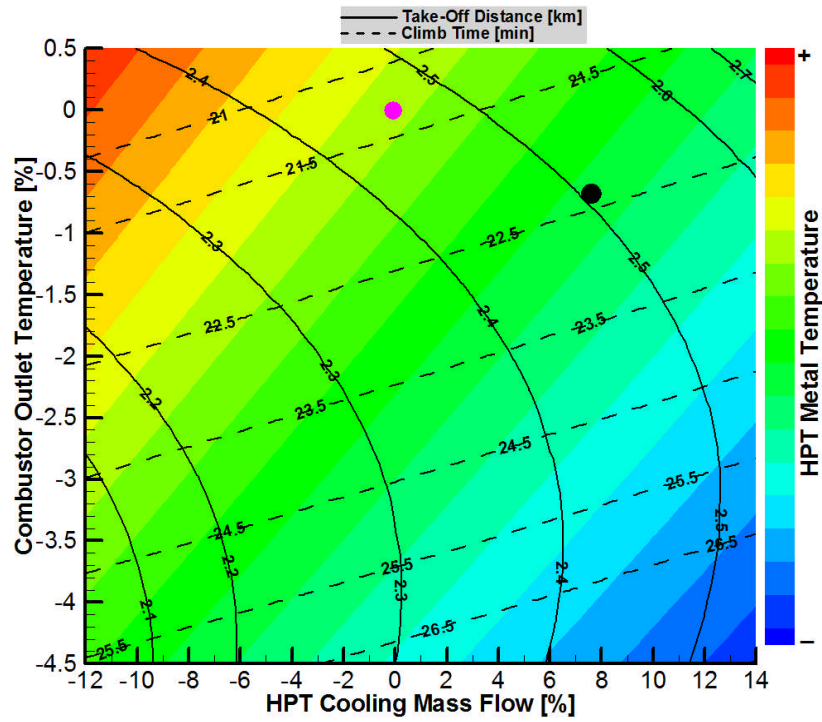


Figure 5-22 Variation of HPT metal temperature with combustor outlet temperature and HPT cooling mass flow

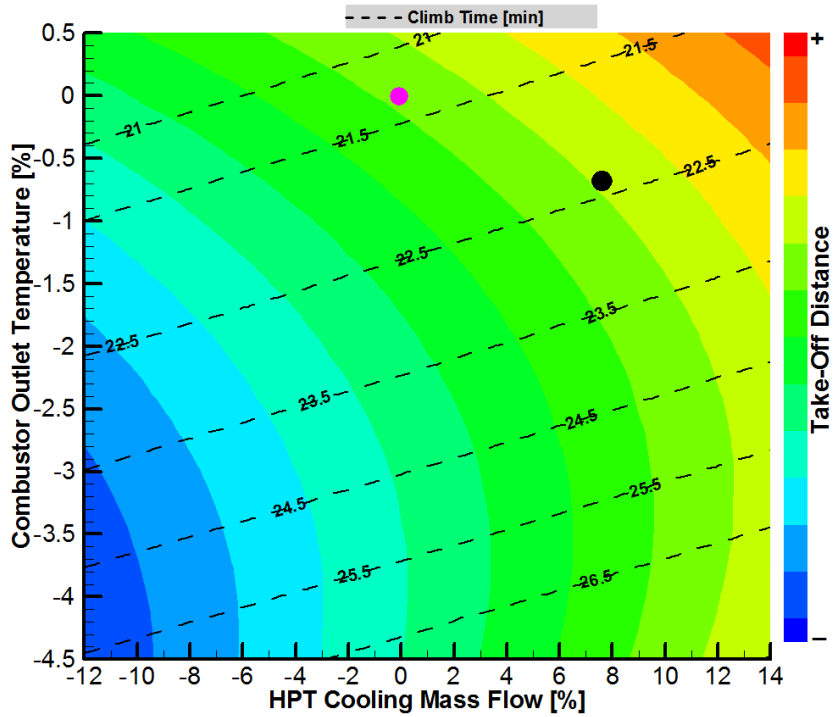


Figure 5-23 Variation of take-off distance with combustor outlet temperature and HPT cooling mass flow

A 0.6% reduction of combustor outlet temperature causes 3% reduction in engine thrust at top of climb. That means that the take-off distance will be longer. Also, reducing combustor outlet temperature level of the engine improves the SFC and block fuel burn. These trends are shown in Figure 5-23 and Figure 5-24. On the other hand a 0.8% engine weight penalty was the effect of turbomachinery changes for the required cooling mass flow.

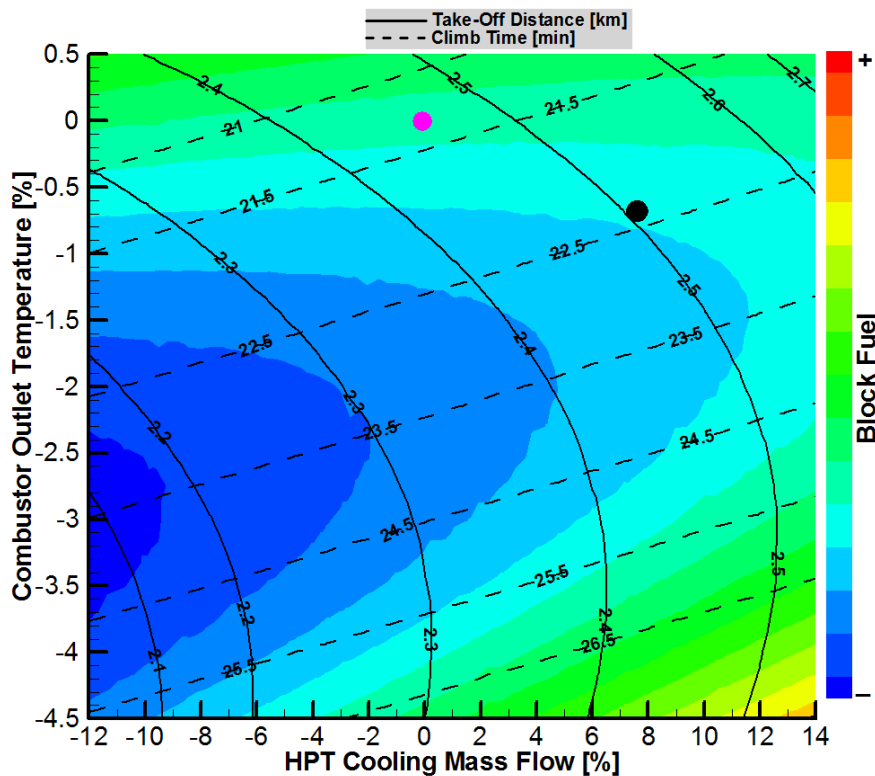


Figure 5-24 Variation of block fuel with combustor outlet temperature and HPT cooling mass flow

With the optimum values of combustor outlet temperature and cooling mass flow a 17% improvement in time between overhaul was achieved, which corresponds to additional 10% life improvement compared to the previous steps. Such a design combination meets all the constraints and it is worth noting that improvement of contradictory targets, namely time between overhaul

and block fuel burn, results in a 0.8% in direct operating cost (DOC), as illustrated in Figure 5-25.

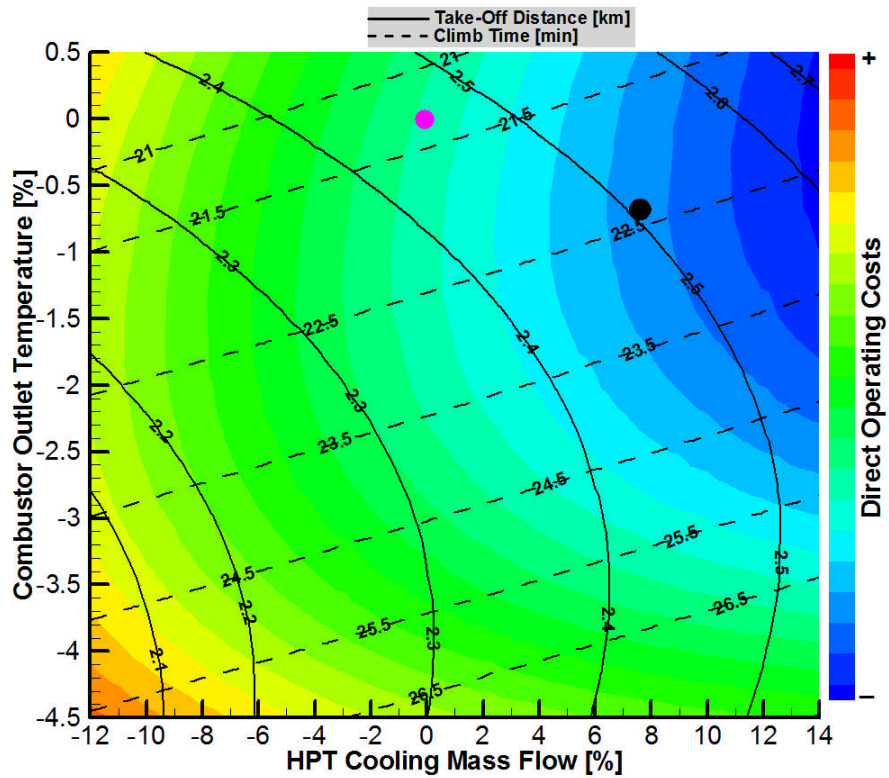


Figure 5-25 Variation of direct operating cost with combustor outlet temperature and HPT cooling mass flow

5.2.4 BASELR Optimised Design

In this section, the BASELR configuration was evaluated and optimised for extending engine life using TERA2020 software. Different parameters as engine design parameters were assessed and their influence on engine life was reported. Then a better combination of engine design parameters with respect to the engine weight, block fuel burn, maintenance and direct operating costs were proposed.

The optimum values of the engine design variables are given in Table 5-6. It should be noted that the optimum values are the percentage deviation of the design parameters from the nominal design.

Table 5-6 *BASELR configuration design variables and optimum values*

Step	Parameter	Optimal Value	Unit
1	Fan inlet mass flow	3.8	%
	Core mass flow	- 3.2	%
	Fan tip pressure ratio	- 4	%
2	IPC Pressure ratio	2.7	%
	HPC Pressure ratio	- 3.5	%
3	Combustor outlet temperature	- 0.6	%
	HPT cooling mass flow	7	%

The optimisation results suggest that an improvement in time between overhaul (TBO) can be expected by reducing the core mass flow, fan and HPC pressure ratios as well as the combustor outlet temperature while increasing the fan inlet mass flow, IPC pressure ratio and HPT cooling mass flow from their respective nominal values. Looking at the values of the optimised design parameters, it can also be concluded that the engine design with a small core size requires more cooling mass flow to further improve engine life.

Performance results are shown in Table 5-7. Comparison is given between the optimum and nominal engine design. The optimal engine design has lower specific thrust, specific fuel consumption and overall pressure ratio. Also, it has higher bypass ratio and overall efficiency. As can be observed, a 17% improvement in time between overhaul was achieved along with the engine weight and production cost penalties. A 0.5% block fuel reduction resulting from the higher cycle efficiency and the thrust reduction effects of rubberized wing aircraft model.

Table 5-7 Comparison of the TBO optimal design of BASELR engine with respect to the nominal design

Performance Parameters	Unit	Top of Climb		
		Nominal	Optimal	Delta %
Fan inlet mass flow	[kg/s]	360	373	3.8
Core mass flow	[kg/s]	61.5	59.5	- 3.2
Bypass ratio	[-]	4.9	5.3	8.6
Fan tip pressure ratio	[-]	1.8	1.7	- 4.0
IPC pressure ratio	[-]	5.2	5.3	2.7
HPC pressure ratio	[-]	4.4	4.2	- 3.5
Overall pressure ratio	[-]	38	35	- 7.5
Combustor outlet temperature	[K]	1620	1609	- 0.6
HPT blade metal temperature	[K]	1123	1099	- 2.1
HPT blade cooling temperature	[K]	807	795	- 1.5
HPT blade cooling effectiveness	[-]	0.48	0.50	3.7
Overall efficiency	[-]	0.32	0.33	0.9
Thermal efficiency	[-]	0.49	0.48	- 1.3
Propulsive efficiency	[-]	0.66	0.68	2.2
Specific fuel consumption	[g/(kN*s)]	17.9	17.7	- 0.9
Specific thrust	[N*s/kg]	189	176	- 6.8
Thrust	[kN]	68	66	- 3.3
Engine weight	[kg]	7140	7200	0.9
Engine production cost	[k€]	5127	5130	0.1
Engine maintenance costs	[k€/h]	0.21	0.19	-11.2
Direct operating costs	[k€/flight]	74.4	73.8	- 0.8
Time between overhaul	[hr]	16400	19200	17
Block fuel	[kg]	32360	32200	- 0.5

5.3 DDICLR Configuration

This is a 3-shaft, 3-nozzle direct drive fan intercooled core turbofan engine configuration for long range application. The auxiliary nozzle in the intercooled module is applied in order to control the intercooler effectiveness. It has a single stage fan, five stages IP compressor, nine stages HP compressor, two stages HP turbine, single stage IP turbine and eight stages LP turbine (1-5-9-2-1-8). The design point is set at Top of climb (TOC) with altitude of 10668 [m] at hot day condition (ISA+10). The table below (Table 5-8) summarises the engine performance specification.

Table 5-8 DDICLR engine performance specifications

Parameter	Unit	Rating		
		Take-off	Top of Climb	Cruise
Altitude	[m]	0	10668	10668
Mach number	[-]	0.25	0.82	0.82
DTAMB	[K]	15	10	0
Inlet mass flow	[kg/s]	1199	500	481
Core mass flow	[kg/s]	85	37	32
Bypass ratio	[-]	13	12.6	14
Fan pressure ratio	[-]	1.49	1.58	1.46
Overall pressure ratio	[-]	67	79	63
Combustor outlet temperature	[K]	2000	1920	1660
SFC	[g/(kN*s)]	10.03	14.95	13.96
Thrust	[kN]	244	67	50

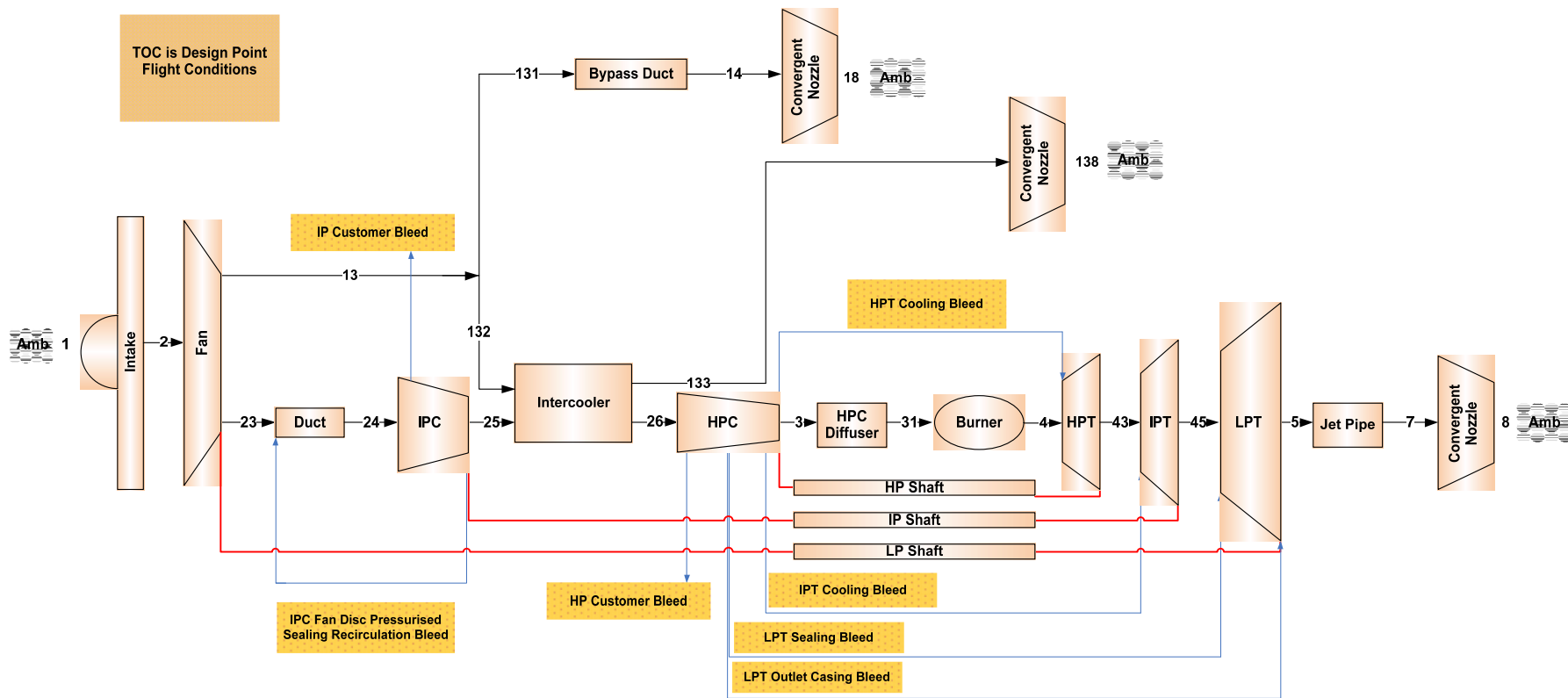


Figure 5-26 DDICLR configuration schematic [77]

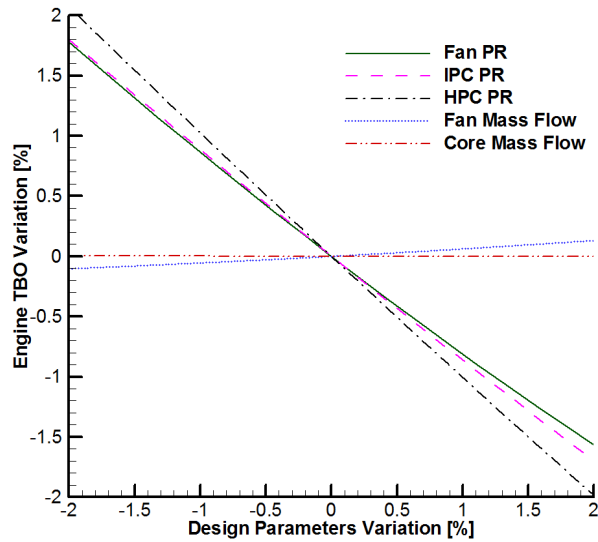
5.3.1 Sensitivity Analysis of DDICLR Configuration

Similar to the BASELR configuration, a sensitivity analysis is performed to investigate the influence of a single design variable perturbation on the values of other design parameters at design point and off-design condition. In fact, perturbation of engine main design parameters is realistic for small changes due to compressor and turbine stage count change, engine specific thrust and velocity ratio variations. More information about the sensitivity analysis and how design parameters perturbation were introduced, are given in CHAPTER 4. Herein, the initial engine design is referred to the engine nominal design point. The engine design parameters and variation range is listed in Table 5-9.

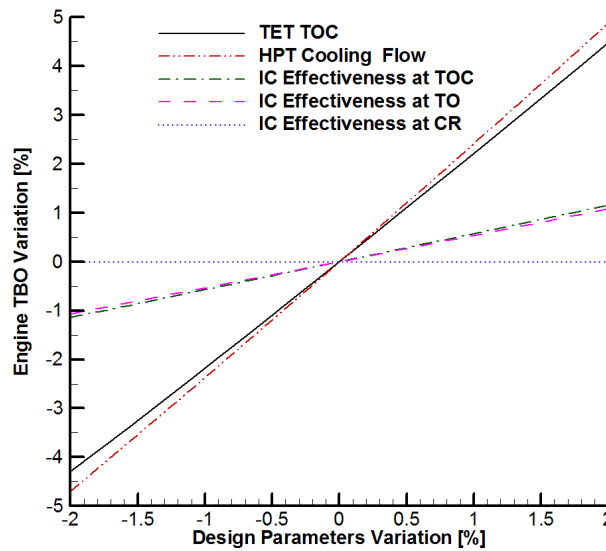
Table 5-9 *DDICLR sensitivity parameters*

Parameter	Range	Unit
Fan tip pressure ratio	-2%... +2%	%
IPC pressure ratio	-2%... +2%	%
HPC pressure ratio	-2%... +2%	%
Intercooler effectiveness at TOC	-2%... +2%	%
Intercooler effectiveness at CR	-2%... +2%	%
Intercooler effectiveness at TO	-2%... +2%	%
Fan inlet mass flow	-2%... +2%	%
Core mass flow	-2%... +2%	%
TET for climb rating	-2%... +2%	%
HPT cooling mass flow	-2%... +2%	%

The presented sensitivity study results indicates that increasing HPT cooling flow, turbine entry temperature and intercooler effectiveness have positive effect on engine life, while increasing fan tip pressure ratio, IPC pressure ratio and HPC pressure ratio deteriorate engine life particularly the engine time between overhaul. The remaining design parameters are not particularly significant. These effects are depicted in the plots of Figure 5-27.



(a)



(b)

Figure 5-27 DDICLR TBO sensitivity analysis

As explained earlier, the engine overall pressure ratio is allowed to vary when fan pressure ratio, IPC pressure ratio or HPC pressure ratio is varied. Therefore, the cooling mass flow required for HPT module raises because of the increased OPR. For that reason, the engine creep and fatigue life deteriorates.

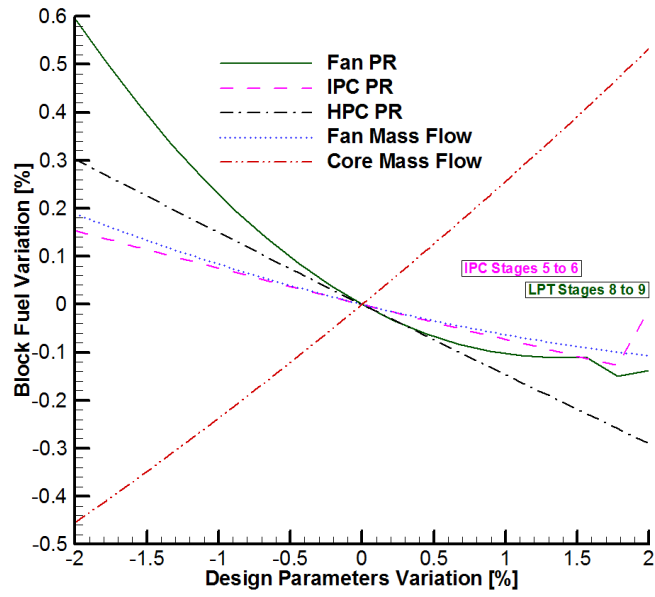
On the other hand increasing OPR means that the IPC and HPC compressors need more stages to achieve so. This makes the engine heavier and resulting with long take-off distance and more time to climb. Again, the hot components life, HPT disk and blades particularly, will be affected.

In fact, HPT blades life benefits from increasing cooling mass flow and reducing combustor outlet temperature. However, increasing combustor outlet temperature improves engine thrust which causes the climb time to be shorter. Although, the HPT metal temperature increased nearly about 2%, at top of climb condition the time is dominant factor rather than temperature. High intercooled effectiveness can reduce the HPC inlet temperature for a given pressure ratio. Then, the HPC delivery temperature will drop and HPT module life benefits from this.

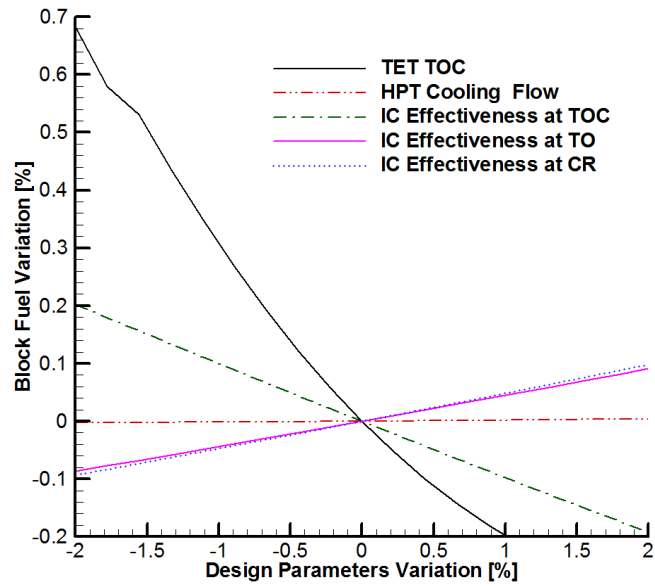
In general, during sensitivity analysis, the variation of the design parameters on engine performance is less marked unlike the engine life. Increasing fan pressure ratio and fan mass flow improve the specific fuel consumption of the engine (hence reducing CO₂) as illustrated in Figure 5-28 and Figure 5-29. As the fan pressure ratio rises, the propulsive efficiency improves results in low fuel consumption.

Similarly, increasing the engine inlet mass flow, thus bigger fan diameter, increases propulsive efficiency which directly related to engine fuel consumption. But, higher fan pressure ratio and bigger fan diameter parameters can be translated as weight and drag penalty that negate the some of the benefits achieved through propulsive efficiency improvement.

As the engine inlet mass flow is fixed, increasing core mass flow essentially reduces the engine bypass ratio. Consequently, increasing the core size will generally result in an increase in engine weight which leads to higher SFC at top of climb.



(a)



(b)

Figure 5-28 DDICLR block fuel sensitivity analysis

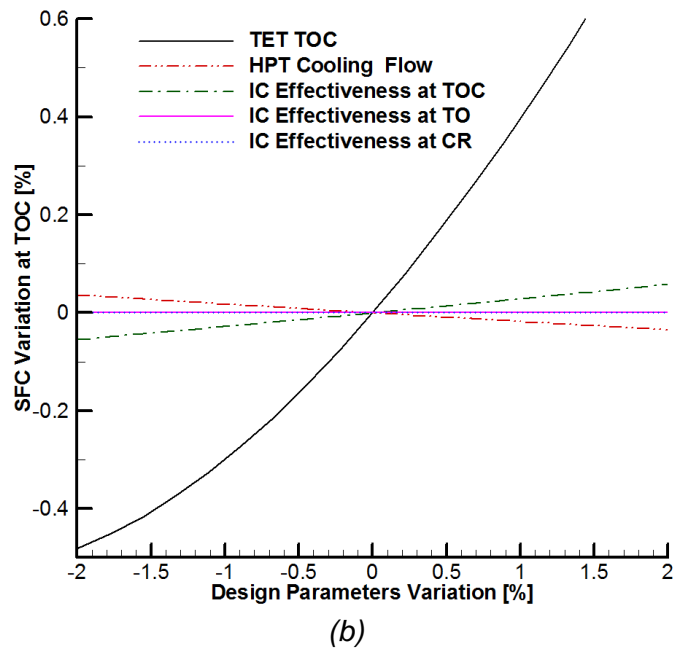
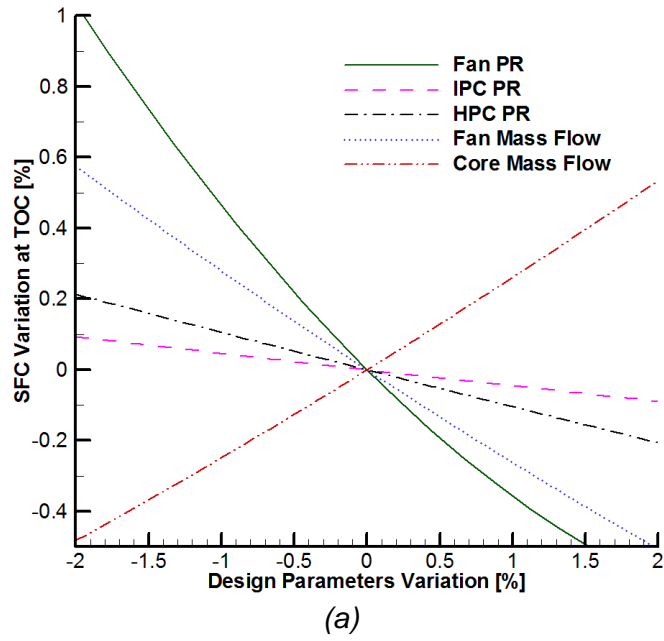


Figure 5-29 DDICLR SFC sensitivity analysis

5.3.2 Parametric study of DDICLR Configuration

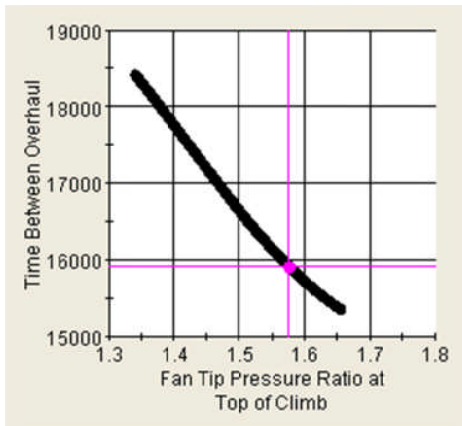
An attempt has been made here to investigate the effect that main engine design parameters have on the time between overhaul, DOC, specific fuel consumption, block fuel and weight of the DDICLR configuration. This study is carried out at hot day top of climb conditions (TOC) and at variable thrust levels. During design space exploration the design variables allowed to vary in a reasonable range. Nevertheless, for some parameters wide ranges are considered to demonstrate the changes on objective functions. In the results presented in this section, the pink dot indicates the nominal design point. From the design parameters listed in Table 5-10 only one parameter at a time is being varied around the initial (nominal) design point, while the rest are kept constant.

Table 5-10 DDICLR design space parameters

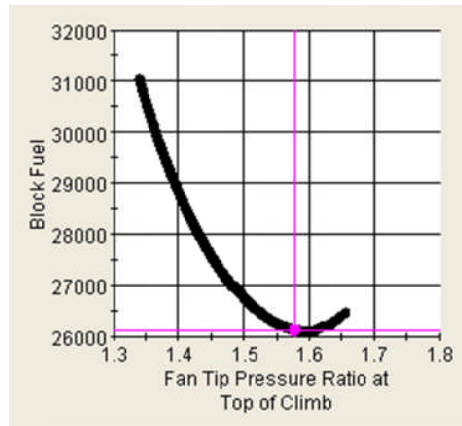
Parameter	Abbreviation	Lower	Upper	Unit
Fan tip pressure ratio	dFanBPPR	-15	+5	%
Fan inlet mass flow	dW1	-35	+15	%
Core mass flow	dW23	-12	+15	%
IPC Pressure ratio	dIPCPR	-20	+25	%
HPC Pressure ratio	dHPCPR	-25	+25	%
Intercooler effectiveness at TO	dIEFFTO	-50	+30	%
HPT cooling mass flow	dW41CQW26	-40	+40	%
Combustor outlet temperature at TOC	dT4TOC	-8	+20	%

5.3.2.1 Fan tip pressure ratio

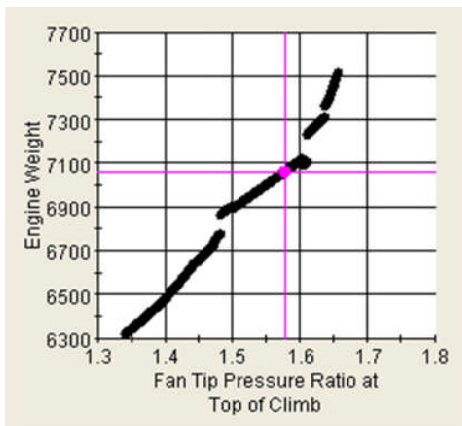
Increasing fan tip pressure ratio up to 2% at constant fan and core mass flow (thus the bypass ratio) results in a 0.05% and 0.14 % improvement in cruise SFC and block fuel, respectively while time between overhaul deteriorates (by roughly 1.5%) as can be seen in Figure 5-30.



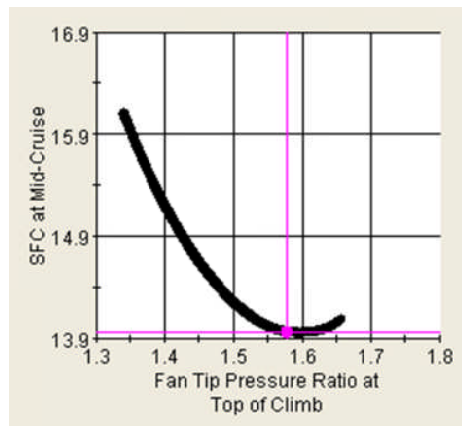
(a)



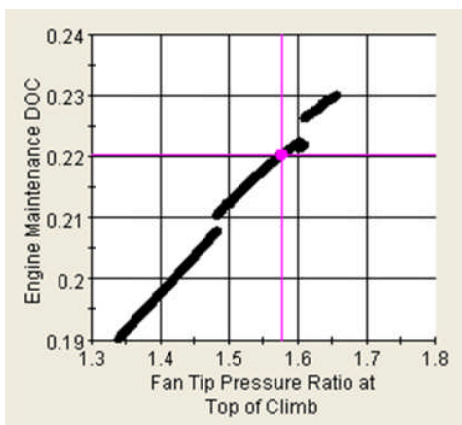
(b)



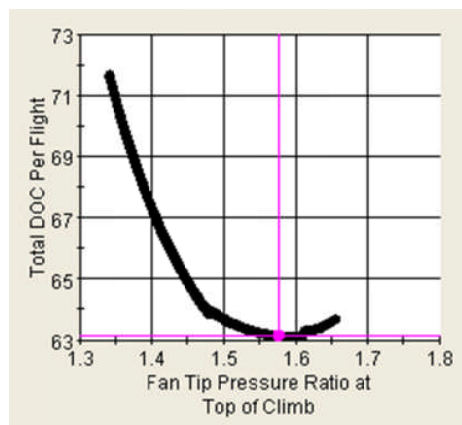
(c)



(d)



(e)



(f)

Figure 5-30 DDICLR Fan tip pressure ratio variation at top of climb

As fan tip pressure ratio is increased, the propulsive efficiency improves until it reaches to the optimal point where further increasing the fan pressure ratio increase engine weight (approximately 0.5%) and very well negate the advantageous. This is mainly attributes to the LPT stage count change from 7 to 9. However, beyond a fan pressure ratio of 1.66, the fan requires more power than that can be delivered by the LPT.

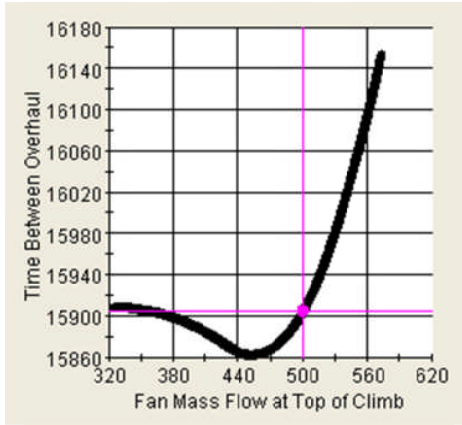
As it can be observed, the effect of fan pressure ration on engine life is linear; increasing fan pressure ration reduces engine life and increase engine maintenance costs and vice versa. This is caused by an increased overall pressure ration which eventually leading to higher cooling flow temperature of the HPT blades and reduce the fatigue life. A 5% reduction in fan pressure ration offers a 4.8% improvement in TBO. (Ref. Appendix C)

5.3.2.2 Fan mass flow

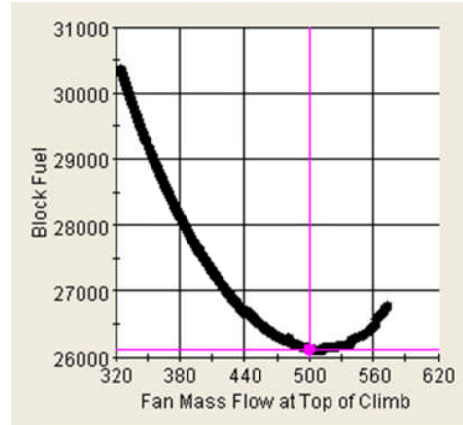
With a fixed fan pressure ratio and core mass flow, the engine fan mass flow at top of climb is varied (and hence the bypass ratio). An increasing fan mass flow reduce the specific thrust, thus improves propulsive efficiency and leading to lower engine fuel burn.

Similarly, better engine life is expected at higher level of fan mass flow. However, fan mass flow cannot go beyond a certain limit since the increased engine weight negates the SFC benefits from the reduced specific thrust.

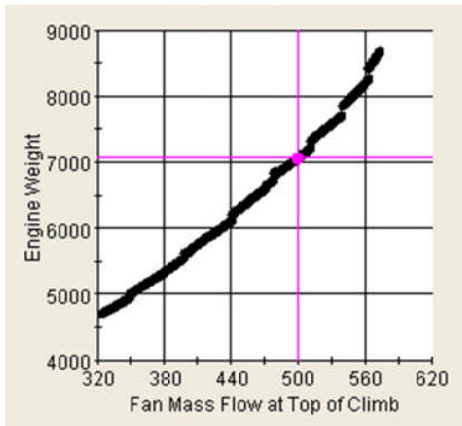
On the hand off-design effect causes an increase in take-off OPR hence leading to higher cooling air temperatures and reduced blade fatigue life. Therefore, a trade-off between the decreasing fuel burn, rising engine weight and maximum time between overhaul is necessary. These trends are illustrated below in Figure 5-31. (Ref. Appendix C)



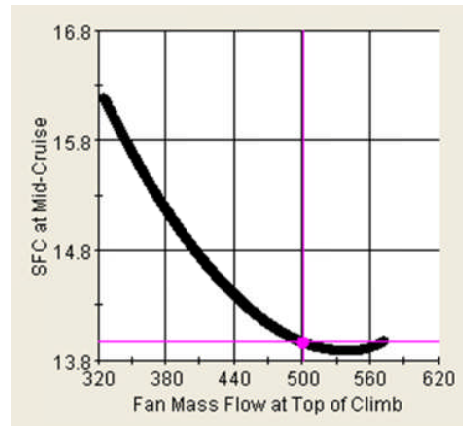
(a)



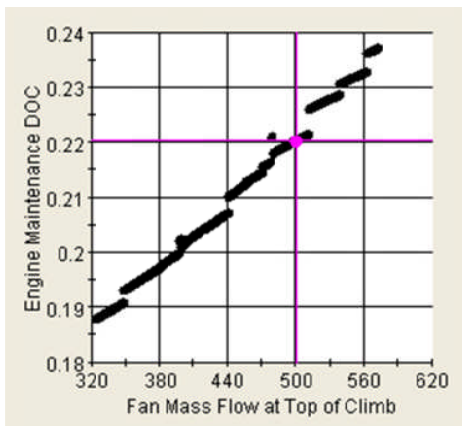
(b)



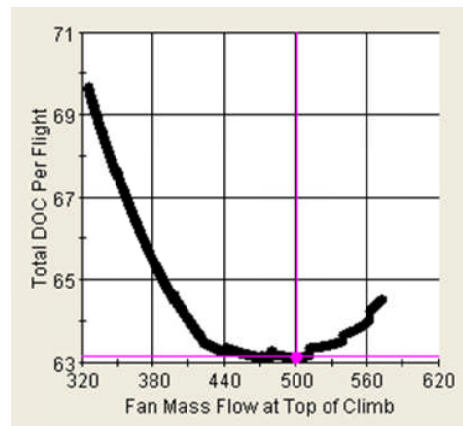
(c)



(d)



(e)



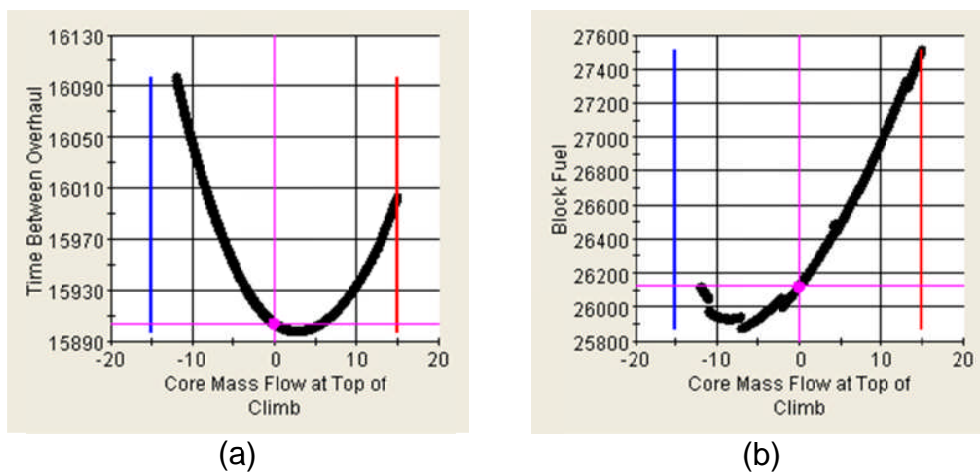
(f)

Figure 5-31 DDICLR Fan mass flow variation at top of climb

5.3.2.3 Core mass flow

Within this investigation the engine core mass flow is varied at a fixed fan mass flow and fan pressure ratio. Increasing the core mass flow principally reduces the engine bypass ratio and increases the core size which elevates the engine weight. Furthermore, specific thrust increases due to the increased fuel flow, which leads to an increase in LPT exit temperature. Since the turbomachinery stage count changes, discontinuity of the design space is predictable. For example the IPC and LPT stages number changes from 5 to 6 and 11 to 6, respectively. With a 7% reduction in core mass flow, the engine SFC and block fuel reaches to the lowest level. At the same time, engine time between overhaul improves by 0.5 %.

Higher core mass flow design is directly associated with substantial increase in engine fuel flow, which leads to an increase in engine thrust level and hence improvement in FAR take-off distance and reduce flight segments time. At a given combustor output temperature, reduce flight time means longer components life and eventually extending the time between overhaul. Furthermore, high core mass flow increases the cooling flow rate (5%) of the HPT component. Lower core mass flow has off-design effects on overall pressure ratio (i.e. OPR reduces at cruise). These observations are illustrated in Figure 5-32.



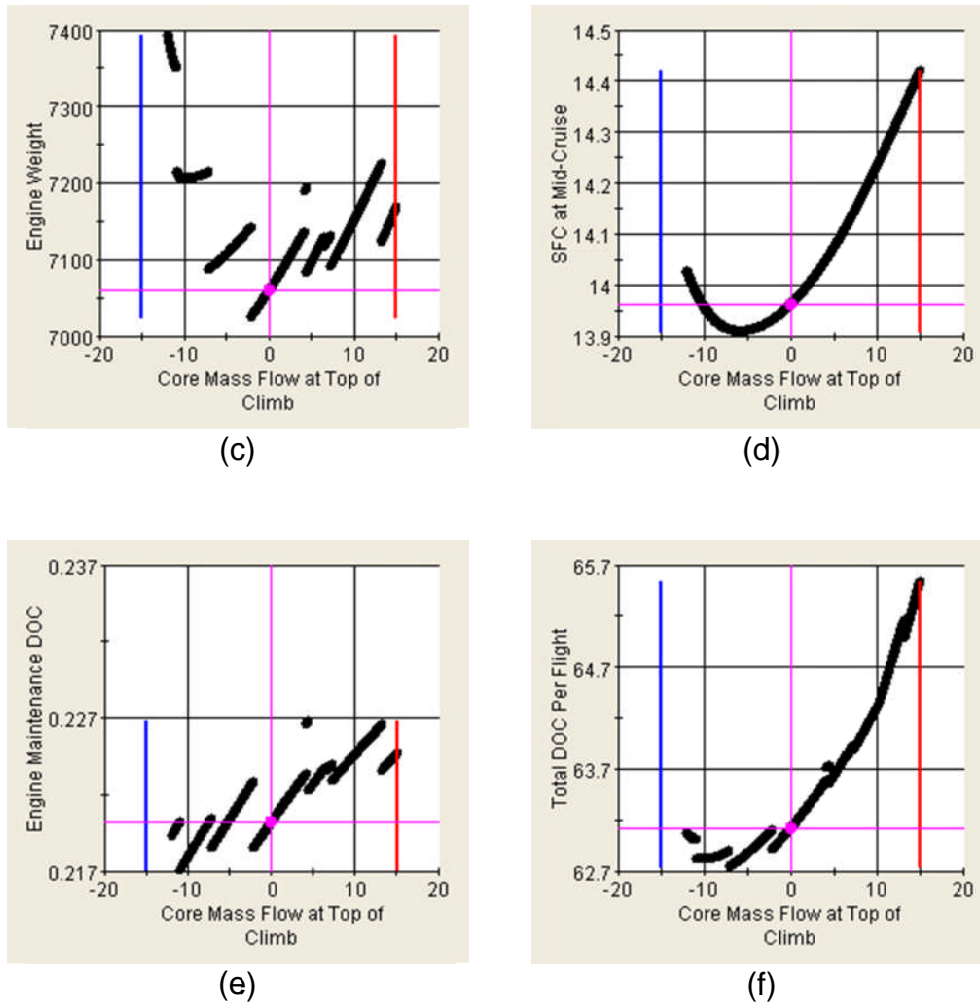


Figure 5-32 DDICLR Core mass flow variation at top of climb

5.3.2.4 IPC / HPC pressure ratio

The intermediate and high pressure compressor pressure ratios are varied (and hence the overall pressure ratio). As the IPC pressure ratio increases, thermal efficiency of the engine improves substantially and thus reduces the amount of engine fuel consumption.

On the other hand, lower IPC pressure ratio is beneficial for the engine weight and time between overhaul. The IPC stage number change from 5 to 6 is

observed and considered reasonable. A similar trend applies to the HPC pressure ratio for to the same reasons.

Looking at the trends illustrated in Figure 5-33 and Figure 5-34, the influence of changing HPC pressure ratio on TBO, SFC and weight is more pronounced compared with IPC pressure ratio.

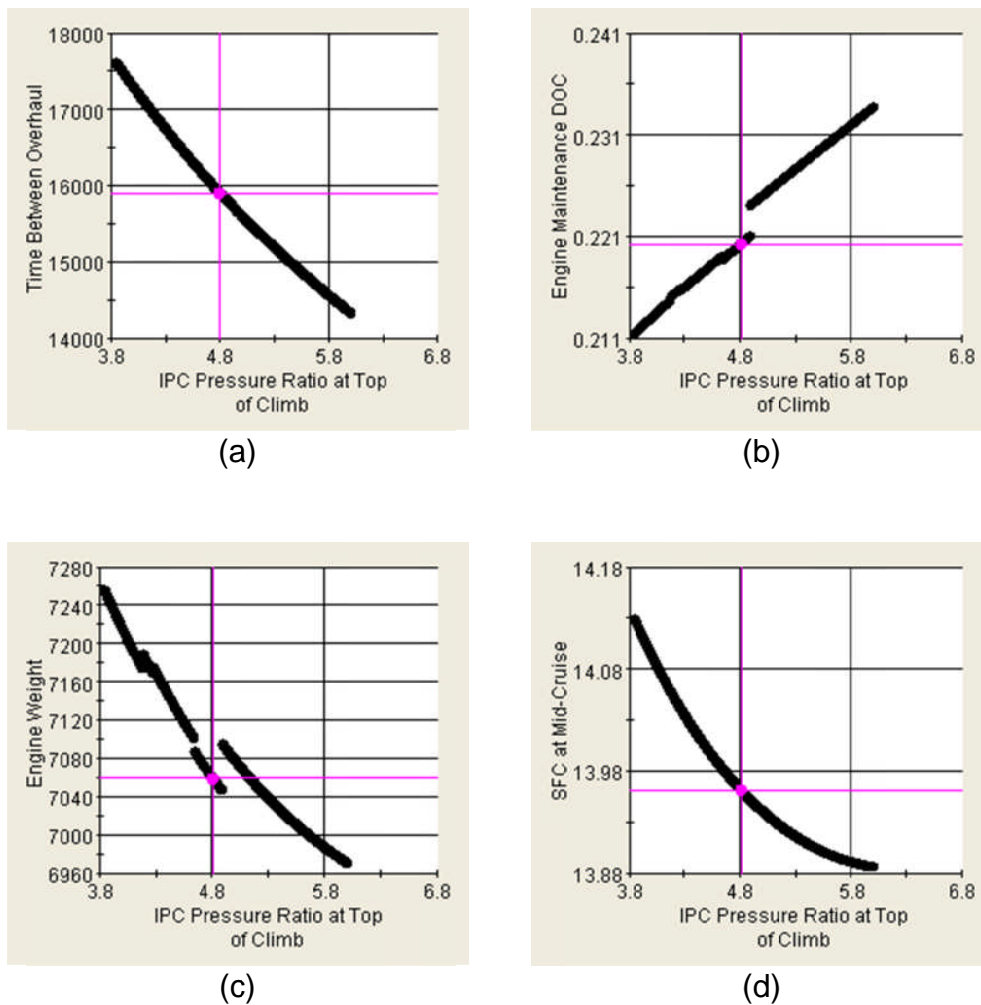


Figure 5-33 *IPC pressure ratio variation at top of climb*

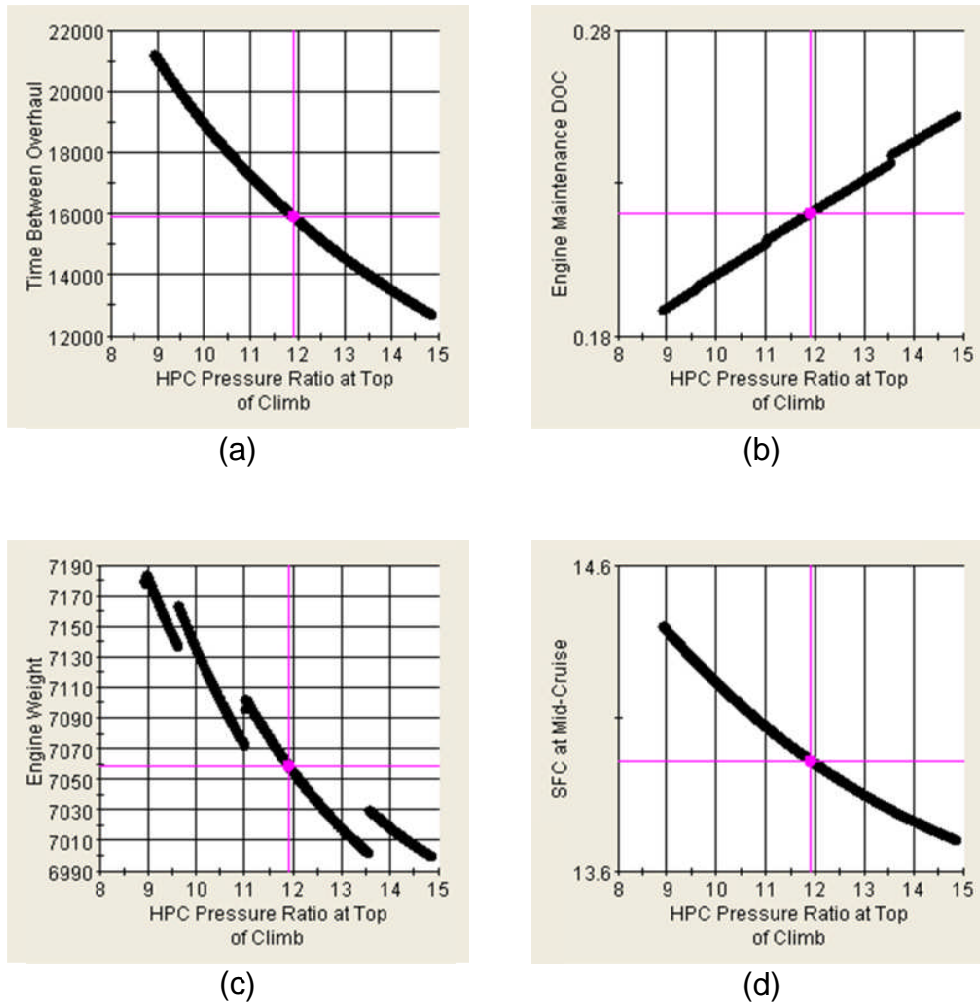


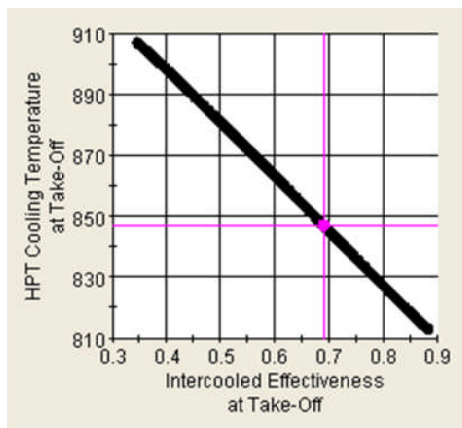
Figure 5-34 *HPC pressure ratio variation at top of climb*

5.3.2.5 Intercooler effectiveness at take-off

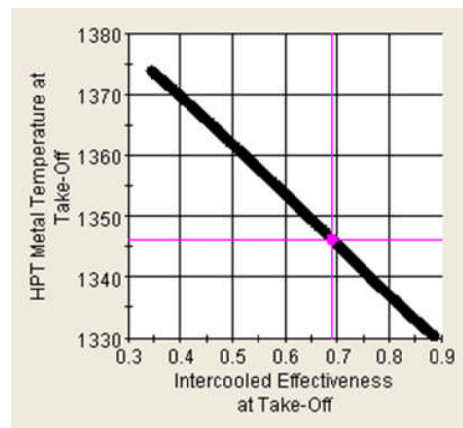
As the intercooler aerodynamic design and sizing is carried out at take-off condition, the engine intercooler effectiveness is varied at take-off by using the variable geometry auxiliary nozzle, to realize the effects on engine life and fuel burn. From the Figure 5-35 it can be observed that changing the intercooler effectiveness at take-off has a significant effect on the HPT blade metal temperature. High intercooler effectiveness can decrease the HPC delivery temperature and hence reduce the HPT cooling temperature. This practice results in a better blade fatigue life and hence higher engine time between overhaul. Also, increasing intercooler effectiveness can increase intercooler

pressure loss which reduce the overall pressure ratio and hence further improve engine life.

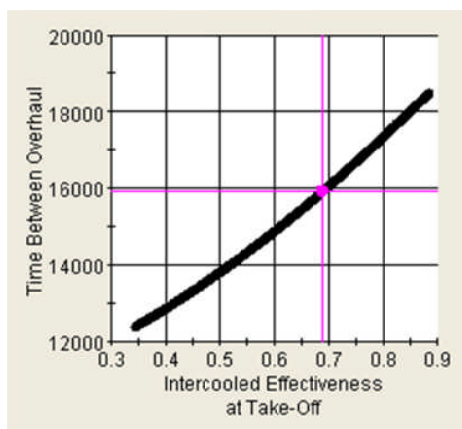
On the hand, higher intercooler effectiveness results in a bulky and heavier intercooler component which can cause installation difficulties. Above that, increased nacelle diameter and associated weigh, cause SFC and block fuel penalties. Therefore, intercooler effectiveness needs to be traded with cooling mass flow to achieve a design that gives minimum block fuel for a given HPT blade metal temperature requirement. It can be observed that increasing the intercooler nozzle area in order to provide the required mass flow ratio, has a negative effect on the engine propulsive efficiency.



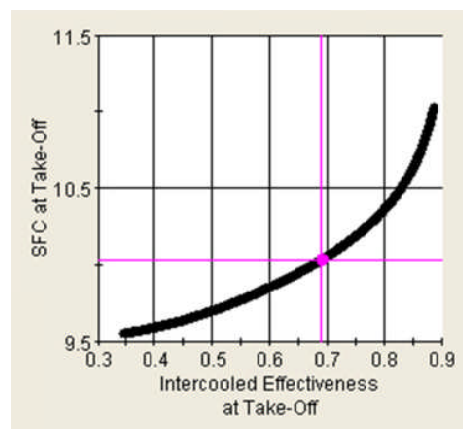
(a)



(b)



(c)



(d)

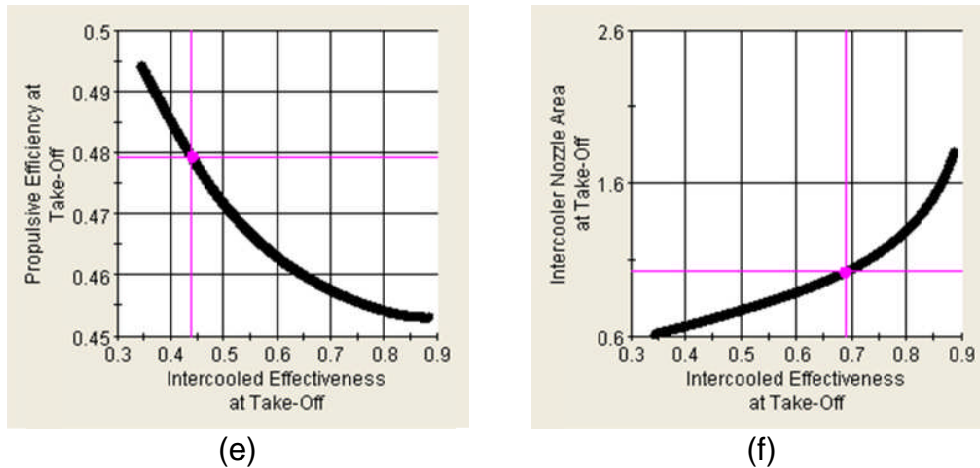


Figure 5-35 *Intercooler effectiveness variation at Take-off*

5.3.2.6 HPT cooling mass flow

The HPT cooling mass flow at top of climb is varied (and hence HPT metal temperature) at a given combustor outlet temperature. It is expected that altering the level of HPT cooling mass flow has a considerable effect on engine life. As can be observed in Figure 5-36, increasing HPT cooling mass flow shows significant improvement in time between overhaul compared to the engine design parameters presented in earlier sections. For example, 5% increasing HPT cooling mass flow results in 12% improvement in time between overhaul compared to the initial engine design.

In a similar manner presented in earlier sections, increasing the engine life has an adverse effect on engine performance and specifically on engine weight. As the cooling mass flow is increased, fuel mass flow drops since the amount of HPC mass flow going to the combustion chamber reduce so does engine thrust. Nevertheless, the velocity ratio increases with increasing cooling mass flow resulting in better propulsive efficiency but eventually causing LPT stage count changing from 8 to 9.

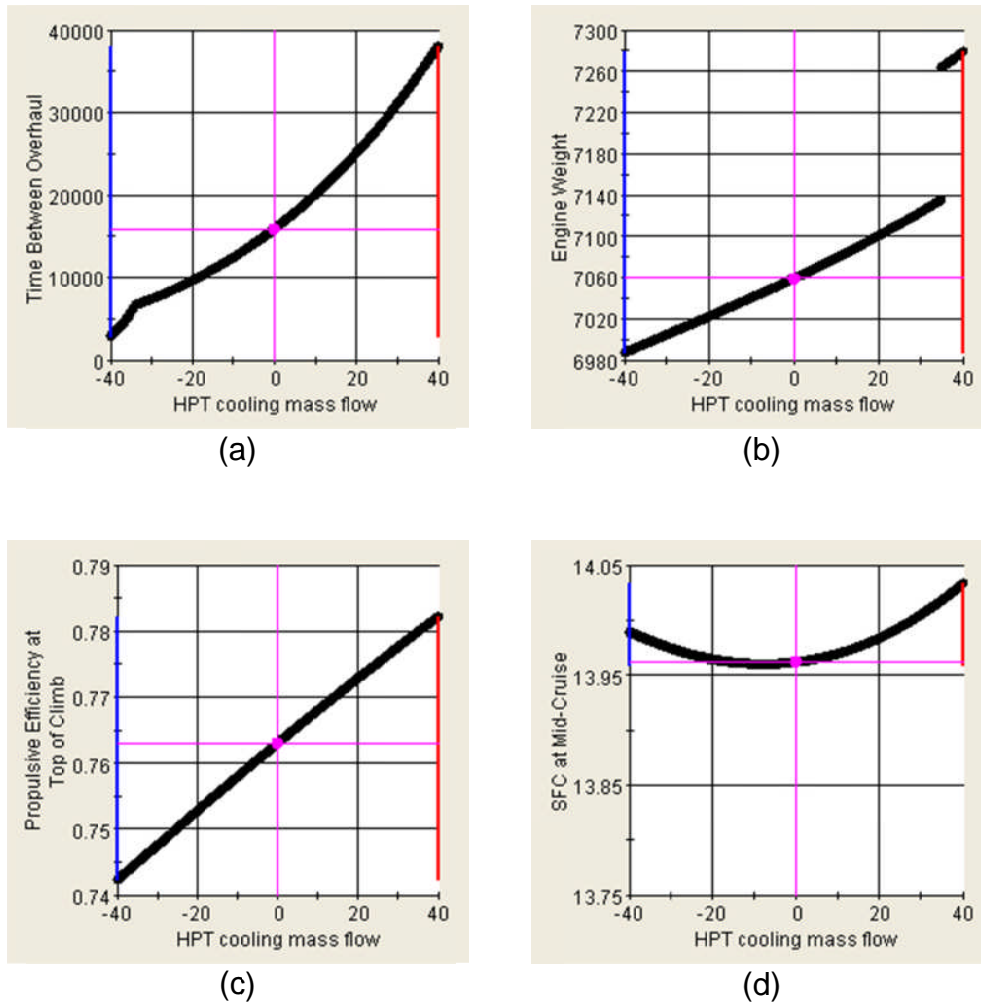


Figure 5-36 *HPT cooling mass flow variation at top of climb*

5.3.2.7 Combustor outlet temperature

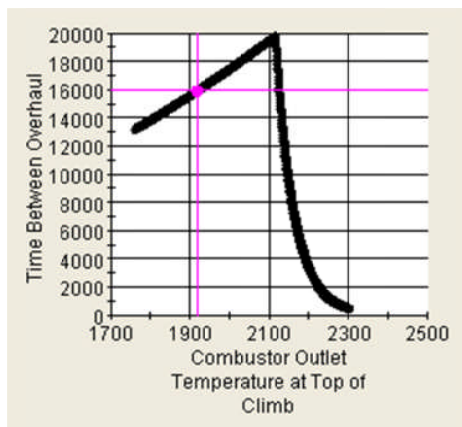
In this investigation the combustor outlet temperature is varied at top of climb condition at a given HPT cooling mass flow. As the combustor outlet temperature is increased, the engine life deteriorates since the HPT blades metal temperature is limited due to material properties. A high combustor outlet temperature is generally advantageous for engine weight where the LPT stage number changes from 7 to 11 stages, as can be observed in Figure 5-37.

Similar to the HPT cooling mass flow variation in previous section, a 5% increase in combustor outlet temperature cause an 11% reduction in engine life.

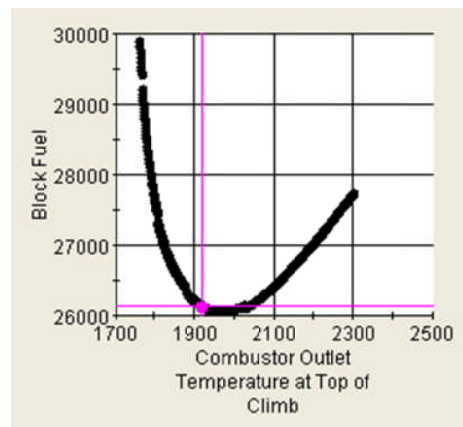
Therefore, one would say that the cooling mass flow and combustor outlet temperature are the key drivers to the engine life.

An increasing in combustor outlet temperature reduces the climb time and meanwhile increases the runway length. The former improves the engine creep life, where the latter deteriorate the engine fatigue life as illustrated in Figure 5-37.

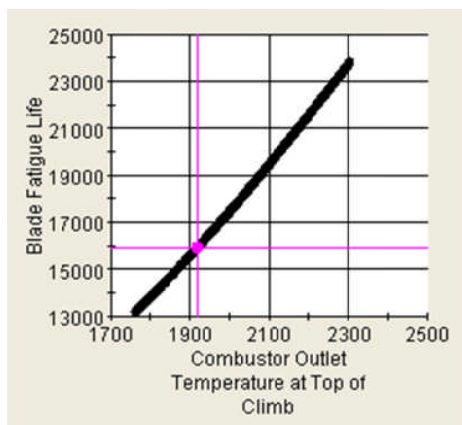
As can be observed, increasing combustor outlet temperature reduces block fuel burn to a certain point where the reduced thermal efficiency negates any benefit from the increased combustor outlet temperature.



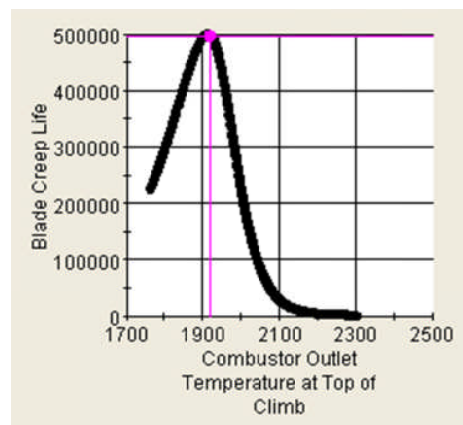
(a)



(b)



(c)



(d)

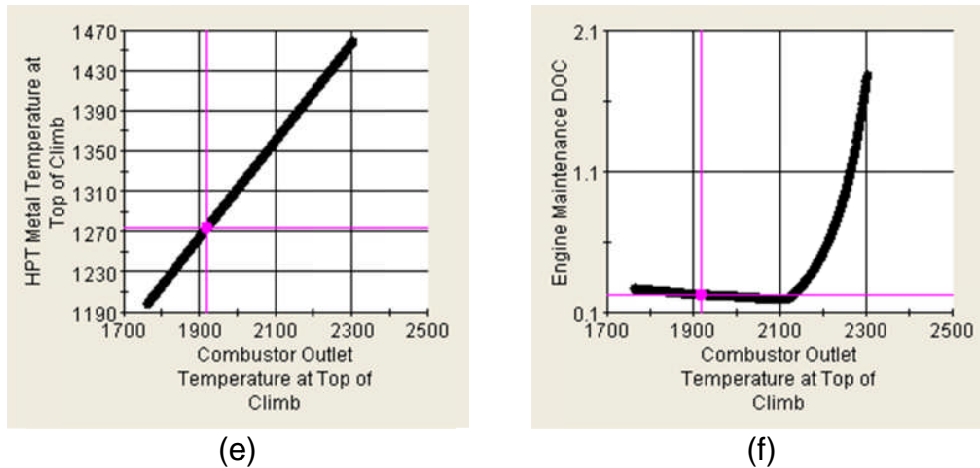


Figure 5-37 *Combustor outlet temperature variation at top of climb*

5.3.3 Optimisation of DDICLR Configuration

The thermodynamic cycle optimisation of the DDICLR configuration with respect to the maximum time between overhaul is presented in this section. Potential block fuel benefits of innovative intercooled aero engine (DDICLR) in order to reduce CO₂ emissions were explored in previous studies [100] [102]. It is already noted that the NEWAC programme intend to improve aero engines fuel consumption.

It is worth noting that the engine maintenance costs depend on time between overhaul (TBO), engine weight and production cost. On the other hand direct operating cost (DOC) is highly dependent on block fuel burn and engine maintenance cost. Therefore, it is reasonable to investigate the engine optimality from engine maintenance costs point of view.

Based on the lessons learned from the sensitivity analysis and the parametric design space exploration, most of the key design variables were considered for the optimisation studies. The selected design variables were allowed to deviate from their nominal value. The component efficiencies are kept constant, since they are considered as the technology parameters. The following engine design

variables that have a major influence on engine and aircraft system were chosen for optimisation, as listed in Table 5-11.

Table 5-11 *DDICLR engine optimisation steps, variables and ranges*

Step	Parameter	Range
1	Fan inlet mass flow	-15%...+5%
	Core mass flow	-15%...+5%
	Fan tip pressure ratio	-15.7%... +0.5%
2	IPC Pressure ratio	-10%... +15%
	HPC Pressure ratio	-10%... +15%
3	Combustor outlet temperature	-5%... +10%
	HPT cooling mass flow	-10%... +15%
4	Intercooler effectiveness	-5%... +10%
	Intercooler inlet mass flow	-40%... +10%

For a better understanding of the design space, the optimisation was performed in four steps. As a first step, the fan pressure ratio, fan mass flow and the core mass flow were optimised to achieve the best engine design in terms of time between overhaul. With these 3 design variables fixed at the optimal design values identified in step 1, the IPC pressure ratio and HPC pressure ratio were optimised next. Then, all the variables in step 1 and 2 were frozen to the optimal values, the combustor outlet temperature and HPT cooling mass flow were optimised. Finally, all the optimisation variables were frozen to the optimal values and step 4 was carried out. The final optimum was the output of all three optimum steps.

During the optimisation procedures using TERA tool, different engine designs were evaluated to find the optimum engine design. The feasibility of the optimum design was judged using the constraints set. Each of the design parameters has a certain limits. For the DDICLR configuration certain bounds was set as constraints such that the final results meet the different requirements i.e. the customer requirements, certification policies, the engine performance and mechanical limitations. These design space constraints set for the current optimisation problem are given in Table 5-12.

Table 5-12 *DDICLR engine design space constraints*

Constraint	Bound		Unit
	<i>Lower</i>	<i>Upper</i>	
FAR take-off distance	-	2.5	km
Climb time to 35000 [ft]	-	22.5	min
IPC design pressure ratio	2.7	-	-
HPC design pressure ratio	-	25	-
HPC last stage blade height	0.01	-	m
Combustor outlet temperature	-	2050	K
HPT blade metal temperature	-	1250	K
Auxiliary nozzle area variation	-	+50	%
Block fuel burned	-	26250	Kg

In the counter plots presented in this section, the Pink point indicates the engine design point and the Black ones represent the optimal design with respect to the time between overhaul.

5.3.3.1 Fan and core sizing

Fan pressure ratio, fan inlet mass flow and core mass flow are the key parameters with respect to the engine overall sizing. These parameters were examined at top of climb to achieve an optimal engine design in terms of time between overhaul (TBO) using TERA2020 software. The results are demonstrated in the form of contour plots and evaluated in terms of engine maintenance costs, direct operating costs, engine weight, fuel burn, and specific fuel consumption.

The contour plot in Figure 5-38 shows the effect of varying fan inlet mass flow and fan pressure ratio (at a fixed core mass flow) on block fuel burn. As expected, higher fan mass flow (bigger fan diameter) leads to a lower specific thrust, which improves the propulsive efficiency and hence reduces fuel consumption. However, this environmental benefit was partly offset by the increased engine weight (Ref. Appendix D.1).

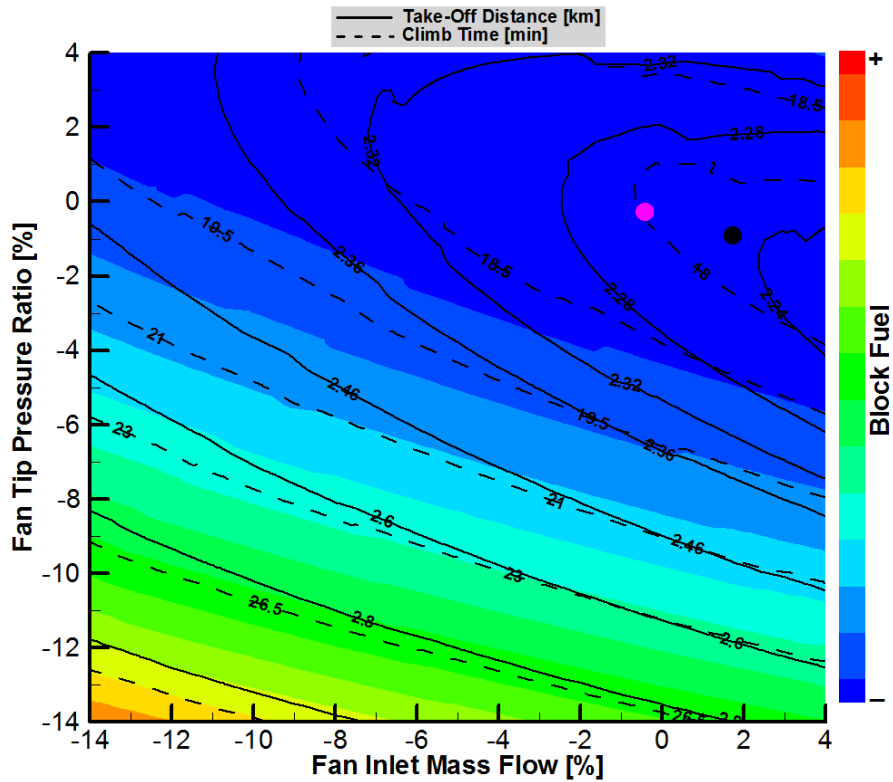


Figure 5-38 Variation of block fuel burn with fan inlet mass flow and fan tip pressure ratio

The improvement in engine maintenance costs from reducing fan tip pressure ratio and increasing fan inlet mass flow is shown in Figure 5-39. In the lower left hand corner of the contour a significant reduction in maintenance costs is predicted which is associated with substantial decreases in overall pressure ratio and hence improved engine component life. Also, increased specific thrust results in a small engine. However, moving towards that direction of the design space was constraint by the block fuel burn and the thrust requirements for the take-off distance and climb to altitude.

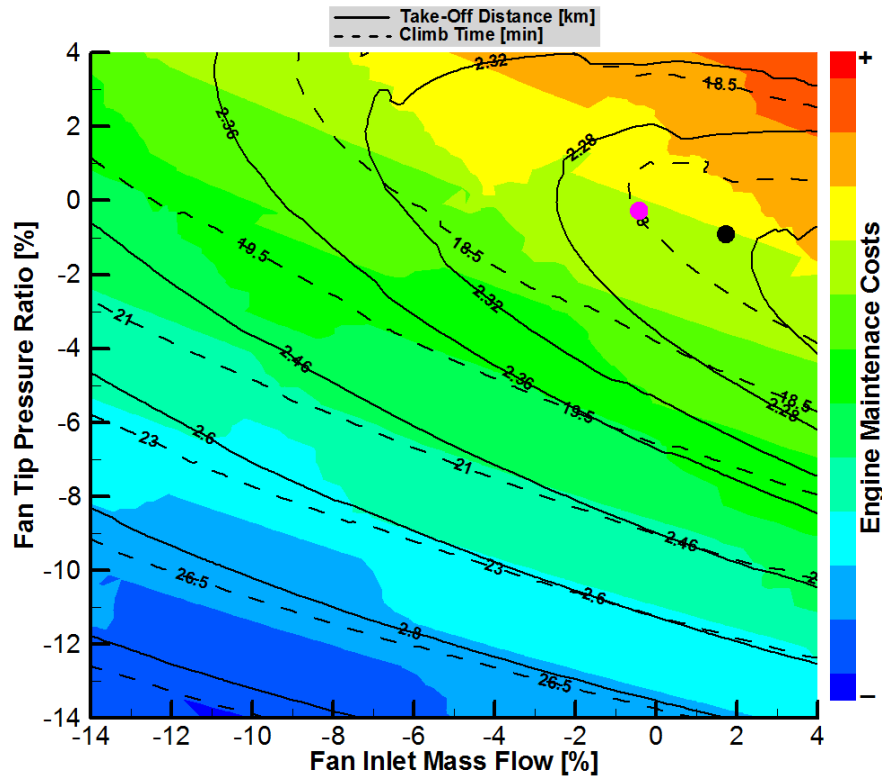


Figure 5-39 Variation of maintenance costs with fan inlet mass flow and fan tip pressure ratio

The variation of direct operating cost (DOC) with the changes in fan mass flow and fan tip pressure ratio is shown in Figure 5-40. The direct operating cost is highly affected by the fuel burn and the maintenance costs. Lower fan tip pressure ratio and higher fan inlet mass flow results in better engine time between overhauls; this in turn reduces the engine maintenance costs and hence direct operating costs.

Better time between overhaul was achieved with higher fan mass flow and slightly lower fan tip pressure ratio. This was attributed to the lower rotational speed of the HP shaft. As the fan rotational is the function of the fan tip pressure ratio, reducing the fan rotational speed affects the downstream components size and rotational speed; this in turn affects the turbomachinery components mechanical lodes and hence stress.

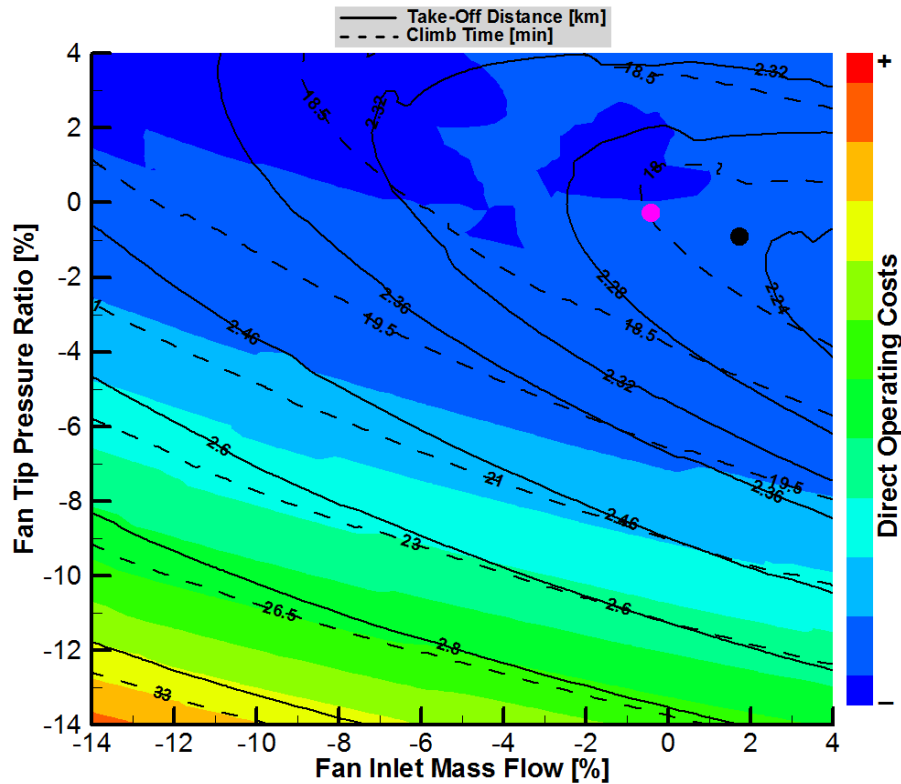


Figure 5-40 Variation of direct operating costs with fan inlet mass flow and fan tip pressure ratio

An increase in fan inlet mass flow by 2.2% and decrease in fan tip pressure ratio by 0.8% translates in an increase of 0.8% in time between overhaul from the engine initial design point. Also the engine maintenance cost was improved about 0.5%. However, a 1.6% engine weight penalty was inevitable.

The contour plot in Figure 5-41 illustrates the effect of varying the core mass flow and fan tip pressure ratio (at a fixed fan inlet mass flow) on block fuel burn. Decreasing the core mass flow directly leads to higher engine bypass ratio and lower engine specific thrust. As the fan diameter was fixed, the reduced engine weight was expected which is related to the smaller engine core size. Unlike the engine fan mass flow, reducing the core mass flow reduces the SFC because of the reduced fuel flow rate and also improved propulsive efficiency.

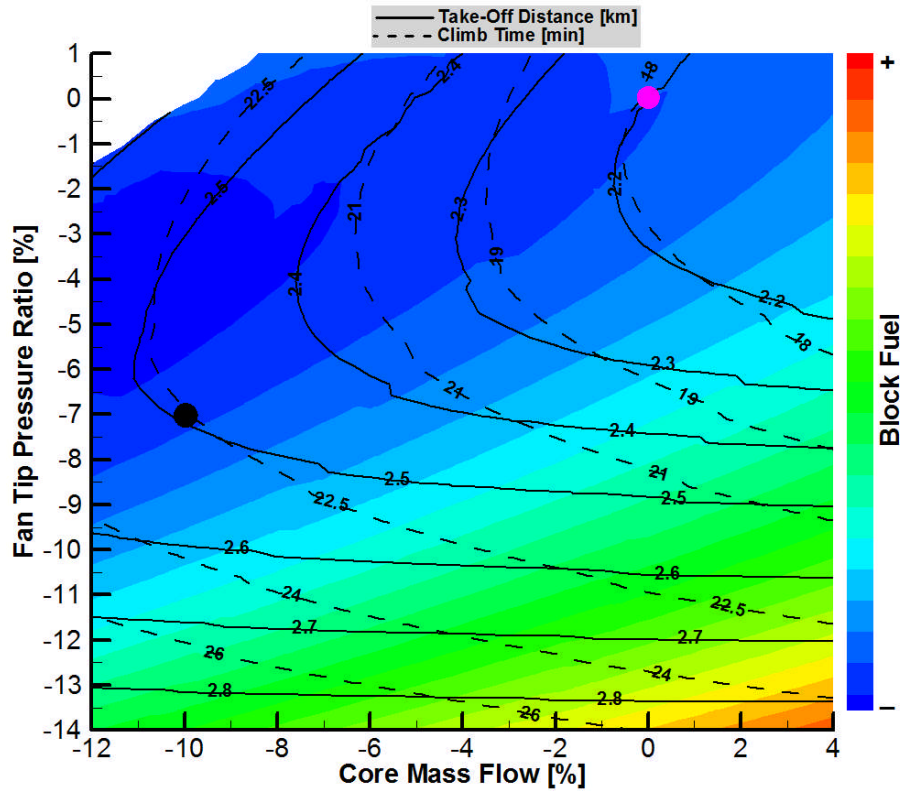


Figure 5-41 Variation of block fuel burn with core mass flow and fan tip pressure ratio

In order to obtain more thermodynamic benefits from reducing specific thrust, the fan pressure ratio needs to be reduced since the increased fan pressure ratio consumes more power delivered by the LPT. Additionally, a lower fan tip pressure ratio was desired due to the stress consideration of the fan blades. However, the thermal efficiency of the engine deteriorates due to reduced fan tip pressure ratio. Because of a temperature decrease at combustor inlet due to the OPR reduction, the fuel flow increases causing an overall increase in fuel consumption. This very well negates the lower specific thrust benefits. Thus, the block fuel burn remains the same. (Ref. Appendix D.2)

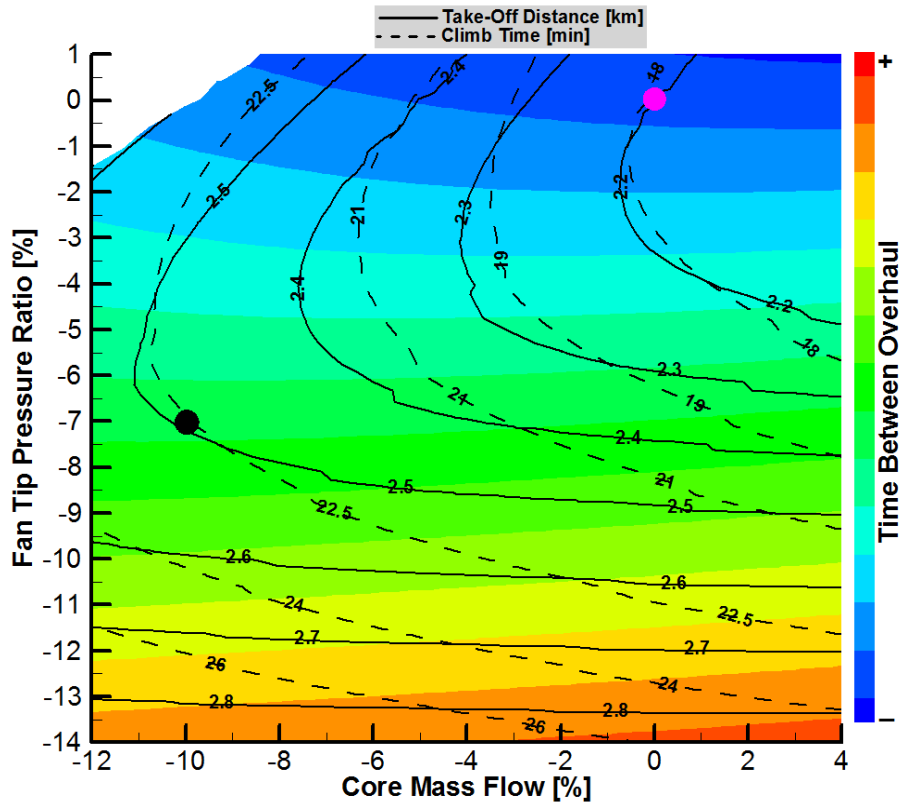


Figure 5-42 Variation of time between overhaul with core mass flow and fan tip pressure ratio

As it can be observed from Figure 5-42, moving towards the lower right corner of the counter, the time between overhaul improves. This is due to the reduction in OPR (which is an off-design effect from the engine performance) and increased cooling flow rate (5% of the HPC exit mass flow) but due to the block fuel burn constraint the optimum TBO is not located in that corner. Similarly, the design space towards the lower left corner of the counter was constrained by the HPC last stage blade height requirement that limiting the core size and fan diameter.

Looking at the trends shown in Figure 5-43, and then comparing with the two previous counters, it can be concluded that the lower core mass flow shall be joined by the reduced fan pressure ratio to achieve a better engine maintenance cost. Again this was constraint by the core size and the engine thrust requirements. Therefore trade-off rises between engine weight, block fuel burn

and time between overhaul. A 10% decrease in core mass flow at top of climb (which translates to a 9% reduction in specific thrust) consequences in reduction by 6% and 0.8% of engine maintenance costs and direct operating costs, respectively. At the same time the take-off distance and time to climb were increased about 7% and 22%, respectively.

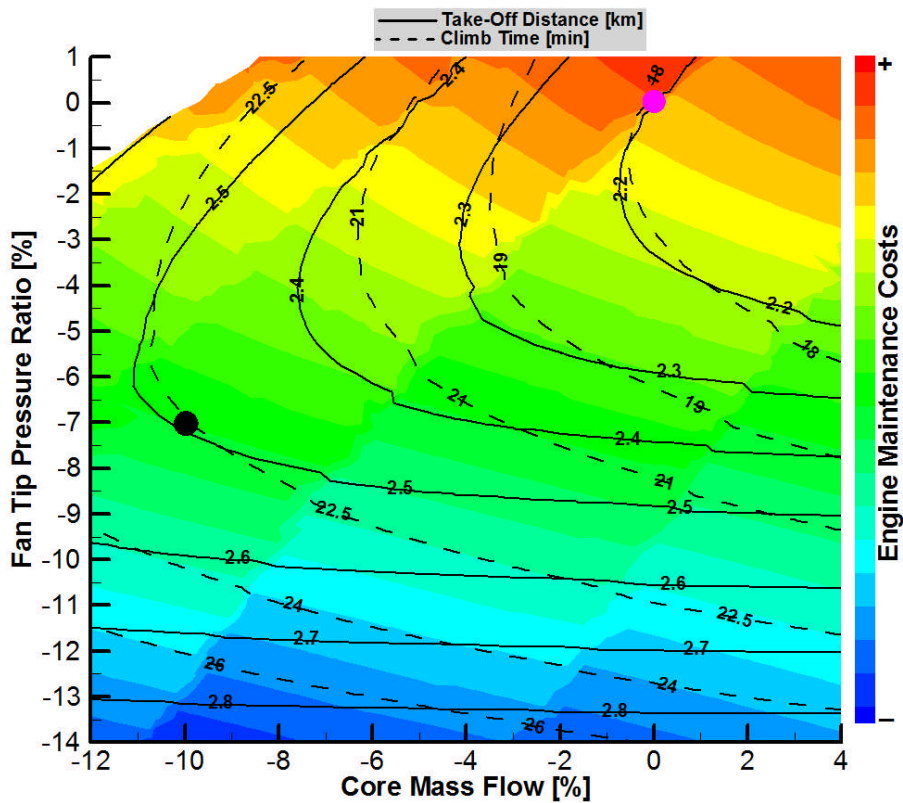


Figure 5-43 Variation of engine maintenance costs with core mass flow and fan tip pressure ratio

With the fan mass flow and core mass flow set at their optimum values, a further improvement in the time between overhaul was achieved through reducing the fan tip pressure ratio, as can be observed in Figure 5-44. In the results illustrated in this section, the Pink dot indicates the design point where the Green dot indicates the optimal point.

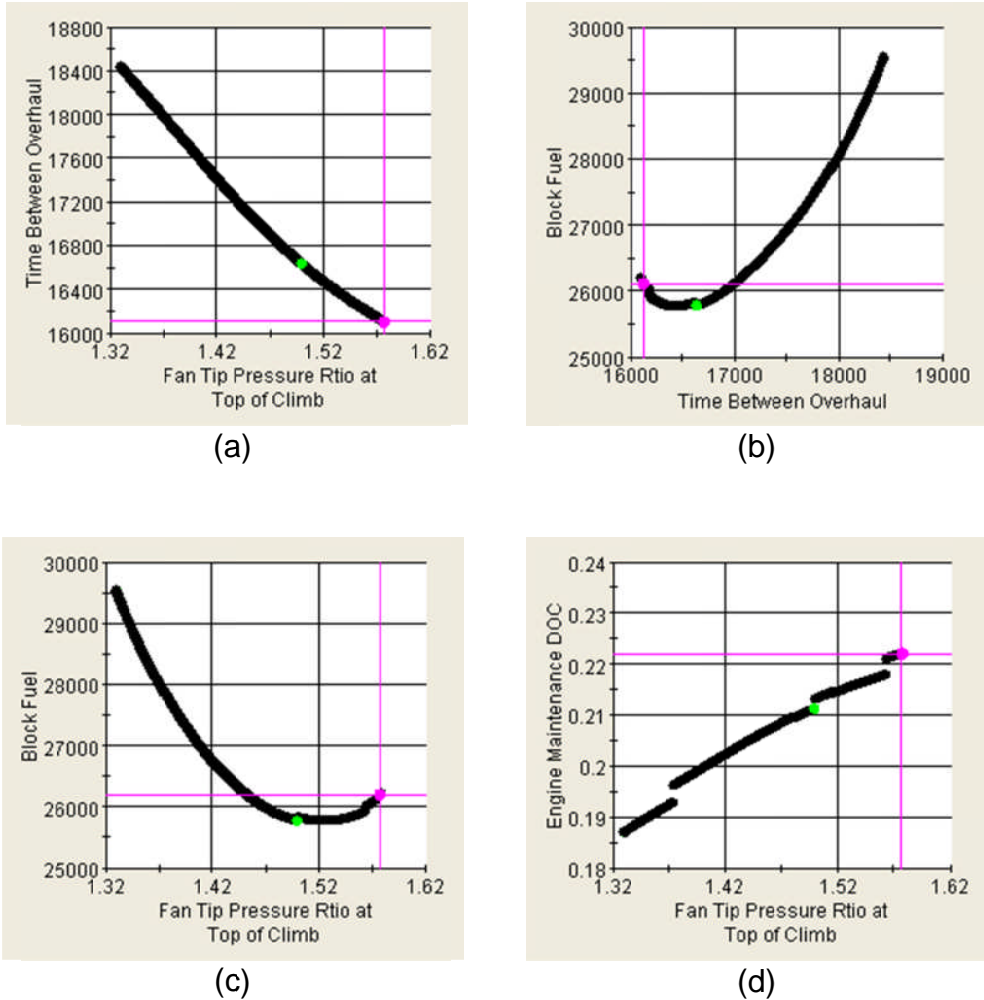


Figure 5-44 Optimum fan tip pressure ratio for maximum TBO

As the fan pressure ratio reduced by 4.9%, a 4.6% increase in the time between overhaul and 1% reduce in the direct operating cost was obtained. Also, the engine fuel burn benefits (roughly 1.3%) from decreasing the fan pressure ratio. This is mainly attributed to the engine weight reduction due to LPT stage count change (from 11 to 9). A large amount of design possibilities were ruled out by the constraints of High Pressure Turbine (HPT) metal temperature, take-off distance and time to climb.

5.3.3.2 IPC/HPC pressure ratio

With the value of the fan mass flow, core mass flow and fan tip pressure ratio fixed at the optimum point, the IPC and HPC pressure ratios were varied (and hence overall pressure ratio) at top of climb to further improve the engine life.

Principally, increasing engine overall pressure ratio, results in a better SFC due to the thermal efficiency improvement. For an intercooled core, increasing the overall pressure ratio reduces the engine core size and hence a lower engine weight. This is because of the increased air density during the intercooling process. Therefore, the overall pressure ratio was limited with the reasonable blade height requirements of the HPC.

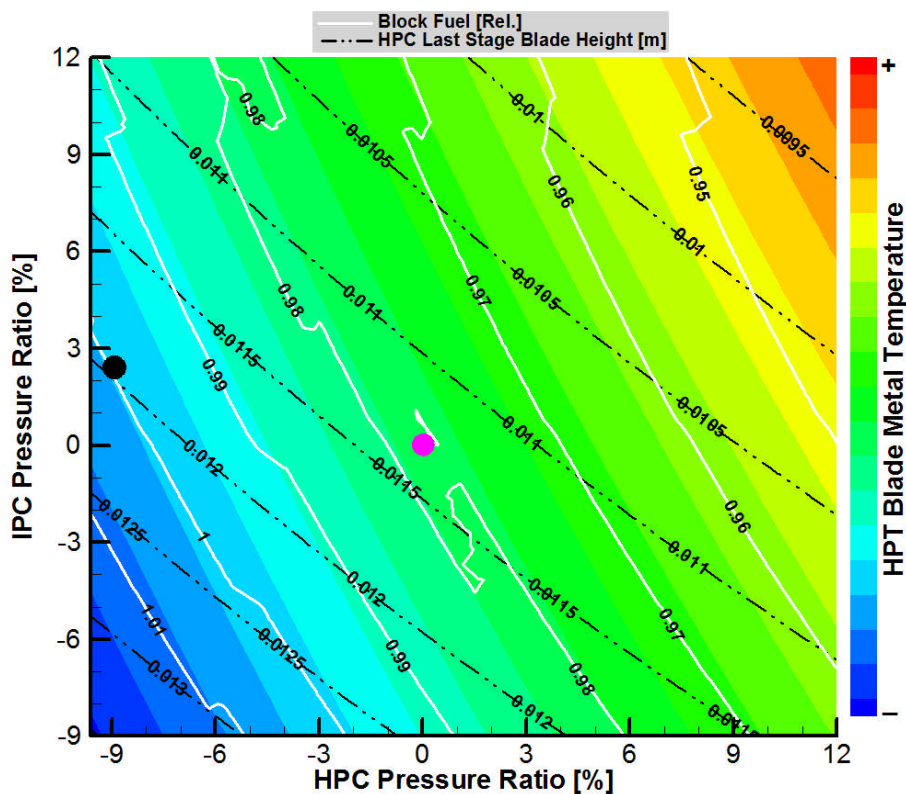


Figure 5-45 Variation of HPT metal temperature with IPC and HPC pressure ratios

The effect of increased overall pressure ratio on engine time between overhaul was almost the opposite of its influence on the fuel consumption. This is mainly attributed to the increased HPC delivery temperature and thus blade metal temperature as illustrated in Figure 5-45. Therefore, trade-off mainly exists between higher time between overhaul and lower specific fuel consumption.

In order to optimise the engine design for maximum time between overhaul and at the same time keeping the block fuel as low as possible, it is required that the increasing OPR is not to be distributed evenly on the IPC and HPC. Thus, when reducing the HPC pressure ratio, it is required to increase the IPC pressure ratio to maintain the optimal OPR with respect to the fuel burn. The variation of engine time between overhaul with IPC and HPC pressure ratio is illustrated in Figure 5-46.

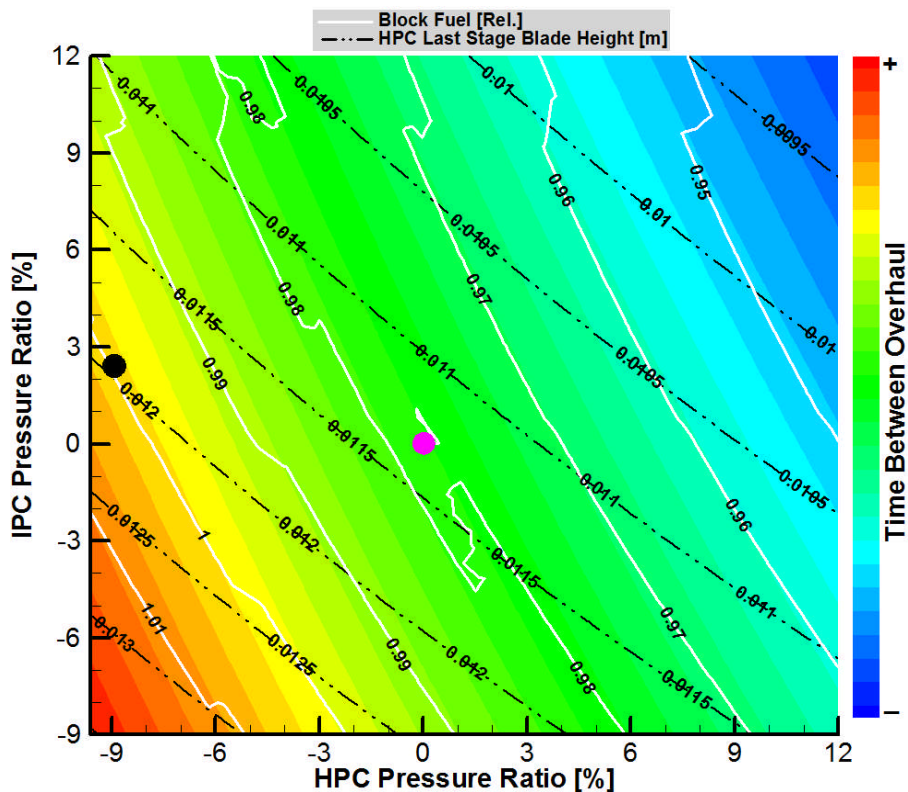


Figure 5-46 Variation of TBO with IPC and HPC pressure ratio

Optimisation results shows that increasing the IPC pressure ratio about 2.5% and reducing the HPC pressure ratio by 9% can improve nearly 14% time between overhaul compared to the nominal engine design. However, this gain was accompanied with a 0.2% engine SFC penalty. Such a design meets all the predefined constraints set.

5.3.3.3 Combustor outlet temperature and HPT cooling flow

With the values from the previous steps set to the optimum, the combustor outlet temperature and HPT cooling mass flow were varied (and hence the engine thrust) at top of climb to further improvement of the engine life. These are crucial parameters to optimise the engine life. This is in agreement with the parametric studies performed in previous sections.

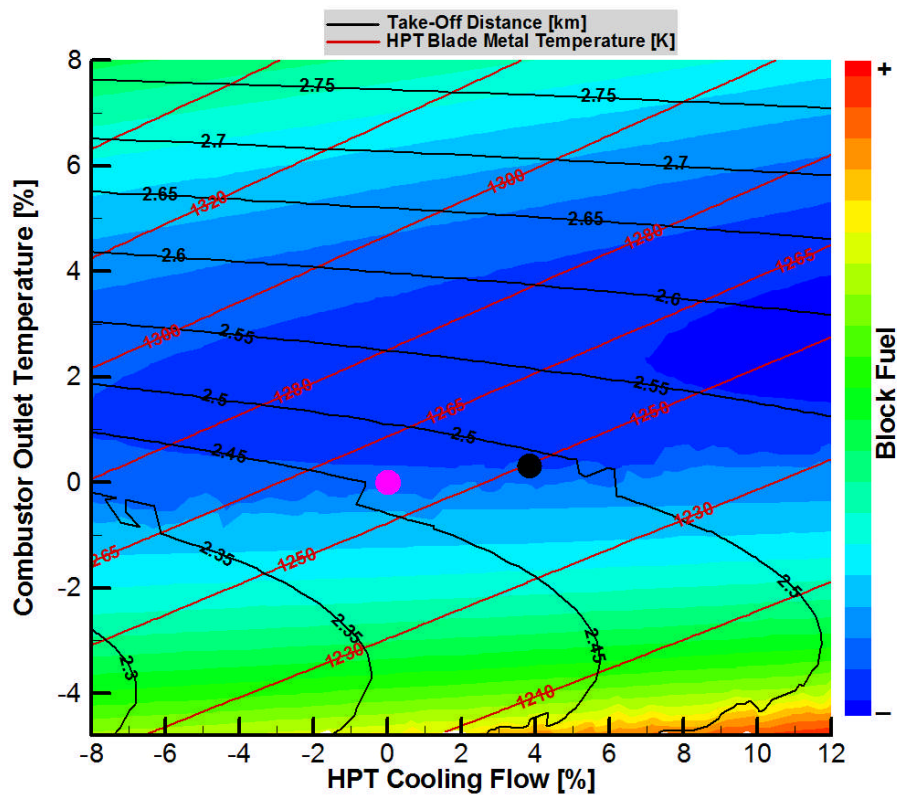


Figure 5-47 Variation of block fuel with Combustor Outlet Temperature and HPT cooling mass flow

Increasing the combustor outlet temperature is desirable to improve the engine thermal efficiency which consequently reduces the engine size and weight. For a given OPR there is an optimal combustor outlet temperature for SFC. At the same time, the propulsive efficiency decreases with the higher level of combustor outlet temperature since the velocity ratio drops with the increasing core outputs. The variation of block fuel burn with combustor outlet temperature and HPT cooling mass flow is given in Figure 5-47. The fact that the value of the combustor outlet temperature was already optimised for minimum block fuel burn explains why its value was increased less than one.

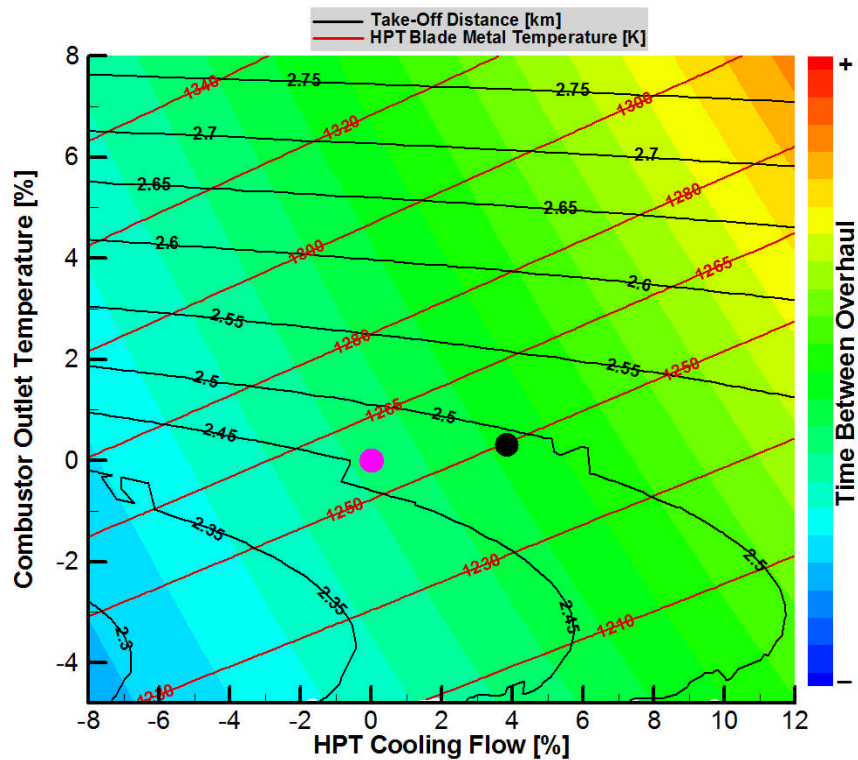


Figure 5-48 Variation of TBO with combustor outlet temperature and HPT cooling mass flow

Although a further increase in time between overhaul was possible by increasing the cooling mass flow, but it worsens the take-off thrust requirements. As shown in Figure 5-48, the time between overhaul was largely

influenced by the combustor outlet temperature rather than HPT cooling mass flow. Optimisation results shows that with the value of combustor outlet temperature reduced by 0.5% and cooling mass flow increased by 3.5%, there is an additional 10% engine life improvement. Nevertheless, an inevitable SFC penalty of about 0.2% was experience due to increased cooling mass flow which deteriorates engine performance.

5.3.3.4 Intercooler effectiveness and cold mass flow

The intercooler effectiveness and intercooler cold mass flow were varied at top of climb (at a variable thrust level and constant combustor outlet temperature) to explore the design space for a better combination of parameters with respect to the engine life.

As the intercooler aerodynamic design was carried out at take-off condition, the effects of varying intercooler mass flow dominates intercooler effectiveness at top of climb. Variation of engine weight with intercooler effectiveness and intercooler cold mass flow is illustrated in Figure 5-49.

With increasing intercooler effectiveness and intercooler mass flow the intercooler pressure losses increases. This can deteriorates the thermal efficiency of the engine. At a fixed fan diameter increasing the intercooler effectiveness reduces the propulsive efficiency. The reason behind this is that higher intercooler effectiveness increases the fuel flow rate and thrust and hence reduces the velocity ratio. Furthermore, it can increase the intercooler weight. Nevertheless the overall engine weight reduces due to reduced size and weight of the HP module. This mainly attributed to the lower work demand of the HPC. On the other hand, high intercooler cold mass flow can increase propulsive efficiency while reduces thermal efficiency and hence overall efficiency. Thus deteriorates the SFC. In order to reduce intercooler pressure losses, the intercooler cold mass flow needs to be reduced. This practice improved the block fuel burn, as illustrated in Figure 5-50.

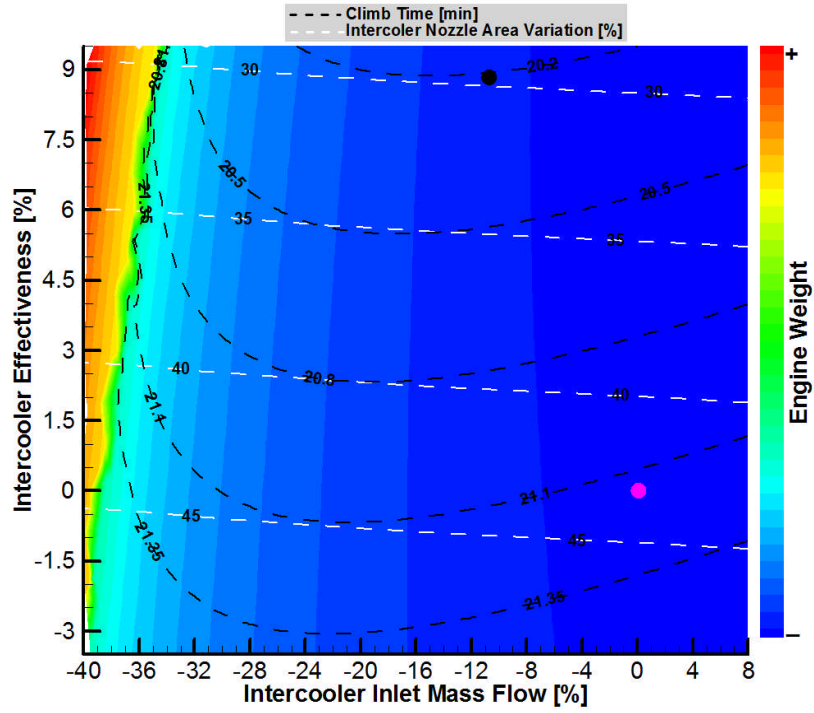


Figure 5-49 Variation of engine weight with Intercooler effectiveness and Intercooler cold mass flow

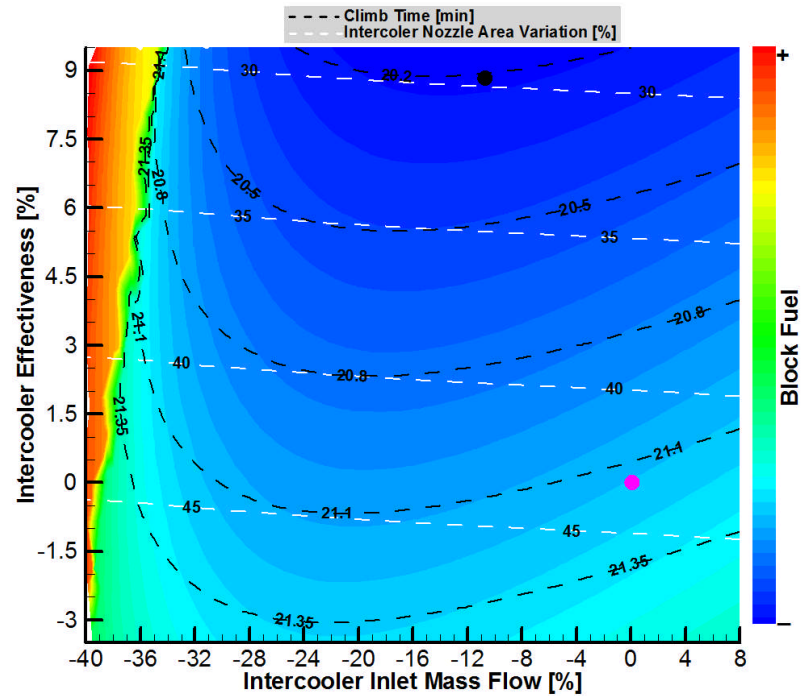


Figure 5-50 Variation of block fuel with Intercooler effectiveness and Intercooler inlet mass flow

Increasing both intercooler effectiveness and cold mass flow was beneficial for engine time between overhaul. Increasing intercooler effectiveness at top of climb reduce the HPC delivery temperature for a given combustor outlet temperature. This means that cooling temperature reduces and thus the blade metal temperature which results in a better engine time between overhaul. Reduced overall pressure ratio also enhances the cooling of the HPT and thus contributes partly to the reduction of the maintenance costs. These are illustrated in Figure 5-51 and Figure 5-52.

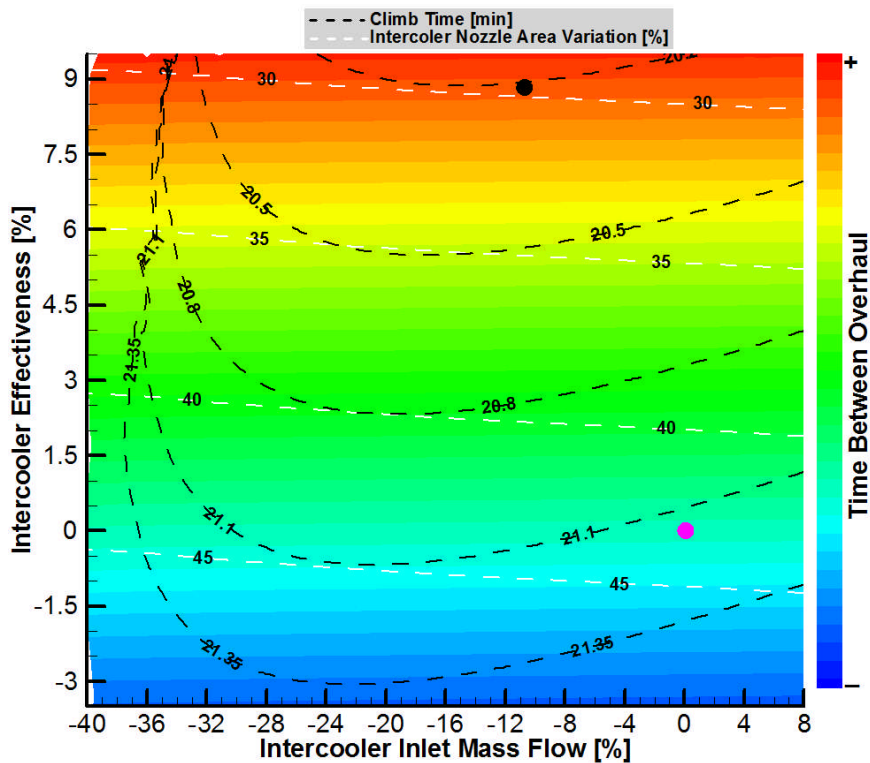


Figure 5-51 Variation of engine time between overhaul with Intercooler effectiveness and Intercooler inlet mass flow

Finally with the all design parameters fixed at the optimum values which were identified in earlier sections, the optimisation results shows that the increased intercooler effectiveness by 9% and reduced intercooler cold mass flow by about 11% can offer approximately 7% improvement in engine time between

overhaul. The reduced time between overhaul thus contributes partly to the reduction of the maintenance costs about 2%.

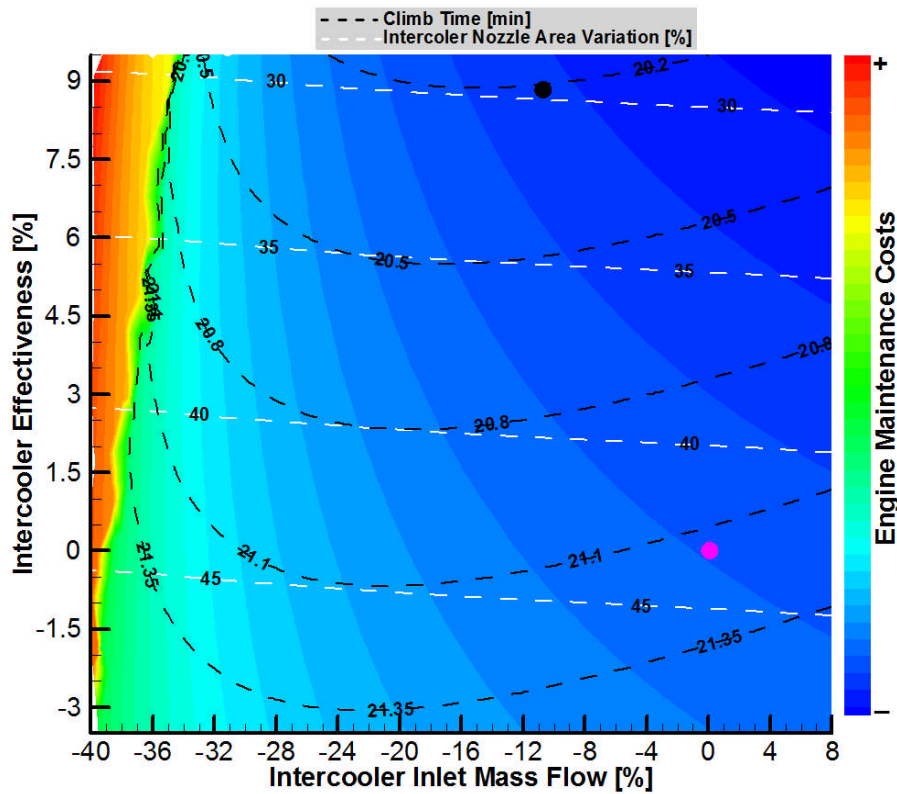


Figure 5-52 Variation of engine maintenance costs with Intercooler effectiveness and Intercooler inlet mass flow

5.3.4 DDICLR Optimised Design

In this section, the DDICLR configuration was evaluated and optimised for extending engine life using TERA2020 software. Different parameters as engine design parameters were assessed and their influence on engine life was reported. Then a better combination of engine design parameters with respect to the engine weight, block fuel burn, maintenance and direct operating costs were proposed.

The optimum values of the engine design variables are given in Table 5-13. It should be noted that the optimum values are the percentage deviation of the design parameters from the nominal design.

Table 5-13 *DDICLR configuration design variables and optimum values*

Step	Parameter	Optimal Value	Unit
1	Fan inlet mass flow	2	%
	Core mass flow	-10	%
	Fan tip pressure ratio	-5	%
2	IPC Pressure ratio	2.5	%
	HPC Pressure ratio	-9	%
3	Combustor outlet temperature	0.5	%
	HPT cooling mass flow	3	%
4	Intercooler effectiveness	9	%
	Intercooler inlet mass flow	-12	%

From the table it can be observed that the engine core mass flow, HPC pressure ratio, intercooler effectiveness and intercooler inlet mass flow were changed significantly. A possible explanation could be that the block fuel constraint tends to move the optimum engine design to a selection of parameters that gives maximum time between overhaul while reducing engine weight and direct operating costs. Thus, a bigger fan diameter and smaller engine core size combined with the reduced pressure losses to satisfy the engine design for higher service life and lower fuel consumption.

Performance results are shown in Table 5-14. Comparison is given between the optimum and nominal engine design. The overall pressure ratio, overall efficiency and engine thrust level of the optimal design are lower compared to the corresponding nominal design point ones while bypass ratio and specific fuel consumption show an increase.

Table 5-14 Comparison of the TBO optimal design of DDICLR engine with respect to the nominal design

Performance Parameters	Unit	Top of Climb		
		Nominal	Optimal	Delta %
Fan inlet mass flow	[kg/s]	500.3	511.4	2.2
Core mass flow	[kg/s]	36.9	33.2	-10
Bypass ratio	[-]	12.6	14.4	14.7
Fan tip pressure ratio	[-]	1.6	1.5	-4.9
IPC pressure ratio	[-]	4.8	4.9	2.5
HPC pressure ratio	[-]	11.9	10.8	-9
Overall pressure ratio	[-]	78	68	-12
Combustor outlet temperature	[K]	1920	1929	0.5
HPT blade metal temperature	[K]	1273	1240	-2.5
HPT blade cooling temperature	[K]	787	730	-7.2
HPT blade cooling effectiveness	[-]	0.5	0.5	2.3
Intercooler effectiveness	[-]	0.65	0.71	9
Intercooler mass flow ratio	[-]	1.4	1.3	-1.9
Overall efficiency	[-]	0.4	0.4	-0.4
Thermal efficiency	[-]	0.51	0.50	-1.4
Propulsive efficiency	[-]	0.76	0.77	0.8
Specific fuel consumption	[g/(kN*s)]	1.95	15	0.4
Specific thrust	[N*s/kg]	133	123	-8
Thrust	[kN]	67	63	-6
Engine weight	[kg]	7059	7048	-0.2
Engine production cost	[k€]	5691	5709	0.3
Engine maintenance costs	[k€/h]	0.22	0.18	-17
Direct operating costs	[k€/flight]	63	62	-1.5
Time between overhaul	[hr]	16000	21000	20
Block fuel	[kg]	26120	25834	-1.1

As can be observed, a 20% improvement in time between overhaul was achieved along with a 17% engine maintenance costs and a 1.5% direct operating costs benefits. Similar to the BASELR configuration, about 1% block fuel reduction arises from the engine performance (re-matching the thermodynamic cycle) and the thrust reduction effects (rubberized wing aircraft model).

5.4 Results Verification

The capability and accuracy of the TERA2020 modules have been proven and accredited through the verified deliverable reports which have been submitted to OEM's and through bilateral technology meeting with the OEM's. Furthermore verifications were made against the specifications provided by the NEWAC project partners in the course of the tool development. The TERA2020 has therefore been verified as a useful tool for the assessments at the preliminary stage of an engine design process for: design space exploration, parametric and sensitivity analysis, and multidisciplinary optimisations.

CHAPTER 6 CONCLUSIONS AND FURTHER WORK

The main conclusions of the present research work and recommendations for further work are summarised in this chapter.

6.1 Conclusion

The primary objective of the present research work was to evaluate and optimise civil aero engine cycles to achieve the best engine design with respect to the engine time between overhaul (TBO) via a multidisciplinary optimisation approach (TERA). Such an approach was necessary in order to assess the trade-off between asset life, operating costs and technical specification. Hence, the specific objectives comprise the following:

- ✓ Contribution to the development and integration of a multidisciplinary framework, namely TERA2020 which consists of integrated models such as aircraft/engine performance, power plant weight and cost, noise, emissions, environmental impact and economic in order to optimise both conventional and conceptual aero engines.
- ✓ Development of a physics based oxidation model for HPT blades life prediction to make possible the assessment of potential performance and running cost benefits resulting from the adoption of new engine technologies and concepts.
- ✓ Assessment and optimisation of the conventional and conceptual aero engines with respect to the engine time between overhaul (TBO), taking into account the multidisciplinary aspects such as performance, block fuel burn, engine weight, production cost, maintenance and direct operating costs (DOC).

The main contributions of this doctoral thesis to knowledge are the following:

- Multidisciplinary TERA assessment of a novel intercooled conceptual engine with a particular emphasis on design space exploration and optimisation studies to identify the designs that may offer the largest time between overhaul and the consequent implications this may have on mission fuel burn and direct operating costs (DOC).
- Development of a more comprehensive lifing model that calculates the engine life with reasonable level of accuracy by integrating physics based oxidation, creep and fatigue models.

An initial literature review was performed at the early stage of the current research project. It gave an overview of the new technologies and procedures applied within the aviation industry to reduce the negative environmental impacts. Literature indicates that the currently available mitigation options may not be enough to prevent growth in air transport emissions. Hence, technology research and development is essential in order to create sustainable development for the future. The design of aero engines to reduce fuel burn, which leads to reduced CO₂ emission, was considered as a key long-term objective. A variety of promising concepts are being proposed to reduce CO₂ and other emissions, although the best option to pursue for investment is difficult to select. The success or failure of an aero engine business depends on a careful selection of a conceptual engine.

On the other hand, the increasing complexity of aero engine design has encouraged the gas turbine engine designers and manufacturers to develop and implement multidisciplinary design optimisation approach (MDO) from the earliest design stages. This helps to prevent the need for expensive changes during later design stages and full-scale development. The problem is multidisciplinary and has led many within the industry and academia to develop and adopt techno-economic tools such as EDS, NPSS, PMDO and TERA.

TERA is an approach pioneered at Cranfield University. It can be used to evaluate the power systems for use on land, at sea and in the air. The essential function of this approach is to rapidly explore the design space, identify solutions and minimise computational time and costs. The core of this tool is a detailed thermodynamic model of the power plant which provides data required by other modules. This core module was integrated with some additional modules, e.g., engine dimensions and weight module, production cost module, aircraft performance and dimension module, emissions module, noise module and economic module to represent a multidisciplinary tool. In contrast to common industrial procedures where aircraft OEM demand a certain engine thrust, in TERA2020 the thrust is allowed to vary.

The economic module (HESTIA) is the last module in TERA calculation sequence. The existing economic module is composed of three main sub models: a lifing model, an economic model and a risk model. The lifing model measures preliminary serviceable life of the engine, namely high pressure turbine disk and blades, through the analysis of creep, fatigue and oxidation over a full working cycle of the engine. The current developed oxidation model in this work is a physics based model which was developed to estimate the TBC life of the high pressure turbine blades of the first stage. This model was used to represent the oxidation effect on turbine blade failure. The first stage of the high pressure turbine is the part of the aero engine that bears the highest stresses due to pressure, temperature and rotational speeds. Hence in this model the focus is on high pressure turbine blade, being the component that usually limits gas turbine life.

Before carrying out the optimisation processes, sensitivity analysis and parametric studies were performed using TERA2020 tool. The performed sensitivity analysis was crucial for successful design of experiments and optimisation studies. These results were helpful for a better understanding of the design domain for each engine configuration. In particular, the compiled sensitivity parameters allowed the impact of changes in a certain design variable to be assessed and to determine which design parameter was the key

driver to concentrate more efforts on. In order to assess the effect of the main design parameters on the final engine design with respect to the specific fuel consumption, engine weight, time between overhaul, maintenance and direct operating costs, the parametric studies were conducted using the Design of Experiment (DOE) techniques. These assessments provide a rough estimate of the optimal designs which can be used as a starting point for design space approximations and numerical optimisations.

Finally, based on the results obtained from the sensitivity analysis and parametric studies, the engine performance design parameters (at top-of-climb) were varied around their nominal point in groups of two or three parameters at a time. Then the Polynomial response surface models (RSM) were used to approximate the design space produced for each set of parameters. Using the approximate models, different optimisation algorithms were employed to find the maximum time between overhaul (TBO) for a mission that obeys a given set of design constraints.

The optimum engine cycles results show that an improvement in time between overhaul (TBO) can be expected by: reducing the core mass flow, intercooler inlet mass flow (for intercooled core), fan and HPC pressure ratios as well as the combustor outlet temperature while increasing the fan inlet mass flow, intercooler effectiveness (for intercooled core), IPC pressure ratio and HPT cooling mass flow from their respective nominal values. Looking at the values of the optimised design parameters, it can also be concluded that the engine design with a small core size requires more cooling mass flow for same TET.

The optimisation results reflect that the optimal overall pressure ratio (OPR) for both configurations is low related to the nominal point. This is mainly comes from the fact that the higher OPR increases the cooling mass flow temperature and hence deteriorates the HPT blade life. Furthermore, the optimal specific thrust value for both configurations is lower compared to the nominal ones; this is mainly due to the increased fan diameter and reduced core size.

In conclusion, considerable benefits in terms of time between overhaul was estimated for optimised engine cycles. For BASELR configuration the time between overhaul improved by 17% while engine weight increased by 1% and engine thrust level reduced by 3%. For the DDICLR configuration the improvement in time between overhaul is more pronounced because of the OPR was reduced significantly. For this configuration a 20% improvement in time between overhaul was predicted. Nevertheless, the engine thrust level was decreased by 6% and the engine production cost increased by roughly 0.3%.

6.2 Recommendations for Further Work

The following recommendations and suggestions for further work are identified:

Lifing model:

- The cooling system has a major influence on turbine blade and disk life. Currently, the blade metal temperature is calculated from the cooling effectiveness factor that is chosen from a range. The blade life is then calculated based on this single temperature. In reality the blade temperature will vary from the root of the blade to the tip. Hence different regions on the blade will have different temperature, as well as different lives. It is important to include this variation in the heat transfer analysis to determine the critical location on the blade that failure could occur. This can be done by introducing the radial temperature distortion factor (RTDF) to obtain the combustor gas temperature profile, from which the blade metal temperature distribution along the blade span can be calculated.
- The importance of considering the impact on the turbine blade life (hence, TBO) of the interaction of the major damage mechanism have been identified in several literature. The turbine blades are subjected to both thermal and mechanical loadings that make them susceptible to Thermomechanical fatigue (TMF). Hence, the current trend in the life

predictions of gas turbines is to adopt a thermomechanical fatigue approach that considers the interaction of the three major damage mechanisms; creep, fatigue and oxidation. Some of the TMF approaches that have now become popular include the N-S TMF model [103], Miller model [104], Zamrik [105] and recently, the works of khoebel [106] . It is therefore suggested that a review of TMF models is carried out with a view to implement a suitable TMF model in the TERA framework.

- Currently, in the lifing model, the flight envelope has been divided to 5 segments: take-off, climb, cruise, descent and reverse-thrust. A significant improvement would be to break down each segment, especially the climb segment to multiple trajectory points. This could be done by the same way that the aircraft module does in order to predict fuel burn and will enable to identify the impact of the time and temperature on the failure mechanisms.

Optimisation studies:

- Evaluating and optimising the aero engines in terms of optimum direct operating cost (DOC) would identify the best economic compromise between the engine life and fuel burn particularly from the operators perspective. This can be done by considering different fuel price and under variety of emission taxation scenarios.
- As there are no internal loops in the TERA2020 algorithm, some interdependencies could not be considered, e.g. turbomachinery efficiency dependency on designed pressure ratio or cooling mass flow dependency on designed heat exchanger temperature drop. Future studies might consider the development and calibration of an interaction tool. Similarly when optimising the engine fan and core, a tool is required to take into account the effects of core size on engine fan and vice versa.

REFERENCES

- [1] ICAO: Department of Economic and Social Affairs, 2001, "Aviation and Sustainable Development", Ninth Session, Commission on Sustainable Development, New York.
- [2] Intergovernmental Panel on Climate Change, 2007, "Climate Change 2007: Mitigation of Climate Change", Working Group III, IPCC Fourth Assessment Report (AR4).
- [3] Boeing Commercial Airplanes, Market Analysis, 2011, "Current Market Outlook 2011 to 2030", URL <http://www.boeing.com>.
- [4] Airbus GMF 2011-2030 delivering the future, 2011, "Global Market Forecast for 2011-2030", URL <http://www.airbus.com>.
- [5] Green, J. E., 2003, "Civil Aviation and the Environmental Challenge", *The Aeronautical Journal*, Vol. 107, No. 1072, pp. 281-299.
- [6] Advisory Council for Aeronautical Research in Europe, 2001, "European Aeronautics: A vision for 2020 – Meeting Society's Needs and Winning Global Leadership," URL <http://www.acare4europe.org>.
- [7] Sieber, J., 2011, "NEWAC technologies: Highly Innovative Technologies for Future Aero Engines", URL <http://www.newac.eu>.
- [8] Penner, J. E., Lister, D. H., Griggs, D. J., Dokken, D. J., and Farland, M. M., 1999, *Aviation and the Global Atmosphere*, Cambridge, Cambridge University Press.
- [9] Bengue, L. M., 2010, "Toward ACARE 2020: Innovative Engine Architectures to Achieve the Environmental Goals?", ICAS 27th Congress Proceedings, Nice, France.
- [10] Pilidis, P., and Palmer, J.R., 2009, *Gas Turbine Theory and Performance*, Course's lecture notes, School of Engineering, Cranfield University, UK.
- [11] Clarke, J. P., 2003, "The Role of Advanced Air Traffic Management in Reducing the Impact of Aircraft Noise and Enabling Aviation Growth", *Journal of Air Transport Management*, Vol. 9, No. 3, pp. 161-165.
- [12] PARTNER, 2009, URL <http://web.mit.edu/aeroastro/partner>.
- [13] Clean Sky JTI, 2010, URL <http://www.cleansky.eu>.

- [14] Kyprianidis, K. G., Grönstedt, T., Ogaji, S. O. T., Pilidis, P., and Singh, R., 2010, "Assessment of Future Aero-engine Designs with Intercooled and Intercooled Recuperated Cores", *ASME Journal of Engineering for Gas Turbines and Power*, GTP-2010-1056.
- [15] Karl, A., 2010, "Assessing Variability to Achieve Robust Design", INSIGHTS, URL <http://www.simulia.com>.
- [16] Ryan, R., Blair, J., Townsend, J., and Verderaime, V., 1996, "Working on the Boundaries: Philosophies and Practices of the Design Process", NASA Technical Paper 3642, Marshall Space Flight Center, MSFC, Alabama.
- [17] Sobieszczanski-Sobieski, J., and Haftka, R. T., 1996, "Multidisciplinary Aerospace Design Optimization: Survey of Recent Developments, Structural Optimization", AIAA Paper 96-0711, AIAA 34th Aerospace Sciences Meeting and Exhibit, Reno.
- [18] Jones, M. j., Bradbrook, S. J., and Nurney, K., 2012, "A Preliminary Engine Design Process for an Affordable Capability", In RTO AVS Symposium on "Reduction of Military Vehicle Acquisition Time and Cost through Advanced Modelling and Virtual Simulation", Proceedings, RTO-MP-089-52, Paris, France.
- [19] Sobieszczanski-Sobieski, J., 1993, "Multi-disciplinary Design Optimization: An Emerging, New Engineering Discipline". NASA Technical Memorandum 107761, Langley Research Centre, Virginia.
- [20] Whellens, M. W., 2003, "Multidisciplinary Optimisation of Aero-Engines Using Genetic Algorithms and Preliminary Design Tools", PhD Thesis, School of Engineering, Cranfield, Bedfordshire, Cranfield University, UK.
- [21] Antoine, N. E., Kroo, I. M., Willcox, K., and Barter, G., 2004, "A Framework for Aircraft Conceptual Design and Environmental Performance Studies", AIAA-2004-4314, 10th AIAA/ISSMO Multidisciplinary Analysis and Optimization Conference, Albany, NY, US.
- [22] US Representative, ICAO Committee on Aviation Environmental Protection "CAEP/7 WG2 – Aircraft Operations and Modelling", 2006, TG2 Meeting –Sixth Meeting, Tucson, AZ, USA.
- [23] Lytle, J. K., 1999, "The Numerical Propulsion System Simulation: A Multidisciplinary Design System for Aerospace Vehicles", NASA/TM-1999-209194, NASA Glenn Research Center, Cleveland, Ohio, US.
- [24] Follen, G. and auBuchon, M., 2000, "Numerical Zooming between NPSS Engine Simulation and a One-Dimensional High Compressor Analysis Code", NASA/TM-2000-209913, NASA Glenn Research Center, Cleveland, Ohio, US.

- [25] Tong, M., Halliwell, I., and Ghosn, L., 2004, "A Computer Code for Gas Turbine Engine Weight and Disk Life Estimation", *Journal of Engineering for Gas Turbine and Power*, Vol. 126, No.2, pp.265-612.
- [26] Schutte, J., Tai, J., Sands, J., and Mavris, D., 2012, "Cycle Design Exploration Using Multi-design Point Approach", ASME Paper GT2012-69334, Proceedings of GT2012, ASME TURBO EXPO 2010: Power for Land, Sea and Air, Copenhagen, Denmark.
- [27] Krishnan, R., 1998, "Evaluation of Frameworks for HSCT Design Optimization", NASA/CR-1998-208731, Computer Science Corporation, Hampton, Virginia, US.
- [28] Antoine, N. E., and Kroo, I. M., 2005, "Framework for Aircraft Conceptual Design and Environmental Performance Studies", *AIAA Journal*, Vol. 43, No.10, pp. 2100-2109.
- [29] Lytle, J. K., 1999, "The Numerical Propulsion System Simulation: A Multidisciplinary Design System for Aerospace Vehicles", 14th International Symposium on Air Breathing Engines sponsored by the International Society for Air Breathing Engines, NASA/TM-1999-209194, Florence, Italy.
- [30] Panchenko, Y., Moustapha, H., Mah, S., Patel, K., Dowhan, M. J., and Hall, D., 2002, "Preliminary Multi-Disciplinary Optimization in Turbomachinery Design", RTO AVS Symposium on Reduction of Military Vehicle Acquisition Time and Cost through Advanced Modelling and Virtual Simulation, Proceedings, RTO-MP-089-57, Paris, France.
- [31] Ogaji, S.O.T., Pilidis, P. and Hales, R., 2007, "TERA – A Tool for Aero-engine Modelling and Management", Second World Congress on Engineering Asset Management and the Fourth International Conference on Condition Monitoring, Harrogate, UK.
- [32] Gayraud, S., 1998, "Design of a Decision Support System for Combined Cycle Schemes", MPhil Thesis, School of Engineering, Cranfield University, Cranfield, Bedfordshire, UK.
- [33] Whellens, M.W., and Singh, R., 2002, "Propulsion System Optimisation for Minimum Global Warming Potential", ICAS 23rd Congress Proceeding, Toronto, Canada.
- [34] Kyprianidis, K.G., Quintero, R.F.C., Pascovici, D.S., Ogaji, S.O.T., Pilidis, P., and Kalfas. A.I., 2008, "EVA - A Tool for Environmental Assessment of Novel Propulsion Cycles", ASME Paper GT2008-50602, Proceedings of GT2008, ASME TURBO EXPO 2008: Power for Land Sea and Air, June 9-13, Berlin, Germany.

- [35] Di Lorenzo, G., Friconneau, V., Brandt, P., Lonneux, V., Marinai, L., Pilidis, P., and Ruiz-Olalla, G., 2007, "Technoeconomic Environmental Risk Analysis Technological Perspective Application to Low Carbon Plant", IDGTE Conference, Milton Keynes, UK.
- [36] Ogaji, S.O.T., Pilidis, P., and Sethi, V., 2009, "Advanced Power Plant Selection: The TERA (Techno-economic Environmental Risk Analysis) Framework", ISABE-2009-1115, Montréal, Canada.
- [37] Doulgeris, G., Korakianitis, T, Pilidis, P., and Tsoudis, E., 2012, "Technoeconomic and environmental risk analysis for advanced marine propulsion systems", *Applied Energy*, Vol. 99, pp. 1-12.
- [38] Khan, R. S. R., Lagana, M. J., Ogaji, S. O. T., Pilidis, P., and Bennett, I., 2010, "Risk Analysis of Gas Turbines for Natural Gas liquefaction", ASME Paper GT2010-23261, Proceedings of the ASME TURBO EXPO 2010: Power for Land Sea and Air, Glasgow, Scotland, UK.
- [39] Morquillas, J. M., and Pilidis, P., 1990, "Recycling of Gas Turbines from Obsolete Aircraft", ASME Paper 90-GT-309, Presented in Brussels, Belgium.
- [40] Ulizar, I. and Pilidis, P., 2000, "Handling of a Semi closed Cycle GT with a Carbon Dioxide-Argon Working Fluid", *ASME Journal of Engineering for gas turbines and power*, vol.122, No.3, pp.437-442.
- [41] Ulizar Alvarez, J. I., 1998, "Simulation of Multi Fuel Gas Turbine", PhD Thesis, School of Engineering, Cranfield, Bedfordshire, Cranfield University, UK.
- [42] Zwebek, A., and Pilidis, P., 2003, "Degradation Effects on CCGT Plant Performance: Part II: Steam Turbine Cycle Component Degradation Effects", *ASME Journal of Engineering for Gas Turbines and Power*, Vol. 125, No.3, pp.658-664.
- [43] Kumar, K. N. P., Tourlidakis, A., and Pilidis, P., 2002, "HTGR Closed Cycle Gas Turbine Plant Analysis: Options & Procedures for start-up with Hot Gas Injection", ASME Paper GT2002-30146, Proceedings of the ASME TURBO EXPO 2002: Land, Sea, and Air, June 3–6, Amsterdam, The Netherlands.
- [44] Al-Abri, B., 2011, "A surface-subsurface model for the tecno-economic and risk evaluation of thermal EOR projects", PhD Thesis, School of Engineering, Cranfield, Bedfordshire, Cranfield University, UK.
- [45] Isight & SIMULIA Execution Engine, Engineous Software Inc., 2012, North Carolina, URL <http://www.3ds.com/products/simulia>.
- [46] LMS Engineering Innovation, 2012, URL <http://www.lmsintl.com>.

- [47] Phoenix Integration, 2012, URL <http://www.phoenix-int.com>.
- [48] ENGIN SOFT, 2012, URL <http://www.enginsoft.it>.
- [49] The DAKOTA Project, 2012, URL <http://dakota.sandia.gov>.
- [50] CFDRC, 2012, URL <http://www.cfdr.com>.
- [51] Spera, D. A., and Grisaffe, S. J., 1973, "Life prediction of turbine components On-going studies at the NASA Lewis Research Center", NASA TM X 2664, NASA Lewis Research Center, Cleveland, Ohio, US.
- [52] Enright, M. P. and Huyse, L., 2006, "Methodology for Probabilistic Life Prediction of Multiple-Anomaly Materials", *AIAA Journal*, vol. 44, no. 4, pp. 787-793.
- [53] Tong, M., Halliwell, I., Ghosn, L., 2004, "A Computer Code for Gas Turbine Engine Weight and Disk Life Estimation", *Journal of Engineering for Gas Turbine and Power*, Vol.126, No.2, 265-271.
- [54] Schutz, W., 1996, "A History of Fatigue", *Engineering Fracture Mechanics*, Vol. 54, No. 2, pp. 263-300.
- [55] Haslam, A.S., and Cookson, R.A, 2007, *Mechanical Design of Turbomachinery*, Course's lecture notes, School of Engineering, Cranfield University, UK.
- [56] Laskaridis, P., 2011, *Mechanical Integrity of Gas Turbine Engine*, Course's lecture notes, School of Engineering, Cranfield University, UK.
- [57] ETBX, Strain-Life Fatigue Analysis, 2009, Engineers Toolbox, URL: http://www.fea-optimization.com/ETBX/strainlife_help.html
- [58] Carter, T.J., 2005, "Common failures in gas turbine blades", *Engineering Failure Analysis*, Vol. 12, No. 2, pp. 237-247.
- [59] Li, B., 2003, Long-term cyclic oxidation behaviour of wrought commercial alloys at high temperatures. PhD thesis, Material Science and Engineering, Iowa State University, Ames, Iowa.
- [60] Izquierdo, A., 2010, "A Review of Suitable oxidation Models for Aero Gas Turbine Engines", MSc thesis, School of Engineering, Cranfield University, Cranfield, Bedfordshire, UK.
- [61] Chan, K. S., Cheruvu, N. S., and Leverant, G. R., 1998, "Coating life prediction under cyclic oxidation conditions", *Journal of Engineering for Gas Turbines and Power*, Vol. 120, No. 3, pp. 609-614.
- [62] IMR Test Labs. Ithaca, NY, 2010. URL http://www.imrtest.com/what_we_do/Thermal_Spray_Coatings/

- [63] Padture, N. P., Gell, M., and Jordan, E. H., 2002, "Thermal barrier coatings for gas-turbine engine applications", *Science*, Vol. 296, No. 5566, pp. 280-284.
- [64] Birks, N., Meier, G. H., and Pettit, F. S., 2006, *High temperature oxidation of metals*, Cambridge University, 2nd Edition, Cambridge, UK.
- [65] Rolt, A. M., and Kyprianidis, K. G., 2010, "Assessment of New Aero Engine Core Concepts and Technologies in the EU Framework 6 NEWAC Programme", ICAS 27th Congress Proceedings, Nice, France.
- [66] NEWAC, 2009, URL <http://www.newac.eu>.
- [67] Sixth Framework Programme, 2005. FP6-2003-AERO-1, Annex I: Description of Work, December 5-12 2005.
- [68] Walsh, P.P., and Fletcher, P., 2004, *Gas Turbine Performance*, Blackwell Science, 2nd Edition, UK.
- [69] Deliverable D1.1.1B, 2007, "Summary of NEWAC engine geometry specifications", NEWAC-SN-DEL-1.1.1B-R1.0. (Unpublished report)
- [70] Boggia, S., and Rüd, K., 2005. "Intercooled Recuperated Gas Turbine Engine Concept", AIAA 2005-4192, 41st AIAA/ASME/SAE/ASEE Joint Propulsion Conference and Exhibit, Tucson, Arizona, US.
- [71] Kyprianidis, K. G., Ogaji, S. O. T., Pilidis, P., Singh, R., Rolt, A. M., and Gronstedt, T., 2010, "Aero Engine Conceptual Design - Part I: Multi-Disciplinary Framework Development", *AIAA Journal of Propulsion and Power*.
- [72] MacMillan, W. L., 1974, "Development of a Modular Type Computer Program for the Calculation of Gas Turbine off Design Performance", PhD Thesis, Cranfield Institute of Technology, Cranfield, Bedfordshire, UK.
- [73] Pachidis, V., 2008, *Gas Turbine Performance Simulation*, Course's lecture notes, School of Engineering, Cranfield University, Cranfield, Bedfordshire, UK.
- [74] Palmer, J. R., 1999, *The TurboMatch Scheme for Gas-Turbine Performance Calculations*, User's Guide, Cranfield University, Cranfield, Bedfordshire, UK.
- [75] Kyprianidis, K. G., Colmenares, R. F., Pascovici, D. S., Ogaji, S. O. T., Pilidis, P., and Kalfas A.I., 2008, "EVA - A Tool for EnVironmental Assessment of Novel Propulsion Cycles", ASME Paper GT-2008-50602 , Proceedings of the ASME TURBO EXPO 2008, Berlin, Germany.

- [76] Kyprianidis, K.G., and Kalfas, A.I., 2008, "Dynamic Performance Investigations of a Turbojet Engine using a Cross-Application Visual Oriented Platform", *Royal Aeronautical Society, Aeronautical Journal*, Vol. 112, No. 1129, UK.
- [77] Kyprianidis et al., 2009, "NEWAC TERA2020 Engine Performance Module Specification – EVA Code", NEWAC WP1.3 Internal Document, NEWAC-WP1.3-CU-T-1009-012-R1.1. (Unpublished report)
- [78] Sethi, V., 2008, "Advanced Performance Simulation of Gas Turbine Components and Fluid Thermodynamic Properties", PhD Thesis, Cranfield University, Cranfield, Bedfordshire, UK.
- [79] EcosimPro, 2012, URL <http://www.proosis.com>.
- [80] Onat, E., and Klees, G. W., 1979, "A Method to Estimate Weight and Dimensions of Large and Small Gas Turbine Engines", NASA CR-159481, Glenn Research Center, Cleveland, Ohio, US.
- [81] Tong, M. T., Halliwell, I., and Ghosn, L., 2004, "A Computer Code for Gas Turbine Engine Weight and Life Estimation", *ASME Journal of Engineering for Gas Turbine and Power*, Vol. 126, No. 2.
- [82] Laskaridis, P., 2005, "Performance Investigations and Systems Architecture for the more Electric Aircraft", PhD Thesis, Cranfield University, Cranfield, Bedfordshire, UK.
- [83] Laskaridis, P., Pilidis, P., and Kotsiopoulos, P., 2005, "An Integrated Engine-Aircraft Performance Platform for Assessing new Technologies in Aeronautics", ISABE-2005-1165, Munich, Germany.
- [84] ISAE, 2012, URL <http://www.isae.fr/en/>.
- [85] Suria, O. V., 2006, "A flexible lifing model for gas turbines: Creep and Low cycle Fatigue approach", MSc Thesis, School of Engineering, Cranfield, Bedfordshire, Cranfield University, UK.
- [86] Pascovici, D. S., 2008, "Thermo Economic and Risk Analysis for Advanced Long Range Aero Engines", PhD Thesis, School of Engineering, Cranfield, Bedfordshire, Cranfield University, UK.
- [87] Spera, D. A., and Grisaffe, S. J., 1973, "Life prediction of turbine components On-going studies at the NASA Lewis Research Center", NASA TM X 2664, NASA Lewis Research Center, Cleveland, Ohio, US.
- [88] Enright, M. P., and Huyse, L., 2006, "Methodology for Probabilistic Life Prediction of Multiple-Anomaly Materials", *AIAA Journal*, Vol. 44, No. 4, pp. 787-793.

- [89] Tong, M., Halliwell, I., and Ghosn, L., 2004, "A Computer Code for Gas Turbine Engine Weight and Disk Life Estimation", *Journal of Engineering for Gas Turbine and Power*, Vol. 126, No.2, pp.265-612.
- [90] Deb, K., 2001, *Multi-objective optimization using evolutionary algorithms*, John Wiley and Sons, Chichester, England.
- [91] VITAL, 2009, URL <http://www.project-vital.org>.
- [92] DREAM, 2012, URL <http://www.dream-project.eu>.
- [93] DREAM, 2012, URL <http://www.dream-project.eu>.
- [94] Rolt, A. M., and Kyprianidis, K. G., 2010, "Assessment of New Aero Engine Core Concepts and Technologies in the EU Framework 6 NEWAC Programme", ICAS 27th Congress Proceedings, Nice, France.
- [95] Ogaji, S.O.T., Pilidis, P., and Hales, R., 2007. "TERA- A Tool for Aero-engine Modelling and Management". Second World Congress on Engineering Asset Management and the 4th International Conference of Condition Monitoring, Harrogate, UK.
- [96] Eshelby, M. E., 2000, *Aircraft Performance: Theory and practice*, Arnold, London.
- [97] Vicente, E., 1994, "Effect of Bypass Ratio on Long Range Subsonic Engines", MSc Thesis, School of Engineering, Cranfield, Bedfordshire, Cranfield University, UK.
- [98] Pilidis, P., and Palmer, J.R., 2009, *Gas Turbine Theory and Performance*, Course's lecture notes, School of Engineering, Cranfield University, UK.
- [99] Pascovici, D.S., Colmenares, F., Ogaji, and Pilidis, P., 2007, "An Economic and Risk Analysis Model for Aircraft and Engines". ASME Paper GT-2007-27236, Proceedings of the ASME TURBO EXPO 2007, Montreal, Canada.
- [100] Kyprianidis, K. G., Gronstedt, T., Ogaji, S. O. T., Pilidis, P., and Singh, R., 2011, "Assessment of Future Aero Engine Designs with Intercooled and Intercooled Re-cuperated Cores", *ASME Journal of Engineering for Gas Turbines and Power*, Vol. 133, No.1, pp. 909-920.
- [101] Kyprianidis et al., 2009, "TERA2020 Sensitivity Analysis for NEWAC Powerplants", NEWAC WP1.3 Deliverable D1.3.2B R1.0. (Unpublished report)

- [102] Kyprianidis, K. G., Gronstedt, T., Ogaji, S. O. T., Pilidis, P., and Singh, R., 2010, "Assessment of Future Aero Engine Designs with Intercooled and Intercooled Recuperated Cores", ASME Paper GT-2010-23621, Proceedings of the ASME TURBO EXPO 2010, Glasgow, UK.
- [103] Sehitoglu, H., 1990, "Thermo-mechanical fatigue of mar-m247: Part 2-life prediction", *Journal of Engineering Materials and Technology*, Vol. 112, pp. 80-89.
- [104] Miller, M. P., McDowell, D. L. and Oehmke, R. L. T., 1992, "A Creep-Fatigue-Oxidation Microcrack Propagation Model for Thermomechanical Fatigue", *Journal of Engineering Materials and Technology*, Vol. 114, No. 3, pp. 282-288.
- [105] Zamrik, S. Y., and Renauld, M. L., 2000, "Thermo-mechanical out-of-phase fatigue life of overlay coated in-738lc gas turbine material", *Thermo-Mechanical Fatigue Behavior of Materials*, ASTM, Vol. 3, pp. 119-137.
- [106] Koeberl, H., Winter, G., and Eichlseder, W., 2011, "Lifetime calculation of thermo-mechanically loaded materials (Al, Cu, Ni, and Fe Alloys) based on empirical methods", *Journal of ASTM International (JAI)* - 2011 - Volume 8, No.1.

APPENDICES

Appendix A

BASELR Design Parametric Study

A.1 Fan tip pressure ratio

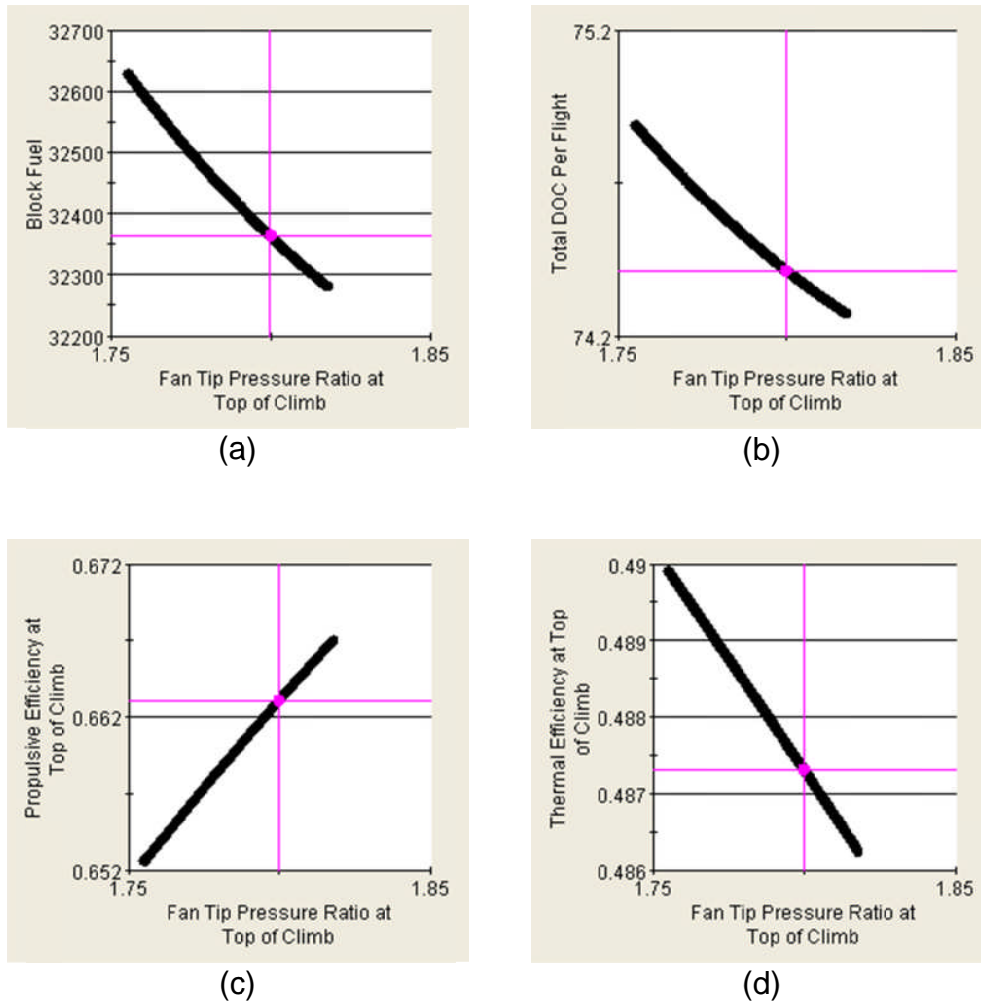
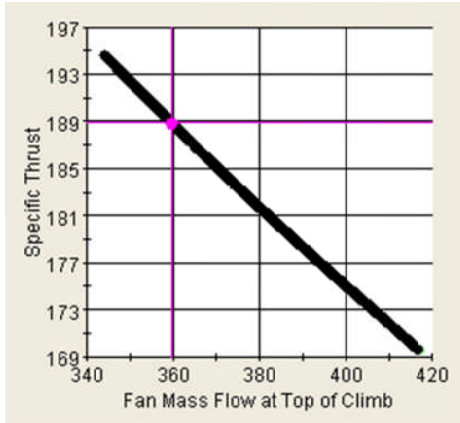
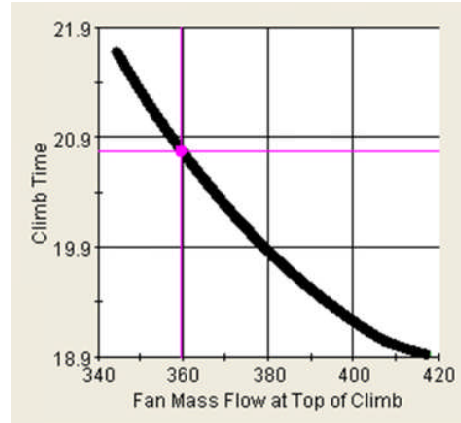


Figure A-1 BASELR Fan tip pressure ratio variation at top of climb

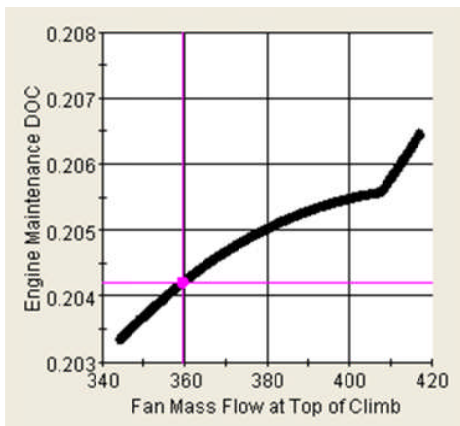
A.2 Fan inlet mass flow



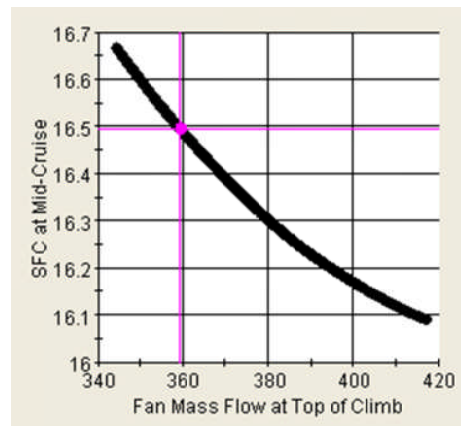
(a)



(b)



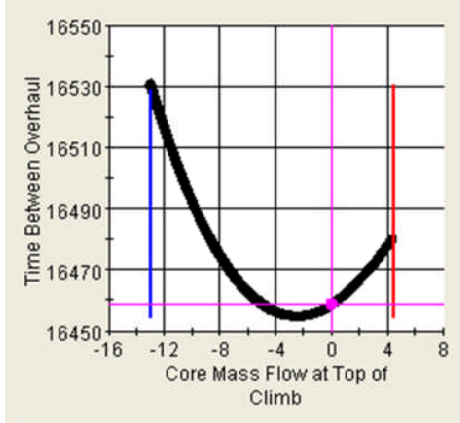
(c)



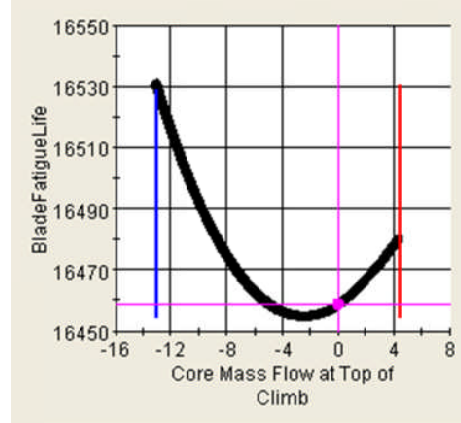
(d)

Figure A-2 BASELR Fan mass flow variation at top of climb

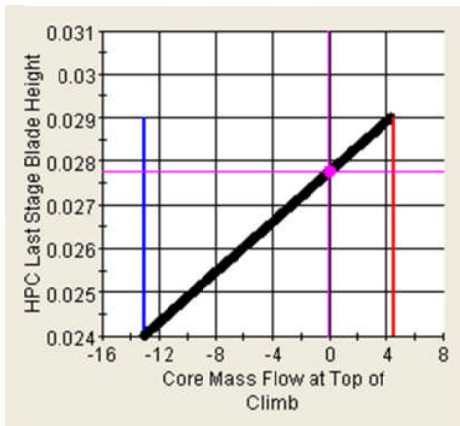
A.3 Core mass flow



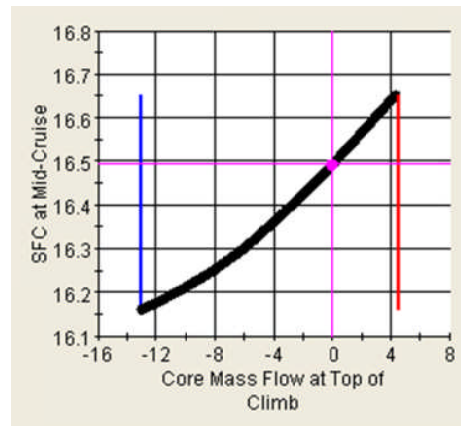
(a)



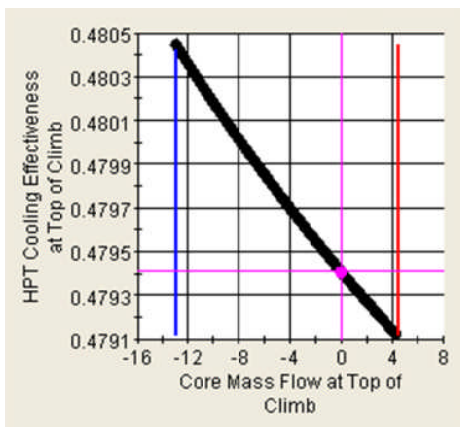
(b)



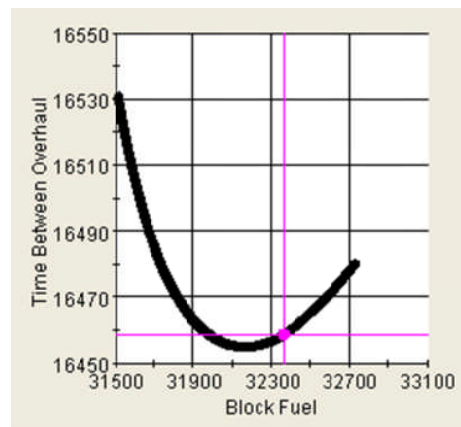
(c)



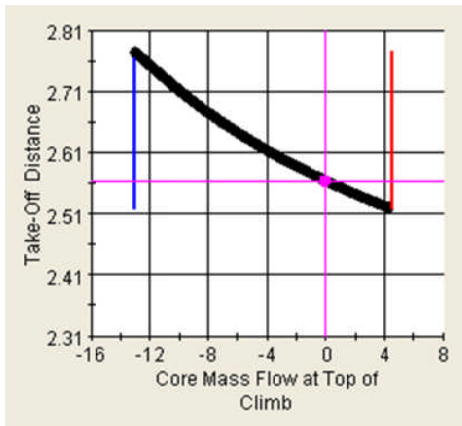
(d)



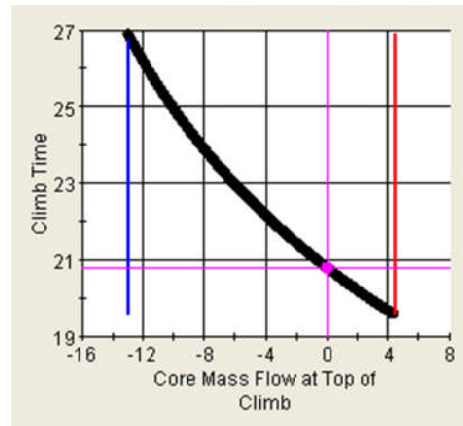
(e)



(f)



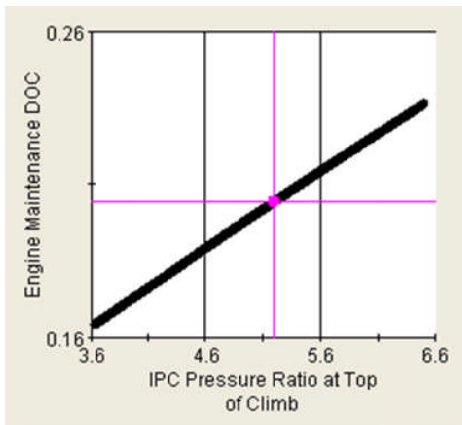
(g)



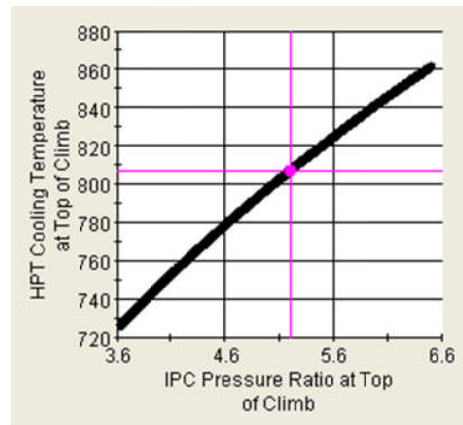
(h)

Figure A-3 BASELR Core mass flow variation at top of climb

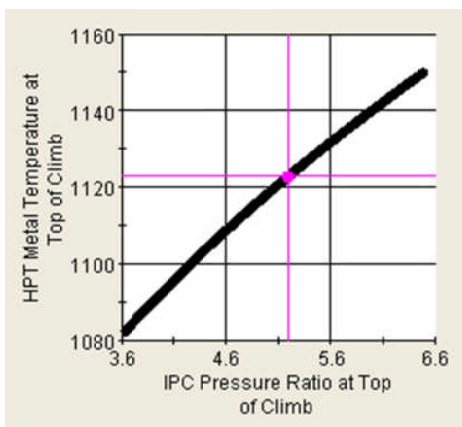
A.4 IPC pressure ratio



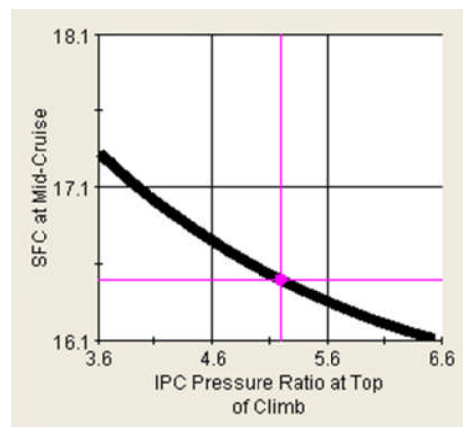
(a)



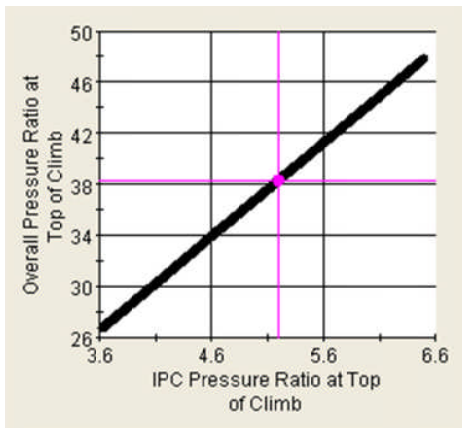
(b)



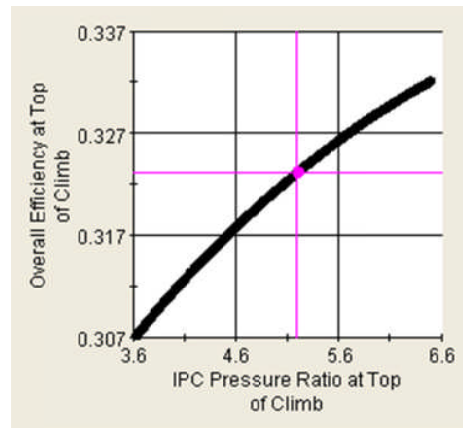
(c)



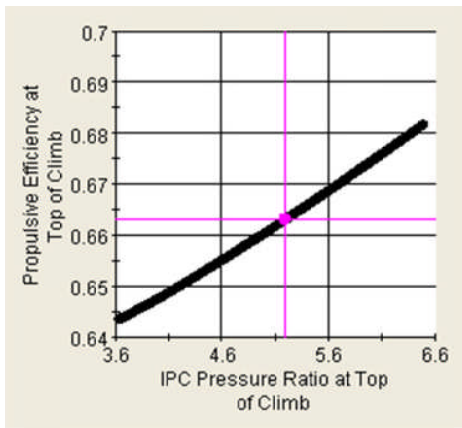
(d)



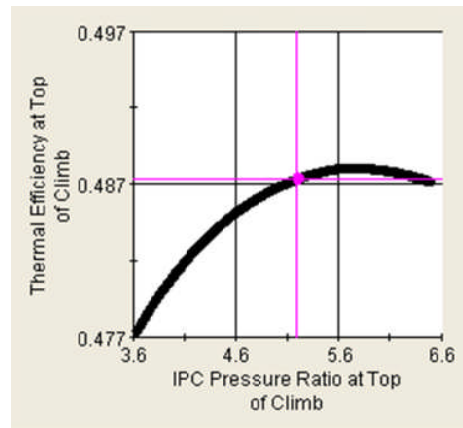
(e)



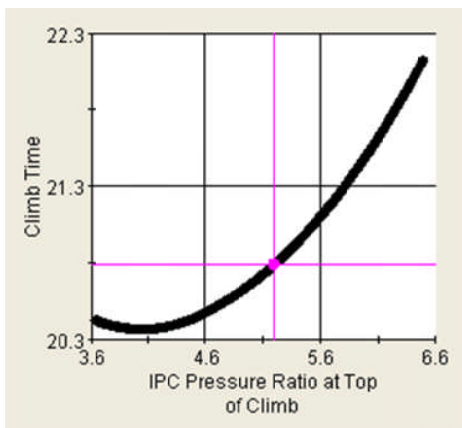
(f)



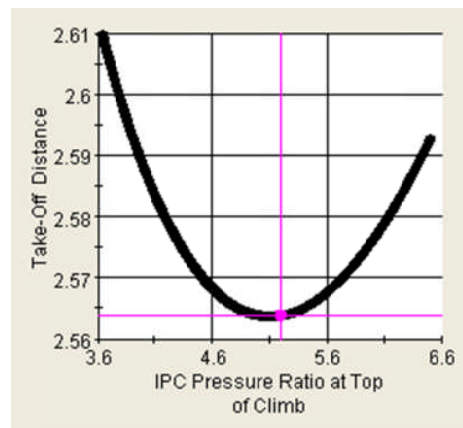
(g)



(h)



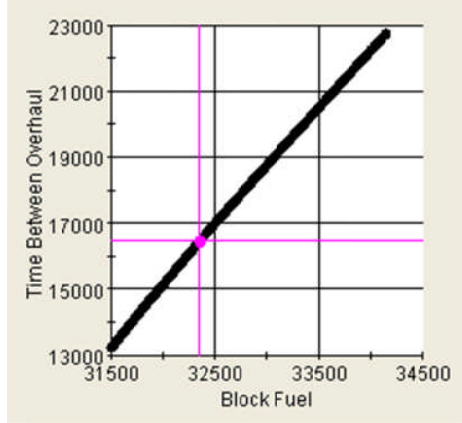
(i)



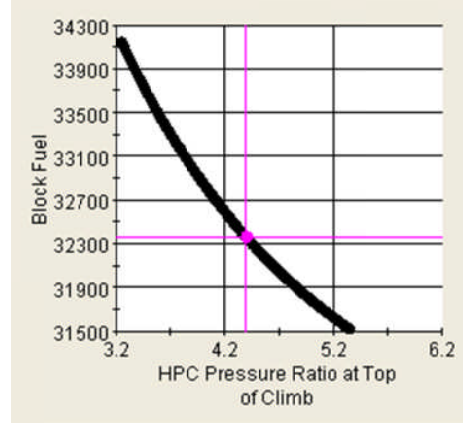
(j)

Figure A-4 *BASELR IPC Pressure ratio variation at top of climb*

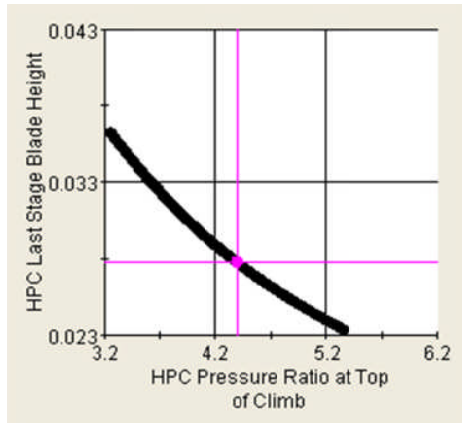
A.5 HPC pressure ratio



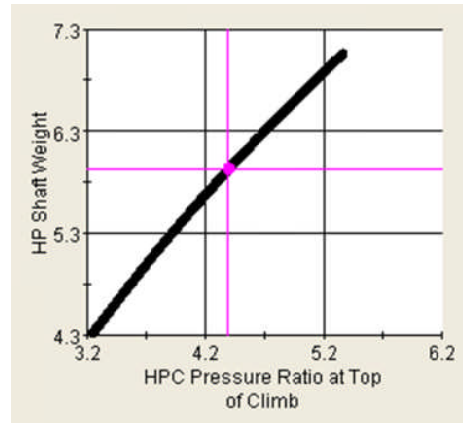
(a)



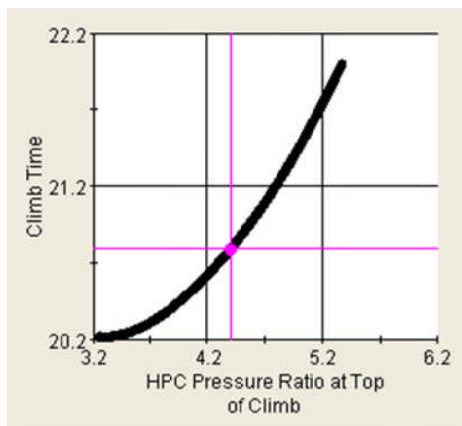
(b)



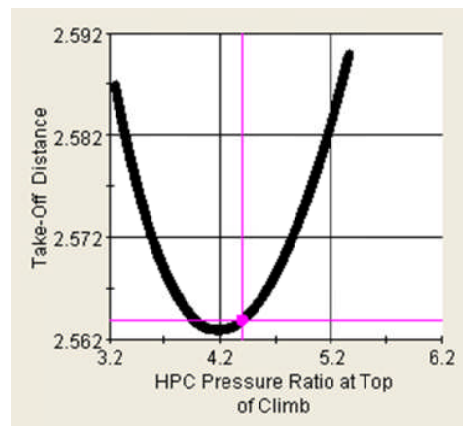
(c)



(d)



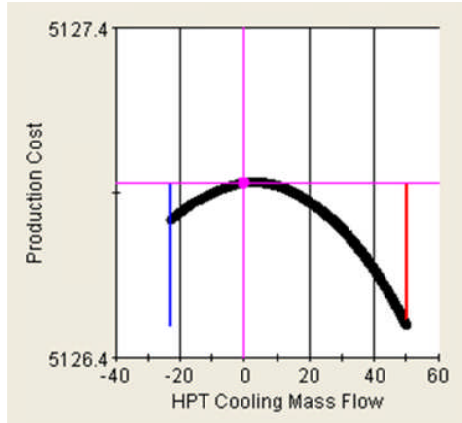
(e)



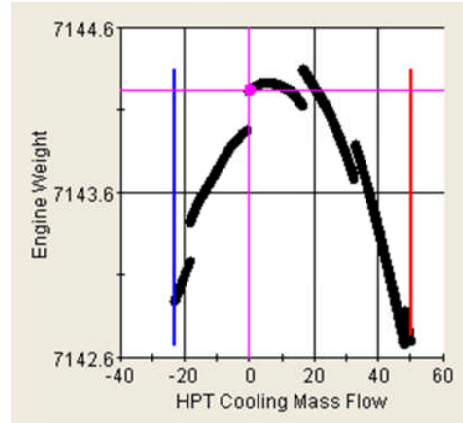
(f)

Figure A-5 BASELR HPC pressure ratio variation at top of climb

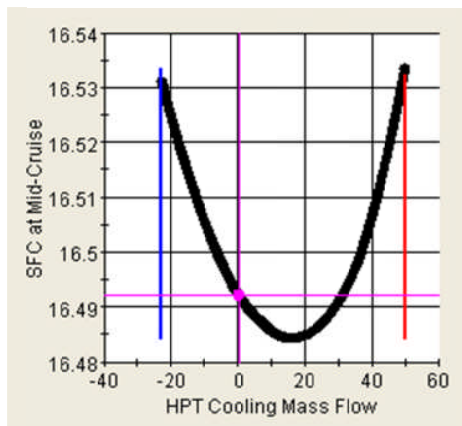
A.6 HPT cooling mass flow



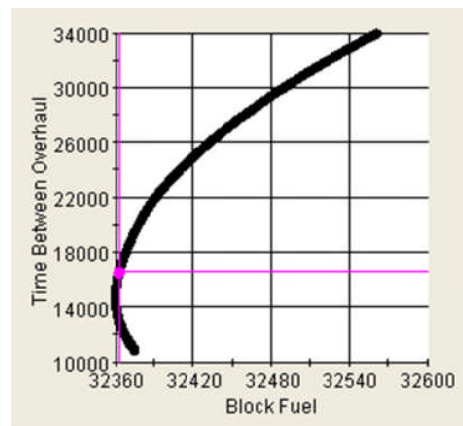
(a)



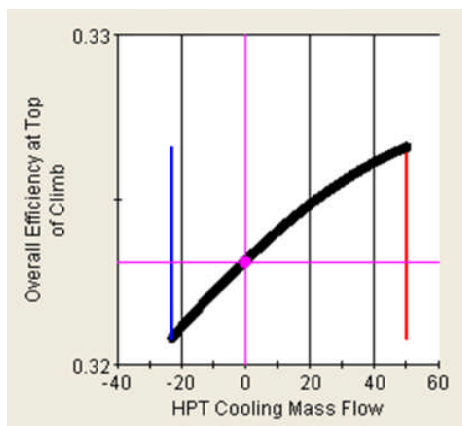
(b)



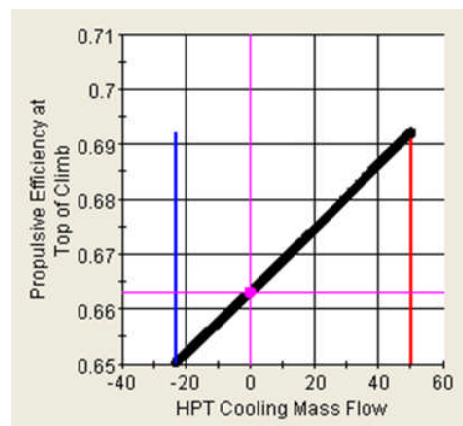
(c)



(d)



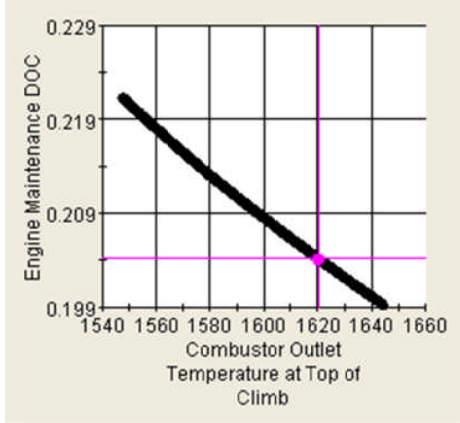
(e)



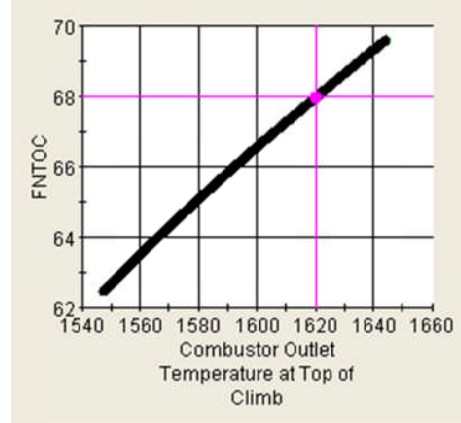
(f)

Figure A-6 BASELR HPT cooling mass flow variation at top of climb

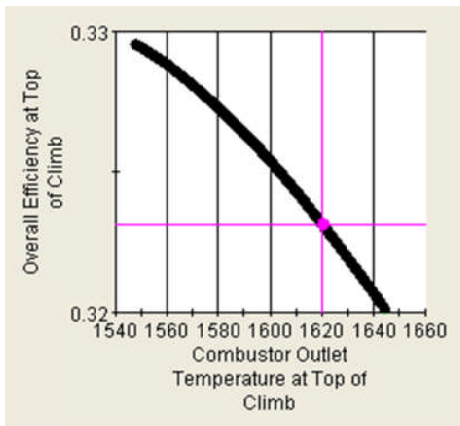
A.7 Combustor output temperature



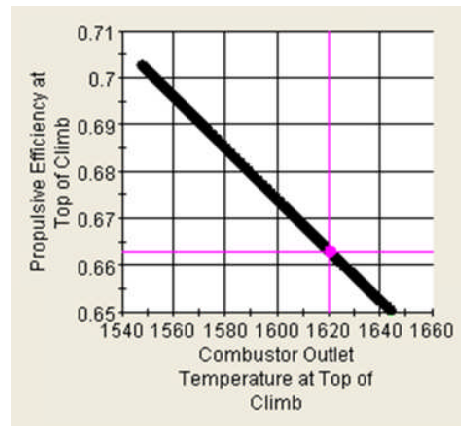
(a)



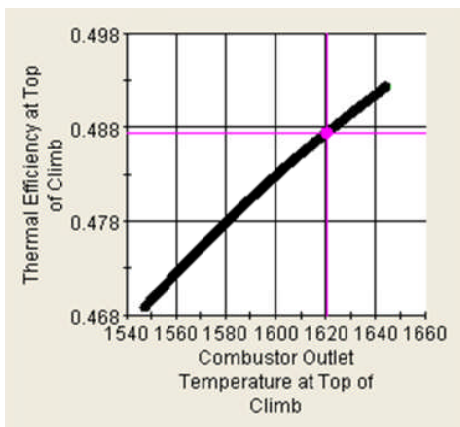
(b)



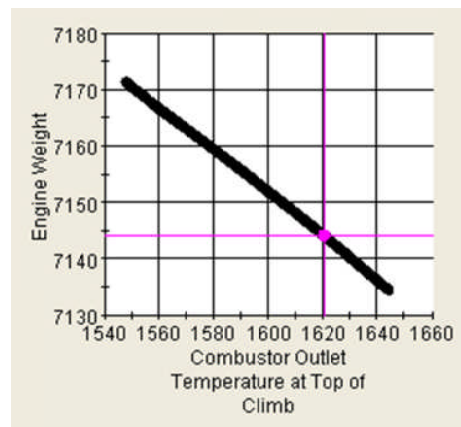
(c)



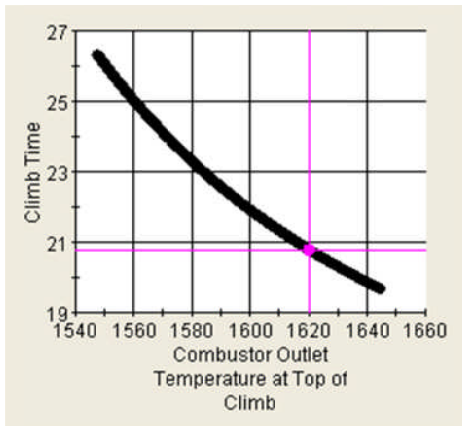
(d)



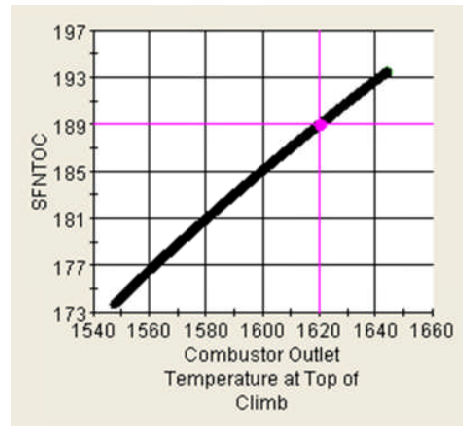
(e)



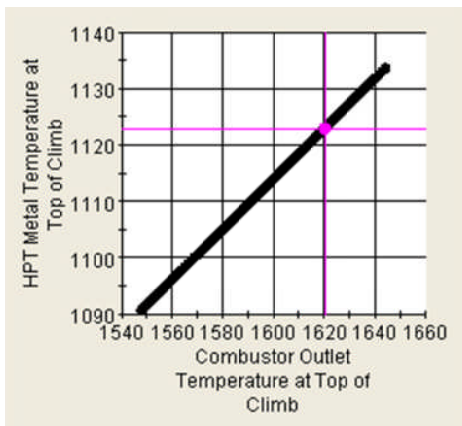
(f)



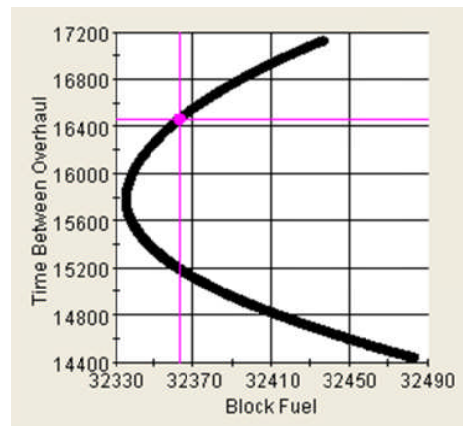
(g)



(h)



(i)



(j)

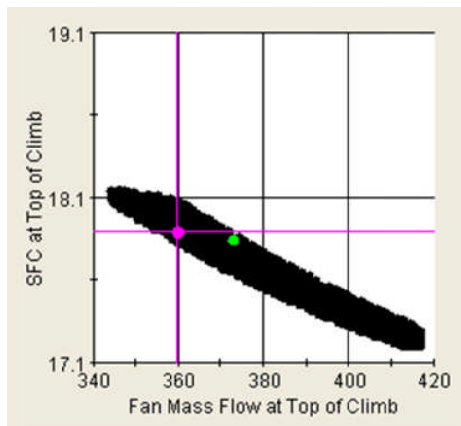
Figure A-7 BASELR Combustor outlet temperature variation at top of climb

Appendix B

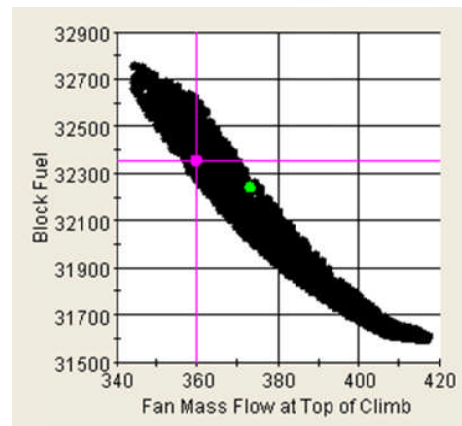
BASELR Design Space Exploration and Optimisation

B.1 Fan and core sizing

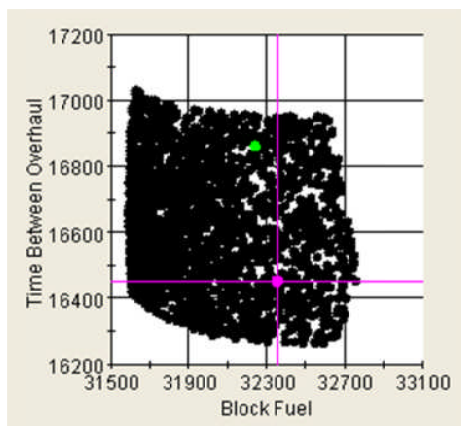
Please note that in the scatter plots, the Pink point indicates the engine design point and the Green ones represent the optimal design with respect to the time between overhaul.



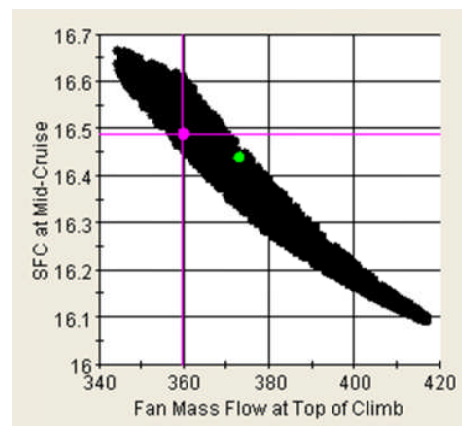
(a)



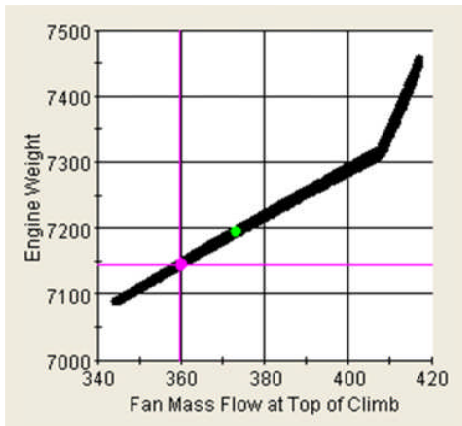
(b)



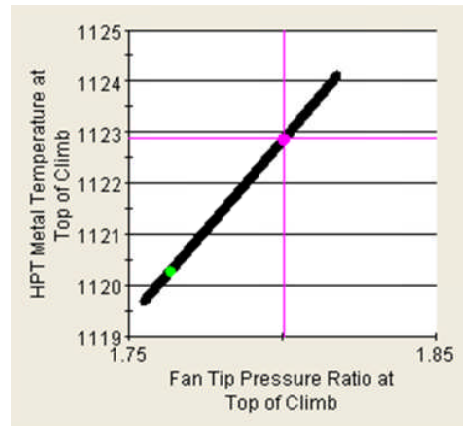
(c)



(d)

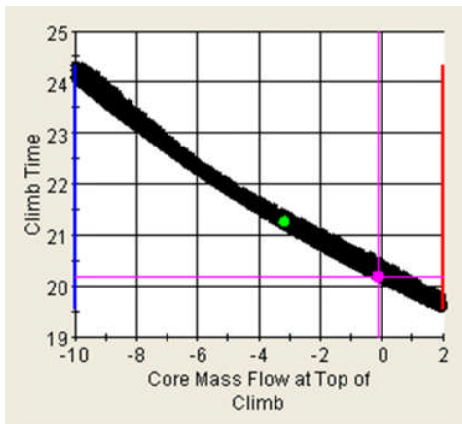


(e)

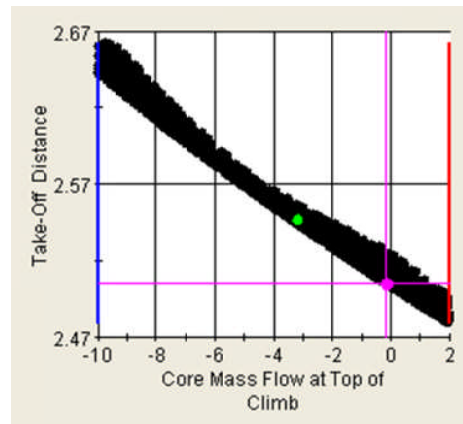


(f)

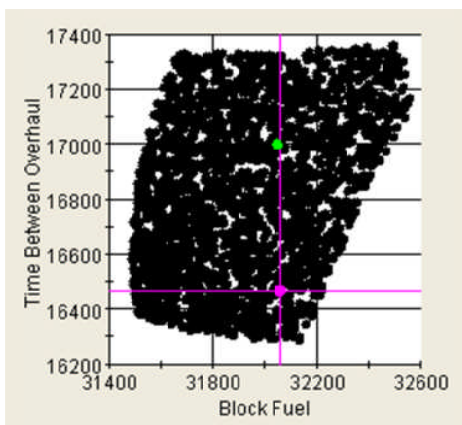
Figure B-8 *BASELR Fan tip pressure ratio and fan mass flow variation*



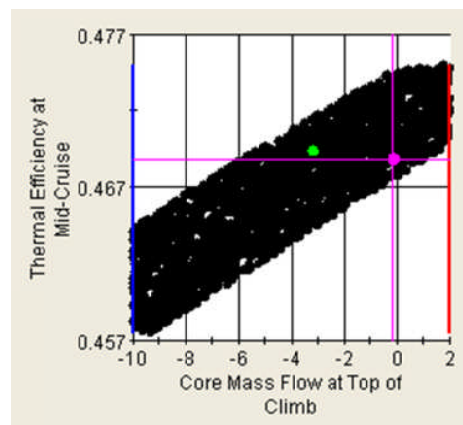
(a)



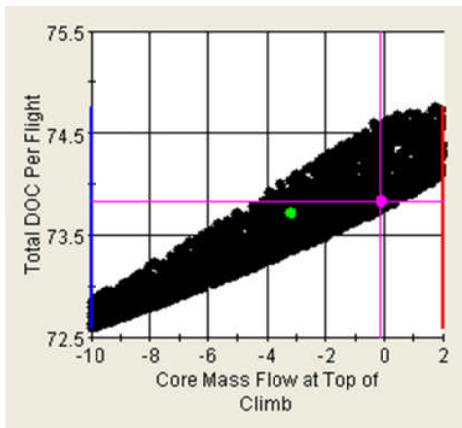
(b)



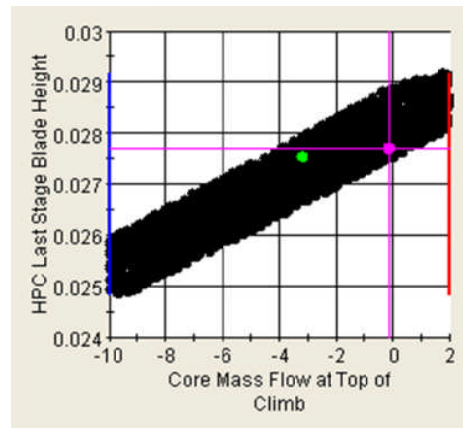
(c)



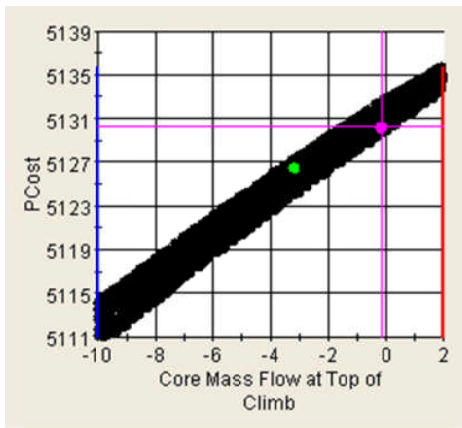
(d)



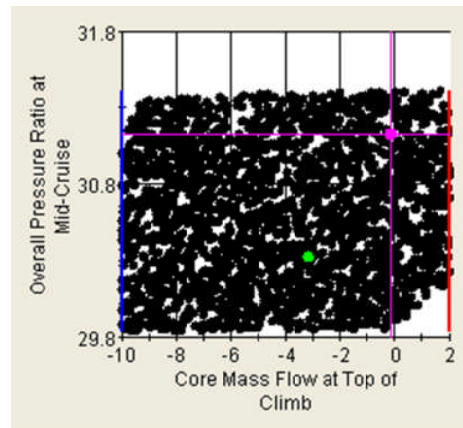
(e)



(f)

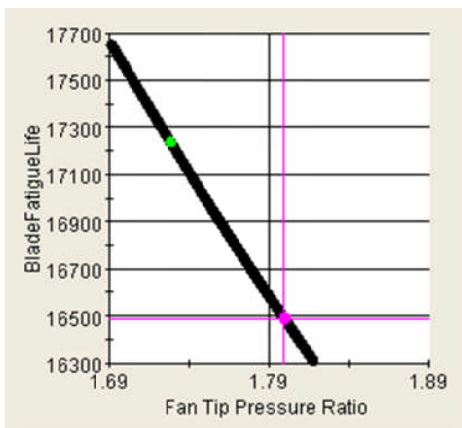


(g)

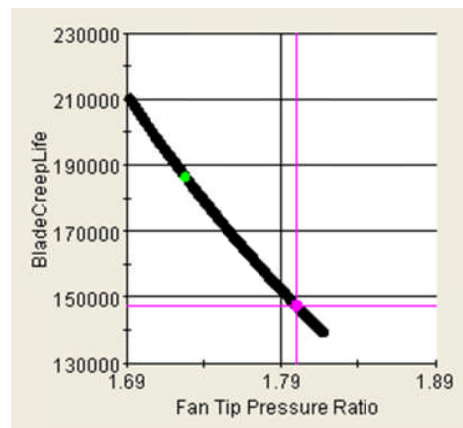


(h)

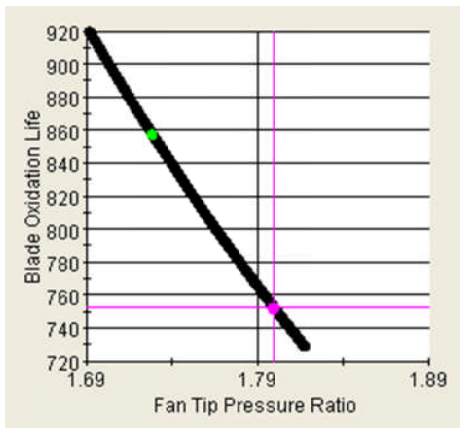
Figure B-9 *BASELR Fan tip pressure ratio and core mass flow variation*



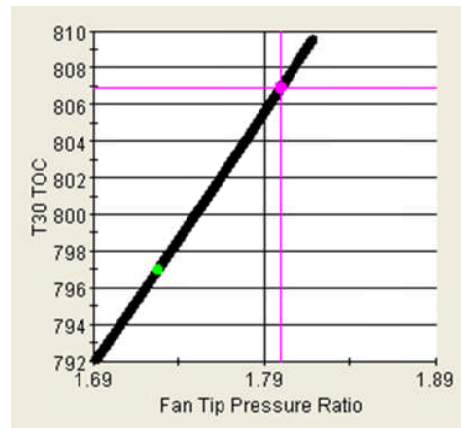
(a)



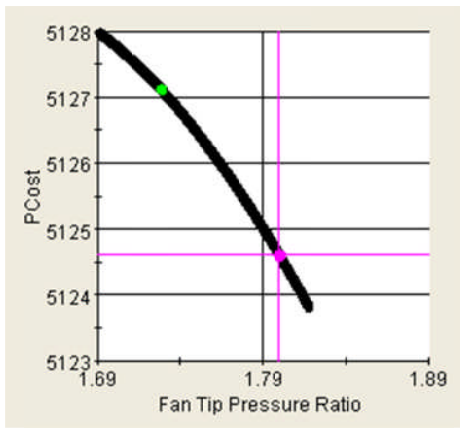
(b)



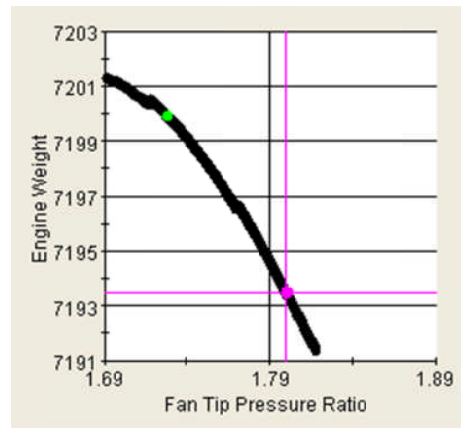
(c)



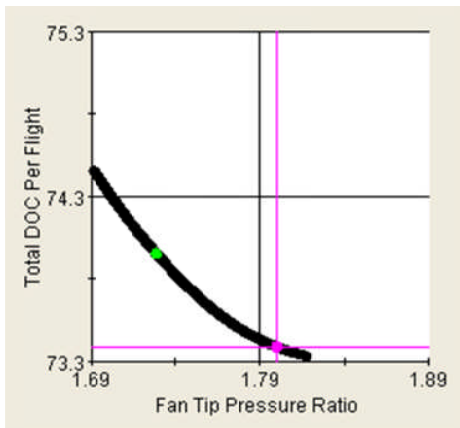
(d)



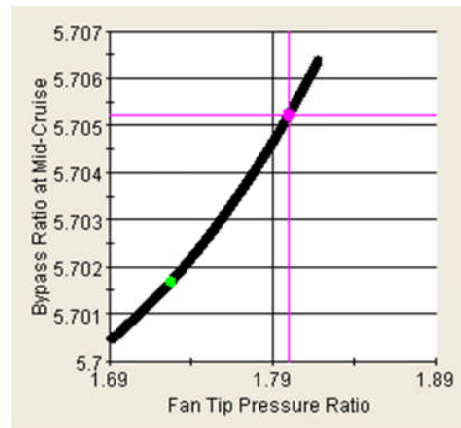
(e)



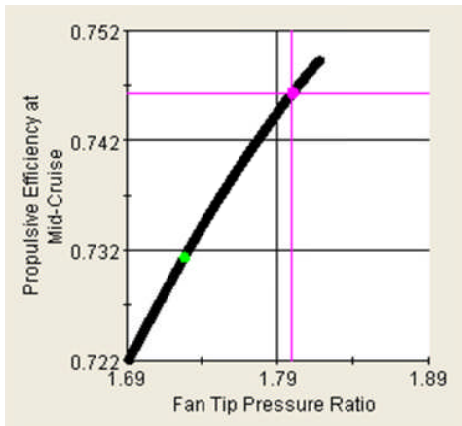
(f)



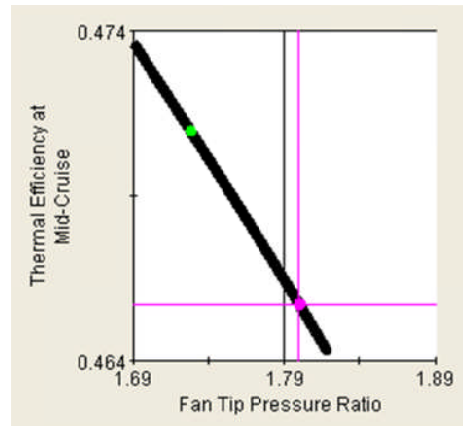
(g)



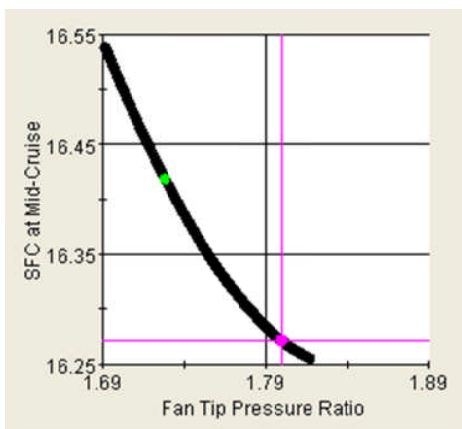
(h)



(i)



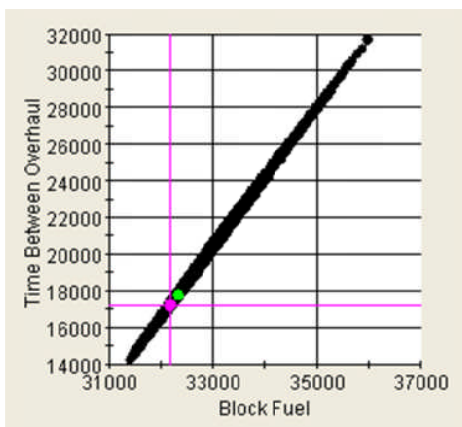
(j)



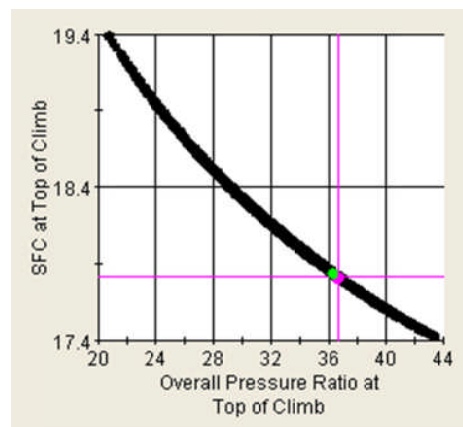
(k)

Figure B-10 BASELR Fan tip pressure ratio variation

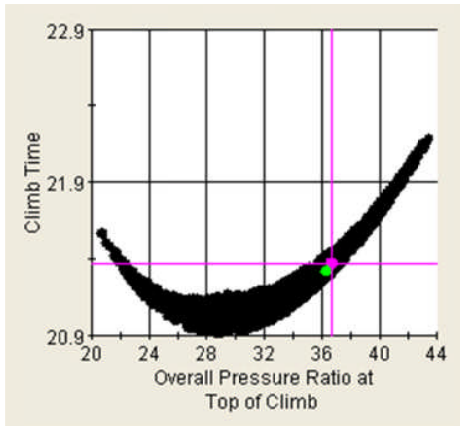
B.2 IPC/HPC work split



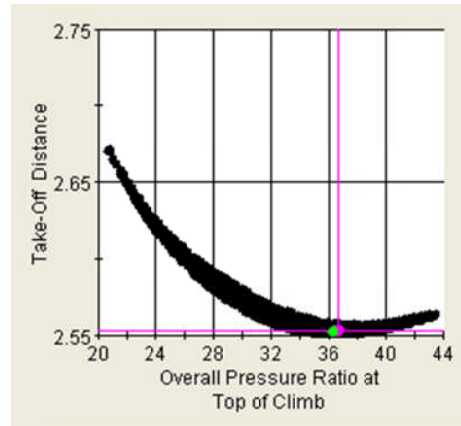
(a)



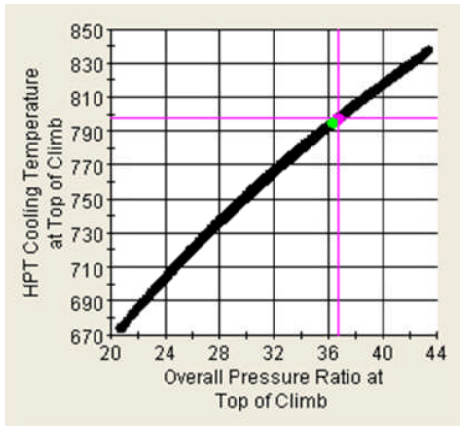
(b)



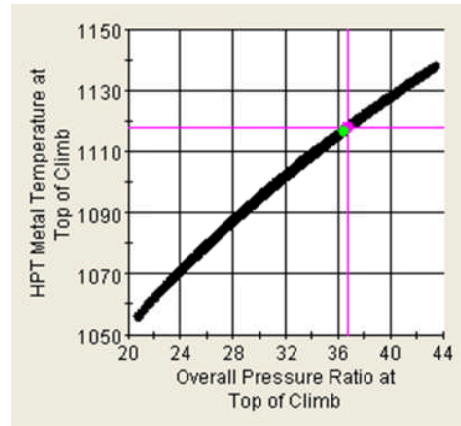
(c)



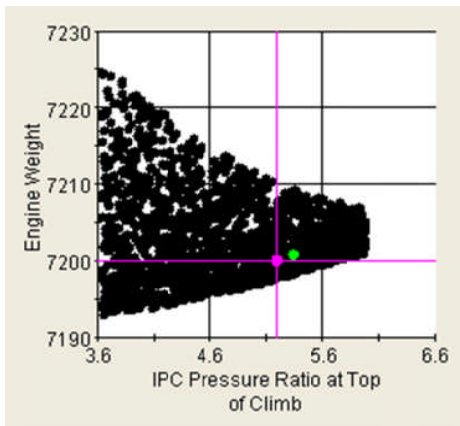
(d)



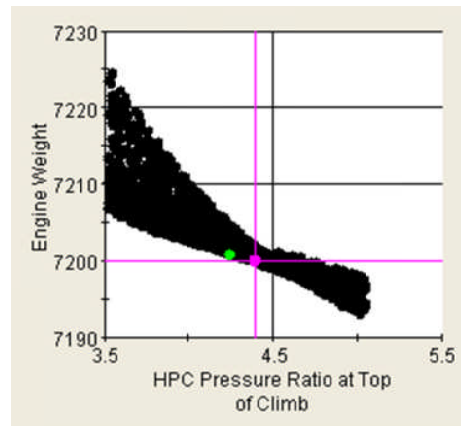
(e)



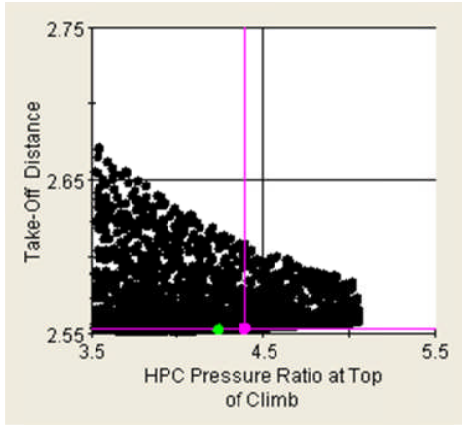
(f)



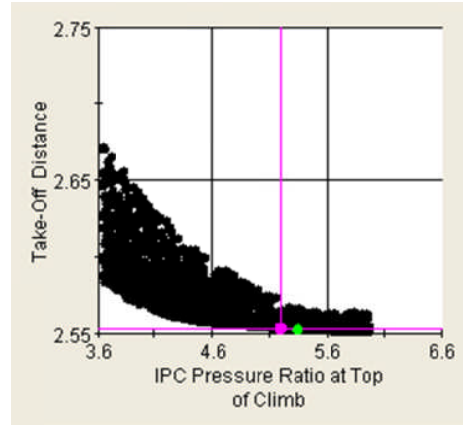
(g)



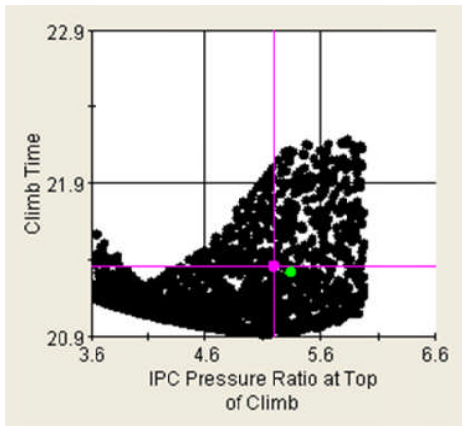
(h)



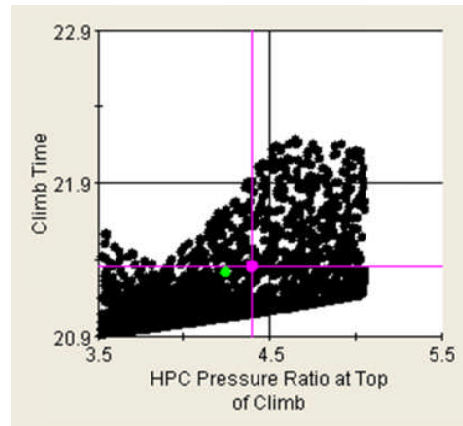
(i)



(j)



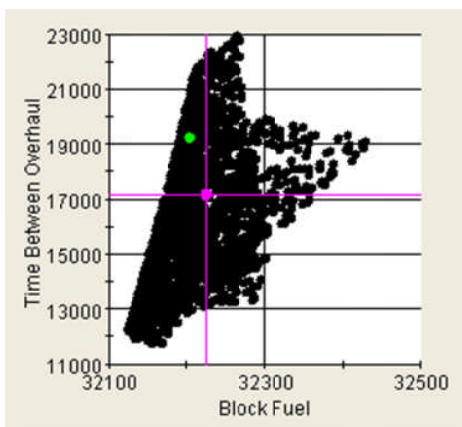
(k)



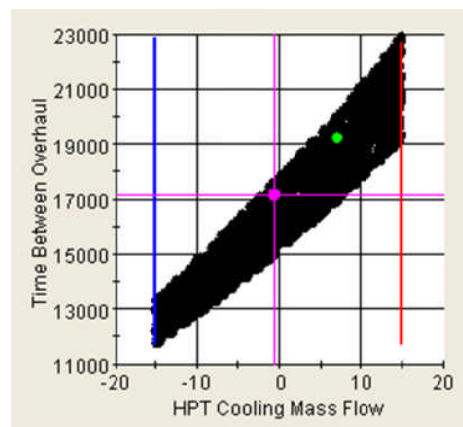
(l)

Figure B-11 BASECLR HPC and IPC pressure ratio variation

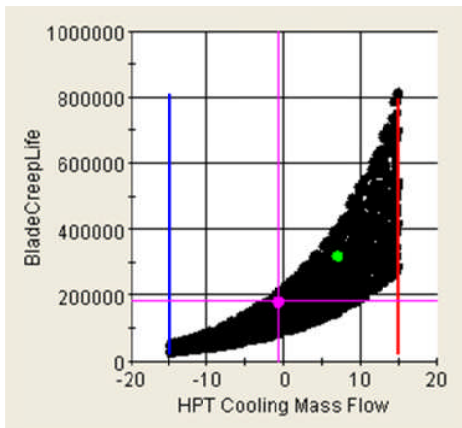
B.3 Combustor outlet temperature and HPT cooling flow



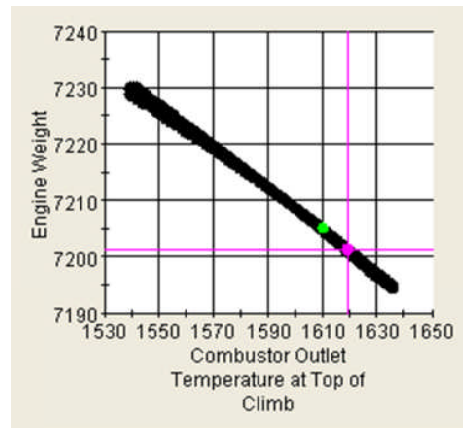
(a)



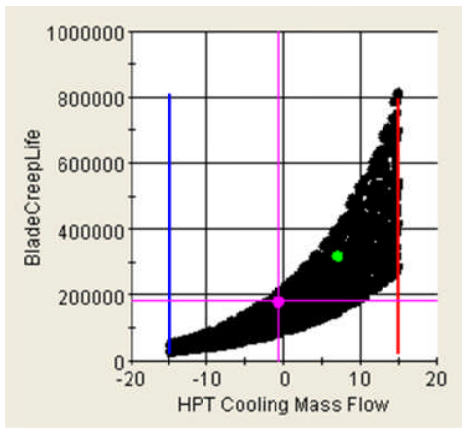
(b)



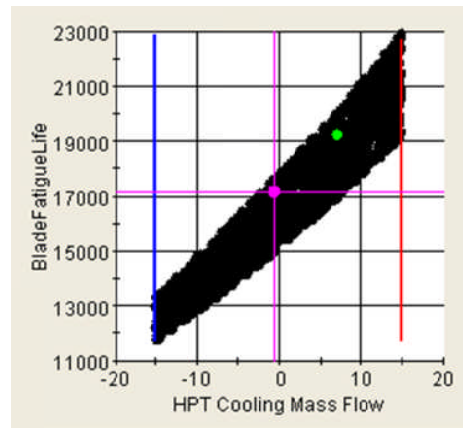
(c)



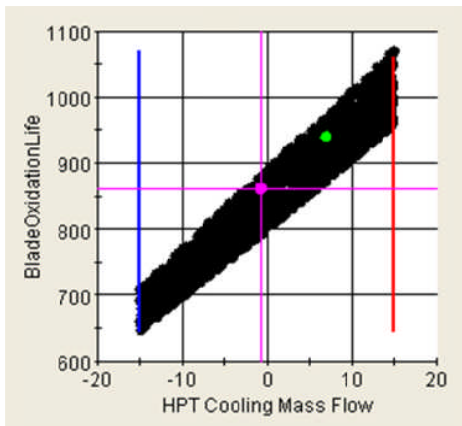
(d)



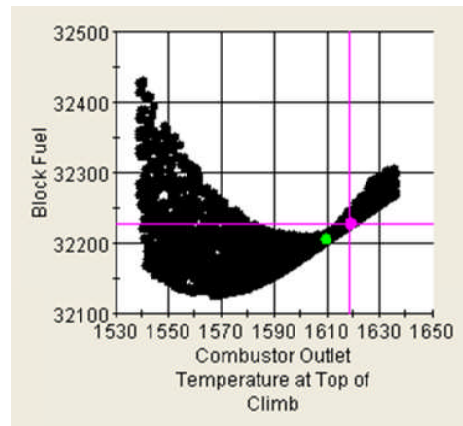
(e)



(f)



(g)



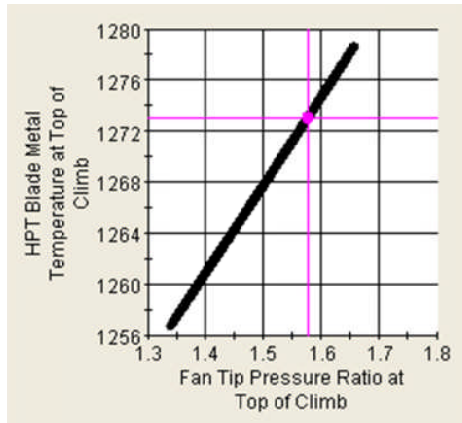
(h)

Figure B-12 *BASECLR Fan tip pressure ratio and core mass flow variation*

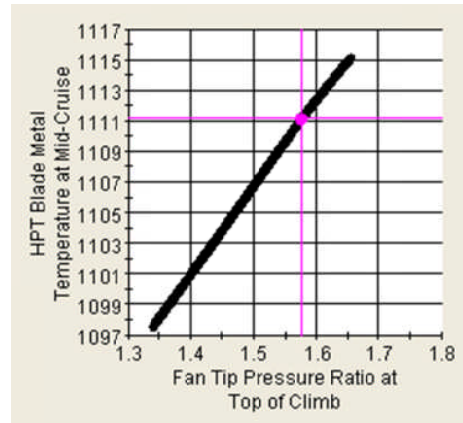
Appendix C

DDICLR Design Parametric Study

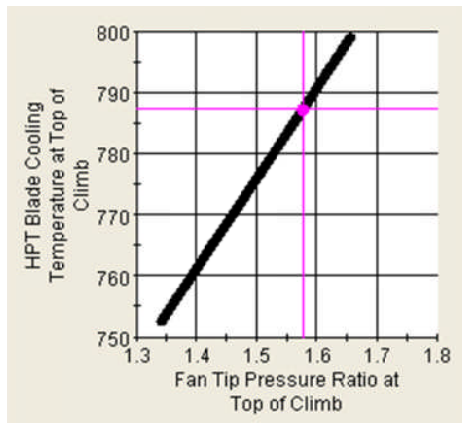
C.1 Fan tip pressure ratio at top of climb



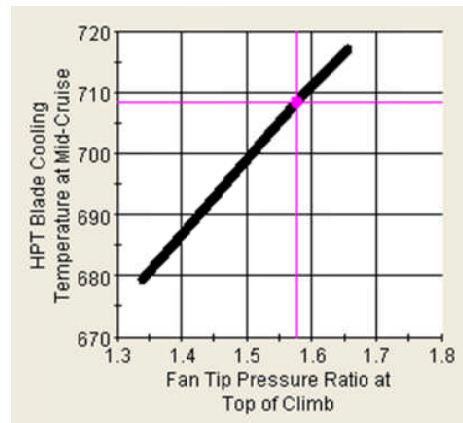
(a)



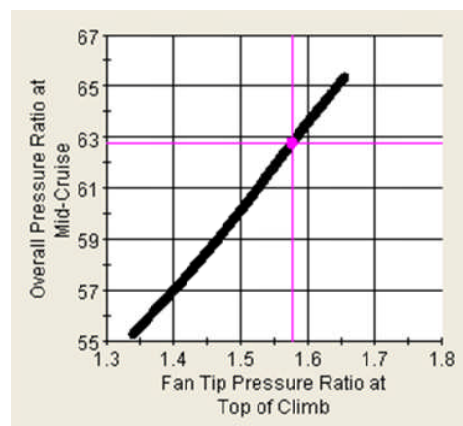
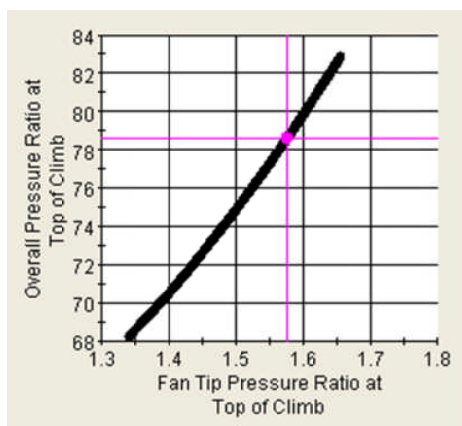
(b)



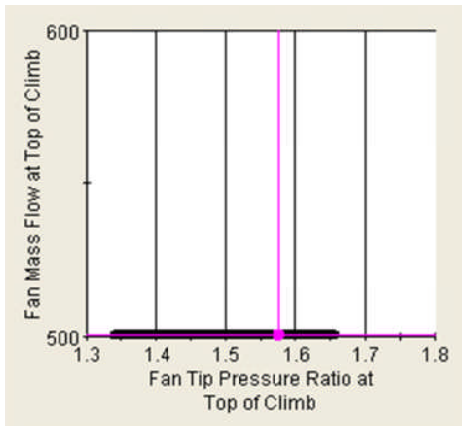
(c)



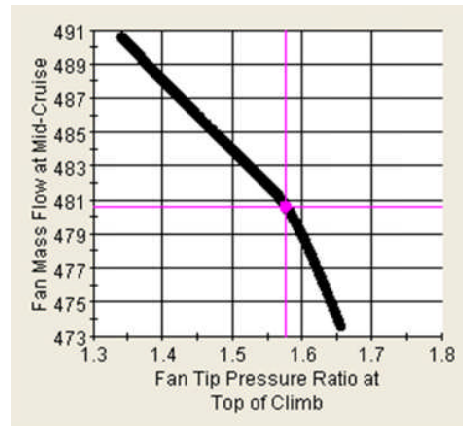
(d)



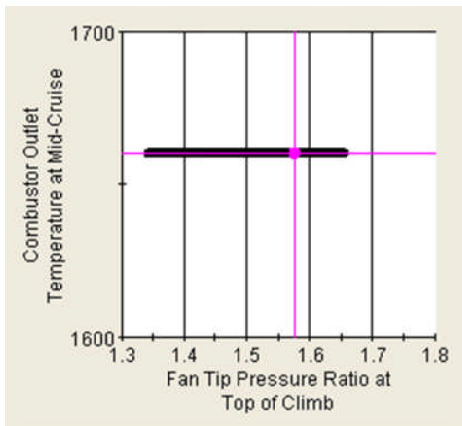
(e)



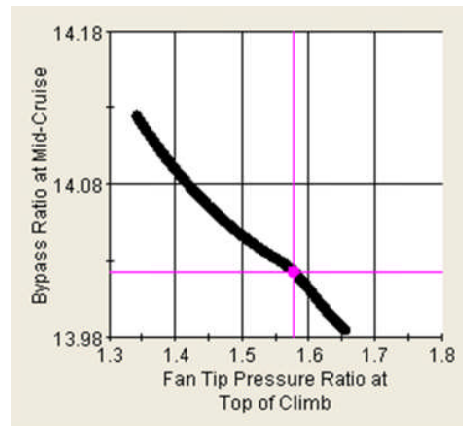
(f)



(g)



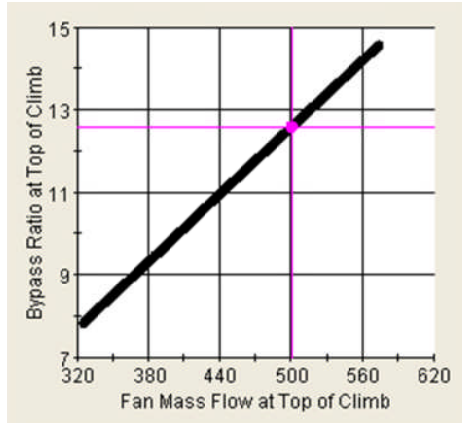
(h)



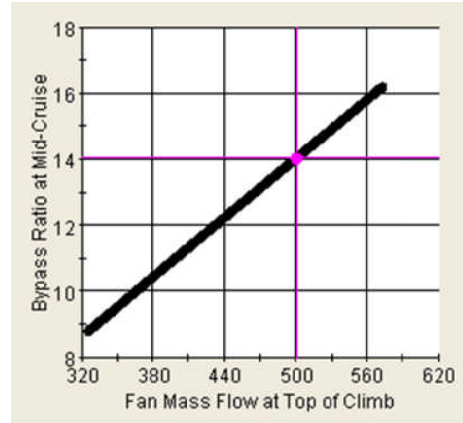
(i)

Figure C-13 DDICLR fan tip pressure ratio variation at top of climb

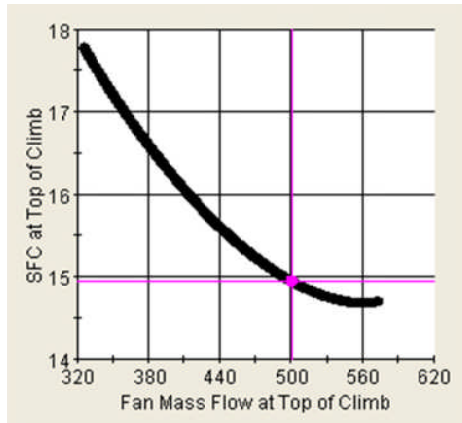
C.2 Fan mass flow at top of climb



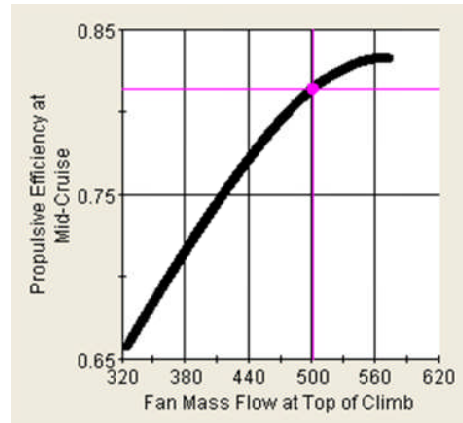
(a)



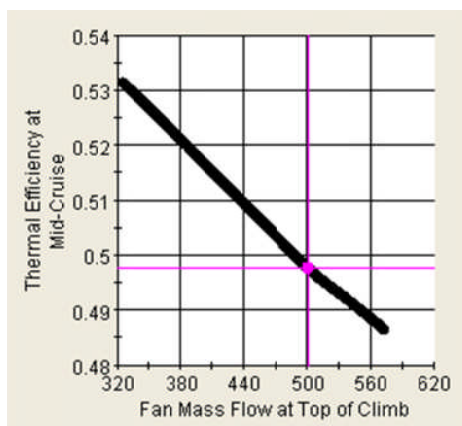
(b)



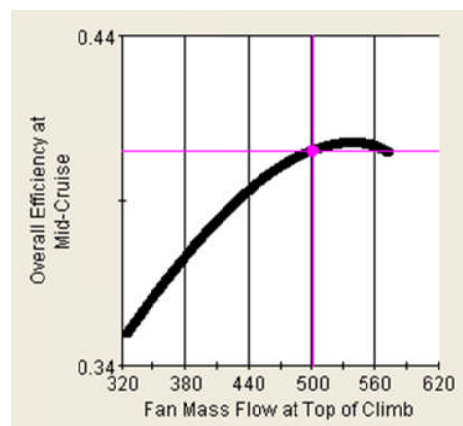
(c)



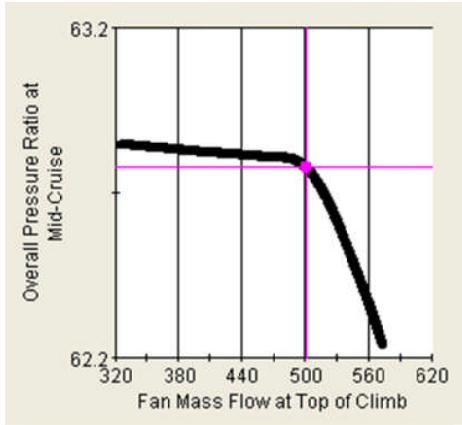
(d)



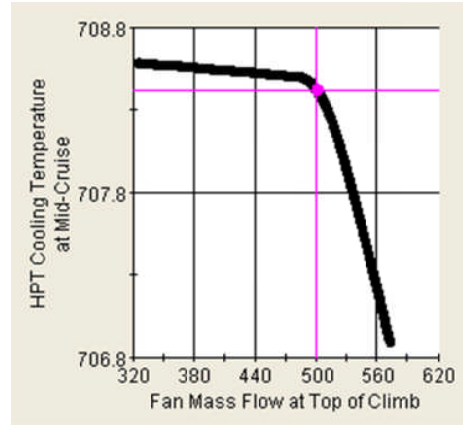
(e)



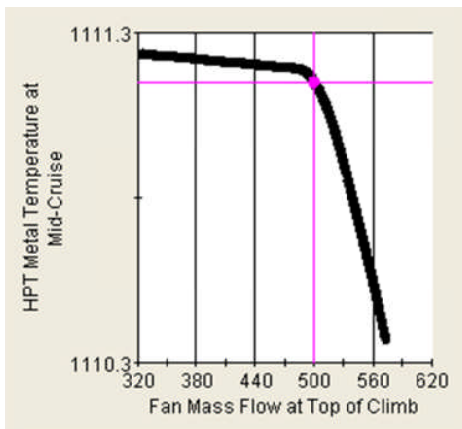
(f)



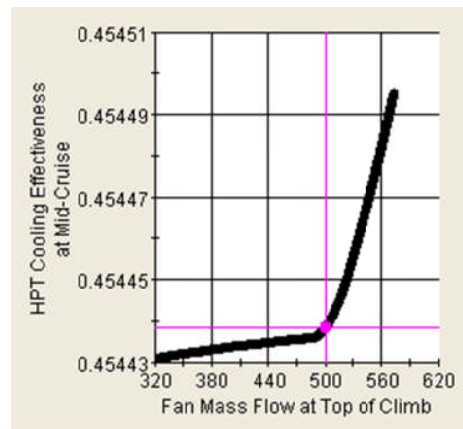
(g)



(h)



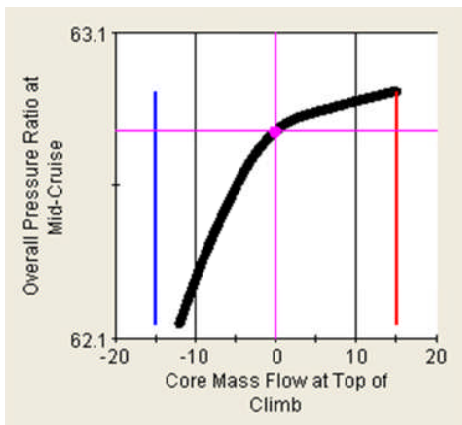
(i)



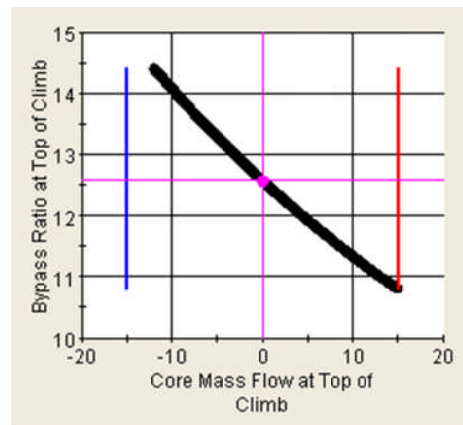
(j)

Figure C-14 Fan mass flow variation at top of climb

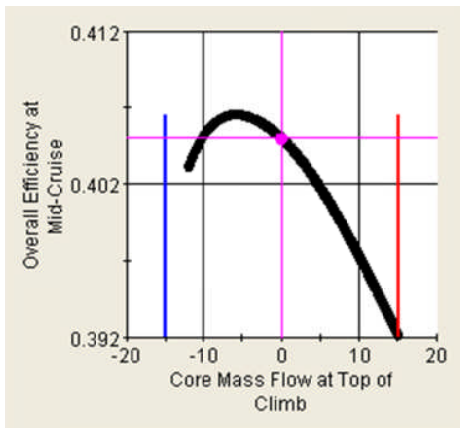
C.3 Core mass flow at top of climb



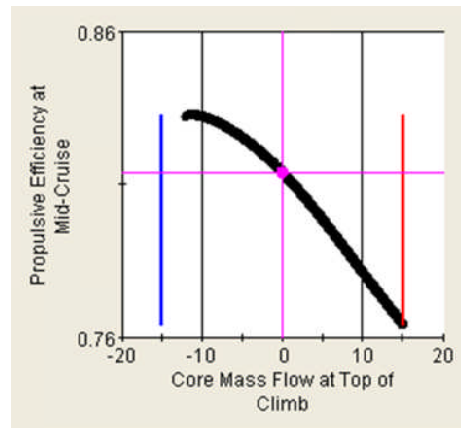
(a)



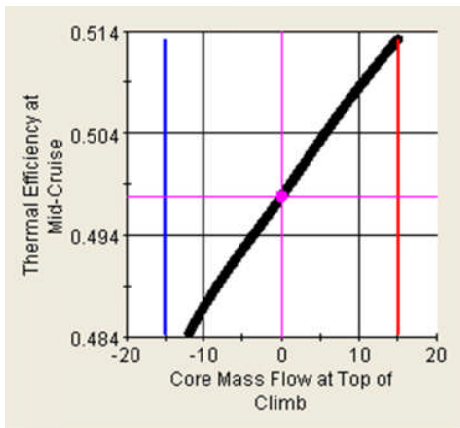
(b)



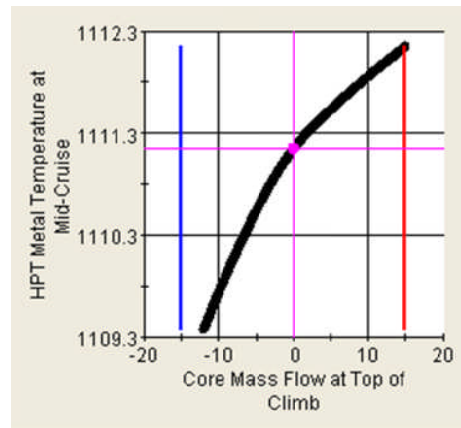
(c)



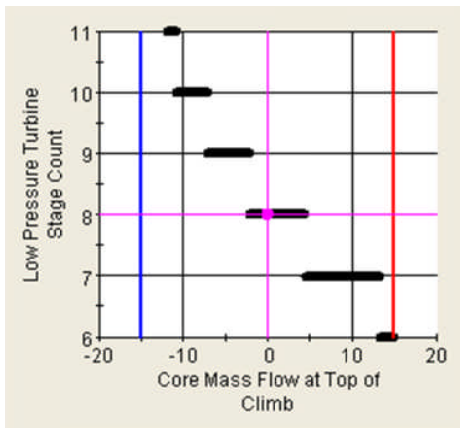
(d)



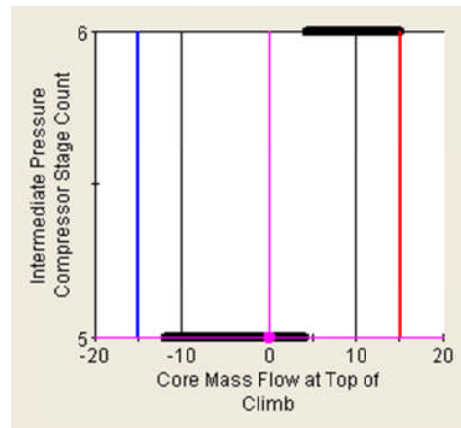
(e)



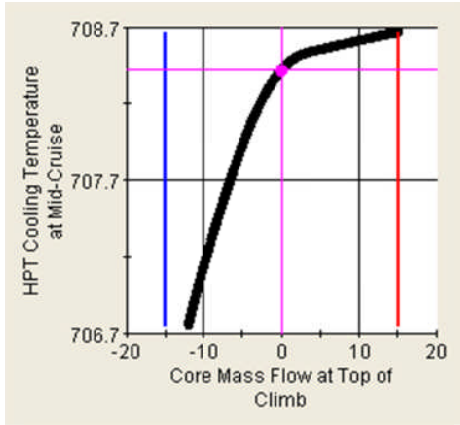
(f)



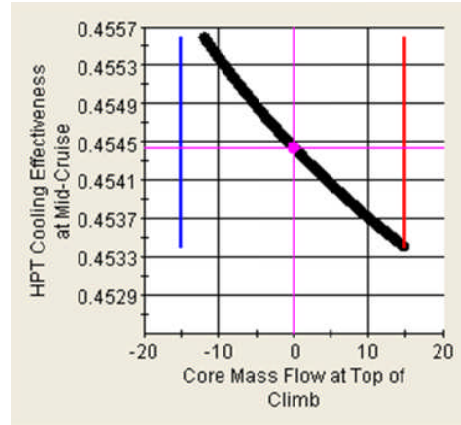
(g)



(h)



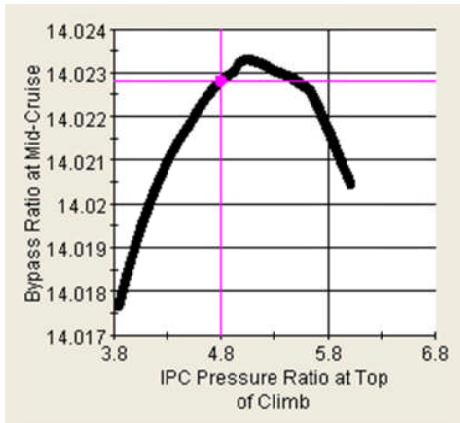
(i)



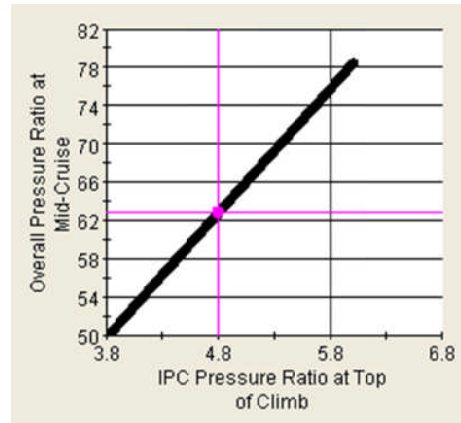
(j)

Figure C-15 Core mass flow variation at top of climb

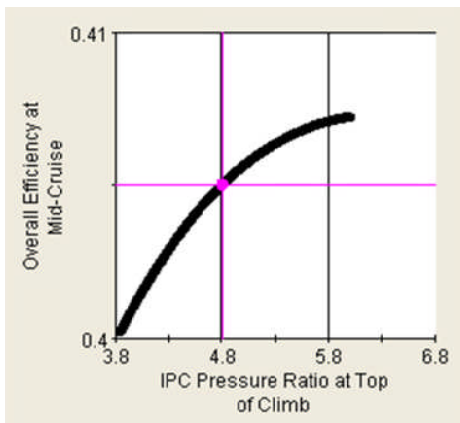
C.4 Intermediate pressure compressor pressure ratio



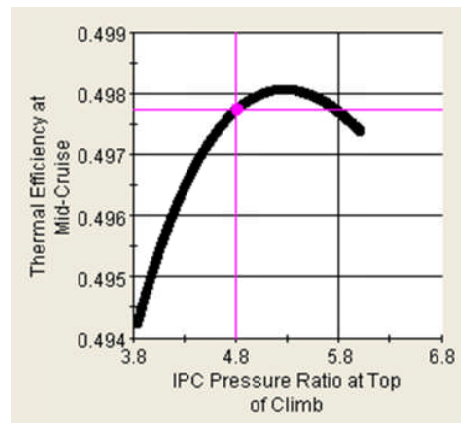
(a)



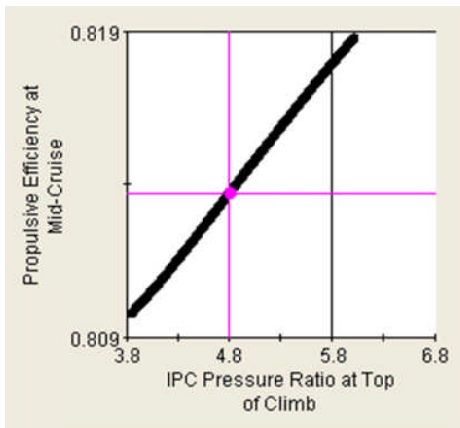
(b)



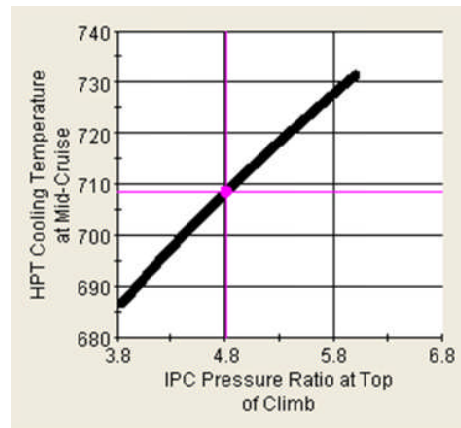
(c)



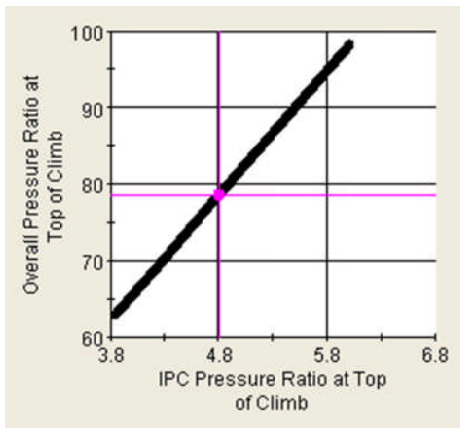
(d)



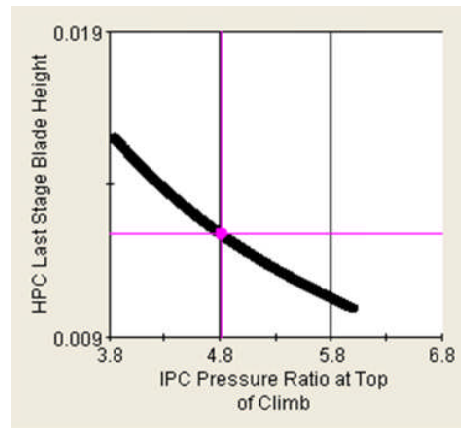
(e)



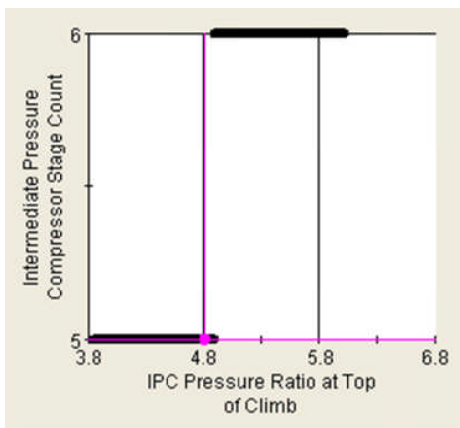
(f)



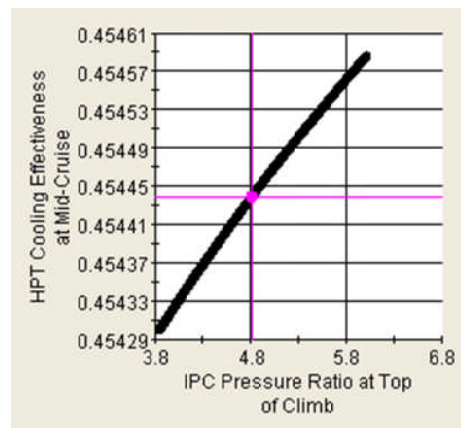
(g)



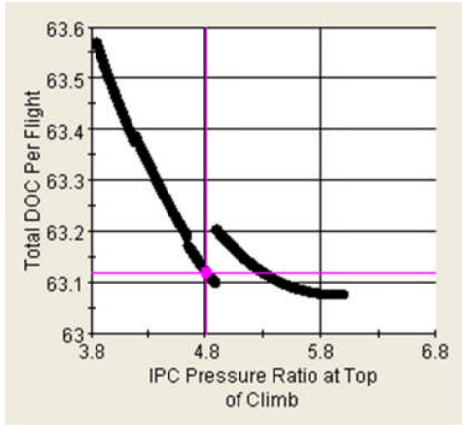
(h)



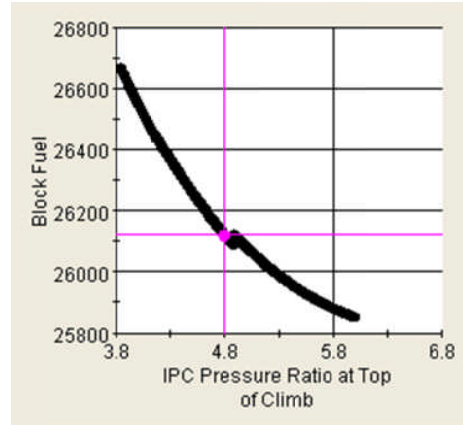
(i)



(j)



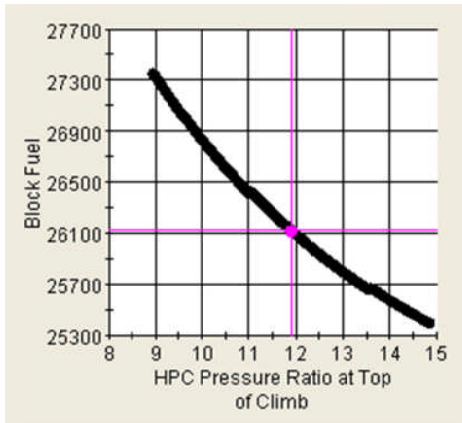
(k)



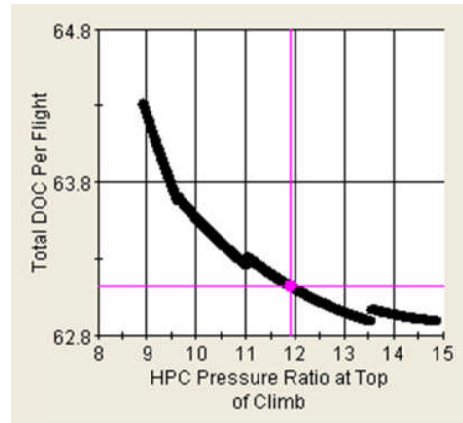
(l)

Figure C-16 IPC pressure ratio variation at top of climb

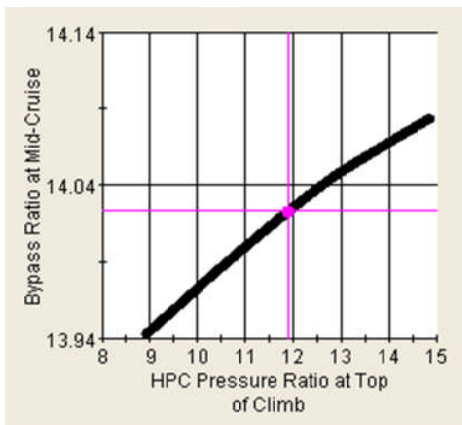
C.5 High pressure compressor pressure ratio



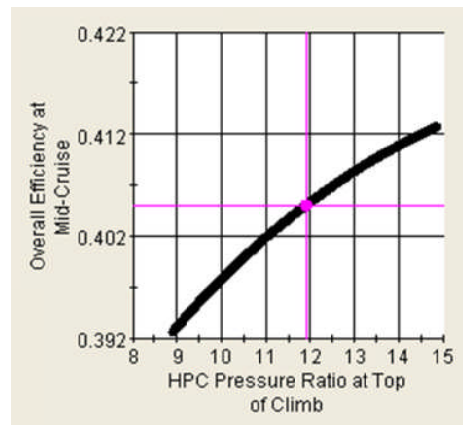
(a)



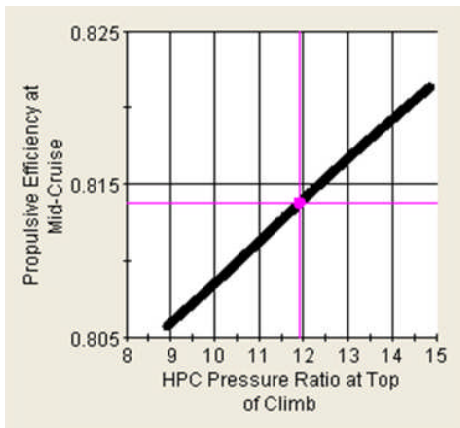
(b)



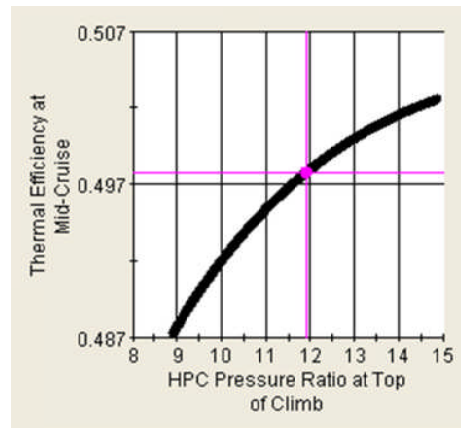
(c)



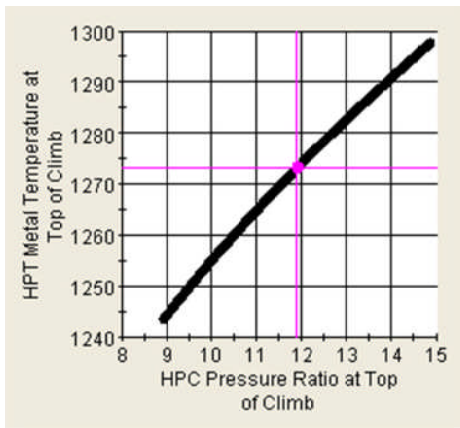
(d)



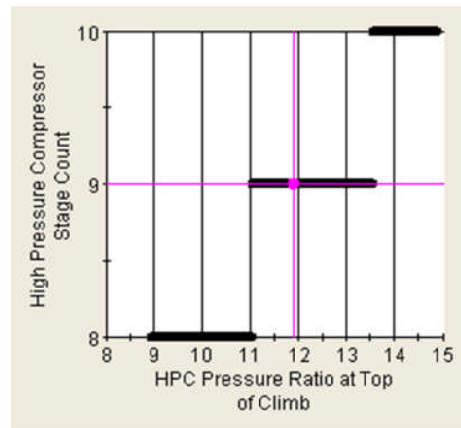
(e)



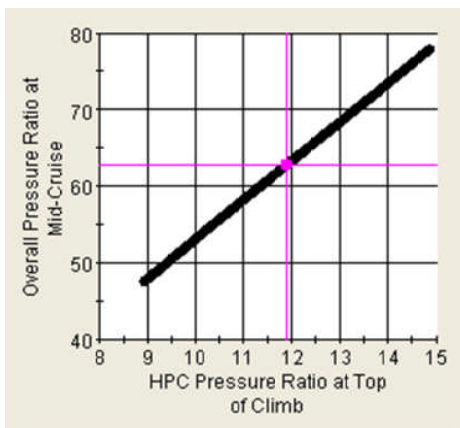
(f)



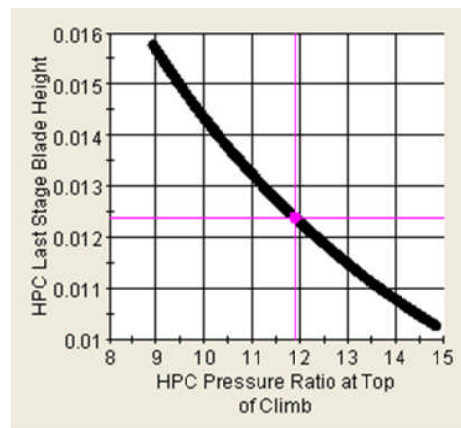
(g)



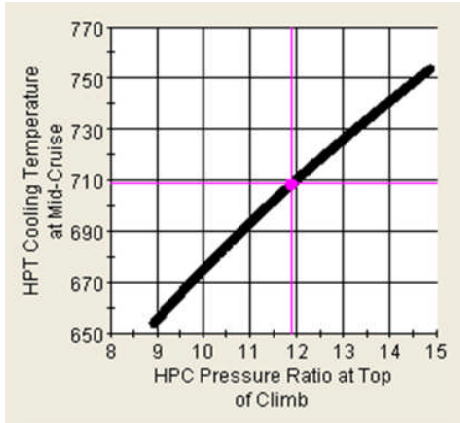
(h)



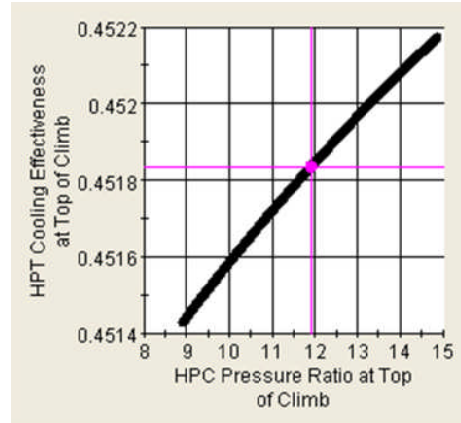
(i)



(j)



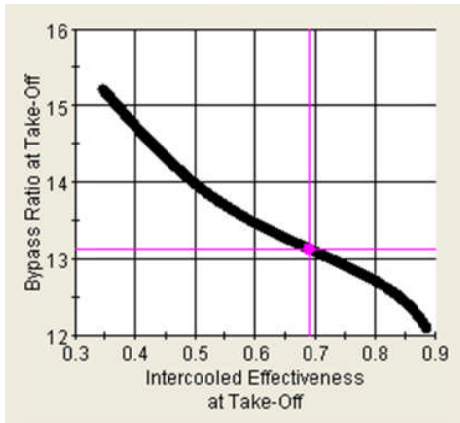
(k)



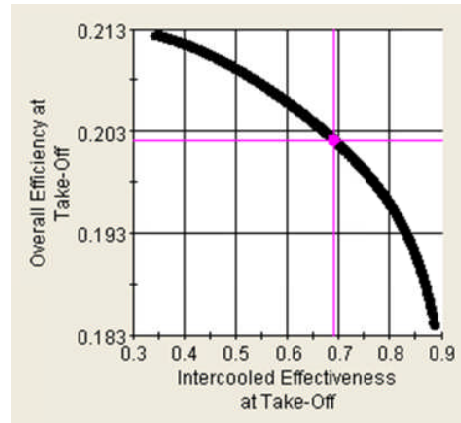
(l)

Figure C-17 HPC pressure ratio variation at top of climb

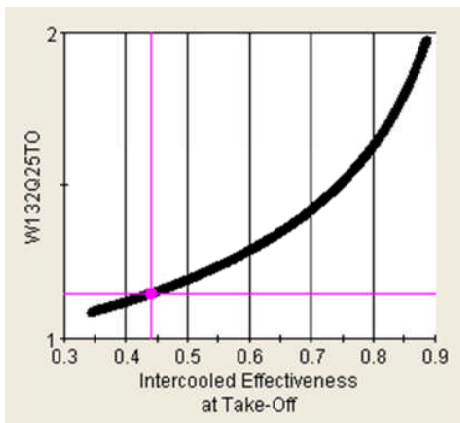
C.6 Intercooler effectiveness at take-off



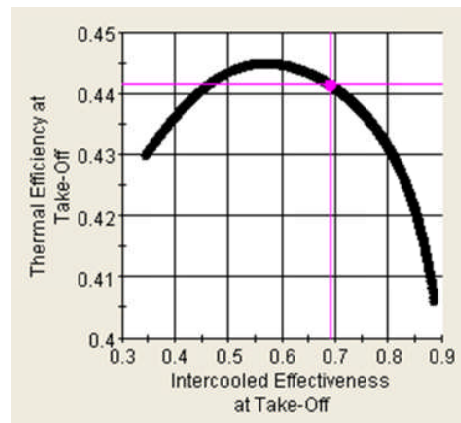
(a)



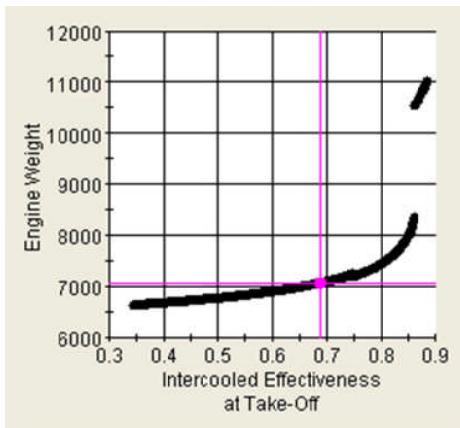
(b)



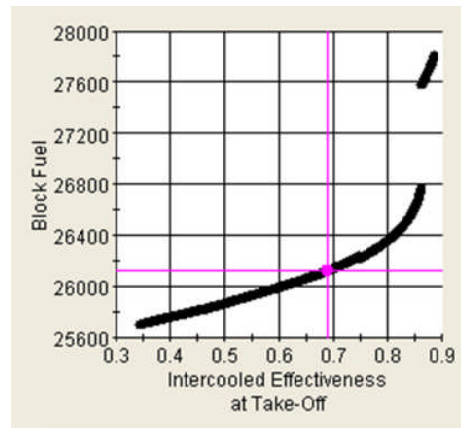
(c)



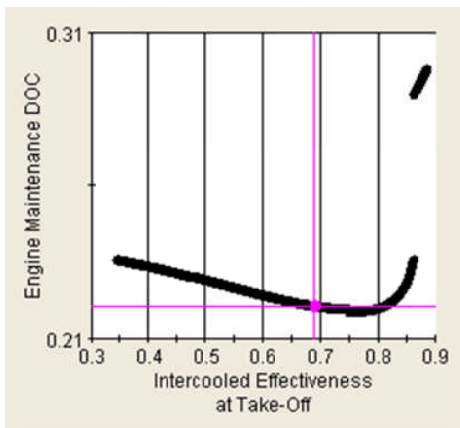
(d)



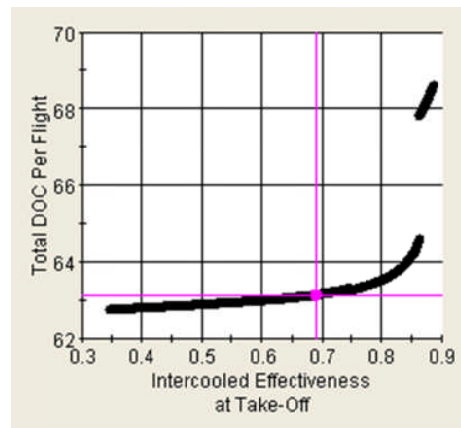
(e)



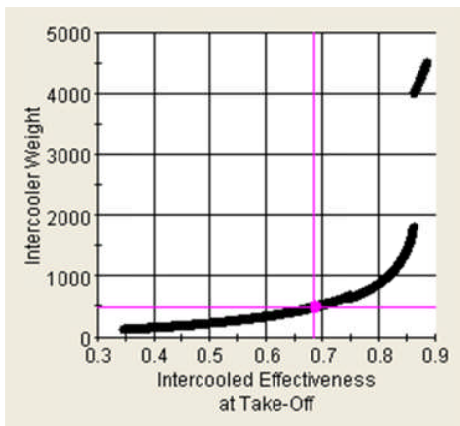
(f)



(g)



(h)



(i)

Figure C-18 *Intercooler effectiveness variation at take-off*

C.7 HPT cooling mass flow at top of climb

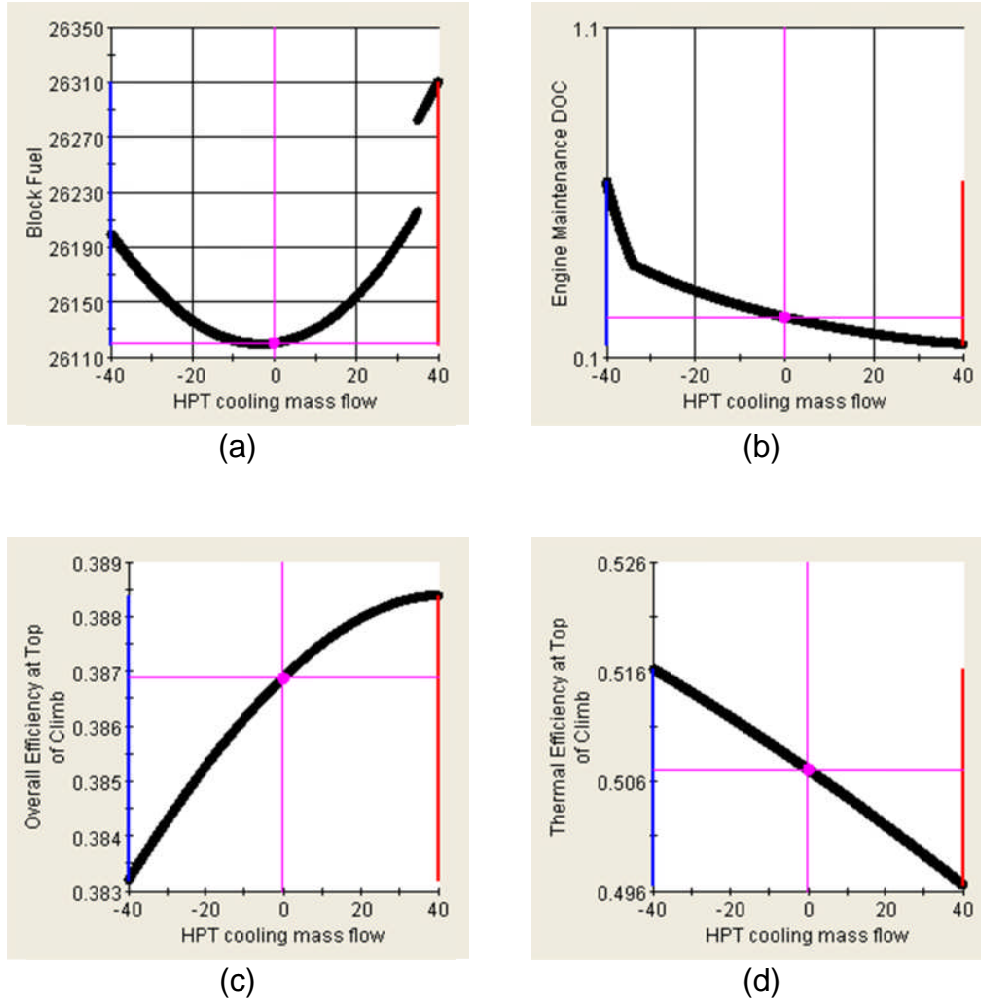
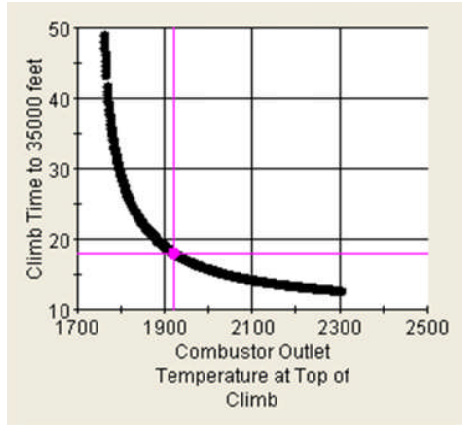
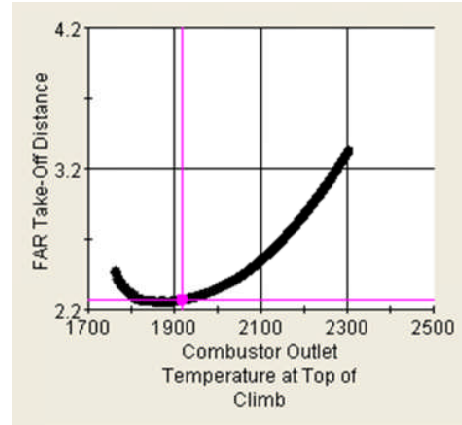


Figure C-19 HPT cooling mass flow variation at top of climb

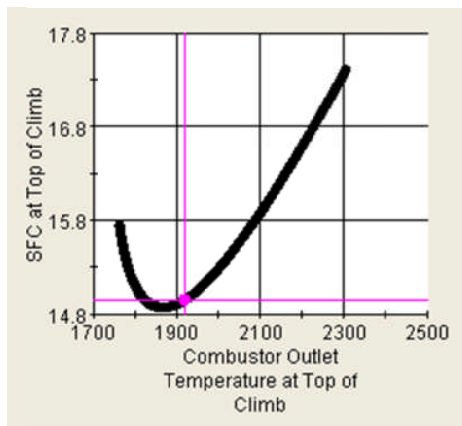
C.8 Combustor outlet temperature at top of climb



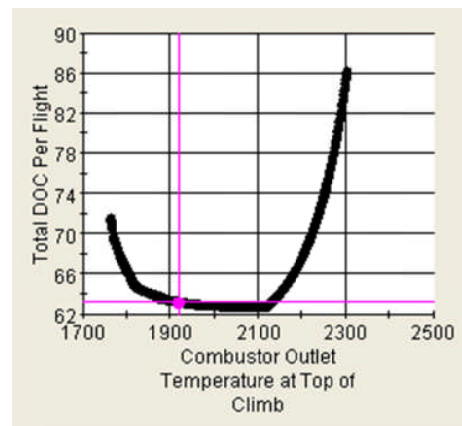
(a)



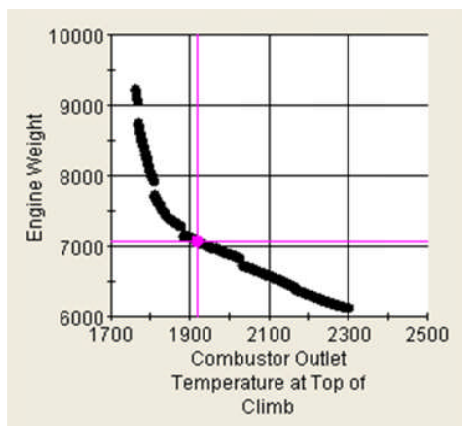
(b)



(c)



(d)



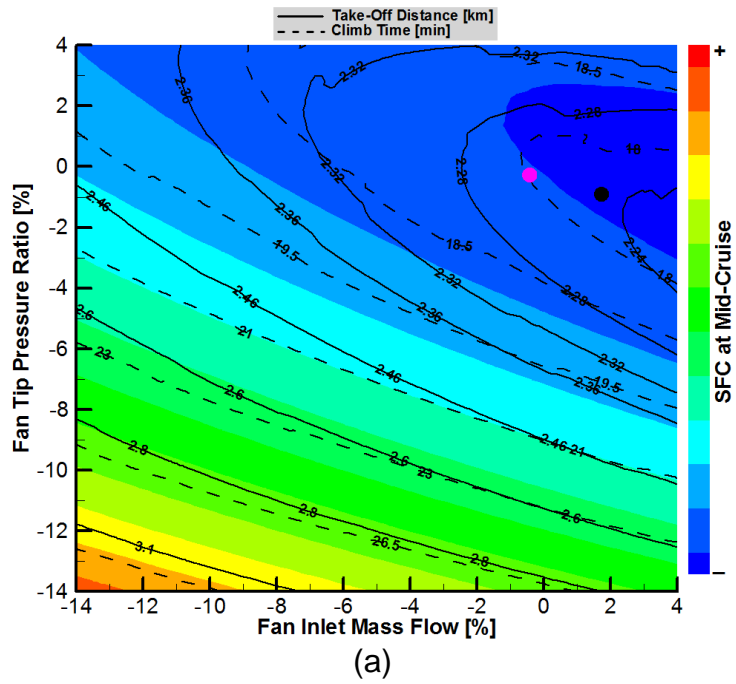
(e)

Figure C-20 Combustor outlet temperature variation at top of climb

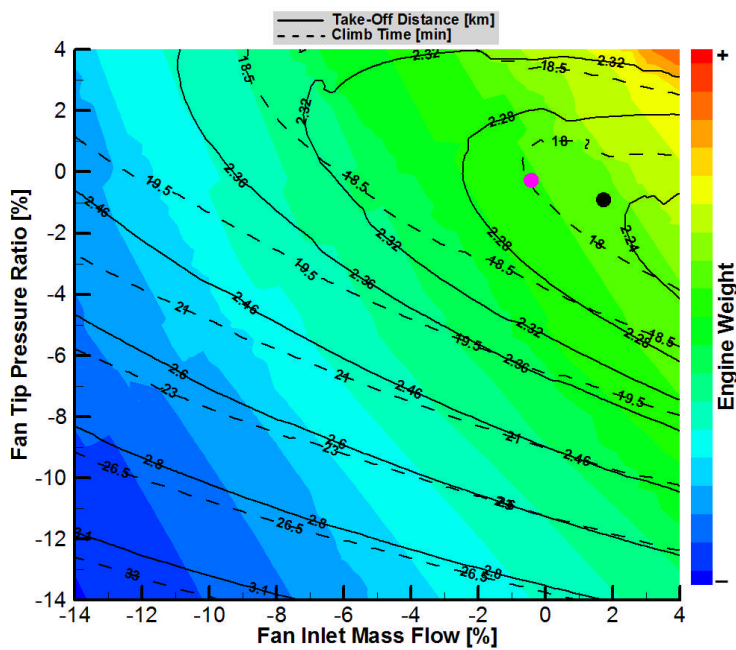
Appendix D

DDICLR Design Space Exploration and Optimisation

D.1 Fan inlet mass flow and fan tip pressure ratio



(a)



(b)

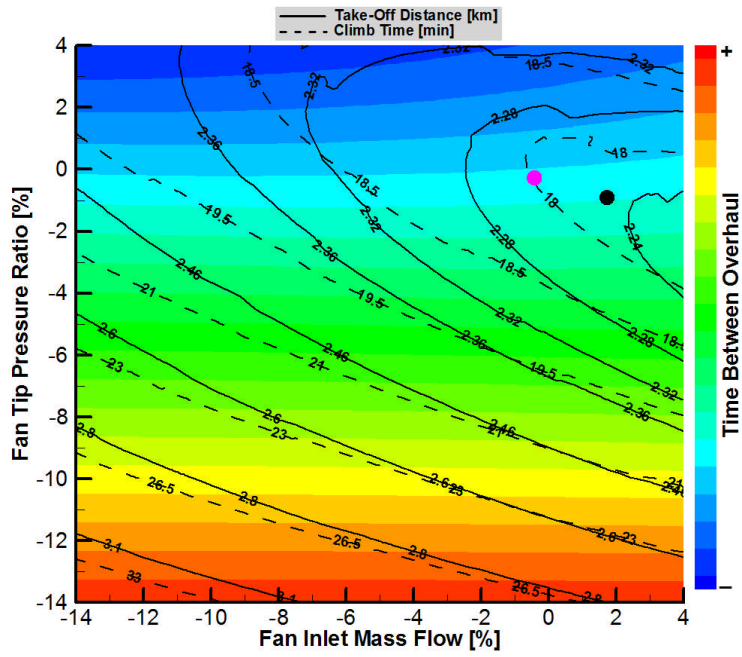
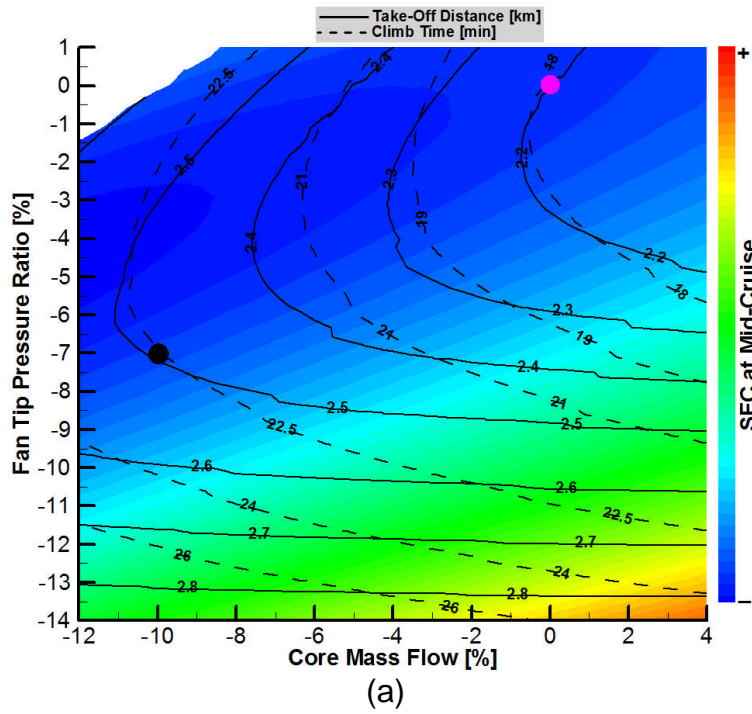


Figure D-21 Variation of fan inlet mass flow and fan tip pressure ratio

D.2 Core mass flow and fan tip pressure ratio



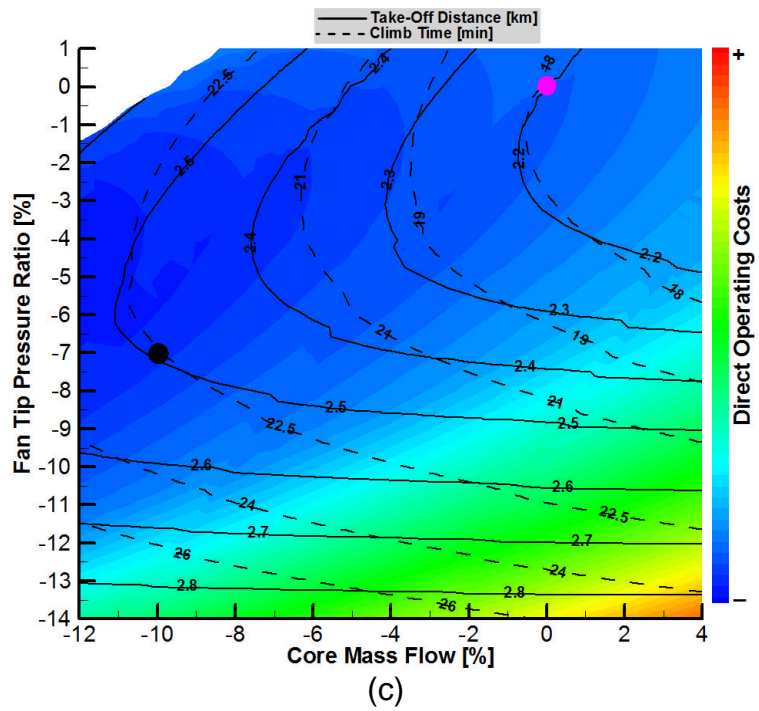
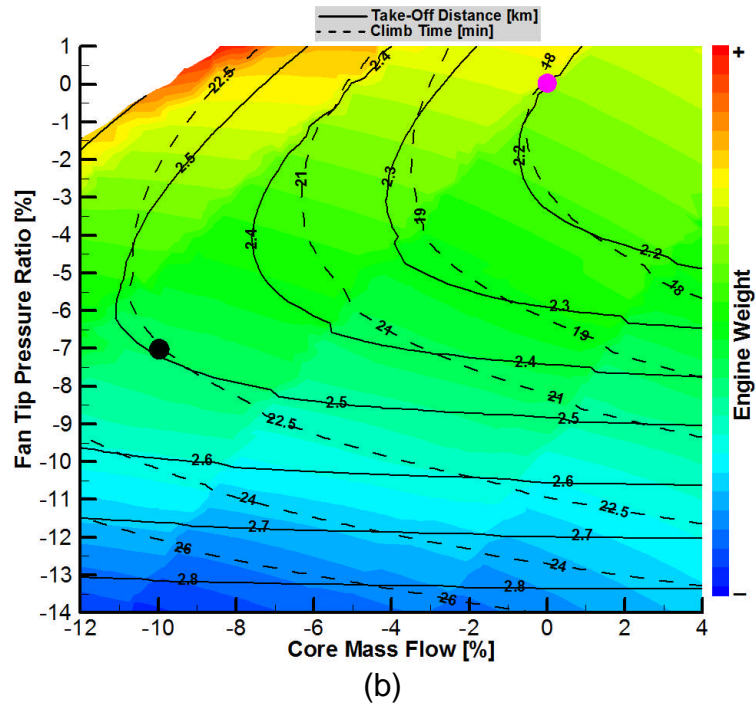


Figure D-22 Variation of core mass flow and fan tip pressure ratio

D.3 Fan tip pressure ratio

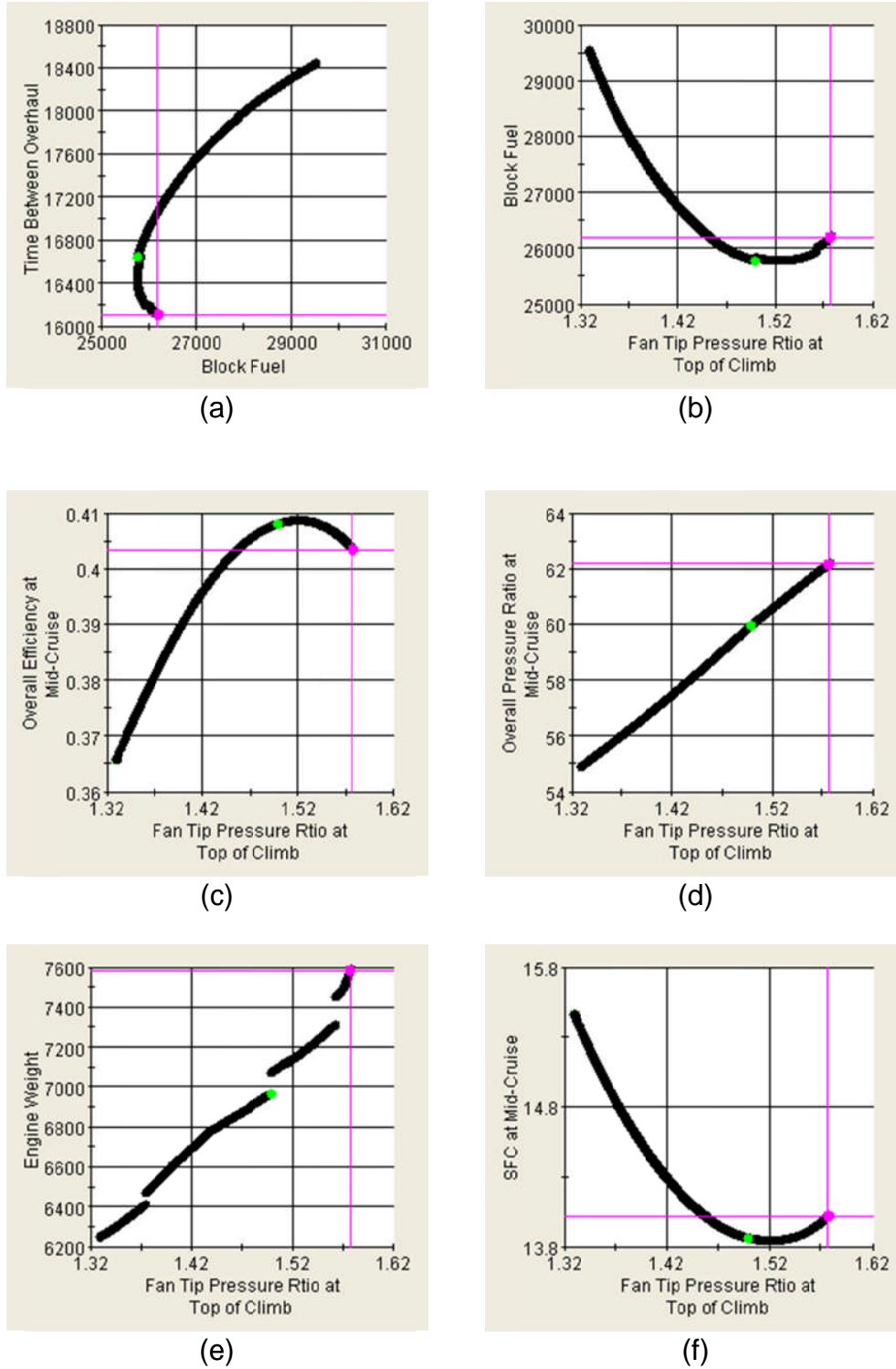
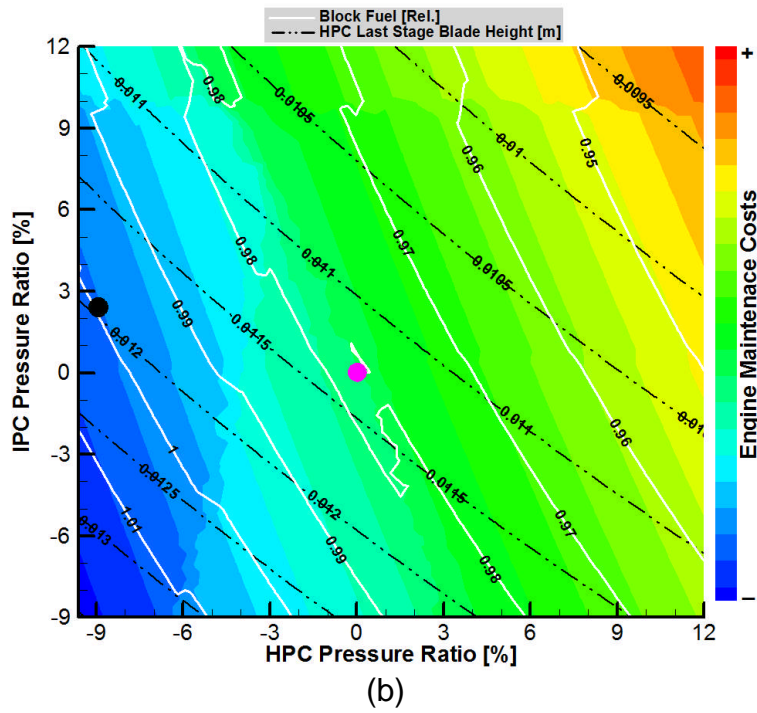
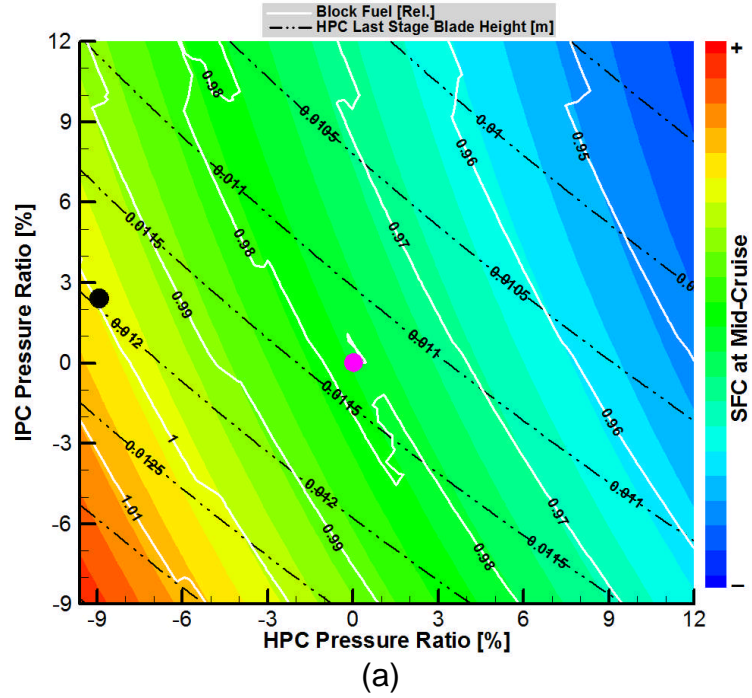


Figure D-23 Optimum fan tip pressure ratio for maximum TBO

D.4 IPC/HPC pressure ratio



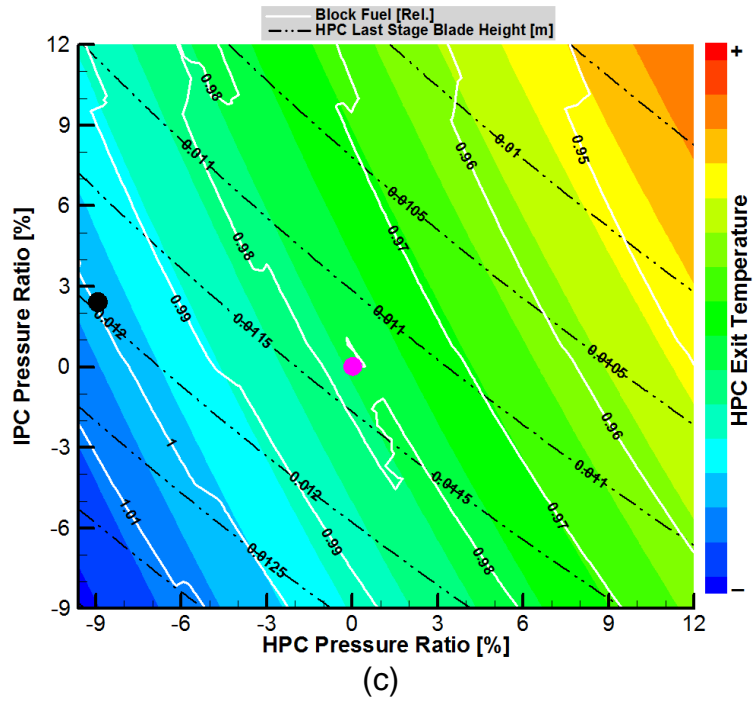
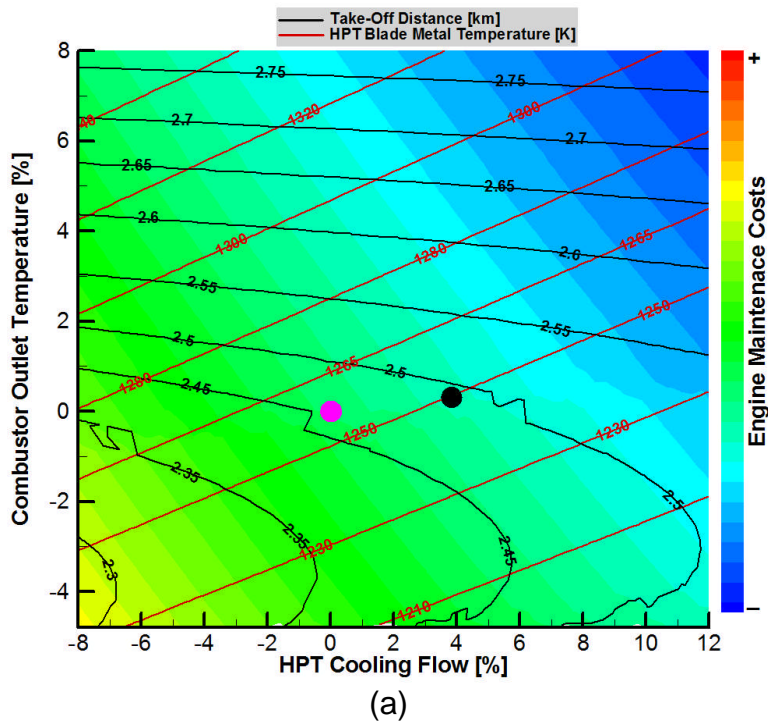


Figure D-24 Variation of IPC and HPC pressure ratio

D.5 Combustor outlet temperature and HPT cooling flow



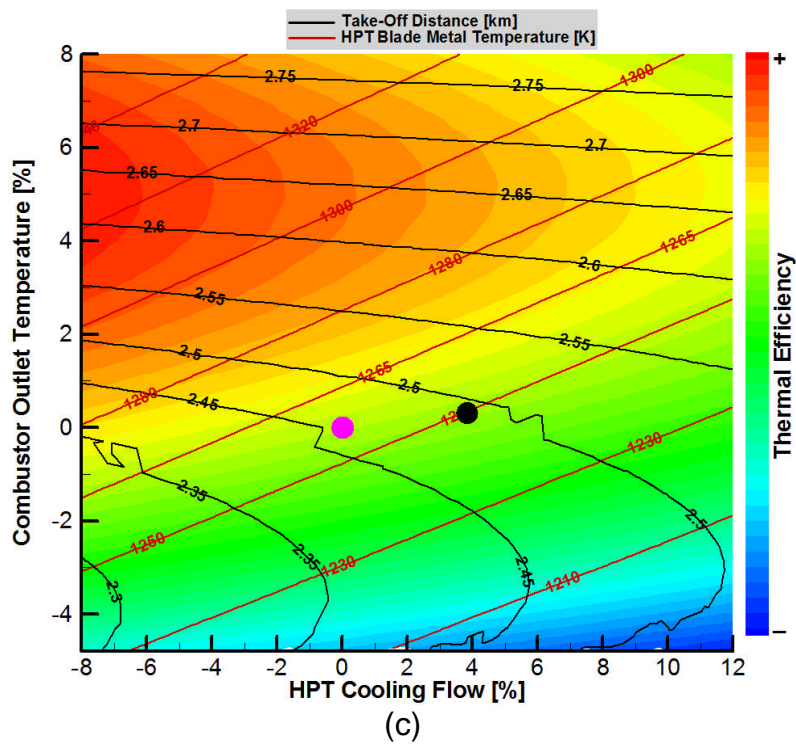
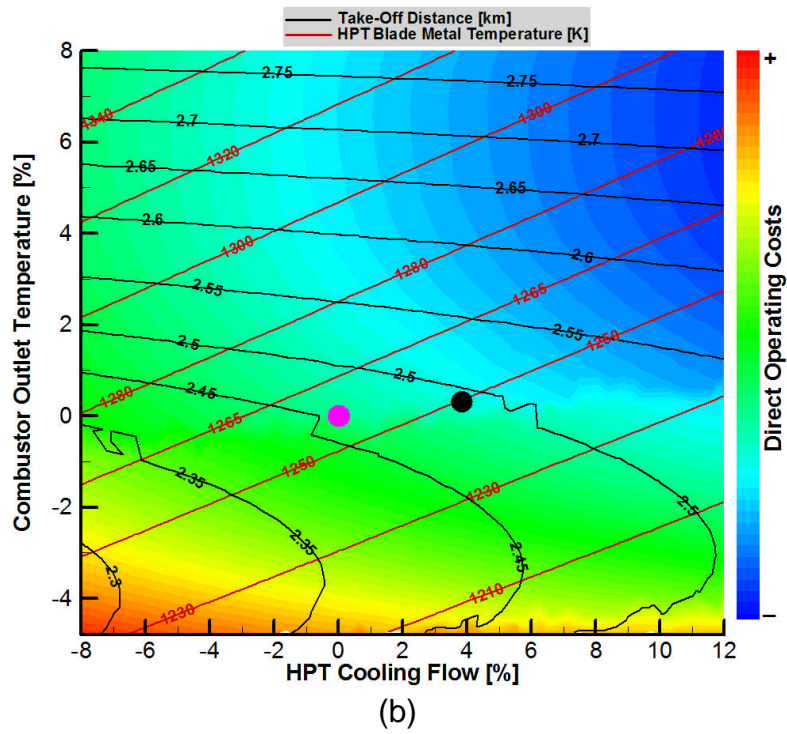
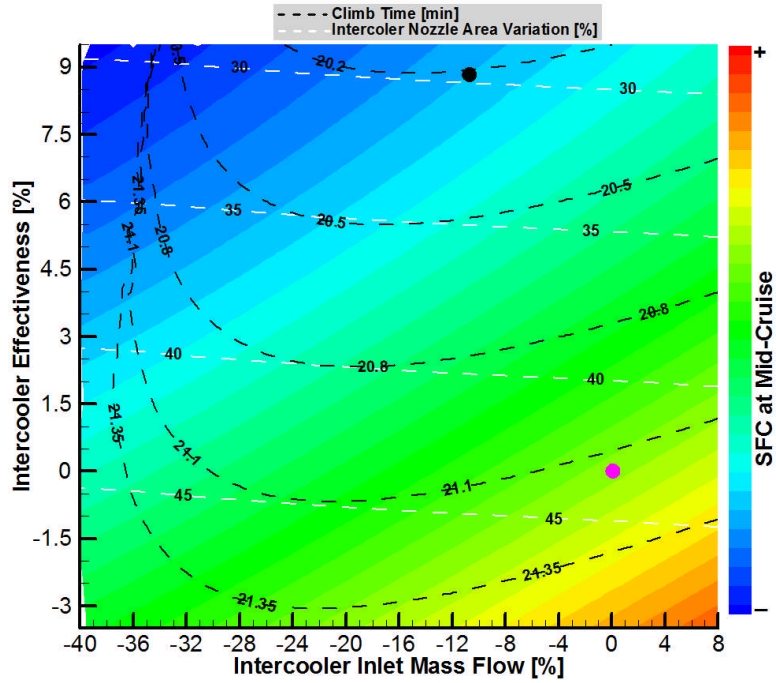
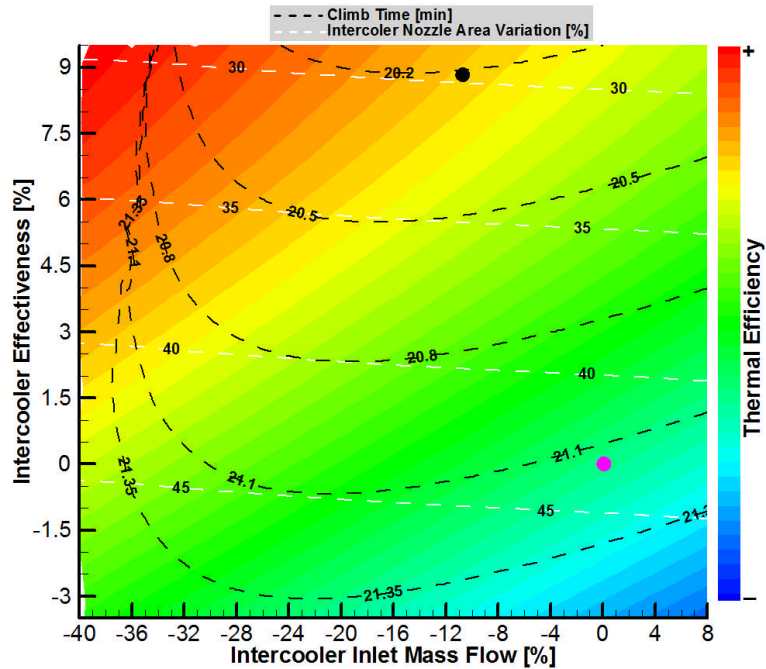


Figure D-25 Variation of combustor outlet temperature and cooling mass flow

D.6 Intercooler effectiveness and inlet mass flow



(a)



(b)

Figure D-26 Variation of intercooler effectiveness and intercooler inlet mass flow

Appendix E

Publications

Conference and Proceedings:

- Abu, A.O., Eshati, S., Najafi, E.S., Laskaridis, P., and Haslam, A., 2013, "Integrated Approach for Physics Based Life Assessment of Gas Turbine Blades", GT-2013-95987, Proceedings of GT2013, ASME Turbo Expo 2013, San Antonio, Texas, USA. (Draft paper submitted for publication)
- Najafi, E.S., Kyprianidis, K.G., Abu, A.O., Sethi, V., and Pilidis, P., 2013, "Techno-Economic and Environmental Assessment of Conceptual Intercooled Aero Engine Design for Long Range Application", ISABE-2013-10407, 21st Conference of the International Society for Air Breathing Engines, Busan, Korea. (Extended abstract submitted for publication)
- Navaratne, R., Najafi, E.S., Sethi, V., and Pilidis, P., 2013, "Preliminary Engine Life Assessment in Techno-Economic Environmental Risk Analysis Framework", ISABE-2013-10368, 21st Conference of the International Society for Air Breathing Engines, Busan, Korea. (Extended abstract submitted for publication)
- Navaratne, R., Najafi, E.S., Sethi, V., and Pilidis, P., 2013, "Preliminary Engine Life Assessment in Techno-Economic Environmental Risk Analysis Framework", GT-2013-94830 Proceedings of GT2013, ASME Turbo Expo 2013, San Antonio, Texas, USA. (Abstract submitted for publication)

Reports:

- Specification Document, Preliminary Specification of the CUTSTF Engine Performance Model for Use in GATAC V1, DI-3.1.2-1, September 16, 2009.
- Deliverable D1.3.3A, TERA2020 Optimisation Results for the three additional NEWAC Powerplants, NEWAC-D1.3.3A-R1.3, April 05, 2011.

Poster:

- Evaluation and Optimisation of Conceptual Aero Engine Cycles, Cranfield University, January, 2011.

This page intentionally left blank.